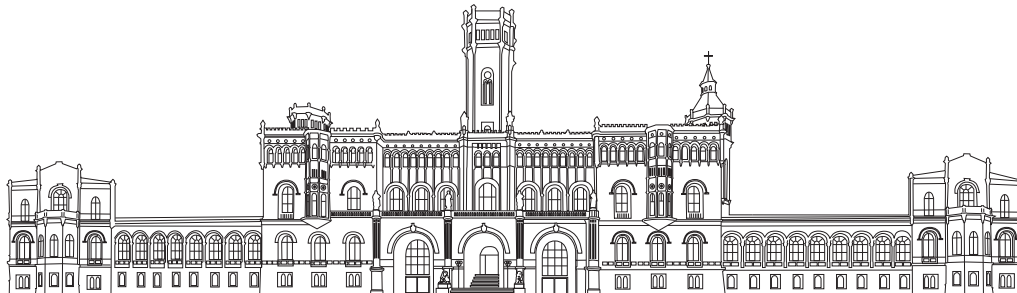


Spin chains and vertex models based on superalgebras



Von der Fakultät für Mathematik und Physik
der Gottfried Wilhelm Leibniz Universität Hannover

zur Erlangung des akademischen Grades

Doktor der Naturwissenschaften

Dr. rer. nat.

genehmigte Dissertation von

M.Sc. Konstantin Hobuß

Referent: Prof. Dr. Holger Frahm,
Leibniz Universität Hannover

Korreferenten: Prof. Dr. Andreas Klümper,
Bergische Universität Wuppertal
PD Dr. Michael Flohr,
Leibniz Universität Hannover

Vorsitz der Promotionskommission: Prof. Dr. Rolf J. Haug,
Leibniz Universität Hannover

Tag der Disputation: 03.12.2019

Abstract

The thermodynamic limit of superspin chains can show several intriguing properties, including the emergence of continua of scaling dimensions and the appearance of discrete states when imposing toroidal boundary conditions. Nevertheless, the former's exhaustive characterization in terms of Conformal Field Theories is still lacking.

In order to study the thermodynamic limit of the $U_q[sl(2|1)]$ $3 \otimes \bar{3}$ superspin chain in the antiferromagnetic regime, we analyze the low lying excitations by means of the model's exact solution using the Algebraic Bethe Ansatz. In the isotropic limit, this model may be used as a toy model for the description of plateau transitions in Quantum Hall systems. The definition of a quasimomentum operator allows for a characterization of the continua of scaling dimensions, thereby giving rise to a quantum number for the corresponding non-compact component of the spectrum in the thermodynamic limit. The associated degeneracies are lifted on the lattice by logarithmic fine structures. Based on the extrapolation of our finite size data we find that under a variation of the boundary conditions from periodic to antiperiodic for the fermionic degrees of freedom, levels from the continuous part of the spectrum flow into discrete levels and vice versa.

Investigating the thermodynamic limit of the q -deformed $osp(3|2)$ superspin chain, corresponding to an intersecting loop model in the rational limit, we seek to uncover its low-lying critical exponents. We present evidences that the latter are built in terms of composites of anomalous dimensions of two Coulomb gases with distinct radii and exponents associated to $Z(2)$ degrees of freedom. This view is supported by the fact that the $S = 1$ XXZ integrable chain spectrum is present in some of the sectors of the superspin chain at a particular value of the deformation parameter. We find that the fine structure of finite-size effects is very rich for a typical anisotropic spin chain. In fact, we argue on the existence of a family of states with the same conformal dimension whose lattice degeneracies are lifted by logarithmic corrections. On the other hand, we also report on states of the spectrum whose finite-size corrections seem to be governed by a power law behaviour. We finally observe that under toroidal boundary conditions the ground state dependence on the twist angle has two distinct analytical structures.

Keywords: Bethe Ansatz, superspin chains, Conformal Field Theories, quasimomentum, critical exponents

Zusammenfassung

Der thermodynamische Grenzwert von Superspinketten kann viele faszinierende Eigenschaften aufweisen, beispielsweise die Ausbildung von Kontinua von Skalendimensionen sowie das Auftreten diskreter Zustände, wenn verdrillte Randbedingungen betrachtet werden. Allerdings fehlt bisher eine allgemeine Klassifizierung dieser Grenzwerte in Bezug auf konforme Feldtheorien.

Um den thermodynamischen Grenzwert der $U_q[sl(2|1)]$ $3 \otimes \bar{3}$ -Superspinkette im antiferromagnetischen Regime zu untersuchen, analysieren wir die niederenergetischen Anregungen vermöge der exakten Lösung des Modells mittels des algebraischen Bethe-Ansatzes. Im isotropen Grenzfall kann die untersuchte Superspinkette zur Modellierung von Plateau-Übergängen in Quanten-Hall-Systemen verwendet werden. Die Definition eines Quasi-Impuls-Operators ermöglicht durch die Einführung einer Quantenzahl für den nicht-kompakten Anteil des Spektrums die Charakterisierung derselben innerhalb des untersuchten Modells. Die entsprechenden Entartungen werden auf dem Gitter durch logarithmische Feinstrukturen aufgehoben. Ausgehend von Extrapolationen unserer Daten für endliche Systemgrößen zeigen wir, dass unter Variationen der Randbedingungen von periodisch zu antiperiodisch für die fermionischen Freiheitsgrade Zustände des Kontinuums in diskrete Zustände übergehen und umgekehrt.

Anschließend untersuchen wir den thermodynamischen Grenzwert der q -deformierten $osp(3|2)$ Superspinkette, die im rationalen Limes zur Beschreibung des “intersecting loop”-Modells verwendet werden kann, indem wir die niederenergetischen kritischen Exponenten bestimmen. Wir präsentieren Anhaltspunkte, dass jene aus zwei Coulomb-Gasen unterschiedlicher Radien und den Exponenten der $Z(2)$ -Freiheitsgrade bestehen. Diese Sichtweise wird unterstützt durch die Tatsache, dass das Spektrum des $S = 1$ XXZ-Heisenbergmodells bei einer bestimmten Anisotropie im Spektrum der Superspinkette enthalten ist. Insbesondere legen wir dar, dass eine Klasse von Zuständen mit gleicher konformer Dimension, deren Gitterentartungen durch logarithmische Korrekturen aufgehoben werden, existiert. Andererseits finden wir ebenfalls Zustände im Spektrum, deren Korrekturen bei endlicher Systemgröße einem Potenzgesetz folgen. Schließlich beobachten wir zwei verschiedene analytische Verhalten des Grundzustandes in Abhängigkeit des Drehwinkels in den Randbedingungen.

Schlagnote: Bethe-Ansatz, Superspinketten, konforme Feldtheorie, Quasi-Impuls, kritische Exponenten

Contents

Abstract	i
Zusammenfassung	iii
Introduction	1
Part I Preliminaries	5
1 Integrability	7
1.1 Quantum Inverse Scattering Method	7
1.2 Algebraic Bethe Ansatz	10
2 Superalgebras	13
2.1 Definitions	13
2.2 Examples: $gl(n m)$ and $sl(2 1)$	16
2.2.1 The general Lie superalgebra $gl(n m)$	16
2.2.2 The special linear Lie superalgebra $sl(2 1)$	16
2.3 Cartan-Weyl and Chevalley basis	18
2.4 Representation theory	20
2.4.1 Definitions	21
2.4.2 Example: $sl(2 1)$	24
2.5 Quantum deformations	26
2.5.1 Construction	26
2.5.2 Example: $U_q(sl(2 1))$	27
2.6 Graded Quantum Inverse Scattering Method	28
3 Conformal Field Theory	29
3.1 Critical phenomena	29
3.2 Conformal invariance	31
3.2.1 Conformal transformations	31
3.2.2 Fields and their correlation functions	34
3.2.3 The Virasoro algebra and its representations	35
3.3 Finite size scaling	40
3.4 Supersymmetric extensions	42
4 From the Integer Quantum Hall effect to superspin chains	45

Part II	Finite size study of integrable superspin chains	49
1	The $U_q[sl(2 1)]$ superspin chain	51
1.1	Definition and solution of the model	52
1.2	Low-energy spectrum	62
1.2.1	Periodic boundary conditions	63
1.2.2	Antiperiodic boundary conditions	65
1.2.3	Conformal Field Theory for the isotropic model	66
1.3	Quasimomentum: Characterization of the continuous spectrum	68
1.4	Spectral flow between the Neveu-Schwarz and Ramond-sector	73
1.5	Summary	77
2	The operator content of the $U_q[osp(3 2)]$ superspin chain	81
2.1	The $osp(3 2)$ Lie superalgebra	83
2.2	Definition and solution of the $U_q[osp(3 2)]$ superspin chain	84
2.2.1	Bethe Ansatz in the $bfbfb$ grading	87
2.2.2	Bethe Ansatz in the $fbbbf$ grading	90
2.3	Finite-size spectrum	91
2.3.1	Root density approach	92
2.3.2	Relation to the spin $S = 1$ XXZ model	93
2.4	Numerical study of the operator content	95
2.4.1	Sector $(0, 0)$	98
2.4.2	Sector $(0, 1)$	102
2.4.3	Sector $(0, 2)$	106
2.4.4	Sector $(1, 0)$	111
2.4.5	Sector $(1, 1)$	115
2.4.6	Sector $(1, 2)$	119
2.4.7	Sector $(2, 0)$	122
2.4.8	Sector $(2, 1)$	125
2.4.9	Sector $(2, 2)$	129
2.5	Summary	132
	Conclusions	139
A	Supplements for the $U_q[osp(3 2)]$ superspin chain	145
	References	151

Introduction

Although magnetism is intuitively familiar to us, the theoretical description of this purely quantum mechanical phenomenon can be rather complicated. While studying ferromagnetism in a solid, Werner Heisenberg [1] and Paul Dirac [2] both realized that the spin degrees of freedom solely determine the magnetic properties of the system. These thoughts resulted in the famous Heisenberg model consisting of particles with spin-1/2 (e.g. electrons) sitting at each lattice site and interacting with each other. A few years later, the one-dimensional Heisenberg model for spin-1/2 particles was solved exactly by Hans Bethe [3]. In general, lattice models of interacting spins in one spatial dimension are called *spin chains*.

Consecutively, spin chain Hamiltonians were shown to be generated by transfer matrices of classical statistical lattice models in two dimensions [4]. This equivalence became manifest mathematically in the theory of integrable models. Within this theory each Lie algebra allows for the construction of a spin chain [5, 6] by means of its equivalent two dimensional vertex model. Moreover, generalizing the ideas of Bethe enables their subsequent exact solution. Particularly, the Heisenberg chain with spin- S particles can be reproduced within this framework when studying the vertex model associated with the spin- S representation of the $su(2)$ Lie algebra. Other spin chains may be seen as mathematical generalizations thereof.

Since the most relevant spin chains like the one-dimensional Heisenberg model with arbitrary spin provide examples of quantum mechanical systems which are completely solvable it is tempting to calculate macroscopic properties for a comparison with experiments or to study phase transitions. In both cases the thermodynamic limit (e.g. enlarging the lattice size to infinity while keeping the density of particles constant) is of extraordinary relevance.

If spin chains based on two dimensional statistical vertex models can be shown to have a massless region in the spectrum, their thermodynamic limit is expected to be described by a Conformal Field Theory (CFT). To be more precise, spin chains based on simply laced Lie algebras were shown to be lattice regularizations of Wess-Zumino-Novikov-Witten (WZNW) models [7]. Generally speaking, the thermodynamic limit of spin chains is well understood.

The scenario completely changes when considering spin chains based on Lie superalgebras instead of ordinary Lie algebras. For this class of models, a complete understanding of the thermodynamic limit is still lacking. Superalgebras allow for a simultaneous description of both bosonic and fermionic degrees of freedom. In a physical context such objects appeared first in the 1970's when Julius Wess and Bruno Zumino constructed transformations between bosonic and fermionic states [8, 9] which is not possible using

‘normal’ Lie algebras.

In principle, superspin chains can be constructed in a very similar way as ordinary spin chains with a few slight modifications. Despite being extremely interesting from the purely mathematical point of view, the question arises in which context spin chains based on superalgebras appear in physics. One example of applications of superspin chains are plateau transitions in the integer Quantum Hall Effect [10]. In 1980, Klaus von Klitzing studied a setup using electrons confined to two spatial dimensions with a strong magnetic field perpendicular to the plane in which the electrons can move. When exposing this setup to low temperatures he found that the resistivity exhibits plateaus at $\rho = 2\pi\hbar/\nu e$ with integer ν and the electron charge $-e$. It can be shown that an effective field theory describing plateau transitions is in fact the thermodynamic limit of a superspin chain with infinitely many local degrees of freedom [11–17]. Since models of interacting particles with an infinite-dimensional Hilbert space may be treated exactly neither analytically nor numerically, toy models which can be constructed by truncating the local Hilbert space have to be used. One example of such a toy model is the $sl(2|1)$ superspin chain which is one of the models studied extensively within this work.

The applicability of superspin chains in statistical physics is not exclusively restricted to order-disorder transitions in Quantum Hall systems. A different class of models for whose description superspin chains can be used are intersecting loops. These models allow for the study of the diffusion of particles through barriers which are placed randomly on a square lattice [18, 19] and tilted left and right w.r.t. the lattice. Incoming particles will change their direction when hitting a scatterer but will pass through a node if it is empty. Hence the particles’ paths form intersecting loops on the lattice which is eponymous for the model. In a special case it may be reformulated in terms of the superspin chain built from representations of the $osp(3|2)$ superalgebra. This model will be investigated thoroughly within this thesis.

While not completely characterized, thermodynamic limits of superspin chains have been shown to exhibit rather unusual features. Several superspin chains have been revealed to possess infinitely many states with the same conformal dimension in the thermodynamic limit [19–22] - although the amount of local degrees of freedom on the lattice is finite. Hence, effective field theories for these models feature a quantum number which describes the corresponding non-compact degree of freedom. This observation indicates that the associated effective field theories may be characterized in terms of non-unitary CFTs. Besides, the latter reveal other interesting features, e.g. the emergence of non-normalizable states which may appear in the spectrum of the corresponding superspin chain for certain boundary conditions only. Note, thermodynamic limits with similar properties do appear not only for superspin chains. The staggered six-vertex model [23–26] as well as models describing the physical properties of two-dimensional

polymers [27, 28] have been proven to correspond to non-unitary CFTs as well.

In this context, the present work aims to provide new insights in the thermodynamic limits of two superspin chains. The first example to be studied, the staggered superspin chain based on quantum deformations of $sl(2|1)$, was previously shown to exhibit a series of levels which tend to the same conformal dimension in the thermodynamic limit [21]. Hence, we seek for a characterization of these states. Further, we investigate the spectral flow when a twist in the boundary conditions is imposed and thereby search for non-analyticities which are expected for lattice regularizations of non-unitary CFTs in order to ultimately study properties of the thermodynamic limit. Consecutively, we investigate a superspin chain built from quantum deformations of $osp(3|2)$. In the corresponding isotropic model, again continua of scaling dimensions have been found [19]. Thus, we are intrigued by the question if such continua can survive in the presence of quantum deformations. To go even beyond, we search for a complete characterization of the operator content in order to provide a solid basis for subsequent studies hopefully leading to an understanding of the thermodynamic limit of the q -deformed $osp(3|2)$ superspin chain.

Thesis outline

In order to provide a clear structure this thesis is divided into two parts. Part I is dedicated to introduce briefly the main concepts needed to understand and construe the results presented in part II. In more detail, we will start by reviewing the Quantum Inverse Scattering Method and the Algebraic Bethe Ansatz in I.1. The following section will familiarize the mathematical concepts of superalgebras in I.2 where we will discuss the basic ideas needed for the subsequent construction and solution of superspin chains. Since the thermodynamic limit of such models is believed to be described by a CFT, we will establish the notion of conformally invariant field theories and discuss their implications for finite size studies in I.3. The preliminary part will be closed by a short discussion of the integer Quantum Hall Effect. It will be shown how superspin chains emerge for the theoretical description of the aforementioned order-disorder transition in Quantum Hall systems in I.4.

The latter section serves as motivation for the second part of this thesis in which two examples of superspin chains will be studied in detail, namely the quantum deformations of $sl(2|1)$ in II.1 and $osp(3|2)$ in II.2. While both sections will contain a finite size study of several states belonging to the low-energy spectrum the scope of these studies is rather different. For the q -deformed $sl(2|1)$ superspin chain in II.1 the operator content for a subset of the spectrum as well as the existence of continua of scaling dimensions has already been established [21]. Hence, in order to study its thermodynamic limit we will seek for a description of these continua in terms of an operator which commutes with the

Hamiltonian and therefore provides us with a good quantum number. Subsequently, we will impose a twist in the boundary conditions and investigate the emergence of discrete states. On the other hand, for the q -deformed $osp(3|2)$ model in II.2 the operator content is still unknown. Hence, we pursue to establish a proposal for the scaling dimensions corresponding to the primary fields by a thorough numerical study of some tens of low-energy states. Our conjecture will be underpinned by analytical arguments using a correspondence with the Heisenberg XXZ spin-1 chain at a certain anisotropy.

Part I

Preliminaries

1 Integrability

In classical mechanics, a system with n degrees of freedom is referred to as *completely integrable* if it possesses n independent conserved quantities, i.e. n integrals of motion. In this case, the system is said to be *completely solvable*. Since this definition is unambiguous it seems surprising that there is no precise quantum equivalent [29]. In this thesis, for the definition of *quantum integrability*, we will follow the notion by Faddeev [30], Izergin and Korepin [31] and call a (1+1)-dimensional vertex model or its equivalent one-dimensional quantum spin chain integrable if it can be constructed and solved by means of the *Quantum Inverse Scattering Method* (QISM) and the *Algebraic Bethe Ansatz* (ABA), respectively.

In this section we will introduce the main concepts of the QISM in 1.1 following [32] and [33]. We will see that it is a powerful tool for constructing integrable models. The second subsection 1.2 is dedicated to a brief discussion of ABA and how it uses the outcome of the QISM to solve the eigenvalue problem for one-dimensional quantum spin chains.

1.1 Quantum Inverse Scattering Method

The starting point for the construction of an integrable model by means of the QISM is the *Yang-Baxter equation* (YBE) which goes back to independent works by C.N. Yang [34, 35] and R.J. Baxter [4],

$$\mathcal{R}_{1,2}(\lambda)\mathcal{R}_{1,3}(\lambda + \mu)\mathcal{R}_{2,3}(\mu) = \mathcal{R}_{2,3}(\mu)\mathcal{R}_{1,3}(\lambda + \mu)\mathcal{R}_{1,2}(\lambda) \quad (\text{I.1})$$

where λ and μ are complex numbers called *spectral parameters*. As we will see below, each solution of (I.1) allows for the construction of an integrable model since it imposes an integrability condition for the building blocks of such models, the *\mathcal{R} -matrix*.

In general, \mathcal{R} -matrices $\mathcal{R}_{a,b}(\lambda)$ are maps from a tensor product $V_a \otimes V_b$ of two vector spaces V_a ($a, b = 1, 2, 3$) onto itself where the vector spaces V_a up to this point are arbitrary. The \mathcal{R} -matrix can be seen as the scattering matrix for one-dimensional quantum systems since the YBE can be understood in the following way. If a system is integrable, i.e. its \mathcal{R} -matrix fulfills (I.1), then every three-particle scattering process can be decomposed into two-particle scattering processes, thus the order of the (artificial) two-particle scattering processes is irrelevant, see fig. 1 for a graphical representation. In fact, this interpretation provides an alternative way to define a (quantum) integrable model. A discussion about the assets and drawbacks of several definitions of quantum integrable models can be found in [29].

For the construction of a physical integrable model (having a spin chain in mind)

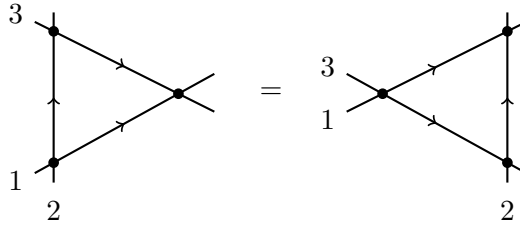


Figure 1: Graphical representation of the Yang-Baxter equation (I.1): The YBE can be seen as condition for the decomposition of any three-particle scattering process into two particle processes such that the order of the two-particle scatterings (denoted as black dots) is irrelevant.

we define the *Lax operator* $L_{n,a}$ to be a map between the tensor product of the local Hilbert space \mathcal{H}_n of the n -th site and a so-called *auxiliary space* \mathcal{V}_a onto itself. The total N -site Hilbert space is defined as the tensor product of all sites and will be denoted by $\mathcal{H} = \otimes_{n=1}^N \mathcal{H}_n$. The Lax operators are related to the \mathcal{R} -matrix in virtue of

$$\mathcal{R}_{a,b}(\lambda - \mu)L_{n,a}(\lambda)L_{n,b}(\mu) = L_{n,b}(\mu)L_{n,a}(\lambda)\mathcal{R}_{a,b}(\lambda - \mu). \quad (\text{I.2})$$

Eqs. (I.2) are called the RLL-relations. If the \mathcal{R} -matrix satisfies (I.1) the Lax operator exists and is unique [36, 37].

In contrast to \mathcal{H}_n which is fixed by the local degrees of freedom there is essentially no constraint regarding the auxiliary space. If $\mathcal{V}_a = \mathcal{H}_n$ the \mathcal{R} -matrix and the Lax operators are basically the same.

Since the Lax operator $L_{n,a}$ describes the ‘transport’ [32] of an auxiliary particle at site a to site n the ordered product over all sites

$$T_a(\lambda) \equiv L_{N,a}(\lambda) \dots L_{1,a}(\lambda) \quad (\text{I.3})$$

defines a *monodromy* around the spin chain when periodic boundary conditions are imposed [32]. Note, the monodromy matrix is an operator valued matrix in the auxiliary space whose entries act on the whole Hilbert space \mathcal{H} . For the effect of general boundary conditions, see below.

Since the monodromy matrix is built from Lax operators which satisfy the RLL-relations (I.2), so does the monodromy,

$$\mathcal{R}_{a,b}(\lambda - \mu)T_a(\lambda)T_b(\mu) = T_b(\mu)T_a(\lambda)\mathcal{R}_{a,b}(\lambda - \mu). \quad (\text{I.4})$$

Analogously, these relations are referred to as RTT-relations.

To make contact with more familiar physical quantities acting on the Hilbert space \mathcal{H} only we define the *transfer matrix* as the trace of the monodromy matrix over the

auxiliary space,

$$\tau(\lambda) = \text{tr}_a T_a(\lambda). \quad (\text{I.5})$$

The RTT-relations (I.4) guarantee that transfer matrices with different spectral parameters commute,

$$[\tau(\lambda), \tau(\mu)] = 0. \quad (\text{I.6})$$

Therefore, it can be used to generate a series of conserved quantities Q_i , e.g.

$$Q_i = \frac{d^i}{d\lambda^i} \log \tau(\lambda) \Big|_{\lambda=\eta}, \quad i = 0, \dots, N-1, \quad (\text{I.7})$$

where η denotes the *shift point*, the spectral parameter where the Lax operator becomes proportional to the permutation operator.¹ The definition of these conserved charges connects the notion of quantum and classical integrability. It can be shown that the momentum and the energy are related to the Q_0 and Q_1 [32],

$$P \propto Q_0 \quad \text{and} \quad H \propto Q_1. \quad (\text{I.8})$$

To summarize we have argued that a specific solution of the YBE (I.1) yields the Hamiltonian and other conserved charges of the corresponding integrable model. Let us close this overview with a few remarks:

- The YBE generates a rich algebraic structure, known as *Yang-Baxter algebra* in which the Lax operators and the monodromy matrix appear as local and global representations, respectively, see [39] and the references therein.
- In this thesis we will investigate spin chains based on superalgebras which leads to some subtleties in the QISM scheme. We will discuss these issues in sec. 2.6.
- More general boundary conditions that preserve the integrability can be imposed by inserting a matrix \mathcal{G} representing these boundary conditions in the definition of the monodromy matrix,

$$T_a^{\text{bd}}(\lambda) \equiv \mathcal{G}_a L_{N,a}(\lambda) \dots L_{1,a}(\lambda) \quad (\text{I.9})$$

provided that \mathcal{G} also fulfills a Yang-Baxter equation²,

$$\mathcal{R}_{a,b}(\lambda) \mathcal{G}_a \mathcal{G}_b = \mathcal{G}_b \mathcal{G}_a \mathcal{R}_{a,b}(\lambda). \quad (\text{I.10})$$

¹Note, the existence of a shift point is not guaranteed, e.g. if the dimensions of the auxiliary and quantum space are unequal. However, even if there is no trivial shift point, it may be possible to construct Hamiltonians e.g. by means of *fusion* in the auxiliary space [38].

²In other words, $\mathcal{G} \otimes \mathcal{G}$ commutes with \mathcal{R} .

In (I.9), the matrix \mathcal{G}_a acts in the auxiliary space only. One example of such integrable boundary conditions are twisted boundaries where \mathcal{G}_a is generated by the generator of rotations in the auxiliary space.

1.2 Algebraic Bethe Ansatz

The Bethe Ansatz dates back to Hans Bethe in 1931 who used a superposition of plane waves in order to compute eigenstates of the Heisenberg XXX spin-1/2 chain [3]. His technique was later on called *Coordinate Bethe Ansatz*. Afterwards, this method has been successfully extended to many other one-dimensional models like the Hubbard-model [40]. Here we will focus on the *Algebraic Bethe Ansatz* which naturally hooks up with the results of the QISM and allows for a systematic calculation of the eigenstates and eigenenergies of the corresponding integrable model.

To start, we study for simplicity a model with $sl(2)$ symmetry or deformations thereof. In this case, the auxiliary space is isomorphic to \mathbb{C}^2 such that the monodromy matrix can be written as operator-valued 2×2 matrix,

$$T_a(\lambda) = \begin{pmatrix} A(\lambda) & B(\lambda) \\ C(\lambda) & D(\lambda) \end{pmatrix}. \quad (\text{I.11})$$

We further assume that there is a *reference state* $|0\rangle$, also called *pseudo vacuum*³, such that $|0\rangle$ is an eigenstate of $A(\lambda)$ and $D(\lambda)$ and therefore it is also an eigenstate of the Hamiltonian. In addition we demand $|0\rangle$ to be annihilated by $C(\lambda)$. In this case candidates for eigenstates of the integrable model can be constructed by

$$|\lambda_1 \dots \lambda_M\rangle = \prod_{j=1}^M B(\lambda_j) |0\rangle. \quad (\text{I.12})$$

Up to this point the λ_j are arbitrary complex numbers.

For $|\lambda_1 \dots \lambda_M\rangle$ to be an eigenstate of the Hamiltonian it is sufficient to be an eigenstate of $A(\lambda) + D(\lambda)$ with eigenvalue $\Lambda(\lambda; \{\lambda_j\})$,

$$(A(\lambda) + D(\lambda)) |\lambda_1 \dots \lambda_M\rangle \stackrel{!}{=} \Lambda(\lambda; \{\lambda_j\}) |\lambda_1 \dots \lambda_M\rangle. \quad (\text{I.13})$$

The RTT-relations allow for an explicit calculation of $(A(\lambda) + D(\lambda)) |\lambda_1 \dots \lambda_M\rangle$ leading to consistency equations which ensure for $|\lambda_1 \dots \lambda_M\rangle$ to be an eigenstate of the Hamiltonian, thereby fixing the λ_j . The corresponding consistency equations are referred to as *Bethe Ansatz Equations* (BAE), their solutions λ_j are called *Bethe roots* or *rapidities*. Solving these equations completely fixes an eigenstate of the Hamiltonian. The BAE

³Note, there are integrable models where a reference state does not exist although this is the main ingredient for the following, e.g. for non-diagonal boundary conditions [41].

also guarantee that the eigenvalues $\Lambda(\lambda; \{\lambda_j\})$ are analytic functions in λ (or, at least, that $\Lambda(\lambda; \{\lambda_j\})$ can be analytically continued), i.e. all residues vanish. For the XXX Heisenberg chain with spin $S = 1/2$ it can be shown that Bethe states are highest weight states w.r.t. the symmetry of the model [42].

For higher-rank models, the lowest possible dimension of the auxiliary space is larger than 2, e.g. in the case of models with $gl(n)$, $n \in \mathbb{N}$ symmetry [41, 43]. For models based on its fundamental representation, the auxiliary space is n -dimensional. In this case, the transfer matrix

$$\tau(\lambda) = \text{tr} T_a(\lambda) \tag{I.14}$$

cannot be diagonalized in one step. In fact, when applying the above scheme the obtained Bethe Ansatz equations will themselves impose a new eigenvalue problem for a *nested transfer matrix* with reduced dimension. This procedure is called *nested Bethe Ansatz* [43, 44]. In an iterative scheme, the nested transfer matrix can be diagonalized by the Algebraic Bethe Ansatz as described above which leads to a second set of Bethe Ansatz equations. The ‘depth’ of nesting necessary to finally arrive at Bethe Ansatz equations only containing the Bethe roots is equal to the rank of the symmetry Lie algebra of the system.

2 Superalgebras

This section is concerned with the discussion of superalgebras. These mathematical objects will serve as symmetry algebras used for the construction of the models which will be investigated in part II of this thesis.

Superalgebras were introduced in the mathematical literature to study deformation theory by Nijenhuis [45] and Fröhlicher [46] in the 1950's. In physics, superalgebras appeared first in the 1970's when J. Wess and B. Zumino used these objects to construct transformations between bosonic and fermionic states. Using normal Lie algebras such a transformation cannot be designed because the generator which connects a bosonic and a fermionic state is itself a fermion, hence its density only comprises an odd amount of fermionic fields. Therefore, it is not possible to extract the essential information to build up a Lie algebra commutator between two fermionic states from the relations between the fields and the corresponding canonical momenta [8, 9].

Two decades later, in 1986, Kulish [47] investigated solutions of the graded Yang-Baxter equations and thereby for the first time constructed superspin chains based on the general linear and the orthosymplectic supergroup. Subsequently it was discovered that superalgebras also play a role in the theory of strongly correlated electrons. It can be shown that the $t - J$ -model, as introduced by Zhang and Rice in 1988 [48], is supersymmetric for the value $J = 2t$, that is, its Hamiltonian commutes with all generators of a specific Lie superalgebra. This allows for the construction of the corresponding spin chain using the Quantum Inverse Scattering Method and its subsequent solution by means of the Algebraic Bethe Ansatz [49].

This section is organized as follows: In subsection 2.1, we will provide the necessary definitions required for the construction of integrable models in part II which will be followed by two examples in 2.2, where we will discuss briefly the Lie superalgebras $gl(n|m)$ and $sl(2|1)$. The latter is one of the most important superalgebras in the context of this thesis. It turns out that two specific bases are very well suited for the following discussions, namely the Cartan-Weyl and the Chevalley basis which will be defined in 2.3. Consecutively, in subsection 2.4 we will discuss shortly the representation theory for superalgebras which can be quite different compared to the representation theory for Lie algebras, and mention the concept of quantum deformations in 2.5. The last subsection will deal with the modifications of the QISM which are necessary for the construction of integrable models based on superalgebras in 2.6.

2.1 Definitions

We shortly list some necessary definitions. For a full mathematical discussion of superalgebras see [50–52] which also provides the basis for this subsection.

Definition 1. Let V be a vector space over a field K . A \mathbb{Z}_2 -gradation (or, grading) of V is a decomposition of V such that

$$V = V_0 \oplus V_1. \quad (\text{I.15})$$

In this case V is said to be \mathbb{Z}_2 -graded. The elements of V_0 (V_1) are called even (odd).

The gradation of a \mathbb{Z}_2 -graded vector space defines a natural decomposition for its elements:

$$\forall v \in V \quad \exists v_0 \in V_0, v_1 \in V_1 : v = v_0 + v_1. \quad (\text{I.16})$$

The component v_0 (v_1) is called *even* (*odd*) component of v . Elements which fulfill $v \in V_0$ ($v \in V_1$) are called *homogeneous*. Homogeneous elements have *degree* $\deg(v) = 0$ if $v \in V_0$ and $\deg(v) = 1$ if $v \in V_1$.

Definition 2. Let V and W be two \mathbb{Z}_2 -graded vector spaces over the same field K . The graded tensor product $V \otimes W$ is also a \mathbb{Z}_2 -graded vector space with the natural grading

$$(V \otimes W)_\gamma = \bigoplus_{\alpha+\beta=\gamma} (V_\alpha \otimes W_\beta), \quad \gamma \in \mathbb{Z}_2. \quad (\text{I.17})$$

Definition 3. Let A be an algebra over a field K . A is said to be a superalgebra, if

$$A = A_0 \oplus A_1 \quad (\text{I.18})$$

$$A_\alpha A_\beta \subset A_{\alpha+\beta} \quad \forall \alpha, \beta \in \mathbb{Z}_2 \quad (\text{I.19})$$

Definition 4. A left ideal I of a superalgebra A is a subalgebra such that $ax \in I \quad \forall a \in A, x \in I$. A subalgebra of a superalgebra is a subset which is also an algebra. A graded subalgebra (ideal) of a superalgebra is a subalgebra (ideal) which is also a graded subspace of the underlying vector space.

For every superalgebra, A_0 is a subalgebra of A .

Definition 5. Let A and B be two superalgebras. The graded tensor product $A \otimes B$ is defined by the multiplication

$$(a \otimes b)(a' \otimes b') = (-1)^{\beta\alpha'} (aa') \otimes (bb') \quad (\text{I.20})$$

$$\forall a \in A, b \in B_\beta, a' \in A'_\alpha, b' \in B; \quad \beta, \alpha' \in \mathbb{Z}_2.$$

on the graded vector space $A \otimes B$.

There is a unique linear map

$$s : A \otimes B \rightarrow B \otimes A \quad (\text{I.21})$$

such that

$$s(a \otimes b) = (-1)^{\alpha\beta} b \otimes a \quad \forall a \in A_\alpha, b \in B_\beta; \alpha, \beta \in \mathbb{Z}_2. \quad (\text{I.22})$$

Thus, the two tensor products $A \otimes B$ and $B \otimes A$ are canonically isomorphic.

Definition 6. Let $\mathcal{L} = \mathcal{L}_0 \oplus \mathcal{L}_1$ be a superalgebra and denote its multiplication by $[\cdot, \cdot]$. \mathcal{L} is said to be a Lie superalgebra if

$$[a, b] = -(-1)^{\alpha\beta} [b, a] \quad (\text{I.23})$$

$$(-1)^{\gamma\alpha} [a, [b, c]] + (-1)^{\alpha\beta} [b, [c, a]] + (-1)^{\beta\gamma} [c, [a, b]] = 0 \quad (\text{I.24})$$

for all $a \in \mathcal{L}_\alpha, b \in \mathcal{L}_\beta, c \in \mathcal{L}_\gamma$ and $\alpha, \beta, \gamma \in \mathbb{Z}_2$.

Equation (I.23) defines the *super Lie product*: For even as well as mixed a, b , it is identical to the Lie product. When thinking of matrices, it is in these cases identical to the commutator while for both a, b odd, it is the *anti-commutator*. The second of the above equations, (I.24), can be read as a graded version of the Jacobi identity.

It can be easily seen that the odd part \mathcal{L}_1 of a Lie superalgebra is the carrier space for a representation of the even part \mathcal{L}_0 which is itself a Lie algebra [52] in the usual sense of representations which is called *representation of \mathcal{L}_0 on \mathcal{L}_1* . This fact allows for a simple way to construct Lie superalgebras: Choose a Lie algebra \mathcal{L}_0 and specify a representation Γ of \mathcal{L}_0 . Then, the direct sum $A = \mathcal{L}_0 \oplus \Gamma$ is a graded vector space provided the elements of \mathcal{L}_0 are defined as even and the ones of Γ as odd. However, it is difficult to construct a super Lie product consistent with the defining equations, (I.23) and (I.24) [52].

Definition 7. A Lie superalgebra \mathcal{L} is said to be simple if there is no graded ideal different from $\{0\}$ and \mathcal{L} and if, moreover, $[\mathcal{L}, \mathcal{L}] \neq 0$.

Definition 8. A simple Lie superalgebra \mathcal{L} is called classical if the representation of the even part on the odd part is either irreducible or completely reducible.

Let us conclude this subsection with two remarks:

- The equations (I.23) and (I.24) indicate the difference to Lie algebras where the multiplication is defined to be the commutator and to fulfill the normal Jacobi identity. Nevertheless, most of the definitions are quite similar compared to the ones for Lie algebras.
- All definitions can be generalized to more complex gradings like \mathbb{Z} . In this case, all direct sums run over all elements of the chosen gradings instead of just the two elements of \mathbb{Z}_2 .

2.2 Examples: $gl(n|m)$ and $sl(2|1)$

In the following, we discuss some basic aspects of the Lie superalgebras $\mathcal{L} = gl(n, m)$ and $\mathcal{L} = sl(2|1)$ over the field of complex numbers.

2.2.1 The general Lie superalgebra $gl(n|m)$

For the *general Lie superalgebra* $gl(n|m)$, the *even* elements (when thinking of matrices) are of the form

$$M = \begin{pmatrix} A & 0 \\ 0 & D \end{pmatrix} \quad (\text{I.25})$$

where A and D are $n \times n$ and $m \times m$ matrices. The odd elements look like

$$M = \begin{pmatrix} 0 & B \\ C & 0 \end{pmatrix} \quad (\text{I.26})$$

where B and C are $n \times m$ and $m \times n$ matrices, respectively. There are no restrictions on the block matrices A, B, C, D at all, similar to the elements of the general Lie algebra $gl(n)$.

All superalgebras which appear in this thesis are subsets of $gl(n|m)$. Having constructed the general Lie superalgebra, we can now define a linear form analogously to the trace for ordinary matrices:

Definition 9. *Let V be a \mathbb{Z}_2 graded vector space and consider the linear map*

$$\gamma : V \rightarrow V, \quad \gamma(x) = (-1)^\xi x \quad (\text{I.27})$$

if $x \in V_\xi$ and $\xi \in \mathbb{Z}_2$. Define a linear form on $gl(n|m)$ by

$$\text{str}(A) = \text{tr}(\gamma A). \quad (\text{I.28})$$

The linear form str is called supertrace.

2.2.2 The special linear Lie superalgebra $sl(2|1)$

For the *special linear Lie superalgebra* $sl(2|1)$, the *even* elements are of the form

$$M = \begin{pmatrix} A & 0 \\ 0 & D \end{pmatrix} \quad (\text{I.29})$$

where A is a 2×2 matrix and D is a number fulfilling $\text{str}(M) = \text{tr}(A) - D = 0$. Thus, there are two different kinds of matrices in the even part $\mathcal{L}_0 = sl(2|1)_0$:

(i) Elements with $\text{tr}(A) = 0$ and $D = 0$. These elements form a Lie subalgebra isomorphic to $sl(2)$, therefore it is 3-dimensional. Note, there is no complement in which the roles of A and D are interchanged since D is just a number.

(ii) Multiples of

$$\begin{pmatrix} 1/2E_2 & 0 \\ 0 & 1 \end{pmatrix} \quad (\text{I.30})$$

where E_n is the $n \times n$ unit matrix. Such elements form a one-dimensional Abelian Lie algebra, thus isomorphic to $gl(1)$.

Hence, \mathcal{L}_0 is the direct sum

$$sl(2|1)_0 \cong sl(2) \oplus gl(1) \quad (\text{I.31})$$

and has dimension $\dim(sl(2|1)_0) = 3 + 1 = 4$. The odd elements consist of

$$M = \begin{pmatrix} 0 & B \\ C & 0 \end{pmatrix} \quad (\text{I.32})$$

where B and C are 2×1 and 1×2 matrices with no additional constraint. Therefore the dimension of the odd part is given by $\dim(sl(2|1)_1) = 4$. In summary, we have shown that $sl(2|1)$ is a $4 + 4 = 8$ dimensional Lie superalgebra.

Lie (super-)algebras alternatively can be characterized by specifying the (super-)commutator-relations for their generators. Since $sl(2|1)_0$ decomposes as eq. (I.31), the even generators are given by the generators of $sl(2)$ which we will denote as Q_m , $m = 1, 2, 3$ ('isospin') together with one additional $gl(1)$ generator denoted by B ('baryon number'). The odd generators are designated by V_{\pm} and W_{\pm} . They are $sl(2) - 1/2$ spinors with baryon number $+1/2$ and $-1/2$. As usual, we can define creation and annihilation operators for the isospin, $Q_{\pm} = Q_1 \pm iQ_2$. The commutation relations of these generators are given by

$$\begin{aligned} [Q_3, Q_{\pm}] &= \pm Q_{\pm}, & [Q_+, Q_-] &= 2Q_3, & [B, Q_{\pm}] &= [B, Q_3] = 0 \\ [Q_3, V_{\pm}] &= \pm \frac{1}{2}V_{\pm}, & [Q_3, W_{\pm}] &= \pm \frac{1}{2}W_{\pm}, & [Q_{\pm}, V_{\mp}] &= V_{\pm}, & [Q_{\pm}, W_{\mp}] &= W_{\pm} \\ [Q_{\pm}, V_{\pm}] &= 0, & [Q_{\pm}, W_{\pm}] &= 0, & [B, V_{\pm}] &= \frac{1}{2}V_{\pm}, & [B, W_{\pm}] &= -\frac{1}{2}W_{\pm} \\ [V_{\pm}, V_{\pm}] &= [V_{\pm}, V_{\mp}] = [W_{\pm}, W_{\pm}] = [W_{\pm}, W_{\mp}] = 0 \\ [V_{\pm}, W_{\pm}] &= \pm Q_{\pm}, & [V_{\pm}, W_{\mp}] &= -Q_3 \pm B. \end{aligned} \quad (\text{I.33})$$

More detailed discussions about $sl(2|1)$ can be found in [50–57].

2.3 Cartan-Weyl and Chevalley basis

For the subsequent discussion of the representation theory as well as the construction of quantum deformations, it is useful to consider different bases for Lie superalgebras. To this extent, we define the *Cartan subalgebra* \mathcal{H}_s of a classical simple complex Lie superalgebra \mathcal{L} to be the largest Abelian subalgebra, i.e.

$$[h, h'] = 0 \quad \forall h, h' \in \mathcal{H}_s. \quad (\text{I.34})$$

The dimension of the Cartan subalgebra is called the *rank* l of $\mathcal{L} = \mathcal{L}_0 \oplus \mathcal{L}_1$. As an example, $\text{rank}(sl(2|1)) = 2$.

Consider now linear functionals on the Cartan subalgebra, $\alpha : \mathcal{H}_s \rightarrow \mathbb{C}$. α is called *root* if there is at least one element $a_\alpha \in \mathcal{L}$ such that

$$[h, a_\alpha] = \alpha(h)a_\alpha \quad \forall h \in \mathcal{H}_s. \quad (\text{I.35})$$

The root α is called *even* (*odd*), if $a_\alpha \in \mathcal{L}_0$ ($a_\alpha \in \mathcal{L}_1$). The set of all elements $a_\alpha \in \mathcal{L}$ which fulfill (I.35) for a given root is called the *root subspace* \mathcal{L}_α corresponding to the root α .

The definition of roots allows for the construction of the *Cartan-Weyl basis* for an n -dimensional Lie superalgebra \mathcal{L} . Instead of characterizing a Lie superalgebra by means of the super-commutation relations for its generators, the first l elements of the Cartan-Weyl basis are given by the elements of the Cartan subalgebra \mathcal{H}_s . The $n - l$ missing elements are associated with the elements a_α corresponding to the non-zero roots according to (I.35). Hence, the commutation relations for the generators within this basis read

$$[h, h'] = 0, \quad (\text{I.36})$$

$$[h, a_\alpha] = \alpha(h)a_\alpha, \quad (\text{I.37})$$

$$[a_\alpha, a_\beta] = \begin{cases} N_{\alpha\beta}a_{\alpha+\beta} & \text{if } \alpha + \beta \text{ is a root and } \alpha \neq -\beta, \\ \sum_h \tilde{N}_{\alpha\beta}^h h & \text{if } \alpha = -\beta, \\ 0 & \text{if } \alpha + \beta \text{ is not a root.} \end{cases} \quad (\text{I.38})$$

Here $N_{\alpha\beta}$ and $\tilde{N}_{\alpha\beta}^h$ are some constants. The first two of these relations are obvious due to the definitions, the third one follows immediately from the graded Jacobi identity,

$$[h, [a_\alpha, a_\beta]] = (\alpha(h) + \beta(h))[a_\alpha, a_\beta] \quad (\text{I.39})$$

for $h \in \mathcal{H}_s$ with $\text{deg}(h) = 0$. Thus, by constructing the Cartan-Weyl basis we have

shown that a Lie superalgebra can be decomposed into the Cartan subalgebra and the sum of the root subspaces,

$$\mathcal{L} = \mathcal{H}_s \oplus_{\alpha \text{ root}} \mathcal{L}_\alpha. \quad (\text{I.40})$$

Similar to Lie algebras, roots are called *positive* or *negative*. To define this notion properly, note that each simple classical Lie superalgebra \mathcal{L} with Cartan subalgebra \mathcal{H}_s can be decomposed,

$$\mathcal{L} = \mathcal{N}^+ \oplus \mathcal{H}_s \oplus \mathcal{N}^- \quad (\text{I.41})$$

where $[\mathcal{H}_s, N^\pm] \subset N^\pm$ and $\dim(N^+) = \dim(N^-)$. A root is said to be positive (negative) if $L_\alpha \cap \mathcal{N}^+ \neq \emptyset$ ($L_\alpha \cap \mathcal{N}^- \neq \emptyset$).

To make further progress, we define a classical simple Lie superalgebra to be *basic* if it possesses a non-degenerate bilinear supersymmetric consistent invariant form $B(\cdot, \cdot)$. Using this bilinear form we can associate each root α to a unique element $h_\alpha \in \mathcal{H}_s$ by demanding

$$B(h, h_\alpha) = \alpha(h) \quad \forall h \in \mathcal{H}_s. \quad (\text{I.42})$$

In a similar way, a quadratic form for the roots themselves can be constructed,

$$\langle \alpha, \beta \rangle = B(h_\alpha, h_\beta). \quad (\text{I.43})$$

A non-zero positive root of a basic classical simple Lie superalgebra is called *simple* if it cannot be decomposed into a sum of two other positive roots. For the Lie superalgebras investigated in this thesis, the number of positive roots matches the rank of the Lie superalgebra.

Another important quantity is the *Cartan matrix* A of a basic classical simple Lie superalgebra. Its matrix elements read

$$A_{jk} = \frac{2\langle \alpha_j, \alpha_k \rangle}{\langle \alpha_j, \alpha_j \rangle}, \quad j = 1, 2, \dots, l \quad (\text{I.44})$$

if $\langle \alpha_j, \alpha_j \rangle \neq 0^4$ for the simple roots α_j . The matrix elements then read $A_{jj} = 2$ and $A_{jk} \in \{0, -1, -2\}$ for $j \neq k$.

Finally, we can construct the *Chevalley basis*. This basis serves as a starting point for the subsequent construction of quantum deformations. In the Chevalley basis, a basic classical simple Lie superalgebra is described in terms of rescaled elements of the Cartan subalgebra (assuming $\langle \alpha_j, \alpha_j \rangle \neq 0^5$),

⁴Otherwise, one of the α_j 's in the denominator can be replaced by any of the roots $\alpha_{j'}$ such that $\langle \alpha_j, \alpha_{j'} \rangle \neq 0$. Then, the matrix elements can be quite different [52].

⁵Otherwise, one of the α_j 's in the denominator can be replaced by any of the roots $\alpha_{j'}$ like above. Then the factor 2 in the numerator has to be dropped.

$$H_j = \frac{2}{\langle \alpha_j, \alpha_j \rangle} h_{\alpha_j}, \quad (\text{I.45})$$

where h_{α_j} is the element in the Cartan subalgebra corresponding to the simple root α_j in the sense defined above, and the *raising and lowering operators* corresponding to the simple roots,

$$e_i = a_{\alpha_i} \quad (\text{I.46})$$

$$f_i = a_{-\alpha_i}, \quad (\text{I.47})$$

where a_α is the element used to define the root α (cf. (I.35)). The super Lie products for the generators within this basis read

$$\begin{aligned} [H_i, H_j] &= 0, & [e_i, f_j] &= \delta_{ij} H_j, \\ [H_i, e_j] &= A_{ij} e_j, & [H_i, f_j] &= -A_{ij} f_j, \end{aligned} \quad (\text{I.48})$$

where $A = (A_{ij})$ denote the elements of the Cartan matrix. The super Lie products for the raising and lowering operators can be read off from those for the Cartan-Weyl basis. Up to now, our basis consists of $3l$ with $l = \text{rank}(\mathcal{L})$ elements. The remaining degrees of freedom are fixed by the repeated commutation of the generators e_i, f_i [58] by means of the *Serre relations*,

$$\begin{aligned} \text{ad}(e_i)^{1-\tilde{A}_{ij}}(e_j) &= 0, \\ \text{ad}(f_i)^{1-\tilde{A}_{ij}}(f_j) &= 0 \end{aligned} \quad (\text{I.49})$$

where the matrix \tilde{A}_{ij} can be constructed from the Cartan matrix by replacing the non-vanishing positive elements in the row with $a_{ii} = 0$ by -1 [59]. The adjoint operator $\text{ad}(e_i)$ is defined by

$$\text{ad}(e_i)(a) = [e_i, a] \quad \forall a \in \mathcal{L}. \quad (\text{I.50})$$

The adjoint operators form an irreducible representation of each Lie superalgebra which will be discussed in the next subsection.

2.4 Representation theory

The superspin chains and vertex models discussed in the second part of this thesis are built using *representations* of several Lie superalgebras as carrier space for the models' local Hilbert spaces. Since for Lie superalgebras, the representation theory is more involved than for Lie algebras, we present in this subsection the main concepts and results of the representation theory for Lie superalgebras followed by a discussion of some irreducible representations of $sl(2|1)$ and their properties. The definitions and

theorems presented here can be found with detailed commentaries in [50, 52].

2.4.1 Definitions

The basic definitions read almost identically compared to the representation theory for Lie algebras except for the notion of grading.

Definition 10. *A graded representation of a Lie superalgebra $\mathcal{L} = \mathcal{L}_0 \oplus \mathcal{L}_1$ is a map*

$$\Gamma : \mathcal{L} \rightarrow gl(d_0|d_1) \quad (\text{I.51})$$

with finite d_0, d_1 such that

$$(i) \quad \forall a, b \in \mathcal{L} \text{ and } \alpha, \beta \in \mathbb{C}: \Gamma(\alpha a + \beta b) = \alpha \Gamma(a) + \beta \Gamma(b),$$

$$(ii) \quad \forall a, b \in \mathcal{L}: \Gamma([a, b]) = [\Gamma(a), \Gamma(b)]$$

(iii) Γ preserves the degree of the elements, that is,

(a) if $a \in \mathcal{L}_0$:

$$\Gamma(a) = \begin{pmatrix} \Gamma_{00}(a) & 0 \\ 0 & \Gamma_{11}(a) \end{pmatrix}, \quad (\text{I.52})$$

where $\Gamma_{00}(a)$ and $\Gamma_{11}(a)$ are $d_0 \times d_0$ and $d_1 \times d_1$ -matrices, respectively;

(b) if $a \in \mathcal{L}_1$:

$$\Gamma(a) = \begin{pmatrix} 0 & \Gamma_{01}(a) \\ \Gamma_{10}(a) & 0 \end{pmatrix}, \quad (\text{I.53})$$

where $\Gamma_{01}(a)$ and $\Gamma_{10}(a)$ are $d_0 \times d_1$ and $d_1 \times d_0$ -matrices.

The representation Γ is said to be $d_0 + d_1$ -dimensional.

The super Lie product for the elements of a representation is given by

$$[\Gamma(a), \Gamma(b)] = \Gamma(a)\Gamma(b) - (-1)^{\deg(a)\deg(b)}\Gamma(b)\Gamma(a) \quad (\text{I.54})$$

if a and b are homogeneous elements of \mathcal{L} . Thus, in accordance to the remark above, it is identical to the commutator for even and mixed elements whereas it is the anti-commutator for odd elements.

Each representation provides us with a *carrier space* which we will use in the second part of this thesis in order to construct superspin chains. The carrier space can be seen as the graded vector space the representation can act on. For the construction, given a $d_0 + d_1$ -dimensional representation Γ , let the carrier space V^c be a $d_0 + d_1$ dimensional graded vector space⁶ $V^c = V_0^c \oplus V_1^c$. We demand the even (odd) part

⁶Sometimes, the carrier space is additionally demanded to have an inner product. For our purpose in this section, this is not necessary.

to be d_0 (d_1)-dimensional. Consider now the bases ψ_j ($j = 1, \dots, d_0$) of V_0^c and ψ_j ($j = d_0 + 1, \dots, d_0 + d_1$) of V_1^c . The action of each element $a \in \mathcal{L}$ in the representation Γ on the basis ψ_j is mediated by a linear operator $\Phi(a)$ via

$$\Phi(a)\psi_j = \sum_{k=1}^{d_0+d_1} \Gamma(a)_{kj} \psi_k. \quad (\text{I.55})$$

Thus, the set of operators $\Phi(a)$ itself form a Lie superalgebra isomorphic to \mathcal{L} .

Two representations Γ and Γ' are said to be *equivalent* if there is a matrix S with

$$S = \begin{pmatrix} S_0 & 0 \\ 0 & S_1 \end{pmatrix} \quad (\text{I.56})$$

where S_0 and S_1 are $d_0 \times d_0$ and $d_1 \times d_1$ -dimensional non-singular submatrices such that

$$\Gamma'(a) = S^{-1}\Gamma(a)S \quad \forall a \in L. \quad (\text{I.57})$$

Definition 11. A reducible graded representation of a Lie superalgebra \mathcal{L} is a graded representation of \mathcal{L} for which the carrier space V^c possesses a proper invariant subspace $V^{c'}$ under the action of $\{\Phi(a), a \in \mathcal{L}\}$.

An irreducible graded representation of \mathcal{L} is a graded representation which is not reducible.

A completely reducible graded representation of \mathcal{L} is a graded representation for which the carrier space V^c can be decomposed into a direct sum of graded subspaces which are all invariant under the action of $\{\Phi(a), a \in \mathcal{L}\}$ and none of which possess a proper invariant subspace.

An example of an irreducible graded representation is the *adjoint representation*: Let $\mathcal{L} = \mathcal{L}_0 \oplus \mathcal{L}_1$ be a Lie superalgebra whose even and odd parts are d_0 and d_1 -dimensional, respectively, and let $a_1, \dots, a_{d_0+d_1}$ be a basis consisting of homogeneous elements. To each $a \in \mathcal{L}$ we can assign a $(d_0 + d_1) \times (d_0 + d_1)$ matrix $\text{ad}(a)$ via

$$[a, a_j] = \sum_{k=1}^{d_0+d_1} \{\text{ad}(a)\}_{kj} a_k. \quad (\text{I.58})$$

The set of matrices $\{\text{ad}(a), a \in \mathcal{L}\}$ forms an irreducible graded representation which is called the *adjoint representation of \mathcal{L}* .

Now, we introduce the concepts of *weights*. This will help us to point out one major difference to the representation theory of Lie algebras. To this purpose, let us remark that for any given graded representation Γ of a basic classical simple Lie superalgebra, a similarity transformation can be applied to diagonalize all representation matrices

of the Cartan subalgebra, $\Gamma(h)$, simultaneously. Therefore, we can assume that this transformation has already been carried out. It follows that there is a basis of the carrier space consisting of eigenvectors $\psi(\lambda)$ with

$$\Phi(h)\psi(\lambda) = \lambda(h)\psi(\lambda) \quad \forall h \in \mathcal{H}_s. \quad (\text{I.59})$$

Here, λ is a linear functional defined on the Cartan subalgebra and yields the eigenvalues of the operators $\Phi(h)$, $h \in \mathcal{H}_s$. The functional $\lambda(h)$ is referred to as *weight*. The dimension of the subspace spanned by $\psi(\lambda)$ for a fixed weight, $m(\lambda)$, is called *multiplicity*. If $m(\lambda) = 1$, the weight is said to be *simple*.

If λ is a weight of a given graded representation and α any root then $\lambda + \alpha$ is also a weight of the same representation if α satisfies $\Phi(a_\alpha)\psi(\lambda) \neq 0$ (for a_α see (I.35)). If instead Λ is a weight such that $\Phi(a_\alpha)\psi(\lambda) = 0$ for every positive root α , then Λ is called *highest weight of the representation*.

Definition 12. *A typical graded irreducible representation ('irrep') Γ with highest weight Λ of a basic classical simple Lie superalgebra \mathcal{L} is an irreducible graded representation such that any reducible graded representation Γ' of \mathcal{L} with the same highest weight can be written as the direct sum of Γ and some other graded representations. Otherwise, it is called atypical.*

Hence, if there exists an atypical graded irreducible representation with highest weight Λ , there is also at least one graded reducible representation with the same highest weight which is not completely reducible, in contrast to the situation for Lie algebras.

Theorem 1. *Let Γ be a graded irreducible representation of a basic classical simple Lie superalgebra, and let Λ be the highest weight of Γ . Γ is atypical if and only if*

$$\langle \Lambda + \rho, \alpha \rangle = 0 \quad (\text{I.60})$$

for some positive root α such that 2α is not a root and

$$\rho = \frac{1}{2} \sum_{\beta \in \Delta_0^+} \beta - \frac{1}{2} \sum_{\beta \in \Delta_0^-} \beta \quad (\text{I.61})$$

where Δ_0^+ (Δ_0^-) is the set of positive even (odd) roots.

Finally, Casimir operators can be defined in the same way as for Lie algebras.

Definition 13. *Let X_j be a set of generators of a simple Lie superalgebra \mathcal{L} in a matrix representation. We can write their commutation relation in the following way,*

$$[X_i, X_j] = \sum_k C_{ij}^k X_k \quad (\text{I.62})$$

with some structure constants C_{ij}^k . Let us also define a metric by

$$g_{ij} = \text{str}(X_i X_j). \quad (\text{I.63})$$

Then the operators constructed by

$$K_n = g_{s_1 \dots s_n} X^{s_1} \dots X^{s_n} \quad (\text{I.64})$$

with

$$g_{s_1 \dots s_n} = \text{str}(X_{s_1} \dots X_{s_n}) \quad \text{and} \quad X^s = g^{sj} X_j \quad (\text{I.65})$$

are Casimir operators [53], that is, they commute with all the generators.

2.4.2 Example: $sl(2|1)$

The irreducible representations of $sl(2|1)$ can be constructed by studying how the generators act on the elements of the carrier space. This procedure yields a labeling of the irreducible representations in terms of the eigenvalue of the isospin $j = 0, 1/2, 1, \dots$ and baryon number $b \in \mathbb{C}$ as well as the states included in the representation under consideration [53]. It can be shown that all (b, j) -irreps of $sl(2|1)$ can be decomposed into irreps of $su(2)$ with spin j for which the baryon number operator B takes the value b . Such an $su(2)$ -irrep will be denoted by ρ_j^b .

Details for the construction of the irreps can be found in [53–55]. Let us briefly discuss the most relevant irreducible representations in the context of this work.

- (a) $j = 0$: For any value of b , this is the trivial one-dimensional representation.
- (b) $b = j$: This irrep is $4j + 1$ -dimensional and atypical. Its decomposition reads

$$(j, j) = \rho_j^j \oplus \rho_{j-1/2}^{j+1/2}. \quad (\text{I.66})$$

In the special case $j = 1/2$, this representation is the fundamental representation of $sl(2|1)$ and will be denoted by $\mathbf{3} \equiv (1/2, 1/2)$.

- (c) $b = -j$: Like the previous irrep, $(-j, j)$ is $4j + 1$ -dimensional and also atypical with decomposition

$$(-j, j) = \rho_j^{-j} \oplus \rho_{j-1/2}^{-j-1/2}. \quad (\text{I.67})$$

These representations are duals of the (j, j) -representations. In the special case $j = 1/2$, this representation will thus be denoted by $\bar{\mathbf{3}} \equiv (-1/2, 1/2)$.

- (d) In the general case $b \neq \pm j$ and $j > 0$, this irrep is $8j$ -dimensional. Its decomposi-

tion reads

$$(b, j) = \rho_j^b \oplus \rho_{j-1/2}^{b+1/2} \oplus \rho_{j-1/2}^{b-1/2} \oplus \rho_{j-1}^b. \quad (\text{I.68})$$

These irreps are the typical ones since typicality requires $b \neq j$ [20].

The two independent Casimir operators, \mathcal{K}_1 and \mathcal{K}_2 , can be constructed by the introduction of new generators

$$U_1 = V_+, \quad U_2 = V_-, \quad U_3 = W_+, \quad U_4 = W_-, \quad (\text{I.69})$$

see (I.33). The Casimirs read

$$\begin{aligned} \mathcal{K}_1 &= \mathbf{Q}^2 - B^2 + \frac{1}{2}UC_4U \\ \mathcal{K}_2 &= BK_1 + \frac{1}{2}BUC_4U + \frac{1}{6}U\mathbf{Q}\varepsilon_4\tau_4C_4U + \frac{1}{12}U\varepsilon_4\tau_4C_4U\mathbf{Q}, \end{aligned} \quad (\text{I.70})$$

using the notation

$$C_4 = \begin{pmatrix} 0 & C \\ C & 0 \end{pmatrix}, \quad C = \begin{pmatrix} 0 & 1 \\ -1 & 0 \end{pmatrix}, \quad \varepsilon_4 = \begin{pmatrix} E_2 & 0 \\ 0 & E_2 \end{pmatrix}, \quad (\tau_4)_m = \begin{pmatrix} \sigma^m & 0 \\ 0 & \sigma^m \end{pmatrix}, \quad (\text{I.71})$$

where σ_m are the usual Pauli-matrices and E_2 the 2×2 unit matrix. For typical irreps, the eigenvalues of the Casimirs read

$$K_1 = j^2 - b^2, \quad K_2 = b(j^2 - b^2), \quad (\text{I.72})$$

while for the atypical ones (i.e. $b = \pm j$) both Casimirs are zero. In particular they are degenerate, thus they cannot be used to specify the irrep in contrast to the situation for Lie algebras.

We will use the carrier space of the representations $\mathfrak{3}$ and $\bar{\mathfrak{3}}$ in part 2 of this thesis as local Hilbert space of a superspin chain. Thus, it is useful to consider the decomposition of the tensor product $(\mathfrak{3} \otimes \bar{\mathfrak{3}})^L$ with the system size L . For $L = 1, 2$, it reads [20]

$$\begin{aligned} \mathfrak{3} \otimes \bar{\mathfrak{3}} &= (0, 0) \oplus (0, 1) \\ (\mathfrak{3} \otimes \bar{\mathfrak{3}})^2 &= (0, 0) \oplus 4(0, 1) \oplus (0, 2) \oplus \left(\frac{1}{2}, \frac{3}{2}\right) \oplus \left(-\frac{1}{2}, \frac{3}{2}\right) \oplus \left(0, -\frac{1}{2}, \frac{1}{2}, 0\right). \end{aligned} \quad (\text{I.73})$$

The representation $(0, -1/2, 1/2, 0)$ is atypical and reducible, but not decomposable. It can be written as a semi-direct sum [54, 60],

$$\left(0, -\frac{1}{2}, \frac{1}{2}, 0\right) = (0, 0) \oplus_s \left(\frac{1}{2}, \frac{1}{2}\right) \oplus_s \left(-\frac{1}{2}, \frac{1}{2}\right) \oplus_s (0, 0). \quad (\text{I.74})$$

The notion of the semi-direct sum in this representation is depicted graphically by

means of a quiver diagram [61] in fig. 2. This representation and its generalization are discussed in [20]. A more detailed discussion of the representation theory of $sl(2|1)$ can be found in [62].

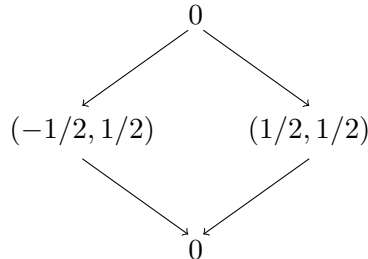


Figure 2: Quiver diagram for the indecomposable representation $(0, -1/2, 1/2, 0)$ of $sl(2|1)$. This picture indicates the notion of the semi-direct sum: The indecomposable contains a trivial representation 0 at the bottom which is an invariant subspace of the indecomposable. Next, there are two three-dimensional submodules which are again invariant subspaces modulo the trivial representation, and finally, on top there is a second one-dimensional trivial representation which is an invariant subspace modulo all the others [20].

2.5 Quantum deformations

In this subsection, we briefly introduce the notion of *quantum deformations* of Lie (super-) algebras. Originally, those structures arose in the Quantum Inverse Scattering Method when investigating several properties of the Yang-Baxter equation [63, 64]. One famous example where quantum deformations of Lie algebras play a crucial role is the Heisenberg XXZ spin chain [65] which has a $U_q[su(2)]$ -symmetry. Here, the deformation parameter is directly related to the anisotropy in the interaction.

Intuitively, the terminus *quantum* can be understood as deforming something commutative (like observables in classical physics) into something *non*-commutative (like observables in quantum mechanics). In our context, the object being deformed can be thought of as the algebra of functions that map the Lie superalgebra \mathcal{L} under consideration onto the underlying field. This object is commutative by definition. For more details see e.g. [59, 66].

2.5.1 Construction

There are several ways to construct quantum deformations of Lie superalgebras including the following three,

- (i) deformation of the super-commutation relations [59, 66],
- (ii) solution of the Yang-Baxter equation [67],
- (iii) direct construction of the Hopf algebra structure [66].

Here, we utilize the first method. To this extent, we use the Chevalley basis (I.48) together with the Serre relations (I.49) of a Lie superalgebra \mathcal{L} . The corresponding quantum deformation $U_q[\mathcal{L}]$ has an analogous set of operators denoted by H_i, X_i, Y_i where the commutation relations are slightly changed,

$$\begin{aligned} [H_i, H_j] &= 0, & [X_i, Y_j] &= \delta_{ij} \frac{\sin(\gamma H_i)}{\sin(\gamma)}, \\ [H_i, X_j] &= a_{ij} X_j, & [H_i, Y_j] &= -a_{ij} Y_j, \end{aligned} \quad (\text{I.75})$$

where a_{ij} denote the elements of the Cartan matrix. Also the Serre relations get deformed,

$$\text{ad}_q(X_i)^{1-\tilde{a}_{ij}}(X_j) = 0, \quad \text{ad}_q(Y_i)^{1-\tilde{a}_{ij}}(Y_j) = 0, \quad (\text{I.76})$$

with $q = \exp(i\gamma)$ parametrizing the deformation. The q -deformed adjoint operator is defined by a deformed supercommutator,

$$\text{ad}_q(X)(Y) \equiv [X, Y]_q \equiv XY - q(-1)^{\deg(X)\deg(Y)} YX \quad (\text{I.77})$$

The equations (I.75) and (I.76) define the quantum deformed Lie superalgebra $U_q[\mathcal{L}]$ [59]. Obviously, the limit $q \rightarrow 1$ yields the original superalgebra \mathcal{L} . Note, this mathematical object is neither a Lie (super-) algebra nor a group - despite its name, *quantum group* - but rather a *Hopf algebra*. A detailed discussion about Hopf algebras can be found in [66].

2.5.2 Example: $U_q(sl(2|1))$

As an example, we consider the quantum deformation of $sl(2|1)$. We work with the following Cartan matrix [59, 68]⁷,

$$A = \begin{pmatrix} 0 & 1 \\ 1 & -2 \end{pmatrix}. \quad (\text{I.78})$$

For convenience we rewrite the elements of the Cartan subalgebra,

$$k_i^2 \equiv q^{H_i}. \quad (\text{I.79})$$

The commutation relation then read

$$k_i k_j = k_j k_i, \quad k_i X_j = q^{a_{ij}} X_j k_i \quad (\text{I.80})$$

⁷Since the Cartan matrix is not unique, we could have equivalently worked with another choice. The results are identical up to an appropriate transformation.

$$k_i Y_j = q^{-a_{ij}} Y_j k_i, \quad [X_i, Y_j] = \delta_{ij} \frac{k_i^2 - k_i^{-2}}{q - q^{-1}}. \quad (\text{I.81})$$

Together with the deformed Serre relations, this defines the quantum deformed Lie superalgebra $U_q[sl(2|1)]$.

Let us briefly mention the impact of quantum deformations on the representation theory [21]. In general, quantum deformations lead to a break of degeneracies present in some $sl(2|1) - (b, j)$ -multiplets. For example, the octet $(0, 1)$ splits into two doublets with $b = 0$ and $s_3 = \pm 1$ (s_3 being the eigenvalue of the generator Q_3) and $s_3 = 0$ together with quartets $b = \pm 1/2$ and $s_3 = \pm 1/2$. The states included in such a subset will be denoted by $|b, s_3\rangle$. Thus, the octet decomposes in the following way,

$$(0, 1) \rightarrow \{|0, 1\rangle, |0, -1\rangle\} \cup \{|0, 0\rangle, |0, 0\rangle\} \cup \left\{ \left| \frac{1}{2}, \frac{1}{2} \right\rangle, \left| \frac{1}{2}, -\frac{1}{2} \right\rangle \right\} \cup \left\{ \left| -\frac{1}{2}, \frac{1}{2} \right\rangle, \left| -\frac{1}{2}, -\frac{1}{2} \right\rangle \right\}. \quad (\text{I.82})$$

2.6 Graded Quantum Inverse Scattering Method

Having defined the basic tools how to handle physical models where the local degrees of freedom are carried by a representation of a Lie superalgebra, we briefly mention its influence on the QISM. The tools developed in section 1 still hold if all tensor products are replaced by super tensor products since the underlying vector spaces are now graded vector spaces. In the same way, the permutation operator turns into a graded permutation operator and the transfer matrix is defined as the super trace over the auxiliary space of the monodromy matrix [39, 49]. A detailed discussion of the graded QISM applied to the supersymmetric $t - J$ -model can be found in [49].

Although the QISM with the described modifications can be applied to models based on representations of Lie superalgebras, the subsequent solution by means of the Algebraic Bethe Ansatz involves some subtleties. For example, the Hamiltonian generated by an expansion of the transfer matrix, eq. (I.7), is no longer inevitably a hermitian operator⁸. Hence, some of the ‘energies’ may have a non-vanishing imaginary part. Up to now, the role of the corresponding complex ‘energies’ is still unknown. Therefore, in this work, we focus on the study of purely real energies in the low-energy spectrum and the corresponding low-energy effective field theory in the thermodynamic limit if the Hamiltonian is not hermitian.

⁸This is related to the existence of unitary representations of the investigated model. For example, the Hamiltonian of the $t - J$ -model at the supersymmetric point is still hermitian since it can be recast by means of operators acting on the carrier space of the unitary fundamental representation of $u(1|2)$ [49].

3 Conformal Field Theory

Conformal transformations appeared in theoretical physics already in the early 20th century, i.e. the Weyl transformation of the metric tensor [69] is exactly what is called a conformal transformation nowadays. Later on, in 1970 Polyakov pointed out how Conformal Field Theories (CFTs) can be applied in the context of statistical mechanics to study critical phenomena [70]. The growing interest during the last decades on CFTs can be traced back to two influential papers by Belavin, Polyakov and Zamolodchikov in 1984 [71, 72] where its relevance for string theory became apparent. More historical information can be found in [73].

To motivate the investigation of CFTs in the context of statistical mechanics we will begin this section by briefly reviewing critical phenomena in 3.1 followed by a short introduction into conformally invariant field theories in 3.2. Note, this subsection is not intended to provide the reader a complete discussion of the broad field of CFTs. A detailed study of CFTs can be found in [58] and [74]. Here, we will focus on its precise definition and its most important implications for the purpose of this thesis. Subsequently we will discuss how conformal symmetry characterizes the finite size scaling of lattice realizations of CFTs in 3.3. Since the critical properties of the spin chains which are studied in part II of this thesis are believed to be described in some specific ‘massless regions’ by two-dimensional Conformal Field Theories [19–22] the discussed results will be used intensively throughout this work. We will close the study of CFTs by discussing two minimal supersymmetric extensions of Conformal Field Theories in 3.4.

3.1 Critical phenomena

This subsection provides for a short motivation for the study of CFTs. A more detailed but still brief introduction into critical phenomena in the context of CFTs (which is the basis of this subsection) can be found in [74].

For the sake of simplicity, we study critical phenomena using the classical two-dimensional *Ising model*,

$$H = -J \sum_{\langle i,j \rangle} \sigma_i \sigma_j - B \sum_i \sigma_i, \tag{I.83}$$

defined by N classical spin variables $\sigma_i = \pm 1$ sitting at the sites of some lattice being exposed to an external magnetic field B . We focus on ferromagnetic interactions, $J > 0$. The summation $\langle i, j \rangle$ indicates that only nearest neighbour interactions are taken into account.

The variation of the temperature T and the external field B allows for an investigation

of the phase diagram which is schematically depicted in fig. 3. For low temperatures

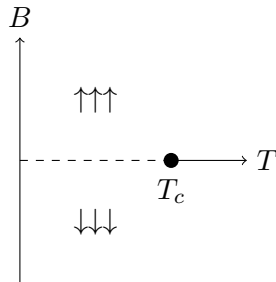


Figure 3: Phase diagram of the classical Ising model, eq. (I.83), taken from [74]. Note, to be more precise, although the model is defined on a finite lattice with N sites, continuous transitions between the phases are only present in the thermodynamic limit, $N \rightarrow \infty$.

and non-zero magnetic field, two ordered ferromagnetic phases emerge: the majority of the spins tend to the same direction defined by the external field, thus the system shows a finite magnetization per size,

$$M = \langle \sigma_i \rangle = -\frac{1}{N} \frac{\partial F}{\partial B} \neq 0, \quad (\text{I.84})$$

with the free energy F . When crossing the line $B = 0$, M (as a *first* partial derivative of the free energy) remains finite and therefore shows a jump discontinuity. By definition, the system traverses a *first order phase transition*. In general, a phase transition is of n -th order if one of the n -th partial derivatives of the free energy is a non-analytic function at the phase transition. At high temperatures thermal fluctuations become apparent and lead to one single disordered phase such that the magnetization vanishes when $B = 0$.

The three described phases merge at the *critical point* at $T = T_c$, $B = 0$ such that the two ordered phases are physically indistinguishable. When crossing criticality the system shows a second-order phase transition. In order to study the critical point, we define the *two-point spin-correlation function* for two spins at sites i and j ,

$$G(i, j) = \langle \sigma_i \sigma_j \rangle - \langle \sigma_i \rangle \langle \sigma_j \rangle \propto |i - j|^{-\tau} e^{-|i-j|/\xi} \quad (\text{I.85})$$

for $T \neq T_c$, $B = 0$ with the correlation length $\xi = \xi(T, B)$ and an exponent τ which depends on the sign of the reduced temperature $t = (T - T_c)/T_c$. The modulus $|i - j|$ denotes the distance of the sites i and j on the lattice. The correlation length describes the average size of ordered clusters in which the spins tend to point in the same direction. At a second order phase transition (i.e. at the critical point of the Ising model discussed here) ξ diverges, thus correlations are present on *all* length scales. In contrast, the correlation length remains finite for first order phase transitions. In the vicinity of a

second order phase transition the behaviour of quantities like the magnetization or the specific heat are completely described by the *critical exponents*, i.e.

$$M \propto (-t)^\beta, \quad t < 0, B = 0 \tag{I.86}$$

with β the critical exponent for the magnetization M . The critical exponents are independent of microscopic details of the model like the chosen lattice or the ratio of the couplings if we had added next nearest neighbour ferromagnetic interactions. Therefore, the critical exponents are referred to as being *universal*.

To figure out the possible corresponding universality classes, we note that a diverging correlation length leads to scale invariance. In [75] it was argued that quantum field theories with scale invariance also are *conformally invariant* - otherwise such systems are not compatible with some axioms of quantum field theory. Conformal transformations are angle-preserving transformations of the space-time. In particular, they contain scale transformations. Hence, studying Conformal Field Theories is of great interest when investigating critical points as the possible values of the critical exponents (or, their universality classes) unfold as scaling dimensions of certain fields, see e.g. [74].

3.2 Conformal invariance

A quantum field theory in d dimensions which is invariant under conformal transformations is called *Conformal Field Theory*. As discussed above those field theories are of exceptional relevance in describing critical points by means of their scaling dimensions. Mathematically conformal transformations are those that preserve angles, thus leaving the metric tensor of the space-time invariant up to a *local* scaling factor $\Lambda(\mathbf{x})$,

$$g_{\mu\nu}(\mathbf{x}) \rightarrow g'_{\mu\nu}(\mathbf{x}') = \Lambda(\mathbf{x})g_{\mu\nu}(\mathbf{x}). \tag{I.87}$$

In 3.2.1, we will investigate the allowed conformal transformations. Subsequently we will discuss the implications of conformal invariance for quantum field theories in 3.2.2. Finally we will study the Hilbert-space structure of CFTs by investigating the Virasoro algebra and its representations in 3.2.3.

3.2.1 Conformal transformations

The definition (I.87) yields the allowed conformal transformations [58],

$$\text{translations:} \quad x'^\mu = x^\mu + a^\mu, \tag{I.88}$$

$$\text{dilations:} \quad x'^\mu = \alpha x^\mu, \tag{I.89}$$

$$\text{rigid rotations:} \quad x'^\mu = M^\mu_\nu x^\nu, \tag{I.90}$$

special conformal transformations:
$$x'^{\mu} = \frac{x^{\mu} - b^{\mu} \mathbf{x}^2}{1 - 2\mathbf{b} \cdot \mathbf{x} + \mathbf{b}^2 \mathbf{x}^2}. \quad (\text{I.91})$$

with $a^{\mu}, \alpha, M_{\nu}^{\mu}, b^{\mu} \in \mathbb{R}$ and $M^{-1} = M^T$. These transformations form the conformal group. In particular (with $\Lambda(\mathbf{x}) = 1$), it contains the Poincaré-group as a subgroup. It can be shown that the conformal group in d dimensions is isomorphic to $SO(d+1, 1)$. Note, the special conformal transformation is equivalent to a translation with a preceding and following inversion.

The case $d = 2$ is rather special. We will parametrize the two-dimensional plane by coordinates $z = (z^0, z^1)$ and consider a transformation $z^{\mu} \rightarrow w^{\mu}(z^0, z^1)$. It is easy to show that (I.87) is equivalent to the Cauchy-Riemann equations for holomorphic functions,

$$\frac{\partial w^0}{\partial z^1} = \frac{\partial w^1}{\partial z^0} \quad \text{and} \quad \frac{\partial w^0}{\partial z^0} = -\frac{\partial w^1}{\partial z^1}, \quad (\text{I.92})$$

or to those for antiholomorphic functions,

$$\frac{\partial w^0}{\partial z^1} = -\frac{\partial w^1}{\partial z^0} \quad \text{and} \quad \frac{\partial w^0}{\partial z^0} = \frac{\partial w^1}{\partial z^1}. \quad (\text{I.93})$$

Thus, every holomorphic function defines a conformal transformation on the plane. This motivates the usage of complex coordinates,

$$z = z^0 + iz^1, \quad z^0 = \frac{z + \bar{z}}{2}, \quad (\text{I.94})$$

$$\bar{z} = z^0 - iz^1, \quad z^1 = \frac{z - \bar{z}}{2i}, \quad (\text{I.95})$$

$$\partial_z = \frac{1}{2}(\partial_0 - i\partial_1), \quad \partial_0 = \partial_z + \partial_{\bar{z}}, \quad (\text{I.96})$$

$$\partial_{\bar{z}} = \frac{1}{2}(\partial_0 + i\partial_1), \quad \partial_1 = i(\partial_z - \partial_{\bar{z}}). \quad (\text{I.97})$$

Note, formally z and \bar{z} are independent components. For explicit calculations \bar{z} obviously has to be the complex conjugate of z .

Since the holomorphicity of a function is a local property, the transformations obeying (I.92) (or, (I.93)) are called *local conformal transformations*. There is no need for these functions to be defined on the entire complex plane. For the construction of the algebra corresponding to local conformal transformations we consider the impact of an infinitesimal local conformal transformation on a spinless and dimensionless field $\phi(z, \bar{z})$. We write

$$z \rightarrow z' = z + \epsilon(z) \quad (\text{I.98})$$

with the Laurent expansion in the vicinity of $z = 0$,

$$\epsilon(z) = \sum_{n=-\infty}^{\infty} c_n z^{n+1}. \quad (\text{I.99})$$

Since the field ϕ is spin- and dimensionless, it transforms as⁹

$$\phi(z, \bar{z}) = \phi'(z', \bar{z}') \quad (\text{I.100})$$

leading to an infinitesimal change $\delta\phi$ of the field,

$$\delta\phi \equiv \phi'(z, \bar{z}) - \phi(z, \bar{z}) \quad (\text{I.101})$$

$$= -\epsilon(z)\partial_z\phi(z, \bar{z}) - \bar{\epsilon}(\bar{z})\partial_{\bar{z}}\phi(z, \bar{z}) \quad (\text{I.102})$$

$$\equiv \sum_n \{c_n l_n + \bar{c}_n \bar{l}_n\} \phi(z, \bar{z}). \quad (\text{I.103})$$

In the last line we introduced the generators of local conformal transformations,

$$l_n = -z^{n+1}\partial_z, \quad \bar{l}_n = -\bar{z}^{n+1}\partial_{\bar{z}}. \quad (\text{I.104})$$

The holomorphic and antiholomorphic generators form the *Witt algebra*,

$$[l_n, l_m] = (n - m)l_{n+m}, \quad [\bar{l}_n, \bar{l}_m] = (n - m)\bar{l}_{n+m}, \quad [l_n, \bar{l}_m] = 0. \quad (\text{I.105})$$

The Witt algebra contains a finite-dimensional subalgebra $\{l_{-1}, l_0, l_1\}$ which together with its antiholomorphic counterpart is said to generate *global* conformal transformations as the corresponding finite transformations are well-defined on the compactified complex plane, the Riemann sphere. The global conformal transformations on the Riemann sphere, sometimes also referred to as *projective conformal transformations*, are equivalent to the Möbius-transformations, hence, the group of global conformal transformations is equivalent to $SL(2, \mathbb{C})$. Geometrically, l_{-1} generates translations, l_0 generates scale transformations and l_1 special conformal transformations. Dilations and rotations are generated by the linear combinations $l_0 + \bar{l}_0$ and $i(l_0 - \bar{l}_0)$, respectively. The Cartan subalgebra of the Witt algebra is spanned by $\{l_0, \bar{l}_0\}$. As we will discuss below, physical fields will be eigenstates of this subalgebra. The corresponding eigenvalues Δ and $\bar{\Delta}$ will be referred to as *conformal weights* since they determine how certain fields transform under conformal transformations. Due to $l_0 + \bar{l}_0$ and $i(l_0 - \bar{l}_0)$ generating dilations and rotations, their eigenvalues are consequently called *scaling dimension* $X = \Delta + \bar{\Delta}$ and *conformal spin* $s = \Delta - \bar{\Delta}$.

⁹This is a special case of the general scheme how fields transform under conformal transformations which will be discussed in 3.2.2.

3.2.2 Fields and their correlation functions

In the following, we focus on two dimensional Conformal Field Theories. To define how fields¹⁰ transform when applying a conformal transformation, we call a field $\phi(z, \bar{z})$ with conformal weights $\Delta, \bar{\Delta}$ *quasi primary* if it transforms under any global conformal transformation $z \rightarrow w_p(z)$ according to

$$\phi(z, \bar{z}) \rightarrow \left(\frac{\partial w_p}{\partial z}\right)^\Delta \left(\frac{\partial \bar{w}_p}{\partial \bar{z}}\right)^{\bar{\Delta}} \phi(w_p(z), \bar{w}_p(\bar{z})). \quad (\text{I.106})$$

If the field $\phi(z, \bar{z})$ transforms in the same way under any local conformal transformation it is referred to as *primary field*. Obviously, every primary field is also a quasi primary while the opposite is not true. All fields which are not primary are sometimes referred to as *secondary fields*. In 3.2.3 we will show that all properties of any secondary field can be completely determined by the knowledge of all primary fields.

In discussing the properties of the critical Ising-model, we have seen that the two-point spin-correlation function plays a crucial role. In general, critical models are described by CFTs which motivates a study of correlation functions within the framework of conformal invariance. Using the path-integral formalism, the *two-point function* of the quasi-primary fields ϕ_1 and ϕ_2 is defined by

$$\langle \phi_1(z_1, \bar{z}_1) \phi_2(z_2, \bar{z}_2) \rangle = \frac{1}{Z} \int [d\Phi] \phi_1(z_1, \bar{z}_1) \phi_2(z_2, \bar{z}_2) \exp(-S[\Phi]) \quad (\text{I.107})$$

where $S[\Phi]$ denotes the conformally invariant action and Z the partition function

$$Z = \int [d\Phi] \exp(-S[\Phi]) \quad (\text{I.108})$$

of the model. In both integrals we integrate over all independent fields in the theory. n -point functions can be defined analogously as the correlation function of n quasi primary fields.

From eq. (I.106) it can be deduced how n -point functions transform under a projective conformal transformation $z_i \rightarrow w_p(z_i)$,

$$\begin{aligned} \langle \phi_1(z_1, \bar{z}_1) \dots \phi_2(z_n, \bar{z}_n) \rangle &= \left(\frac{\partial w_p}{\partial z_1}\right)^{\Delta_1} \left(\frac{\partial \bar{w}_p}{\partial \bar{z}_1}\right)^{\bar{\Delta}_1} \dots \left(\frac{\partial w_p}{\partial z_n}\right)^{\Delta_n} \left(\frac{\partial \bar{w}_p}{\partial \bar{z}_n}\right)^{\bar{\Delta}_n} \\ &\cdot \langle \phi_1(w_p(z_1), \bar{w}_p(\bar{z}_1)) \dots \phi_2(w_p(z_n), \bar{w}_p(\bar{z}_n)) \rangle. \end{aligned} \quad (\text{I.109})$$

Using suitable projective conformal transformations, eq. (I.109) determines the form of two- and three-point functions and also yields some constraints on the four-point

¹⁰Although we will speak a lot about ‘fields’ we will not specify their image set. Instead we will focus on the discussion of their dependencies on two complex numbers z and \bar{z} .

functions. This procedure leads to

$$\langle \phi_1(z_1, \bar{z}_1) \phi_2(z_2, \bar{z}_2) \rangle = \begin{cases} \frac{C_{12}}{z_{12}^{-2\Delta} \bar{z}_{12}^{-2\bar{\Delta}}}, & \text{if } \Delta_1 = \Delta_2 \equiv \Delta \\ 0, & \text{otherwise} \end{cases} \quad (\text{I.110})$$

for the two-point and

$$\begin{aligned} \langle \phi_1(z_1, \bar{z}_1) \phi_2(z_2, \bar{z}_2) \phi_3(z_3, \bar{z}_3) \rangle = & C_{123} z_{12}^{-(\Delta_1 + \Delta_2 - \Delta_3)} z_{23}^{-(\Delta_2 + \Delta_3 - \Delta_1)} z_{13}^{-(\Delta_1 + \Delta_3 - \Delta_2)} \\ & \cdot \bar{z}_{12}^{-(\bar{\Delta}_1 + \bar{\Delta}_2 - \bar{\Delta}_3)} \bar{z}_{23}^{-(\bar{\Delta}_2 + \bar{\Delta}_3 - \bar{\Delta}_1)} \bar{z}_{13}^{-(\bar{\Delta}_1 + \bar{\Delta}_3 - \bar{\Delta}_2)} \end{aligned} \quad (\text{I.111})$$

for the three-point function. We used the notation $z_{ij} = |z_i - z_j|$. Note, while the coefficient C_{12} in the two-point function is an arbitrary normalization factor, the factor C_{123} in the three-point function is not arbitrary. It is rather determined by the crossing symmetry of the four-point function. This approach is utilized in the *conformal bootstrap* program [58].

We close this subsection by briefly summarizing what a Conformal Field Theory actually is: A CFT is completely determined by the correlation functions of a set of fields (or, equivalently, operators) $\{A(z, \bar{z})\}$ over the complex plane with the following properties [74],

1. If $\phi \in \{A(z, \bar{z})\}$ then all its derivatives are also in $\{A(z, \bar{z})\}$.
2. There is a subset of fields which transforms under projective conformal transformations like eq. (I.106). These fields are called quasi primary.
3. Every field in $\{A(z, \bar{z})\}$ can be decomposed as linear combination of the quasi-primary fields and their derivatives.
4. There is a vacuum field invariant under projective conformal transformations¹¹.
5. There is a subset of the quasi primary fields which transform under any local conformal transformation like eq. (I.106). These fields are called primary.

Note, a CFT can actually be completely determined by much less information. We will remark on this in the following subsection.

3.2.3 The Virasoro algebra and its representations

Up to this point, we discussed mathematically the implications of conformal transformations. In this subsection, we enrich these results with physical input. Thus, we

¹¹For more details see 3.2.3.

construct the generators of conformal transformations acting on the space of physical fields. Thereby we gain insights into the Hilbert space structure of Conformal Field Theories.

We defined primary fields to transform according to (I.106) under any local conformal transformation. However, by Liouville's theorem, these transformations cannot be bounded in the entire complex plane unless they are constant. Hence, if we demand the infinitesimal conformal transformation $\mathbf{x} \rightarrow \mathbf{x}' = \mathbf{x} + \epsilon(\mathbf{x})$ to be analytic inside a region D_1 , ϵ is a priori non-analytic in the external of D_1 which will be denoted by D_2 . Therefore, it drives the system away from criticality [74] by modifying the Hamiltonian

$$H \rightarrow H - \frac{1}{2\pi} \int_{D_2} d^2\mathbf{x} \partial^\mu \epsilon^\nu T_{\mu\nu}(\mathbf{x}). \quad (\text{I.112})$$

The tensor $T_{\mu\nu}$ is called *energy momentum tensor*¹² and describes the first-order coupling of the small perturbation ϵ and the Hamiltonian. By demanding conformal invariance of T it can be shown that it is symmetric and traceless allowing us to use again complex coordinates,

$$T(z) = T_{11} - T_{22} - 2iT_{12}, \quad \bar{T}(\bar{z}) = T_{11} - T_{22} + 2iT_{12}. \quad (\text{I.113})$$

Before we proceed, we briefly mention some properties of the energy momentum tensor. When inserting T in a n -point function it acts like

$$\begin{aligned} & \langle T(z) \phi_1(z_1, \bar{z}_1) \dots \phi_n(z_n, \bar{z}_n) \rangle \\ &= \sum_i \left(\frac{\Delta_i}{(z - z_i)^2} + \frac{1}{z - z_i} \partial_{z_i} \right) \langle \phi_1(z_1, \bar{z}_1) \dots \phi_n(z_n, \bar{z}_n) \rangle. \end{aligned} \quad (\text{I.114})$$

Eq. (I.114) is often referred to as *conformal Ward identity*. It determines the scaling dimension $X(T) = X(\bar{T}) = 2$ and conformal spin $s(T) = -s(\bar{T}) = 2$ of the energy momentum tensor. The correlation function of T with itself is given by

$$\langle T(z_1) T(z_2) \rangle = \frac{c/2}{(z_1 - z_2)^4}. \quad (\text{I.115})$$

The normalization factor c is called *central charge* and will play a crucial role in the following.

As we already argued T determines how the Hamiltonian changes when applying local conformal transformations. Hence its Laurent coefficients can be seen as generators of conformal transformation acting on physical fields (see below). This motivates the

¹²Alternatively it can be seen as the Noether-current corresponding to infinitesimal coordinate transformations.

definitions

$$L_n = \frac{1}{2\pi i} \oint dz z^{n+1} T(z), \quad T(z) = \sum_{n \in \mathbb{Z}} z^{-n-2} L_n, \quad (\text{I.116})$$

$$\bar{L}_n = \frac{1}{2\pi i} \oint d\bar{z} \bar{z}^{n+1} \bar{T}(\bar{z}), \quad \bar{T}(\bar{z}) = \sum_{n \in \mathbb{Z}} \bar{z}^{-n-2} \bar{L}_n. \quad (\text{I.117})$$

By inverting these relations and applying Cauchy's integral theorems repeatedly the commutators of the L_n 's can be calculated,

$$\begin{aligned} [L_n, L_m] &= (n-m)L_{n+m} + \frac{c}{12}n(n^2-1)\delta_{n+m,0}, \\ [\bar{L}_n, \bar{L}_m] &= (n-m)\bar{L}_{n+m} + \frac{c}{12}n(n^2-1)\delta_{n+m,0}, \\ [L_n, \bar{L}_m] &= 0. \end{aligned} \quad (\text{I.118})$$

These equations define the *Virasoro algebra*. It differs from the Witt algebra only by the central term proportional to c which occurs for $n+m=0$. Before we discuss its representations, we give some remarks regarding this definition.

- c is sometimes referred to as anomaly since it describes the anomalies in statistical systems at criticality due to fluctuations on all length scales. Thus, c is of great interest when describing critical points in terms of Conformal Field Theories.
- c disappears for $n=0, \pm 1$ thereby recovering the generators $l_0, l_{\pm 1}$. The Cartan subalgebra of the Virasoro algebra is spanned by $\{c, L_0, \bar{L}_0\}$.
- As justified above, the generators L_n generate conformal transformations on the Hilbert space corresponding to physical fields - see below - while l_n generate conformal transformations in the space of functions. This observation is in accordance with quantum field theory, i.e. it is demanded that symmetry transformations act on states by means of projective representations which are equivalent to representations of the central extension of the symmetry algebra [76]. In the case of conformal transformation, the central extension of the symmetry algebra (Witt algebra, (I.105)) is the Virasoro algebra.

In the remaining part of this subsection we will focus on the representation theory of the Virasoro algebra which allows for a construction of the Hilbert space corresponding to CFTs. The starting points in constructing representations of the Virasoro algebra are primary fields. Algebraically they may be defined as a field ϕ with conformal weight Δ that satisfies

$$\begin{aligned} L_n \phi &= 0 \text{ if } n > 1 \\ L_0 \phi &= \Delta \phi \end{aligned} \quad (\text{I.119})$$

where we omitted the explicit dependence of the field ϕ on the coordinates. The conformal weight of the primary defines the highest weight of a representation. All other states which belong to this representation can be constructed by means of the operators L_{-n} with $n > 0$,

$$\phi^{(-n_k, \dots, -n_1)} = L_{-n_k} \dots L_{-n_1} \phi. \quad (\text{I.120})$$

These states are called *descendants* of the primary ϕ . Their conformal weight can easily be calculated using the commutator relations (I.118),

$$L_0 \phi^{(-n_k, \dots, -n_1)} = L_0 L_{-n_k} \dots L_{-n_1} \phi = (\Delta + n_1 + \dots + n_k) \phi^{(-n_k, \dots, -n_1)} \quad (\text{I.121})$$

Hence, the operators L_{-n} with $n > 0$ act as ladder operators. The integer $n = n_1 + \dots + n_k$ is called *level* of the descendant. A representation built of a primary and all its descendants is called *Verma module*¹³. The primary ϕ is the only state in the Verma module with conformal weight Δ , the descendant $L_{-1}\phi$ is the only one with weight $\Delta + 1$. As an example, it can be shown that the energy momentum tensor is a level-2 descendant of the identity operator $\mathbf{1}$,

$$T(z) = L_{-2}\mathbf{1} \quad (\text{I.122})$$

which justifies $X(T) = 2$.

We now argue that the operator L_0 should be bounded from below. Assume L_0 were not bounded. Hence, there is a primary field with conformal weight $\Delta = -\infty$. By means of (I.110) it follows that its correlation function with itself would be infinite everywhere which is not physical. Thus, in a physically reasonable theory it is legitimate to assume that L_0 is bounded from below. Moreover, since $L_0 + \bar{L}_0$ generate dilations we may presume for the Hamiltonian of the theory,

$$H \propto L_0 + \bar{L}_0, \quad (\text{I.123})$$

giving L_0 the notion of an energy operator. We will use this result in the next subsection to study finite-size effects in physical systems whose thermodynamic limit is described by a Conformal Field Theory. Finally in order to fix the representation we declare the states on which the representation act. To this end, we define the vacuum state as the highest weight of the identity operator at the origin [74],

¹³Note, there are fields that are primary and descendant at the same time. These states are called null vectors. Therefore, non-degenerate representations of the Virasoro algebra can be constructed by dividing out the null vectors of a Verma module.

$$|0\rangle \equiv \mathbf{1}(z=0), \quad (\text{I.124})$$

which is assumed to satisfy

$$L_n |0\rangle = 0 \quad \text{for } n \geq -1. \quad (\text{I.125})$$

Hence, the vacuum is invariant under global conformal transformations. Further, the vacuum expectation value of the energy momentum tensor vanishes. The true physical vacuum is the tensor product of $|0\rangle$ with $|\bar{0}\rangle$, the latter being the vacuum of the antiholomorphic identity. States corresponding to a primary ϕ with conformal weight Δ can now be defined as

$$\begin{aligned} |\Delta\rangle &\equiv \phi(0) |0\rangle \quad \text{with} \\ L_0 |\Delta\rangle &= \Delta |\Delta\rangle \quad \text{and} \\ L_n |\Delta\rangle &= 0 \quad \text{for } n > 0. \end{aligned} \quad (\text{I.126})$$

Descendants of this primary may be constructed by acting with several ladder operators,

$$|\Delta^{(-n_k, \dots, -n_1)}\rangle \equiv (L_{-n_k} \dots L_{-n_1}) \phi(0) |0\rangle, \quad (\text{I.127})$$

with conformal weight $\Delta + n_1 + \dots + n_k$ as computed above.

In order to obtain a Hilbert space structure we need to define the dual of the vacuum state. The dual of (I.125) should read

$$\langle 0| (L_n)^\dagger = 0 \quad \text{for } n \geq 0 \quad (\text{I.128})$$

leading to

$$(L_n)^\dagger = L_{-n} \quad (\text{I.129})$$

which looks quite natural. Hence, $L_0^\dagger = L_0$ and the Hamiltonian is hermitian with a real spectrum. The dual of primary states can be defined by evaluating the field at infinity,

$$\langle \Delta| \equiv \lim_{z \rightarrow \infty} \langle 0| \phi(z) z^{2\Delta} \quad (\text{I.130})$$

which finally allows for the calculation of scalar products and norms of states. Further, it guarantees orthogonality of primaries with different conformal weights, $\langle \Delta| \Delta' \rangle = \delta_{\Delta, \Delta'}$. We close this subsection by two remarks.

- It is possible to connect the states defined here to fields evaluated at arbitrary positions on the complex plane by

$$\phi(z) |0\rangle \equiv \exp(zL_{-1}) |\Delta\rangle \quad (\text{I.131})$$

since L_{-1} generates translations which allows for the calculation of correlation functions as scalar products. For the two-point function, this leads to

$$\langle 0 | \phi(z_1) \phi(z_2) | 0 \rangle = \frac{1}{(z_1 - z_2)^{2\Delta}} \quad (\text{I.132})$$

for the holomorphic part in total agreement with eq. (I.110).

- It is possible to prove that every quasi primary is the secondary operator of a primary, hence the primaries are the building blocks of a CFT. Thus, a CFT can be completely described by knowing all the primaries, their conformal weights, the central charge and the three-point function normalization factors C_{ijk} . By means of the operator product expansion, the coefficients C_{ijk} determine completely all higher n -point functions. Historically, the reduction of four-point to three-point functions is manifest in the conformal bootstrap approach which allows for a computation of the C_{ijk} using crossing symmetry. More details can be found e.g. in [58].

3.3 Finite size scaling

This subsection treats the calculation of the scaling dimensions and the central charge for a critical system with a *finite* system size, $L < \infty$. To this end we consider the two-point correlation function of a scalar primary field ϕ with conformal weight Δ , eq. (I.110), and study its transformation, (I.109), using

$$w = \frac{L}{2\pi} \log z. \quad (\text{I.133})$$

This conformal transformation corresponds to a mapping between the infinite complex plane and a strip with a finite width L . Eq. (I.109) allows for the calculation of the two-point function on the strip geometry,

$$\langle \phi(w_1, \bar{w}_1) \phi(w_2, \bar{w}_2) \rangle_{\text{strip}} \quad (\text{I.134})$$

$$= \left(\frac{\partial w}{\partial z} \Big|_{z_1} \frac{\partial w}{\partial z} \Big|_{z_2} \right)^{-\Delta} \left(\frac{\partial \bar{w}}{\partial \bar{z}} \Big|_{\bar{z}_1} \frac{\partial \bar{w}}{\partial \bar{z}} \Big|_{\bar{z}_2} \right)^{-\bar{\Delta}} \langle \phi(z_1, \bar{z}_1) \phi(z_2, \bar{z}_2) \rangle \quad (\text{I.135})$$

$$= \left(\frac{2\pi}{L} \right)^{2\Delta+2\bar{\Delta}} \left(\frac{z_1^{1/2} z_2^{1/2}}{z_1 - z_2} \right)^{2\Delta} \left(\frac{\bar{z}_1^{-1/2} \bar{z}_2^{-1/2}}{\bar{z}_1 - \bar{z}_2} \right)^{2\bar{\Delta}} \quad (\text{I.136})$$

3. Conformal Field Theory

$$= \left(\frac{2\pi}{L}\right)^{2\Delta+2\bar{\Delta}} \left(\frac{e^{\pi/L(w_1+w_2)}}{e^{2\pi w_1/L} - e^{2\pi w_2/L}}\right)^{2\Delta} \left(\frac{e^{\pi/L(\bar{w}_1+\bar{w}_2)}}{e^{2\pi\bar{w}_1/L} - e^{2\pi\bar{w}_2/L}}\right)^{2\bar{\Delta}} \quad (\text{I.137})$$

$$= \left(\frac{\pi}{L} \frac{1}{\sinh\left(\frac{\pi}{L}(w_1 - w_2)\right)}\right)^{2\Delta} \left(\frac{\pi}{L} \frac{1}{\sinh\left(\frac{\pi}{L}(\bar{w}_1 - \bar{w}_2)\right)}\right)^{2\bar{\Delta}} \quad (\text{I.138})$$

We write $w_j = u_j + iv_j$. Asymptotically, for $|u_1 - u_2| \gg L$, an expansion of the sinh yields

$$\begin{aligned} & \langle \phi(w_1, \bar{w}_1) \phi(w_2, \bar{w}_2) \rangle_{\text{strip}} \\ &= \left(\frac{2\pi}{L}\right)^{2X} \exp\left(-\frac{2\pi}{L}X(u_1 - u_2) - i\frac{2\pi}{L}s(v_1 - v_2)\right) \end{aligned} \quad (\text{I.139})$$

with the scaling dimension $X = \Delta + \bar{\Delta}$ and conformal spin $s = \Delta - \bar{\Delta}$. A comparison of eq. (I.139) with the definition of the correlation length, e.g. eq. (I.107) finally gives the correlation length for the field ϕ ,

$$\xi = \frac{L}{2\pi X}. \quad (\text{I.140})$$

In [74] equation (I.140) was called

“[...] one of the most important results for the application of conformal invariance to critical phenomena”.

To go even one step further, the Lehmann representation of the two-point function relates the correlation length with the eigenenergies of the Hamiltonian ($\hbar \equiv 1$),

$$\xi_i^{-1} = E_i - E_0 \Rightarrow X_i = \frac{L}{2\pi}(E_i(L) - E_0(L)), \quad (\text{I.141})$$

where $E_0(L)$ is the exact ground state energy of the Hamiltonian and $E_i(L)$ the energy of an excited state for a system with system size L . The lattice constant is set to unity. We will make extensive use of eq. (I.141) in part II of this work since this equation allows us to calculate the scaling dimensions of the Conformal Field Theory describing the thermodynamic limit by simply calculating the energy spectrum of a superspin chain for a given finite system size L .

A similar argument applies to the central charge c . It can be calculated by means of

$$c = -\frac{6L}{\pi}(E_0(L) - Le_\infty) \quad (\text{I.142})$$

again for finite system sizes. Here, we introduced the ground state energy per site in the thermodynamic limit, e_∞ . We recall that we started by studying two-point functions of a scalar primary field. However, it turns out that eq. (I.140) is also true for descendant

fields. Also, we implicitly assumed isotropic interactions. On the other hand, anisotropic interactions manifest themselves only by a slight modification of the above formulas, e.g. for the scaling dimension

$$X_i^{\text{an}} = \frac{L}{2\pi v_F} (E_i(L) - E_0(L)), \quad (\text{I.143})$$

where the information about the anisotropy is solely contained in the *Fermi velocity* v_F .

One example of an application of eq. (I.142) is the calculation of the specific heat for spin chains at small but finite temperatures. It turns out to be proportional to the central charge,

$$C = \frac{\pi c}{3\hbar v_F} k_B^2 T, \quad (\text{I.144})$$

where \hbar is the reduced Plank constant and k_B the Boltzmann constant. Thus, intuitively the central charge counts the critical degrees of freedom of the studied system.

3.4 Supersymmetric extensions

Finishing this short introduction into Conformal Field Theories, we briefly discuss supersymmetric extensions, i.e. Superconformal Field Theories. The corresponding symmetry algebra is called *super Virasoro algebra*. The commutation relation for the generators read [77]

$$[L_n, L_m] = (n - m)L_{n+m} + \frac{c}{12}n(n^2 - 1)\delta_{n+m,0}, \quad (\text{I.145})$$

$$[G_r, G_s] = 2L_{r+s} + \frac{c}{3}\left(r^2 - \frac{1}{4}\right)\delta_{r+s,0}, \quad (\text{I.146})$$

$$[L_n, G_r] = \left(\frac{n}{2} - r\right)G_{n+r}. \quad (\text{I.147})$$

accompanied by the corresponding generators for the complex conjugate coordinate. The even part of the super Virasoro algebra is spanned by the operators L_n , hence, the even part of the super Virasoro algebra is the ordinary Virasoro algebra discussed above. The operators G_n form a basis for the odd part. While n, m are integers, the indices r, s are integers or half integers originating in a possible double-valuedness of the energy-momentum tensor when the spin is half-integer. If r, s are integers the Superconformal Field Theory is said to describe the *Ramond sector* [78] while the half-integer case is called *Neveu-Schwarz sector* [79]. The whole Hilbert space of a Superconformal Field Theory contains both the Ramond- and the Neveu-Schwarz sector

Like for Conformal Field Theories, the operator $L_0 + \bar{L}_0$ generates dilations and acts as a Hamiltonian. Likewise, L_n and G_n are lowering (raising) operators for $n > 0$ ($n < 0$). The vacuum state is defined by the condition that it is annihilated by all

lowering operators. An irreducible representation can again be constructed by acting with all raising operators on a suitable field.

The state-field correspondence described in subsection 3.2 holds only in the Neveu-Schwarz sector while in the Ramond sector it is far more involved and hence beyond the scope of this work.

In part II where superspin chains are constructed and solved by means of the Algebraic Bethe Ansatz, the Ramond- and the Neveu-Schwarz sector are manifest in the boundary conditions: The Ramond-sector correspond to periodic boundary conditions for the fermionic degrees of freedom whereas antiperiodic boundary conditions translate to the Neveu-Schwarz sector in the language of Superconformal Field Theory. The latter implies that the transfer matrix for the Neveu-Schwarz sector in the QISM framework is calculated by means of the trace over the auxiliary space (rather than the supertrace which is used in the Ramond sector).

4 From the Integer Quantum Hall effect to superspin chains

Having discussed the mathematical basics, we seek for the answer of the question: Why should we study integrable superspin chains, i.e. spin chains constructed by means of QISM where the local degrees of freedom are carried by a representation of a certain Lie superalgebra? One pragmatical reason can be formulated in Baxter’s words [4],

“Basically, I suppose the justification for studying these models is very simple: they are relevant and they can be solved, so why not do so and see what they tell us?”

Following this idea, in this section we argue why superspin chains are relevant by briefly studying the Quantum Hall effect based on [80] and show how superspin chains emerge for its theoretical description.

Motivated by a remark of Maxwell [81],

“It must be carefully remembered that the mechanical force which urges a conductor carrying a current across the lines of magnetic force acts, not on the electric current, but on the conductor which carries it. – The only force which acts on electric currents is electromotive force”,

Hall studied the effects of a magnetic field pointing perpendicular (here: z -direction) to an electric current confined to two dimensions (here: (x, y) -plane). The setup is schematically depicted in fig. 4. Using this setup, Hall measured a voltage in y -direction

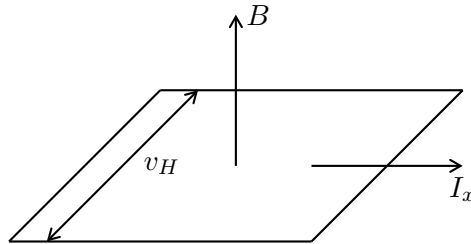


Figure 4: The experimental setup for the classical Hall effect.

although the external current is applied in x -direction [82]. By means of the Drude-model, the *longitudinal* ρ_{xx} and *Hall-resistivity* ρ_{xy} can be calculated,

$$\rho_{xx} = \frac{m}{ne^2\tau} \quad \text{and} \quad \rho_{xy} = \frac{B}{ne} \quad (\text{I.148})$$

with the electron mass m , the electron density n , the electron charge $-e$ and the scattering time τ . This classical calculation therefore predicts a constant longitudinal and a linear dependence of the Hall-resistivity w.r.t. the magnetic field.

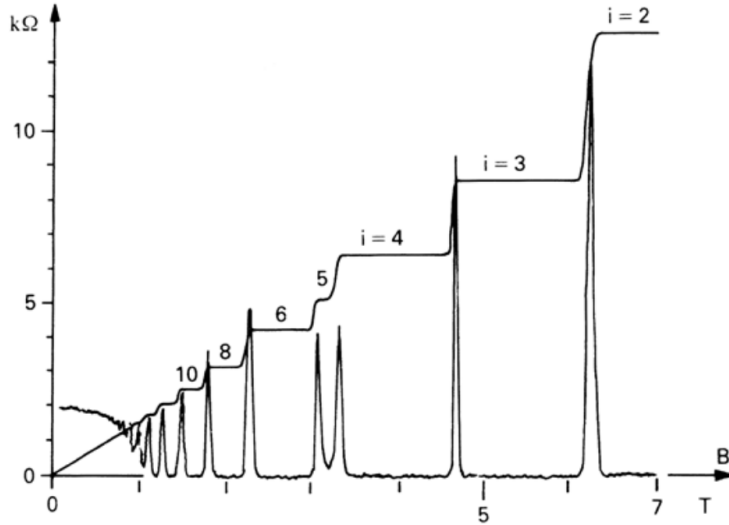


Figure 5: Hall- and longitudinal resistivity for low temperatures and fixed electron density as a function of the magnetic field. Taken from [83].

However, for low temperatures and high magnetic fields, von Klitzing and coworkers observed several plateaus labeled by integers in the Hall resistivity and sharp peaks in the longitudinal resistivity whenever there is a transition between two plateaus in the Hall resistivity [10], see fig. 5. This effect is referred to as *Integer Quantum Hall effect*. In 1985, von Klitzing was rewarded with the Nobel price of physics for the discovery of the Quantum Hall effect. The Hall resistivity at the ν -th plateau was found to be

$$\rho_{xy} = \frac{2\pi\hbar}{e^2} \frac{1}{\nu} \quad (\text{I.149})$$

which can be explained by the quantization of the non-interacting electrons in two dimensions exposed to a magnetic field leading to *Landau levels*. Instead of free electrons described by two quantum numbers corresponding to the two degrees of freedom, the presence of a magnetic field allows for a mapping to a harmonic oscillator with the *cyclotron frequency*

$$\omega_B = \frac{eB}{m}. \quad (\text{I.150})$$

Each Landau level can be filled with

$$\mathcal{N} = \frac{eBA}{2\pi\hbar} \quad (\text{I.151})$$

electrons where A is the area of the sample. Hence, each Landau level is highly degenerate. Whenever the ν -th Landau level is completely filled the Hall resistivity is given by eq. (I.149) which explains the values which ρ_{xy} can take. The persistence of the plateaus over a wide range of the magnetic field can be attributed to the disorder in

4. From the Integer Quantum Hall effect to superspin chains

the sample which leads to additional but localized states (in contrast to the Landau level states which are delocalized). When the magnetic field is decreased each Landau level can be filled with fewer electrons. But instead of occupying the next Landau level, the remaining electrons start to populate the localized states which by default do not contribute to the electric transport. At the same time the current caused by the delocalized electrons occupying the Landau levels increases to compensate for the missing current from the now localized states. Eventually this leads to the plateaus observed by von Klitzing. As mentioned above the role of disorder is crucial for the emergence of plateaus in the Hall resistivity. When studying the very same setup with a perfect sample, i.e. without any disorder, no plateaus would be observable in an experiment.

We now focus on the transition between two plateaus. Numerical studies using the network model to incorporate the effects of disorder indicate that the correlation length diverges at the critical point for the electron gas [11], hence, the plateau transition is of second order. Naively we would expect a description in terms of a Conformal Field Theory. However a multifractal analysis of the moments of the local density of states at the critical point shows a continuous spectrum of critical exponents [12] which can be achieved by non-unitary field theories only.

The first Ansatz for a field theoretical description of the plateau transition was formulated by Pruisken and his coworkers using a nonlinear sigma model [13, 14]. However it does not have the right symmetry to include conformal invariance [15]. To overcome this problem, Weidenmüller constructed a supersymmetric version of Pruisken's nonlinear sigma model [16] by calculating disorder averages of correlation functions [17]. As Zirnbauer showed, in the Hamiltonian limit this supersymmetric nonlinear sigma model can be mapped to a superspin chain [15] in which the local degrees of freedom are carried by alternating infinite dimensional representations of $gl(2|2)$. Thus, superspin chains may be good candidates for lattice models corresponding to field theories for plateau transitions in integer Quantum Hall systems. However, in order to perform analytic or numerical studies, the local Hilbert space has to be truncated which allows for the construction of toy models with finite local degrees of freedom [20, 21, 84, 85]. One of these toy models, the superspin chain with $sl(2|1)$ symmetry, can alternatively be derived directly from the network model [86].

Part II

Finite size study of integrable superspin chains

1 The $U_q[sl(2|1)]$ superspin chain

Since the last decade, a growing number of lattice models including order-disorder transitions in Quantum Hall systems, the anti-ferromagnetic Potts-model, intersecting loops or physical properties of two-dimensional polymers have been shown to exhibit thermodynamic limits that - although having a finite-dimensional Hilbert space for the local degrees of freedom on the lattice - have been found to correspond to non-unitary CFTs [19–21, 23, 27, 28, 84]. The corresponding non-compactness of the target space manifests itself in the emergence of a continuous component in the spectrum of scaling dimensions in the thermodynamic limit. Additionally, in non-unitary CFTs, there may exist (discrete) levels which are not normalizable. Hence, the corresponding states appear in the spectrum of the lattice model only when the norm of the corresponding operator in the CFT becomes finite, e.g. by imposing certain boundary conditions. In the spectrum of the superspin chain, this may lead to a non-analytic dependence of the effective central charge of the lattice model on the boundary conditions.

For some of the following lattice models the spectral data obtained from their exact solution have allowed to identify the CFT describing their thermodynamic limits:

- An integrable vertex model built from the three-dimensional fundamental and dual representations of the superalgebra $sl(2|1)$ was argued to flow to a $SU(2|1)$ Wess-Zumino-Novikov-Witten (WZNW) model at level $k = 1$ [20, 87]. For a physical modular invariant partition function it is only allowed to consider continuous values of the $sl(2|1)$ charge quantum number leading to continua of scaling dimensions.
- A staggered six-vertex model related to the anti-ferromagnetic Potts model [23] (which also appears in the phase diagram of a staggered superspin chain built from four-dimensional representations of $U_q[sl(2|1)]$ [84]) has been argued to provide a realization of the $SL(2, \mathbb{R})/U(1)$ Euclidean black hole sigma model [88, 89]. This identification was based on the density of states in the continuous spectrum corresponding to primary fields [24–26]. However, taking also into account the contribution of descendant states, this identification is no longer true [90].
- The $a_2^{(2)}$ model (equivalent to the 19-vertex Izergin-Korepin model [91]) in 'regime III' has a non-compact thermodynamic limit which can again be described by the $SL(2, \mathbb{R})/U(1)$ black hole sigma model [27]. Here, the spectrum of discrete levels appearing in the lattice model with twisted boundary conditions has been found to be consistent with the predicted appearance of levels related to the principal discrete representations of $SL(2, \mathbb{R})$ states [92, 93]. Similarly, the scaling limit of the general $a_{N-1}^{(2)}$ model has been shown to be a $SO(N)/SO(N-1)$ gauged WZNW model [28].

In this section we will focus upon the thermodynamic limit of the mixed q -deformed $sl(2|1)$ superspin chain based on the three dimensional atypical representation and its dual, labeled 3 and $\bar{3}$ in the following [94]. In previous work on this model, and similar as in the isotropic case $q \rightarrow 1$, the existence of an exact zero energy state and of continua of scaling dimensions have been established [21].

As sketched in section 4 in part I, the corresponding isotropic $sl(2|1)$ superspin chain may be a good candidate for describing order-disorder transitions in Quantum Hall systems. Hence, the investigation of its thermodynamic limit is intriguing, not only because it is mathematically unknown. A better understanding of the latter can also help to gain insights in the field theoretical description of the critical point regarding plateau transitions in Quantum Hall systems.

This section is organized as follows: In the first subsection we will recall the definition and solution of the staggered $U_q[sl(2|1)]$ superspin chain by means of the Algebraic Bethe Ansatz in 1.1 followed by a short reminder of some previous results for the operator content in 1.2. Subsequently we will define an operator which allows for a characterization of the continuous components of the spectrum in 1.3. Further, we will generalize the lattice model to include general toroidal boundary conditions allowing for an adiabatic change from periodic to antiperiodic boundary conditions for the fermionic degrees of freedom. Using the Bethe Ansatz solution of this model, we will find the exact dependence of e.g. the scaling dimensions for some low lying levels on the twist angle in 1.4. Translating our results into the context of the field theory describing the thermodynamic limit of the model, we will find that under the spectral flow states from the continuous part of the spectrum in the Neveu-Schwarz sector are mapped onto discrete levels in the Ramond sectors, and vice versa. This section will be closed by a summary of our findings in 1.5.

1.1 Definition and solution of the model

This subsection is dedicated to the definition of the $U_q[sl(2|1)]$ superspin chain and its equivalent two-dimensional vertex model. Subsequently, its solution by means of the nested Algebraic Bethe Ansatz will be presented. The Lie superalgebra $sl(2|1)$ and its quantum deformation are discussed in section 2 in part I of this work.

We consider the mixed vertex model based on the three dimensional atypical representation of $U_q[sl(2|1)]$ labelled 3 and its dual $\bar{3}$ (see 2.4 in part I) as shown in fig. 6. Arrows pointing to the right or up (left or down) denote the representation 3 ($\bar{3}$). The Boltzmann weights for the different local states are encoded in the elements of four different \mathcal{R} -matrices acting on the tensor products $3 \otimes 3$, $3 \otimes \bar{3}$, $\bar{3} \otimes 3$ and $\bar{3} \otimes \bar{3}$ depending on which representations are sitting at the corresponding vertex [21, 94], see fig. 7.

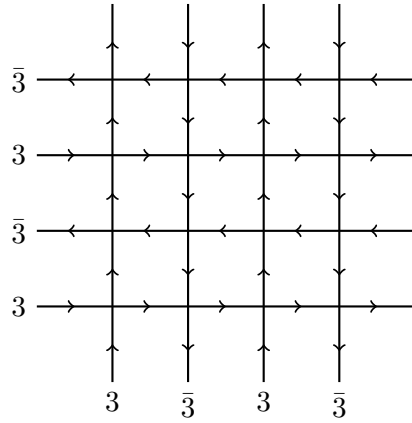


Figure 6: Vertex model corresponding to the staggered $U_q[sl(2|1)]$ superspin chain.

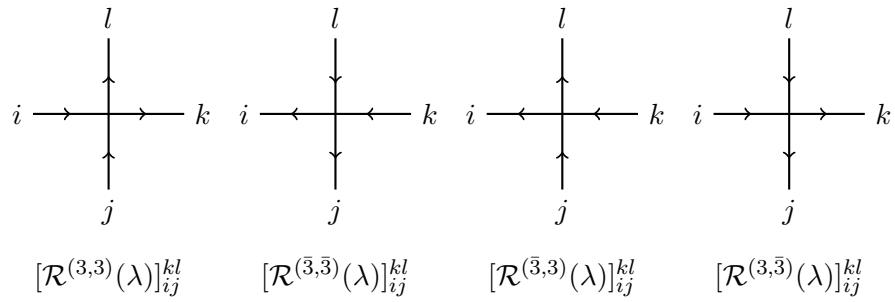


Figure 7: Weights of the four different types of vertices giving rise to four different \mathcal{R} -matrices.

Explicitly, the four different \mathcal{R} -matrices read [21]

$$\begin{aligned} \mathcal{R}_{a,b}^{(3,3)}(\lambda) &= \sum_{j=1}^3 a_j(\lambda) e_{jj}^{(a)} \otimes e_{jj}^{(b)} + \sum_{\substack{j,k=1 \\ j \neq k}}^3 b(\lambda) e_{jj}^{(a)} \otimes e_{kk}^{(b)} \\ &+ c(\lambda) \left(\sum_{\substack{j,k=1 \\ j > k}}^3 (-1)^{p_j p_k} e_{jk}^{(a)} \otimes e_{kj}^{(b)} + e^{-2\lambda} \sum_{\substack{j,k=1 \\ j < k}}^3 (-1)^{p_j p_k} e_{jk}^{(a)} \otimes e_{kj}^{(b)} \right), \end{aligned} \quad (\text{II.1})$$

$$\begin{aligned} \mathcal{R}_{a,b}^{(3,\bar{3})}(\lambda) &= \sum_{j=1}^3 a_j(-\lambda - 2i\gamma) e_{jj}^{(a)} \otimes e_{jj}^{(b)} + \sum_{\substack{j,k=1 \\ j \neq k}}^3 b(-\lambda - 2i\gamma) e_{jj}^{(a)} \otimes e_{kk}^{(b)} \\ &+ c(-\lambda - 2i\gamma) \left(\sum_{\substack{j,k=1 \\ j < k}}^3 (-1)^{p_j} f_{jk} e_{jk}^{(a)} \otimes e_{jk}^{(b)} + e^{2\lambda + 4i\gamma} \sum_{\substack{j,k=1 \\ j > k}}^3 (-1)^{p_j} (f_{jk})^{-1} e_{jk}^{(a)} \otimes e_{jk}^{(b)} \right), \end{aligned} \quad (\text{II.2})$$

$$\begin{aligned} \mathcal{R}_{a,b}^{(\bar{3},3)}(\lambda) &= \sum_{j=1}^3 a_j(-\lambda) e_{jj}^{(a)} \otimes e_{jj}^{(b)} + \sum_{\substack{j,k=1 \\ j \neq k}}^3 b(-\lambda) e_{jj}^{(a)} \otimes e_{kk}^{(b)} \\ &+ c(-\lambda) \left(\sum_{\substack{j,k=1 \\ j > k}}^3 (-1)^{p_k} (\tilde{f}_{jk})^{-1} e_{jk}^{(a)} \otimes e_{jk}^{(b)} + e^{2\lambda} \sum_{\substack{j,k=1 \\ j < k}}^3 (-1)^{p_k} \tilde{f}_{jk} e_{jk}^{(a)} \otimes e_{jk}^{(b)} \right), \end{aligned} \quad (\text{II.3})$$

$$\begin{aligned} \mathcal{R}_{a,b}^{(\bar{3},\bar{3})}(\lambda) &= \sum_{j=1}^3 a_j(\lambda) e_{jj}^{(a)} \otimes e_{jj}^{(b)} + \sum_{\substack{j,k=1 \\ j \neq k}}^3 b(\lambda) e_{jj}^{(a)} \otimes e_{kk}^{(b)} \\ &+ c(\lambda) \left(\sum_{\substack{j,k=1 \\ j < k}}^3 (-1)^{p_j p_k} e_{jk}^{(a)} \otimes e_{kj}^{(b)} + e^{-2\lambda} \sum_{\substack{j,k=1 \\ j > k}}^3 (-1)^{p_j p_k} e_{jk}^{(a)} \otimes e_{kj}^{(b)} \right). \end{aligned} \quad (\text{II.4})$$

Here, $e_{jk}^{(a)}$ are the standard 3×3 Weyl-matrices acting on the a -th copy of \mathbb{C}^3 , p_j denotes the degree of the j -th component of a vector in \mathbb{C}^3 , i.e. $p_j = 0$ if the j -th component is even or *bosonic* and $p_j = 1$ if it is odd or *fermionic*. The functions a_j, b and c are given by

1. The $U_q[sl(2|1)]$ superspin chain

$$a_j(\lambda) = \frac{\sinh(\lambda - 2i\gamma(2p_j - 1))}{\sinh(\lambda + 2i\gamma)}, \quad b(\lambda) = \frac{\sinh(\lambda)}{\sinh(\lambda + 2i\gamma)}, \quad c(\lambda) = \frac{e^\lambda \sinh(2i\gamma)}{\sinh(\lambda + 2i\gamma)}. \quad (\text{II.5})$$

Further, the matrices f_{jk} and \tilde{f}_{jk} depend on the anisotropy $q = e^{-i\gamma}$ only. Their non-zero elements read

$$\tilde{f}_{12} = e^{2i\gamma(1-p_3)}, \quad \tilde{f}_{13} = e^{2i\gamma p_2}, \quad \tilde{f}_{23} = e^{-2i\gamma p_1}, \quad (\text{II.6})$$

as well as

$$\begin{aligned} f_{12} &= (-1)^{1+p_2} e^{2i\gamma(p_1+p_2+2p_3)} \frac{\sin(2\gamma)}{\sin(2\gamma(1-2p_1-2p_3))}, \\ f_{13} &= (-1)^{p_3} e^{2i\gamma(2p_1+p_2+2p_3)} \frac{\sin(2\gamma-4\gamma p_3)}{\sin(2\gamma)}, \\ f_{23} &= (-1)^{1-p_2+p_3} e^{2i\gamma p_1} \frac{\sin(2\gamma(1-2p_1-2p_3)) \sin(2\gamma-4\gamma p_3)}{\sin^2(2\gamma)}. \end{aligned} \quad (\text{II.7})$$

The four different \mathcal{R} -matrices obey Yang-Baxter equations for any combination of the representations $\mathfrak{3}$ and $\bar{\mathfrak{3}}$,

$$\mathcal{R}_{12}^{(\omega_1, \omega_2)}(\lambda) \mathcal{R}_{13}^{(\omega_1, \omega_3)}(\lambda + \mu) \mathcal{R}_{23}^{(\omega_2, \omega_3)}(\mu) = \mathcal{R}_{23}^{(\omega_2, \omega_3)}(\mu) \mathcal{R}_{13}^{(\omega_1, \omega_3)}(\lambda + \mu) \mathcal{R}_{12}^{(\omega_1, \omega_2)}(\lambda) \quad (\text{II.8})$$

for $\omega_j \in \{\mathfrak{3}, \bar{\mathfrak{3}}\}$ and $j = 1, 2, 3$. As a consequence, two families of row-to-row transfer matrices acting on the Hilbert space $(\mathfrak{3} \otimes \bar{\mathfrak{3}})^{\otimes L}$ can be constructed as the supertrace over auxiliary spaces $\mathcal{A} \cong \mathbb{C}^3$ of ordered products of these \mathcal{R} -matrices [47],

$$\begin{aligned} \tau_{\mathfrak{3}}(\lambda) &= \text{str}_{\mathcal{A}} T_{\mathfrak{3}}(\lambda), \\ T_{\mathfrak{3}}(\lambda) &= \mathcal{G}^{(\mathfrak{3})}(\alpha) \mathcal{R}_{\mathcal{A}, 2L}^{(\mathfrak{3}, \mathfrak{3})}(\lambda) \mathcal{R}_{\mathcal{A}, 2L-1}^{(\mathfrak{3}, \bar{\mathfrak{3}})}(\lambda - i\gamma) \mathcal{R}_{\mathcal{A}, 2L-2}^{(\mathfrak{3}, \mathfrak{3})}(\lambda) \dots \mathcal{R}_{\mathcal{A}, 1}^{(\mathfrak{3}, \bar{\mathfrak{3}})}(\lambda - i\gamma), \\ \tau_{\bar{\mathfrak{3}}}(\lambda) &= \text{str}_{\mathcal{A}} T_{\bar{\mathfrak{3}}}(\lambda), \\ T_{\bar{\mathfrak{3}}}(\lambda) &= \mathcal{G}^{(\bar{\mathfrak{3}})}(\alpha) \mathcal{R}_{\mathcal{A}, 2L}^{(\bar{\mathfrak{3}}, \bar{\mathfrak{3}})}(\lambda + i\gamma) \mathcal{R}_{\mathcal{A}, 2L-1}^{(\bar{\mathfrak{3}}, \mathfrak{3})}(\lambda) \mathcal{R}_{\mathcal{A}, 2L-2}^{(\bar{\mathfrak{3}}, \bar{\mathfrak{3}})}(\lambda + i\gamma) \dots \mathcal{R}_{\mathcal{A}, 1}^{(\bar{\mathfrak{3}}, \mathfrak{3})}(\lambda). \end{aligned} \quad (\text{II.9})$$

The boundary conditions are controlled by the diagonal twist matrices $\mathcal{G}^{(\omega)}(\alpha) = \exp(2i\alpha Q_3^{(\omega)})$ with $Q_3^{(\omega)}$ the diagonal generator of the spin-subalgebra in the representation ω . For $\alpha = 0$ the lattice model obeys periodic boundary conditions while for $\alpha = \pm\pi$ bosonic states are periodic while fermions fulfill *antiperiodic* boundary conditions. In the field theory describing the thermodynamic limit of the lattice model, these cases correspond to the Ramond (R) and Neveu-Schwarz (NS) sector, respectively.

Due to the Yang-Baxter equations (II.8), the two transfer matrices commute with each other, in addition to commuting among themselves,

$$[\tau_3(\lambda), \tau_{\bar{3}}(\mu)] = 0 \quad \forall \lambda, \mu. \quad (\text{II.10})$$

Local integrals of motion are generated by the double row transfer matrix

$$\tau(\lambda) = \tau_3(\lambda)\tau_{\bar{3}}(\lambda). \quad (\text{II.11})$$

For example, the Hamiltonian¹⁴ of the mixed $U_q[sl(2|1)]$ superspin chain is defined by

$$\mathcal{H} = i \frac{\partial}{\partial \lambda} \log \tau(\lambda) \Big|_{\lambda=0}. \quad (\text{II.12})$$

The transfer matrix (II.11) (and therefore \mathcal{H} as well as other conserved charges) can be diagonalized using the nested Algebraic Bethe Ansatz (see 1.2 in part I). The resulting expressions obtained within this framework depend on the choice of grading for the underlying superalgebra [47, 49, 95–97]. Note, the expressions above for the \mathcal{R} -matrices are valid for all possible gradings. As in refs. [20, 21] we choose $[p_1, p_2, p_3] = [0, 1, 0]$.

We now explicitly diagonalize the transfer matrix for periodic boundary conditions, $\alpha = 0$, by following the calculation in [98]. Since the two different single row transfer matrices commute with each other, $[\tau_3(\lambda), \tau_{\bar{3}}(\mu)] = 0$, it is sufficient to diagonalize τ_3 .

As discussed in part I, the most important fundament for applying nested Bethe Ansatz techniques is the existence of a suitable reference state. We may use the state¹⁵

$$|0\rangle = |0^{(3)}\rangle_1 \otimes |0^{(\bar{3})}\rangle_2 \otimes |0^{(3)}\rangle_3 \dots \otimes |0^{(\bar{3})}\rangle_{2L} \quad (\text{II.13})$$

with

$$|0^{(3)}\rangle_j = \begin{pmatrix} 1 \\ 0 \\ 0 \end{pmatrix} \quad \text{and} \quad |0^{(\bar{3})}\rangle_j = \begin{pmatrix} 0 \\ 0 \\ 1 \end{pmatrix}. \quad (\text{II.14})$$

To prove that $|0\rangle$ is an appropriate reference state we consider the action of the Lax operators¹⁶ on $|0\rangle$,

$$\mathcal{R}_{A,j}^{(3,3)}(\lambda) |0^{(3)}\rangle_j = \begin{pmatrix} h_1(\lambda) & \# & \# \\ 0 & h_2(\lambda) & 0 \\ 0 & 0 & h_3(\lambda) \end{pmatrix} |0^{(3)}\rangle_j \quad (\text{II.15})$$

¹⁴Note, for this model, $\mathcal{R}^{(3,3)}$ and $\mathcal{R}^{(\bar{3},\bar{3})}$ turn to graded permutation operators at the shift point $\lambda = 0$.

¹⁵Note, there is a different scheme of performing the nested Algebraic Bethe Ansatz for this model and related superspin chains in which the reference state remains undetermined, besides belonging to a certain subspace [97].

¹⁶By the way the monodromy matrices in (II.9) are built we may interpret the \mathcal{R} -matrices as Lax operators.

and

$$\mathcal{R}_{A,j}^{(3,\bar{3})}(\lambda - i\gamma) |0^{(\bar{3})}\rangle_j = \begin{pmatrix} g_1(\lambda) & 0 & \# \\ 0 & g_2(\lambda) & \# \\ 0 & 0 & g_3(\lambda) \end{pmatrix} |0^{(\bar{3})}\rangle_j \quad (\text{II.16})$$

where $\#$ signifies non-zero entries. The diagonal entries are determined by the functions h_i and g_i ,

$$h_i(\lambda) = \begin{cases} 1 & i = 1 \\ b(\lambda) & i = 2, 3 \end{cases} \quad (\text{II.17})$$

$$g_i(\lambda) = \begin{cases} b(-\lambda - i\gamma) & i = 1, 2 \\ 1 & i = 3 \end{cases}. \quad (\text{II.18})$$

Inspired by the structure of the monodromy matrix for $su(n)$ -symmetric models [41] we impose the following Ansatz for the structure of $T_3(\lambda)$ written in the auxiliary space,

$$T_3(\lambda) = \begin{pmatrix} A(\lambda) & B_1(\lambda) & B_2(\lambda) \\ C_1(\lambda) & D_{1,1}(\lambda) & D_{1,2}(\lambda) \\ C_2(\lambda) & D_{2,1}(\lambda) & D_{2,2}(\lambda) \end{pmatrix} \quad (\text{II.19})$$

where $A(\lambda), B_i(\lambda), C_i(\lambda)$ and $D_{i,j}(\lambda)$ are operators acting on the Hilbert space. Given this structure, we may write for the transfer matrix

$$\tau_3(\lambda) = A(\lambda) - D_{1,1}(\lambda) + D_{2,2}(\lambda), \quad (\text{II.20})$$

thus, the eigenvalue problem for τ_3 becomes

$$(A(\lambda) - D_{1,1}(\lambda) + D_{2,2}(\lambda)) |\phi\rangle = \Lambda_3(\lambda) |\phi\rangle. \quad (\text{II.21})$$

By means of eqs. (II.15) and (II.16), the action of the elements of the monodromy matrix on reference state can be calculated,

$$A(\lambda) |0\rangle = g_1(\lambda)^L |0\rangle, \quad (\text{II.22})$$

$$D_{i,i}(\lambda) |0\rangle = f_{i+1}(\lambda)^L g_{i+1}(\lambda)^L |0\rangle, \quad i = 1, 2, \quad (\text{II.23})$$

$$B_i(\lambda) |0\rangle = \#, \quad (\text{II.24})$$

$$C_i(\lambda) |0\rangle = 0, \quad (\text{II.25})$$

$$D_{2,1}(\lambda) |0\rangle = 0, \quad (\text{II.26})$$

$$D_{1,2}(\lambda) |0\rangle = \#, \quad (\text{II.27})$$

which finally proves that $|0\rangle$ is in fact a suitable reference state as it fulfills the require-

ments presented in part I. The equations (II.22)-(II.27) further shows that $B_i(\lambda)$ act as creation operators w.r.t. $|0\rangle$. Therefore, we are led to impose the following Ansatz for the eigenstates of the transfer matrix,

$$|\phi\rangle = \sum_{i_1 \dots i_{N_1}=1,2} F^{i_{N_1} \dots i_1} B_{i_1}(\lambda_1^{(1)}) \dots B_{i_{N_1}}(\lambda_{N_1}^{(1)}) |0\rangle \quad (\text{II.28})$$

with a positive integer N_1 and coefficients $F^{i_{N_1} \dots i_1}$. To solve the eigenvalue problem we need to commute the operators $A(\lambda)$ and $D_{i,i}(\lambda)$ through $B_i(\lambda_j^{(1)})$, hence, we need to know their commutation relations. The latter can be obtained by the RTT equations, (I.4), and read [98]

$$\begin{aligned} A(\lambda)B_j(\mu) &= \frac{B_j(\mu)A(\lambda)}{b(\mu-\lambda)} - \frac{c(\mu-\lambda)e^{-2(\mu-\lambda)}}{b(\mu-\lambda)} B_j(\lambda)A(\mu), \\ D_{i,j}(\lambda)B_k(\mu) &= \sum_{l,q} \frac{B_l(\mu)D_{i,g}(\lambda)}{b(\lambda-\mu)} \check{r}^{(1)}(\lambda-\mu)_{lq}^{jk} (-1)^{p_i+1p_l+1} \\ &\quad - \frac{c(\lambda-\mu)}{b(\lambda-\mu)} B_j(\lambda)D_{i,k}(\mu) (-1)^{p_j+1p_i+1}, \\ B_i(\lambda)B_j(\mu) &= \sum_{l,q} \check{r}^{(1)}(\lambda-\mu)_{lq}^{ij} B_l(\mu)B_q(\lambda) \end{aligned} \quad (\text{II.29})$$

where $\check{r}^{(1)}(\lambda-\mu)_{lq}^{ij}$ are the elements of the \mathcal{R} -matrix for the $U_q[sl(1|1)]$ model [98].

Hence, commuting the fields $A(\lambda)$ and $D_{i,i}(\lambda)$ through $B_i(\lambda_j^{(1)})$ creates terms proportional to $|\phi\rangle$ by considering the first terms on the right hand side in (II.29), i.e. the terms which do not change the argument of the operators. On the other hand, also terms which are *not* proportional to $|\phi\rangle$ occur. Those are called *unwanted terms*. Demanding the unwanted terms to vanish yields for the eigenvalue of the transfer matrix $\tau_3(\lambda)$

$$\Lambda_3(\lambda) = b(-\lambda - i\gamma)^L \prod_{j=1}^{N_1} \frac{1}{b(\lambda - \lambda_j^{(1)})} + \prod_{j=1}^{N_1} \frac{1}{b(\lambda - \lambda_j^{(1)})} \Lambda^{(1)}(\lambda, \{\lambda_k^{(1)}\}), \quad (\text{II.30})$$

given that the *Bethe roots on the first level* $\{\lambda_k^{(1)}\}$ fulfill the Bethe Ansatz equations

$$b(-\lambda_j^{(1)} - i\gamma)^L \prod_{k=1, k \neq j}^{N_1} \frac{b(\lambda_k^{(1)} - \lambda_j^{(1)} - i\gamma)}{b(\lambda_j^{(1)} - \lambda_k^{(1)} - i\gamma)} = \Lambda^{(1)}(\lambda_j^{(1)}, \{\lambda_k^{(1)}\}). \quad (\text{II.31})$$

Within this framework, the Bethe Ansatz equations can be understood as consistency equations for a state of type (II.28) to be an eigenstate of the transfer matrix and, thus, of the Hamiltonian of the model.

The function $\Lambda^{(1)}$ is defined in terms of a different, *nested* eigenvalue problem,

$$\sum_{j_1, \dots, j_{N_1}=1,2} \tau_3^{(1)}(\lambda, \{\lambda_k^{(1)}\})_{i_1 \dots j_{N_1}}^{j_1 \dots j_{N_1}} F^{i_1 \dots i_{N_1}} |0\rangle = \Lambda^{(1)}(\lambda, \{\lambda_k^{(1)}\}) F^{i_1 \dots i_{N_1}} |0\rangle \quad (\text{II.32})$$

with the nested transfer matrix

$$\begin{aligned} \tau_3^{(1)}(\lambda, \{\lambda_k^{(1)}\})_{i_1 \dots j_{N_1}}^{j_1 \dots j_{N_1}} &= \sum_{k_1 \dots k_{N_1}=1,2} \sum_{m=1,2} (-1)^{p_{m+1}} \binom{N_1}{1 + \sum_{l=1}^{N_1} p_{k_l+1}} \\ &\times \check{r}^{(1)}(\lambda - \lambda_1^{(1)})_{i_1 k_1}^{m j_1} \check{r}^{(1)}(\lambda - \lambda_1^{(1)})_{i_2 k_2}^{k_1 j_2} \dots \check{r}^{(1)}(\lambda - \lambda_{N_1}^{(1)})_{i_{N_1} k_{N_1}}^{k_{N_1-1} j_{N_1}} D_{m, k_{N_1}}(\lambda). \end{aligned} \quad (\text{II.33})$$

This problem can again be solved by Algebraic Bethe Ansatz methods [98]. Equation (II.33) may be viewed as supertrace of an auxiliary monodromy matrix $T_3^{(1)}$,

$$T_3^{(1)}(\lambda, \{\lambda_k^{(1)}\}) = \underline{D}_{\mathcal{A}^{(1)}} r_{\mathcal{A}^{(1)}, N_1}^{(1)}(\lambda - \lambda_{N_1}^{(1)}) r_{\mathcal{A}^{(1)}, N_1-1}^{(1)}(\lambda - \lambda_{N_1-1}^{(1)}) \dots r_{\mathcal{A}^{(1)}, 1}^{(1)}(\lambda - \lambda_1^{(1)}). \quad (\text{II.34})$$

where $r_{\mathcal{A}^{(1)}, j}^{(1)}(\lambda) = P_{\mathcal{A}^{(1)}, j} \check{r}_{\mathcal{A}^{(1)}, j}^{(1)}(\lambda)$ with the graded permutation operator P and \underline{D} the 2×2 matrix with elements $D_{i,j}$. Note, the auxiliary space for $T_3^{(1)}(\lambda)$ is now $\mathcal{A}^{(1)} \cong \mathbb{C}^2$. The monodromy matrix $T_3^{(1)}(\lambda)$ and the \mathcal{R} -matrix $r^{(1)}(\lambda)$ fulfill also an RTT relation,

$$\begin{aligned} \check{r}^{(1)}(\lambda - \mu) T_3^{(1)}(\lambda, \{\lambda_k^{(1)}\}) \otimes T_3^{(1)}(\mu, \{\lambda_k^{(1)}\}) \\ = T_3^{(1)}(\mu, \{\lambda_k^{(1)}\}) \otimes T_3^{(1)}(\lambda, \{\lambda_k^{(1)}\}) \check{r}^{(1)}(\lambda - \mu) \end{aligned} \quad (\text{II.35})$$

where the tensor product has to be performed with respect to new parities $p_\alpha^{(1)} = p_{\alpha+1}$, $\alpha = 1, 2$. To solve the nested problem, we impose a nested pseudovacuum state [99],

$$|0\rangle^{(1)} = |0\rangle \otimes \prod_{j=1}^{N_1} \begin{pmatrix} 1 \\ 0 \end{pmatrix}_j. \quad (\text{II.36})$$

The nested monodromy matrix $T_3^{(1)}$ written in auxiliary space reads

$$T_3^{(1)}(\lambda, \{\lambda_k^{(1)}\}) = \begin{pmatrix} A^{(1)}(\lambda) & B^{(1)}(\lambda) \\ C^{(1)}(\lambda) & D^{(1)}(\lambda) \end{pmatrix}. \quad (\text{II.37})$$

Its matrix elements applied to the nested pseudovacuum yield

$$A^{(1)}(\lambda, \{\lambda_k^{(1)}\}) |0\rangle^{(1)} = b(\lambda)^L b(-\lambda - i\gamma)^L \prod_{j=1}^{N_1} a_2(\lambda - \lambda_j^{(1)}) |0\rangle^{(1)}, \quad (\text{II.38})$$

$$D^{(1)}(\lambda, \{\lambda_k^{(1)}\}) |0\rangle^{(1)} = b(\lambda)^L \prod_{j=1}^{N_1} b(\lambda - \lambda_j^{(1)}) |0\rangle^{(1)}, \quad (\text{II.39})$$

$$C^{(1)}(\lambda, \{\lambda_k^{(1)}\}) |0\rangle^{(1)} = 0, \quad (\text{II.40})$$

$$B^{(1)}(\lambda, \{\lambda_k^{(1)}\}) |0\rangle^{(1)} = \# . \quad (\text{II.41})$$

Thus, the auxiliary model we have to diagonalize strongly recalls the famous six vertex model [98]. Hence our Ansatz for eigenstates of (II.33) is given by

$$|\phi\rangle^{(1)} = B(\lambda_1^{(2)})B(\lambda_2^{(2)})\dots B(\lambda_{N_2}^{(2)}) |0\rangle^{(1)} \quad (\text{II.42})$$

with the Bethe roots on the second level, $\{\lambda_k^{(2)}\}$. Again, we can commute the operators $A^{(1)}(\lambda)$ and $D^{(1)}(\lambda)$ through $B^{(1)}(\lambda_j^{(2)})$ and demand the unwanted terms to vanish. This calculation yields for the eigenvalue of $\tau_3^{(1)}(\lambda)$,

$$\begin{aligned} \Lambda^{(1)}(\lambda, \{\lambda_k^{(1)}\}) &= -b(\lambda)^L b(-\lambda - i\gamma)^L \prod_{j=1}^{N_1} a_2(\lambda - \lambda_j^{(1)}) \prod_{k=1}^{N_2} \frac{a_2(-\lambda + \lambda_k^{(2)})}{b(-\lambda + \lambda_k^{(2)})} \\ &+ b(\lambda)^L \prod_{j=1}^{N_1} b(\lambda - \lambda_j^{(1)}) \prod_{k=1}^{N_2} \frac{1}{b(\lambda - \lambda_k^{(2)})} \end{aligned} \quad (\text{II.43})$$

provided that the Bethe roots $\{\lambda_k^{(2)}\}$ fulfill a second set of Bethe Ansatz equations,

$$\begin{aligned} b(-\lambda_j^{(2)} - i\gamma)^L &= \prod_{k=1}^{N_1} \frac{b(\lambda_j^{(2)} - \lambda_k^{(1)})}{a_2(\lambda_j^{(2)} - \lambda_k^{(1)})} \\ &\times \prod_{\substack{k=1 \\ k \neq j}}^{N_2} \frac{1}{a_2(\lambda_k^{(2)} - \lambda_j^{(2)})} \frac{b(\lambda_k^{(2)} - \lambda_j^{(2)})}{b(\lambda_j^{(2)} - \lambda_k^{(2)})}. \end{aligned} \quad (\text{II.44})$$

To simplify the results of this calculation we may use the definitions above. Thereby we arrive at a symmetrical formulation of the Bethe Ansatz equations for the $U_q[sl(2|1)]$ model. By taking into account general toroidal boundary conditions imposed by the matrix \mathcal{G} in the monodromy matrix¹⁷, see eq. (II.9), we arrive at

$$\begin{aligned} \left[\frac{\sinh(\lambda_j^{(1)} + i\gamma)}{\sinh(\lambda_j^{(1)} - i\gamma)} \right]^L &= e^{i\alpha} \prod_{k=1}^{N_2} \frac{\sinh(\lambda_j^{(1)} - \lambda_k^{(2)} + i\gamma)}{\sinh(\lambda_j^{(1)} - \lambda_k^{(2)} - i\gamma)}, \quad j = 1, \dots, N_1, \\ \left[\frac{\sinh(\lambda_j^{(2)} + i\gamma)}{\sinh(\lambda_j^{(2)} - i\gamma)} \right]^L &= e^{i\alpha} \prod_{k=1}^{N_1} \frac{\sinh(\lambda_j^{(2)} - \lambda_k^{(1)} + i\gamma)}{\sinh(\lambda_j^{(2)} - \lambda_k^{(1)} - i\gamma)}, \quad j = 1, \dots, N_2. \end{aligned} \quad (\text{II.45})$$

Note, the numbers N_1 and N_2 were defined as parametrizing the number of Bethe roots on each level. However, they correspond to different sectors of the Hilbert space

¹⁷Since \mathcal{G} is diagonal, it does not break the integrability. It only affects the exact diagonalization by introducing overall factors in the operators entering the monodromy matrix.

with fixed quantum numbers related to the $U(1)$ subalgebras of $U_q[sl(2|1)]$, i.e. charge $b = (N_1 - N_2)/2$ and z -component of the spin $j_3 = L - (N_1 + N_2)/2$.

The corresponding eigenvalue of the single row transfer matrices τ_3 and $\tau_{\bar{3}}$ reads for periodic boundary conditions $\alpha = 0$ [21],

$$\begin{aligned} \Lambda_3(\lambda) &= \left(\frac{\sinh \lambda + i\gamma}{\sinh \lambda - i\gamma} \right)^L \prod_{j=1}^{N_1} \frac{\sinh \lambda_j^{(1)} - \lambda + i\gamma}{\sinh \lambda_j^{(1)} - \lambda - i\gamma} \\ &+ \left(\frac{\sinh \lambda}{\sinh \lambda + 2i\gamma} \right)^L \prod_{j=1}^{N_2} \frac{\sinh \lambda - \lambda_j^{(2)} + 2i\gamma}{\sinh \lambda - \lambda_j^{(2)}} \\ &- \left(\frac{\sinh \lambda + i\gamma}{\sinh \lambda - i\gamma} \frac{\sinh \lambda}{\sinh \lambda + 2i\gamma} \right)^L \prod_{j=1}^{N_1} \frac{\sinh \lambda - \lambda_j^{(1)} - i\gamma}{\sinh \lambda - \lambda_j^{(1)} + i\gamma} \prod_{j=1}^{N_2} \frac{\sinh \lambda_j^{(2)} - \lambda - 2i\gamma}{\sinh \lambda_j^{(2)} - \lambda}, \end{aligned} \quad (\text{II.46})$$

$$\begin{aligned} \Lambda_{\bar{3}}(\lambda) &= \left(\frac{\sinh \lambda + i\gamma}{\sinh \lambda - i\gamma} \right)^L \prod_{j=1}^{N_2} \frac{\sinh \lambda_j^{(2)} - \lambda + i\gamma}{\sinh \lambda_j^{(2)} - \lambda - i\gamma} \\ &+ \left(\frac{\sinh \lambda}{\sinh \lambda + 2i\gamma} \right)^L \prod_{j=1}^{N_1} \frac{\sinh \lambda - \lambda_j^{(1)} + 2i\gamma}{\sinh \lambda - \lambda_j^{(1)}} \\ &- \left(\frac{\sinh \lambda + i\gamma}{\sinh \lambda - i\gamma} \frac{\sinh \lambda}{\sinh \lambda + 2i\gamma} \right)^L \prod_{j=1}^{N_2} \frac{\sinh \lambda - \lambda_j^{(2)} - i\gamma}{\sinh \lambda - \lambda_j^{(2)} + i\gamma} \prod_{j=1}^{N_1} \frac{\sinh \lambda_j^{(1)} - \lambda - 2i\gamma}{\sinh \lambda_j^{(1)} - \lambda}. \end{aligned} \quad (\text{II.47})$$

Due to the symmetry of both the Bethe Ansatz equations and the eigenvalues Λ_3 and $\Lambda_{\bar{3}}$, swapping the Bethe roots on both levels $\{\lambda_k^{(1)}\} \leftrightarrow \{\lambda_k^{(2)}\}$ results in an exchange of the eigenvalues, $\Lambda_3 \leftrightarrow \Lambda_{\bar{3}}$.

Finally, the eigenvalue of the Hamiltonian (II.12) is given by

$$\begin{aligned} E(\{\lambda_j^{(1)}\}, \{\lambda_j^{(2)}\}) &= i \frac{\partial}{\partial \lambda} \log \Lambda(\lambda) \Big|_{\lambda=0} \\ &= 4L \cot(\gamma) + 2 \sum_{a=1,2} \sum_{k=1}^{N_a} \frac{\sin(2\gamma)}{\cos(2\gamma) - \cosh(2\lambda_k^{(a)})}. \end{aligned} \quad (\text{II.48})$$

In the large L limit, the possible root configurations solving the Bethe equations (II.45) can be classified using the string hypothesis [20, 21]. A class of low-energy excitations in the zero charge sector $b = 0$ which we will investigate in the following has been identified with collections of $O(L)$ 'strange 2-strings'. These are complex conjugate pairs of rapidities $\lambda^{(1)} = (\lambda^{(2)})^*$ coming in two types, i.e. (\pm) with $\text{Im}(\lambda^{(1)}) = \pm\gamma/2$. Solutions to the Bethe equations consisting of N_{\pm} type- (\pm) strange strings with $N_+ + N_- = L - j_3$ for some fixed values of j_3 but $\Delta N = N_+ - N_- \neq 0$ have been found to form a continuous component of the finite size spectrum starting at levels with $\Delta N = 0$, see below and refs. [20, 21, 84]. In the rest of this section, we numerically solve the Bethe Ansatz

equations (II.45) for particular states to study the low-energy spectrum of the staggered superspin chain.

1.2 Low-energy spectrum

Since the staggered superspin chain is critical in the region $0 \leq \gamma \leq \pi$ [21], we expect its thermodynamic limit to be described by a Conformal Field Theory. Information on the effective field theory describing the low-energy degrees of freedom in the mixed superspin chain can be obtained from the finite size spectrum of the lattice model, e.g. by studying the central charge and the effective scaling dimensions, see section 3.3 in part I.

Obviously, the choice $\lambda_k^{(a)} = 0$ for $k = 1, \dots, L$, i.e. in the sector $(b, j_3) = (0, 0)$, and $a = 1, 2$, is a solution of the Bethe Ansatz equations [20, 21]. This state has the energy $E = 0$ for all system sizes and is the ground state of the periodic superspin chain for anisotropies $0 \leq \gamma \leq \pi/4$. The existence of a zero energy ground state implies that the effective central charge of the superspin chain is $c = 0$. Hence, the scaling dimensions for the $U_q[sl(2|1)]$ staggered superspin chain with a finite system size L can be determined as follows,

$$X(L) = \frac{LE(L)}{2\pi v_F} \quad (\text{II.49})$$

with the Fermi-velocity

$$v_F = \frac{\pi}{\gamma}. \quad (\text{II.50})$$

Before calculating the effective scaling dimensions for several low-energy states by numerically solving the Bethe Ansatz equations we seek towards some analytical progress. To this purpose, inspecting the sector with $N_1 = N_2 \equiv N$ and $\{\lambda_j^{(1)}\} = \{\lambda_j^{(2)}\}$ we find that the Bethe Ansatz equations (II.45) turn into the equations for the XXZ spin-1 chain with twist $\alpha - \pi$,

$$\left[\frac{\sinh \frac{1}{2}\gamma(\lambda_j + 2i)}{\sinh \frac{1}{2}\gamma(\lambda_j - 2i)} \right]^L = -e^{i\alpha} \prod_{k=1}^N \frac{\sinh \frac{1}{2}\gamma(\lambda_j - \lambda_k + 2i)}{\sinh \frac{1}{2}\gamma(\lambda_j - \lambda_k - 2i)} \quad (\text{II.51})$$

Hence, some of the scaling dimensions of primary operators in the Conformal Field Theory for the staggered superspin chain can be deduced from the known operator content of the low-energy theory for the spin-1 XXZ chain [20, 21, 100–102]. This field theory can be described in terms of composites of an $U(1)$ Kac-Moody field and Ising operators [103]. The results for the corresponding subset of scaling dimensions in the low-energy effective theory for the superspin chain based on such a mapping between the spectra of these lattice models depend on the boundary conditions and will be elaborated in the following subsections.

1.2.1 Periodic boundary conditions

For periodic boundary conditions (i.e. the Ramond sector in the effective field theory for the thermodynamic limit), this mapping yields

$$X_{(m,w)}^R = \frac{m^2}{2k} + \frac{k}{2}w^2 + \begin{cases} 0 & \text{for } m+w \in 2\mathbb{Z} \\ -\frac{1}{4} & \text{for } m+w \in 2\mathbb{Z}+1 \end{cases}, \quad (\text{II.52})$$

with $k = \pi/(\pi - 2\gamma)$ and the compactification radius $R = 1/\sqrt{2k} = \sqrt{(\pi - 2\gamma)/(2\pi)}$ of the free boson. The conformal spin of these primary fields is given by $s = mw$. Here, the integer m is the quantum number j_3 of the corresponding state in both the XXZ spin-1 model and in the superspin chain while w is related to the vorticity of the state.

Note that the level parametrized by $(m, w) = (0, 0)$ corresponds to the exact zero mode and therefore vanishes identically, $X_{(0,0)}^R = 0$. In the related spin-1 XXZ model with antiperiodic boundary conditions, the exact zero mode has been shown to be a singlet under an exact dynamical lattice supersymmetry [104].

The lowest excitation above the vacuum $(m, w) = (0, 0)$ is given by the field with scaling dimension

$$X_{(1,0)}^R = \frac{1}{2k} - \frac{1}{4} = \frac{1}{4} - \frac{\gamma}{\pi}. \quad (\text{II.53})$$

In the superspin chain, this state corresponds to a solution of the Bethe equations consisting of $(L - 1)/2$ narrow strings with centers distributed over the entire real axis [20, 21]¹⁸. This excitation becomes the highest weight state of an $sl(2|1)$ -octet $(b, j_3) = (0, 1)$ in the isotropic limit, $\gamma \rightarrow 0$.

Similarly, the lowest states in the sectors $(b, j_3) = (0, 0)$, $(b, j_3) = (0, 2)$, and $(b, j_3) = (0, 3)$ are described by Bethe root configurations with $(L - j_3)/2$ narrow strings. For $\gamma = 0$, the first of these is the highest weight singlet state within the $sl(2|1)$ -indecomposable $(0, -\frac{1}{2}, \frac{1}{2}, 0)$ and degenerates with the octet, see [20]. The finite size energy gaps of these levels are described by the scaling dimensions $X_{0,1}^R$, $X_{2,0}^R$, and $X_{3,0}^R$, respectively, see fig. 8 where our results from numerically solving the Bethe Ansatz equations for these sectors are presented.

Excitations with $U_q[sl(2|1)]$ quantum numbers $(b, j_3) = (0, 1)$ but outside of the XXZ spin-1 set of levels have been studied in refs. [20, 21]. They correspond to root configurations of N_+ type + and N_- type - strange strings with $N_+ + N_- = L - 1$ but $\Delta N = N_+ - N_- \neq 0$. In the thermodynamic limit, these form a continuum of scaling dimensions starting at $X_{1,0}^R$ leading to a logarithmic fine structure of levels which is

¹⁸Note that for $\pi/4 < \gamma < \pi/2$ the scaling dimensions (II.53) become negative and the singlet ground state disappears within the continuum.

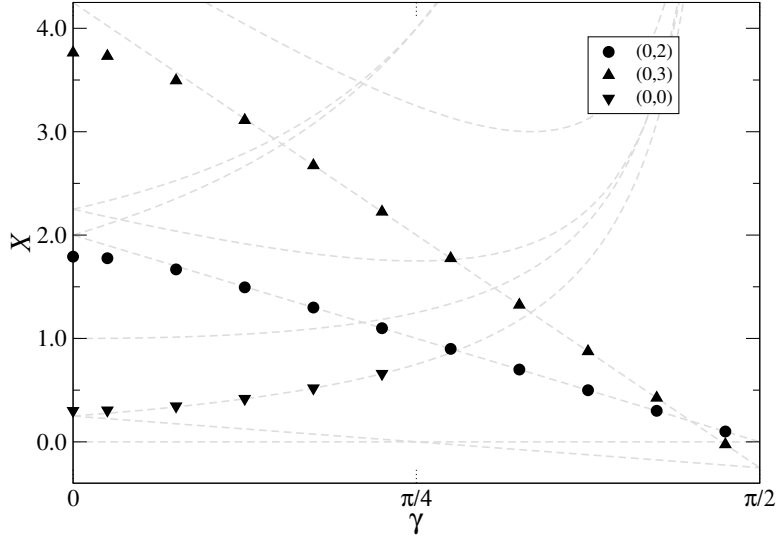


Figure 8: Scaling dimensions for the ground states of the periodic superspin chain (Ramond sector) in sectors (b, j_3) as a function of the anisotropy γ : symbols denote data extracted from the finite size spectra for system size $L = 1024$ for j_3 even ($L = 1025$ for j_3 odd). Dashed lines are the predictions (II.52) from Conformal Field Theory. The deviations of the finite size data for small γ are a consequence of the appearance of a marginal operator at $\gamma = 0$.

determined by the number ΔN for large but finite L ,

$$X_{(1,0)}^R(\Delta N) \simeq X_{(1,0)}^R + A(\gamma) \left[\frac{\Delta N}{\log(L/L_0(\gamma))} \right]^2, \quad (\text{II.54})$$

with an amplitude A and a non-universal length scale L_0 depending on the anisotropy, see fig. 9.

We have extended the investigation of zero charge states with $\Delta N \neq 0$ to sectors with different j_3 .

$(b, j_3) = (0, 3)$: Similarly to the sector $(b, j_3) = (0, 1)$, we have been able to identify a family of excitations described by configurations of $(L-3)/2$ strange 2-strings with varying ΔN . The finite size energies show a strong logarithmic dependence on the system size. Assuming a rational dependence on $1/\log L$, all of them extrapolate to $X_{(3,0)}^R$, see fig. 10. The subleading corrections are quadratic in ΔN with an amplitude consistent with those in eq. (II.54).

$(b, j_3) = (0, 2)$: For small system sizes L we have found root configurations of $(L-2)/2$ strange 2-strings and $\Delta N = 1$. As L is increased, however, these configurations degenerate into a collection of narrow strings and an additional pair of roots $\lambda^{(1)} = 0 = \lambda^{(2)}$, i.e. from the subsector of the spectrum of zero charge states related to that of the spin-1 XXZ model.

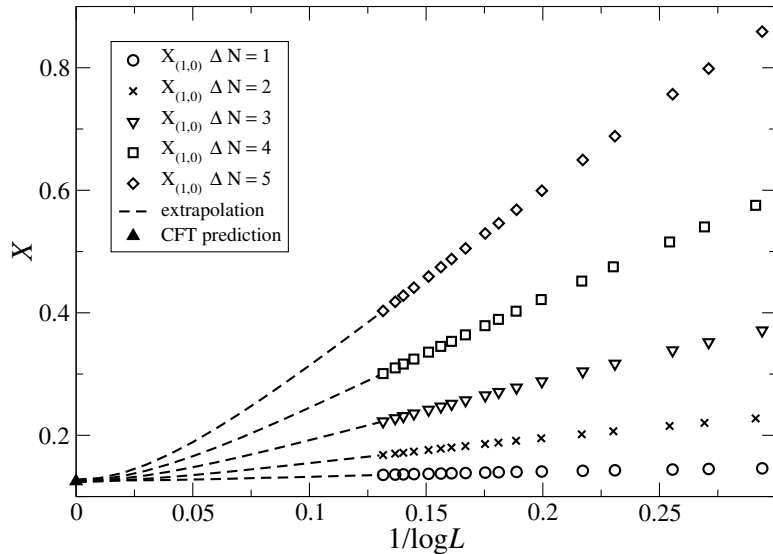


Figure 9: Finite size scaling dimensions of the lowest states for periodic boundary conditions (Ramond sector) in the $(b, j_3) = (0, 1)$ sector for $\gamma = \pi/8$. The results contained in this figure were calculated by numerically solving the Bethe Ansatz equations (II.45). Dashed lines are the results of an extrapolation assuming a rational dependence [105] of the finite size data on $1/\log L$.

$(b, j_3) = (0, 0)$ the lowest state in this sector (with $\Delta N = 0$) has finite momentum and a root configuration which is not symmetric under the reflection $\lambda^{(a)} \rightarrow -(\lambda^{(a)})^*$. We have not been able to identify a solution with $\Delta N \neq 0$.

1.2.2 Antiperiodic boundary conditions

For antiperiodic boundary conditions, $\alpha = \pi$, due to the matrix \mathcal{G} , the transfer matrices are defined by taking the trace rather than the supertrace over auxiliary space in (II.9). Also, the factor $e^{i\alpha}$ leads to an extra sign in the Bethe Ansatz equations (II.45). As discussed above, a part of the spectrum in the zero charge sector of the superspin chain can be related to that of the spin-1 XXZ chain, in this case with periodic boundary conditions. From this mapping we obtain the following scaling dimensions for antiperiodic boundary conditions for the fermionic fields, i.e. in the Neveu-Schwarz sector in the effective field theory for the thermodynamic limit,

$$X_{(m,w)}^{NS} = \frac{m^2}{2k} + \frac{k}{2}w^2 + \begin{cases} -\frac{1}{4} & \text{for } m + w \in 2\mathbb{Z} \\ 0 & \text{for } m + w \in 2\mathbb{Z} + 1 \end{cases}. \quad (\text{II.55})$$

Note, the lowest state for antiperiodic boundary conditions is realized in the sector $(b, j_3) = (0, 0)$ and thus has a scaling dimension $X_{(0,0)}^{NS} = -\frac{1}{4}$, leading to an effective central charge $c_{\text{eff}} = 3$. For even L it is realized in the XXZ subspace of this sector. Hence,

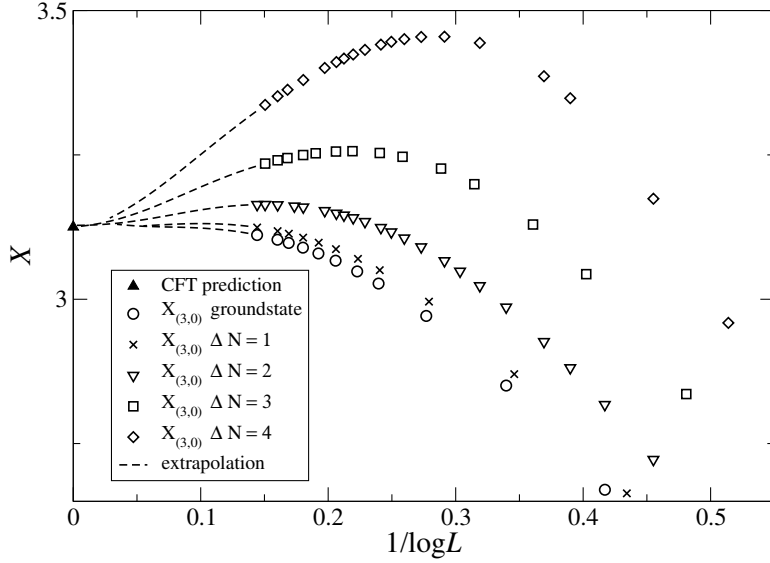


Figure 10: Finite size scaling dimensions of the lowest states for periodic boundary conditions (Ramond sector) in the $(b, j_3) = (0, 3)$ sector for $\gamma = \pi/8$. The results contained in this figure were calculated by numerically solving the Bethe Ansatz equations (II.45). Dashed lines are the results of an extrapolation assuming a rational dependence of the finite size data on $1/\log L$.

the corresponding Bethe root configuration can be mapped to that of the singlet ($j_3 = 0$) ground state of the periodic spin-1 chain. However, for odd L the lowest state is doubly degenerate. One of the Bethe root configurations for this state consists of $N_{\pm} = (L \pm 1)/2$ type-(\pm) strange 2-strings, i.e. $\Delta N = 1$. Other excitations above the ground state can be constructed by increasing ΔN . The scaling dimensions of these states exhibit a logarithmic dependence on the system size, $X_{(0,0)}^{NS}(L) = -\frac{1}{4} + O((\Delta N / \log L)^2)$ [20, 21], consistent with the emergence of a continuum of levels starting at $X^{\text{eff},NS}(0,0) = -\frac{1}{4}$ in the thermodynamic limit, see fig. 11 for finite size data of the states with $\Delta N = 1, 2, 3, 4, 5$. Note, states with odd ΔN are realized for odd system sizes only while for an even ΔN the system size L has to be even.

1.2.3 Conformal Field Theory for the isotropic model

Based on these insights from the lattice model it has been argued that the thermodynamic limit of the isotropic superspin chain flows to a $SU(2|1)$ Wess-Zumino-Novikov-Witten (WZNW) model at level $k = 1$ [20, 87]. These models are certain Conformal Field Theories based on Lie (super-) groups by means of an action involving a coupling constant k which will be referred to as *level* of the theory¹⁹. Investigating the commutation relations for the modes of the conserved currents within the corresponding action

¹⁹Note, although often restricted to $k \in \mathbb{Z}$ by topological arguments, there is no such restrictions for the WZNW model based on the non-compact Lie group $SL(2, \mathbb{R})$ [106] which turns out to be the model of special interest in the context of this work, see e.g. [23–26].

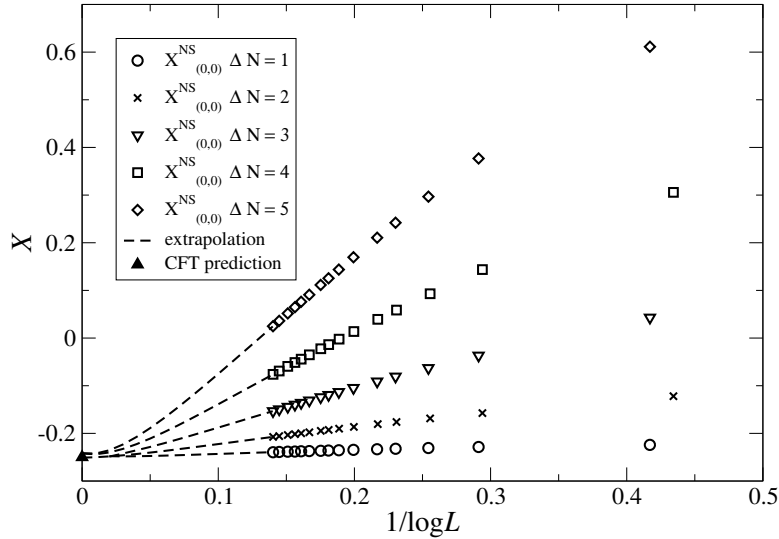


Figure 11: Finite size scaling dimensions of the lowest excitations above the ground state for antiperiodic boundary conditions (Neveu-Schwarz sector) for $\gamma = \pi/8$. The results contained in this figure were calculated by numerically solving the Bethe Ansatz equations (II.45). Dashed lines are the results of an extrapolation assuming a rational dependence of the finite size data on $1/\log L$.

functional it is easy to see that the currents are the generators of an affine Kac-Moody (super-) algebra. By means of the *Sugawara construction* it can be shown that WZNW models are in fact Conformal Field Theories. More details can be found in [58].

The generic class I irreducible representations of the affine superalgebra $\hat{sl}(2|1)_k$ are built over the typical representations (b, j) with charge $b \in \mathbb{C}$ and spin $j = \frac{1}{2}, 1, \dots, \frac{k}{2}$. Their ground states have conformal weight

$$\Delta_{[b,j]}^R = \frac{j^2 - b^2}{k + 1}. \quad (\text{II.56})$$

Bowcock *et al* have computed the characters for these representations [107]. At level $k = 1$ the Ramond characters can be expressed in terms of the integrable $\hat{sl}(2)_1$ characters $\chi_\ell(z, q)$, $\ell = 0, \frac{1}{2}$, as

$$\chi_{[b, \frac{1}{2}]}^R(z, \zeta, q) = \frac{q^{-b^2/2} \zeta^b}{\eta(q)} \left(\chi_0(z, q) \chi_{\frac{1}{2}}(\zeta, q) + \chi_{\frac{1}{2}}(z, q) \chi_0(\zeta, q) \right) \quad (\text{II.57})$$

where the variables z , ζ , and q keep track of spin j_3 , charge b , and conformal weight of the states in the module, respectively. With (II.57) the contribution

$$\chi_{[b, j_+ = \frac{1}{2}]}^R(z, \zeta, q) \chi_{[-b, j_- = \frac{1}{2}]}^R(z, \zeta, \bar{q}) \quad (\text{II.58})$$

to the partition function with $b = 0$ yields a spectrum of scaling dimensions $X^R \in \mathbb{N}_0 + \frac{1}{4}$

with conformal weights $(\Delta^R, \bar{\Delta}^R) = (\frac{1}{8}, \frac{1}{8})$ of the lowest states. The latter can be decomposed into an $sl(2|1)$ octet $[0, 1]$ and an eight-dimensional indecomposable, which are degenerate in the isotropic $3 \otimes \bar{3}$ superspin chain [20]. The charge quantum number b takes discrete values $b \in \mathbb{Z}/2$ in the lattice model.

Requiring modular invariance, however, this restriction leads to a spectrum of conformal weights which is unbounded from below. For a physical partition function which can be compared with the spectrum of the lattice model, we are therefore forced to consider continuous values of b which, after analytical continuation $b \rightarrow i\beta$, yields continua of conformal weights starting at $X^R = n + \frac{1}{4}$ [87].

Note, however, that this proposal does not capture the primary fields with integer scaling dimension (i.e. $m + n$ even in (II.52)), in particular the $sl(2|1)$ singlet state with $\Delta^R = \bar{\Delta}^R = 0$. Since modular invariance appears to preclude the appearance of this singlet on its own it has been argued in ref. [87] that this state is an artifact of the lattice model and disappears in the continuum.

1.3 Quasimomentum: Characterization of the continuous spectrum

In the previous subsections, it has been shown that above the lowest states in the sectors $(b, j_3) = (0, 1)$ and $(b, j_3) = (0, 3)$ for periodic boundary conditions as well as $(b, j_3) = (0, 0)$ for antiperiodic boundary conditions, there exists a continuum of levels with the same scaling dimension in the Conformal Field Theory describing the thermodynamic limit. This subsection is dedicated to a characterization of these continuous components of the spectrum in terms of the eigenvalues of an operator. To this purpose, it is tempting to try to connect the integer ΔN with a conserved quantity of the mixed superspin chain. Clearly, ΔN cannot be related to one of the $U_q[sl(2|1)]$ charges b and j_3 . Note, however, that under the \mathbb{Z}_2 symmetry $(b, j_3) \rightarrow (-b, j_3)$ of the model, the sets of rapidities $\{\lambda_j^{(1)}\}$ and $\{\lambda_j^{(2)}\}$ are interchanged leading to a reversal of the sign of ΔN .

In a notable work Ikhlef *et al.* [24] were interested in the very same question but for the \mathbb{Z}_2 -staggered six-vertex model. This model also exhibits continuous components of the spectrum. For a characterization of the latter they introduced a quasimomentum operator \mathcal{K} , see also refs. [25, 26]. Its (real) eigenvalues K have been identified with the quantum number parametrizing the spin j of the $SL(2, \mathbb{R})$ affine primaries from the continuous series, $j = -1/2 + iK$ [24]. Based on this identification, the staggered six-vertex model has been argued to be described by the $SL(2, \mathbb{R})/U(1)$ Euclidean black hole CFT in the thermodynamic limit. However, Bazhanov *et al.* recently showed that the density of descendant states does not coincide with the expectations from the $SL(2, \mathbb{R})/U(1)$ CFT [90]. So the question of identifying the CFT for the thermodynamic limit of the staggered six-vertex model remains unanswered although

the quasimomentum operator enabled huge progress.

Hence, we aim for a definition of a similar operator for the superspin chain studied here, the mixed $U_q[sl(2|1)]$ model. We may define a *quasimomentum operator* \mathcal{K} by means of

$$\mathcal{K} = \frac{\gamma}{2\pi(\pi - 2\gamma)} \log \left(\tau^{(3)}(\lambda) \left[\tau^{(\bar{3})}(\lambda) \right]^{-1} \right) \Big|_{\lambda=0}. \quad (\text{II.59})$$

Its eigenvalues are parametrized by the Bethe roots according to

$$K(\{\lambda_j^{(1)}\}, \{\lambda_j^{(2)}\}) = \frac{\gamma}{2\pi(\pi - 2\gamma)} \times \left(\sum_{k=1}^{N_1} \log \left(\frac{\sinh(\lambda_k^{(1)} + i\gamma)}{\sinh(\lambda_k^{(1)} - i\gamma)} \right) - \sum_{k=1}^{N_2} \log \left(\frac{\sinh(\lambda_k^{(2)} + i\gamma)}{\sinh(\lambda_k^{(2)} - i\gamma)} \right) \right). \quad (\text{II.60})$$

By construction, this operator commutes with the Hamiltonian (II.12). For a staggered model as the one considered here, it belongs to an expansion of a different (compared to e.g. the Hamiltonian and momentum operator) combination of the single-row transfer matrices, i.e. $\tau^{(3)}(\lambda)[\tau^{(\bar{3})}(\lambda)]^{-1}$, whose logarithm, unlike (II.11), is *odd* under the exchange of the 3 and $\bar{3}$ representation. As an immediate consequence, $K = 0$ for the levels from the spin-1 XXZ chain subset of the spectrum.

Following the mentioned previous work on the staggered six-vertex model [24–26], we are led to study the dependence of the quasimomentum eigenvalue K on ΔN for states belonging to several continua. Hence, we solved the Bethe Ansatz equations (II.45) numerically for some $\Delta N > 0$ and system sizes up to $L \leq 2000$ in the sectors $(b, j_3) = (0, 1)$ and $(b, j_3) = (0, 3)$ in the Ramond sector. We find that the ratio $\Delta N/K$ is a linear function of $\log(L)$ for sufficiently large L , see fig. 12.

Note, for the $\Delta N = 1$ excitation in the sector $(0, 3)$, the corrections to this behaviour are larger but appear to approach the same γ -dependent line asymptotically.

The same observation can be found when studying the continuum of excitations above the ground state with quantum numbers $(b, j_3) = (0, 0)$ in the Neveu-Schwarz sector, see fig. 13.

Based on these data we conjecture the following relation,

$$\frac{\Delta N}{K} = \frac{\pi + 2\gamma}{\pi\gamma} \left[\log \left(\frac{L}{L_0(\gamma)} \right) + B \right]. \quad (\text{II.61})$$

Here, $L_0(\gamma)$ is a non-universal length scale and B is related to the finite part of the density of states in the continuous component of the spectrum of scaling dimensions. Since the allowed values for ΔN at a given system size L differ by multiples of 2, the

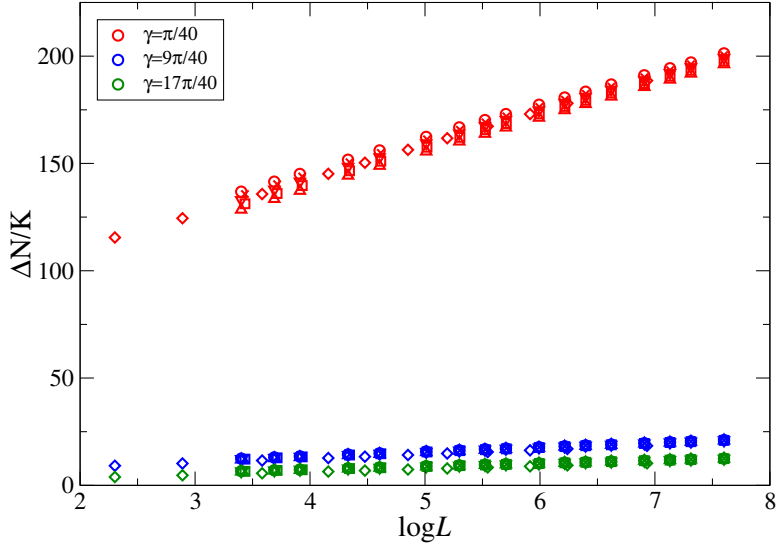


Figure 12: $\Delta N/K$ as a function of $\log(L)$ for several deformation parameters γ for periodic boundary conditions (i.e., in the Ramond sector). The circle symbols denote an excitation in the sector $(b, j_3) = (0, 1)$ with $\Delta N = 1$, crosses $\Delta N = 2$, lower triangles $\Delta N = 3$, squares $\Delta N = 4$ and upper triangles $\Delta N = 5$, respectively. The diamond symbols denote the $\Delta N = 1$ -state in the sector $(0, 3)$.

density of states may be defined by

$$\rho(K) \equiv \frac{1}{2} \frac{\partial}{\partial K} \Delta N = \frac{\pi + 2\gamma}{2\pi\gamma} \left(\log \frac{L}{L_0(\gamma)} + \frac{\partial}{\partial K} (KB(K)) \right). \quad (\text{II.62})$$

As expected, $\rho(K)$ diverges in the thermodynamic limit $L \rightarrow \infty$ while its finite part is determined by the function $B(K)$ entering our conjecture, eq. (II.61). Motivated by the approach from Ikhlef *et al.* described above [23–25], it is tempting to compare the density of states found in the lattice model with that from ‘candidate CFTs’ for the thermodynamic limit. To this purpose, our findings for the function $B(K)$ extracted from our numerical results for the continuum of states in the sector $(b, j_3) = (0, 1)$ at periodic boundary conditions for several values of the anisotropy γ are presented in fig. 14.

Obviously, different anisotropies lead to genuine different curve progressions. In contrast, for the staggered six vertex model, the function $B(K)$ was shown to agree with the expectation from the $SL(2, \mathbb{R})/U(1)$ black hole CFT [23–26] which is in particular independent of γ . Hence, there is still an unknown γ -dependence hidden in the function $B(K)$ and our results do not coincide with those from the $SL(2, \mathbb{R})/U(1)$ CFT. Note, this γ -dependence cannot be absorbed by a different normalization of the quasimomentum: Our results for the spectral flow in the following subsection indicate for the quasimomentum of a state to be related to the spin j of the corresponding primary

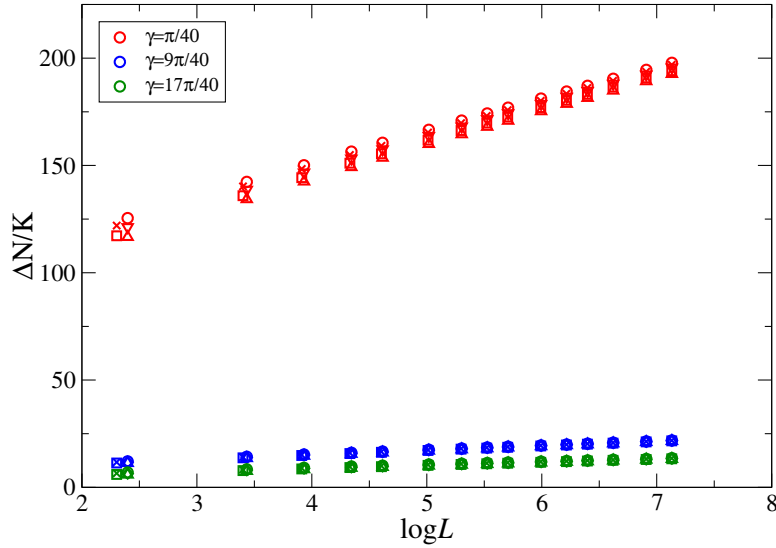


Figure 13: $\Delta N/K$ as a function of $\log(L)$ for several deformation parameters γ for antiperiodic boundary conditions (i.e., in the Neveu-Schwarz sector). The circle symbols denote the excitation above the ground state with $\Delta N = 1$, crosses $\Delta N = 2$, lower triangles $\Delta N = 3$, squares $\Delta N = 4$ and upper triangles $\Delta N = 5$, respectively.

in the CFT by means of $j = -1/2 + iK$. Different normalizations of the quasimomentum would prevent us from this immediate interpretation of the quasimomentum.

Unfortunately, the identification of the CFT by means of calculating the finite part of the density of states as described here is reliant on the knowledge of the latter for any ‘candidate CFT’. Since only little is known about the density of states for continuous components of the spectrum for non-unitary CFTs, we are unable to proceed further towards an identification of the thermodynamic limit.

Instead, in order to provide support for eq. (II.61), we have computed the asymptotic slope of the function $\Delta N/K$ assuming a rational dependence of the data on $\log(L)$. In figure 15 the numerical data from the $(0, 1)$ states are shown together with our conjecture (II.61).

Using (II.61) the subleading contribution to the scaling dimensions (II.54) can be expressed in terms of the quasimomentum K as

$$X_{(1,0)}(K) = X_{(1,0)} + \frac{(\pi + 2\gamma)(\pi - 2\gamma)}{4\gamma^2} K^2. \quad (\text{II.63})$$

In this expression, the quasimomentum K enters as a quantum number for the non-compact degree of freedom in the CFT.

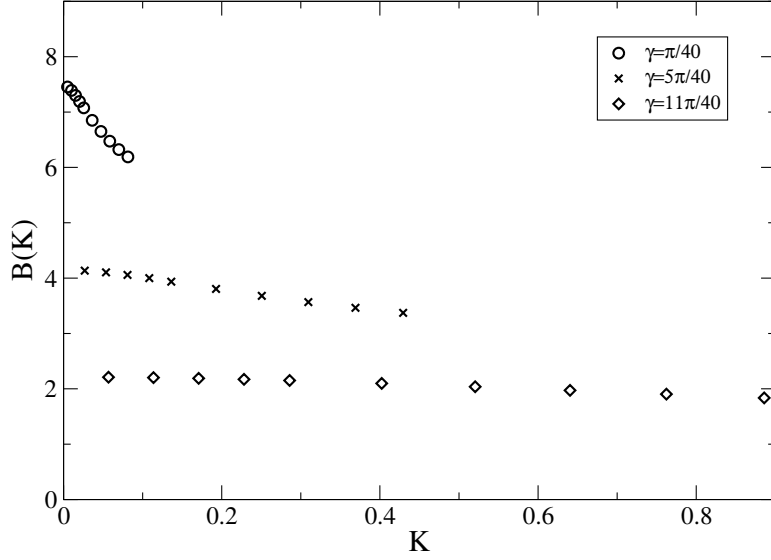


Figure 14: The function $B(K)$ for the largest accessible system size, $L_{\text{even}} = 2000$ and $L_{\text{odd}} = 2001$, respectively, and several anisotropies γ . Clearly, there is still an unknown γ -dependence which is not captured by the well-known $SL(2, \mathbb{R}/U(1)$ ‘candidate CFT’.

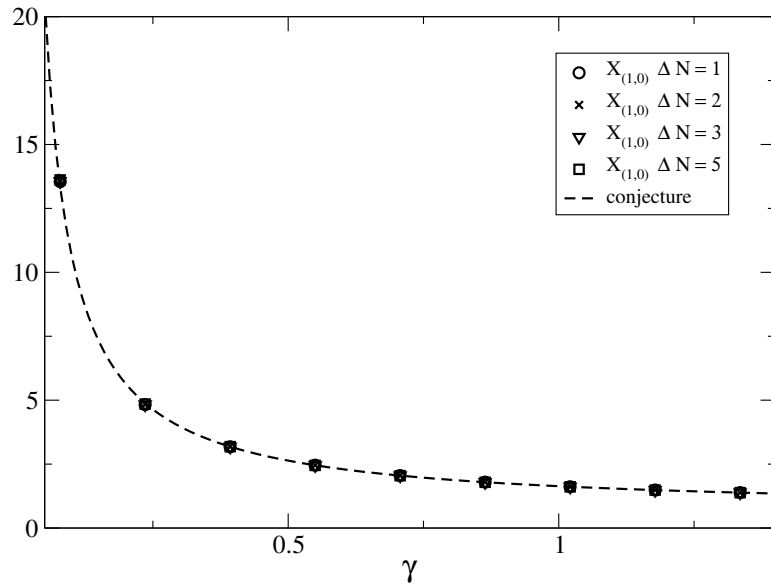


Figure 15: Slope of the function $f(\log(L)) \equiv \Delta N/K$ as a function of the anisotropy γ . The dashed line is the factor $(\pi + 2\gamma)/(\pi\gamma)$ entering our conjecture (II.61).

We have used the numerical estimate for the amplitude $A(\gamma)$ in (II.54)

$$A(\gamma) = \frac{\pi^2}{4} \frac{\pi - 2\gamma}{\pi + 2\gamma}, \quad 0 \leq \gamma < \frac{\pi}{2}. \quad (\text{II.64})$$

Note, this is a refinement of the estimate from ref. [21] where a factor $5/2$ instead of $\pi^2/4$ had been obtained without knowledge of the quasimomentum operator.

1.4 Spectral flow between the Neveu-Schwarz and Ramond-sector

In the previous subsections, we have studied the continuous component of the spectrum and its characterization by means of the quasimomentum operator. In particular, the eigenvalue of the quasimomentum enters in the finite size correction to the effective scaling dimensions as a quantum number for the non-compact degree of freedom in the non-unitary Conformal Field Theory describing the thermodynamic limit. In this subsection, we focus on a different characteristic feature of such non-unitary Conformal Field Theories, namely the appearance of non-normalizable states which emerge in the spectrum of the superspin chain only when the corresponding operator in the CFT becomes normalizable, e.g. for certain boundary conditions. To be more specific, we study the spectrum of the staggered $U_q[sl(2|1)]$ superspin chain as a function of the twist $\varphi = \alpha + \pi$ which, in the thermodynamic limit, corresponds to the spectral flow between the Neveu-Schwarz and the Ramond sector. The results presented within this subsection are published in [85].

In the presence of a twist φ in the boundary conditions, the corresponding effective scaling dimensions of the superspin chain (II.12) are given by

$$X_{(m,w)}^{\text{eff}}(\varphi = \alpha + \pi) = -\frac{1}{4}\delta_{m+w \in 2\mathbb{Z}} + \frac{m^2}{2k} + \frac{k}{2} \left(w + \frac{\varphi}{\pi} \right)^2, \quad k = \frac{\pi}{\pi - 2\gamma}. \quad (\text{II.65})$$

Note, for antiperiodic boundary conditions, $\varphi = 0$, this expression reproduces (II.55) while for the periodic boundary conditions it is equivalent to (II.52) with a shift $w + 1 \rightarrow w$ in the vorticity.

Here, we investigate the scaling dimensions of the $\Delta N = 1$ state in sector $(b, j_3) = (0, 0)$ for antiperiodic boundary conditions as we adiabatically change the twist angle. Hence, we can follow this state under the spectral flow. For $|\varphi| < \varphi_c = \pi/k$, we observe that its scaling dimension $X_{(m,w)=(0,0)}^*(\varphi)$ stays within the continuum above $X_{(0,0)}^{\text{eff}}(\varphi)$. As the twist approaches $\pm\varphi_c$, the strange string with largest real part goes to ∞ . Beyond $\pm\varphi_c$ the root configuration changes and the finite size scaling dimension of the state deviates significantly from (II.65). Unlike higher excitations ($|\Delta N| > 1$) within this class of Bethe states, it splits off from the emerging continuum above $X_{(0,0)}^{\text{eff}}(\varphi)$, see fig. 16. Based on our finite size data, we conjecture the following φ -dependence of the

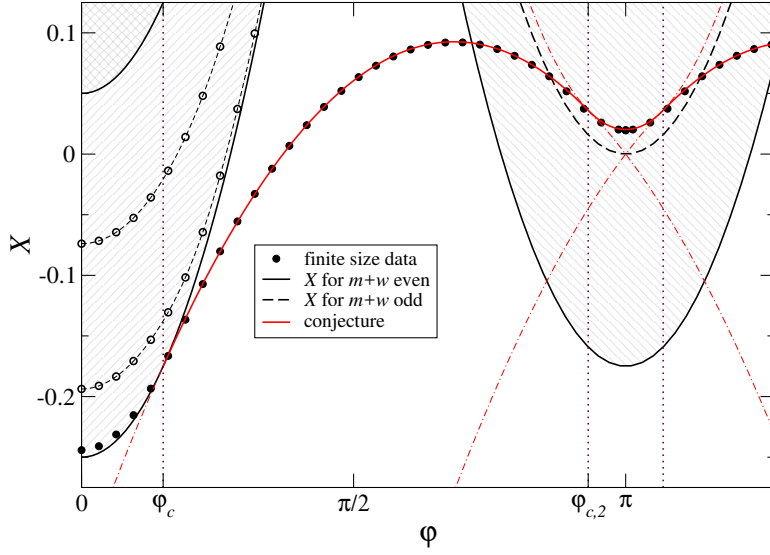


Figure 16: Evolution of the lowest states in the NS sector of the superspin chain of odd length L with the twist angle $\alpha = -\pi + \varphi$: bullets are the scaling dimensions obtained from the solution of the Bethe equations (II.45) for $L = 27$ evolving from a root configuration consisting of strange strings with $|\Delta N| = 1$ for $\varphi = 0$, i.e. the NS ground state, for anisotropy $\gamma = 17\pi/40$. Open circles show the flow of scaling dimensions with $|\Delta N| = 3$ and 5 for the same parameters. Black lines indicate the lowest effective scaling dimensions $X_{(m,w)}^{\text{eff}}(\varphi)$ of the superspin chain, i.e. $(m, w) = (0, 0)$, $(1, -1)$, $(2, 0)$, and $(0, -1)$, for this anisotropy. The shaded areas indicate the observed continua of scaling dimensions starting at $X_{(m,w)}^{\text{eff}}(\varphi)$ with even $m + w$. The conjectured φ -dependence of the discrete level $X_{(0,0)}^*$, eq. (II.66), is shown in red (dash-dotted lines indicate continuations of the functions appearing in the piecewise definition of $X_{(0,0)}^*(\varphi)$ beyond their domain of definition).

scaling dimension,

$$X_{(0,0)}^*(\varphi) = \begin{cases} -\frac{1}{4} + \frac{k}{2} \left(\frac{\varphi}{\pi}\right)^2 - \frac{2k-1}{(k-1)^2} \left(\frac{1}{2} - \frac{k}{2} \left|\frac{\varphi}{\pi}\right|\right)^2 & \text{for } \varphi_c \leq |\varphi| \leq \varphi_{c,2} \\ \frac{k}{2} \left(1 - \frac{\varphi}{\pi}\right)^2 + \frac{1}{4} \frac{1}{2k-1} & \text{for } |\varphi - \pi| \leq |\varphi_{c,2} - \pi| \end{cases} \quad (\text{II.66})$$

where $\varphi_{c,2} = \pi - \frac{\pi(k-1)}{k(2k-1)}$.

In other words, we find that one state from the *continuum* above $X^{\text{eff},NS}(0, 0)$ evolves under the spectral flow $\varphi = 0 \dots \pi$ to a *discrete* level with dimension

$$X_{(0,0)}^*(\pi) = \frac{1}{4} \frac{\pi - 2\gamma}{\pi + 2\gamma} = \frac{1}{4} \frac{1}{2k-1} \quad (\text{II.67})$$

in the Ramond sector. The Bethe root configuration for this state consists of $(L-1)/2$ of the usual 2-strings (built from two complex conjugate rapidities on the same level [108]) and, in addition, one single root at ∞ on either level, i.e.²⁰

²⁰This configuration has already been observed for $L = 3$ in Ref. [21] but not considered further.

$$\lambda_j^{(1)} = -\lambda_j^{(2)} \in \left\{ \mu_k^\pm : \text{Im}(\mu_k^\pm) \simeq \pm \frac{\gamma}{2}, k = 1 \dots \frac{L-1}{2} \right\} \cup \{\infty\}. \quad (\text{II.68})$$

Note that there are strong logarithmic finite size corrections to scaling to (II.67), similar as for the states in the continuum, see figure 17.

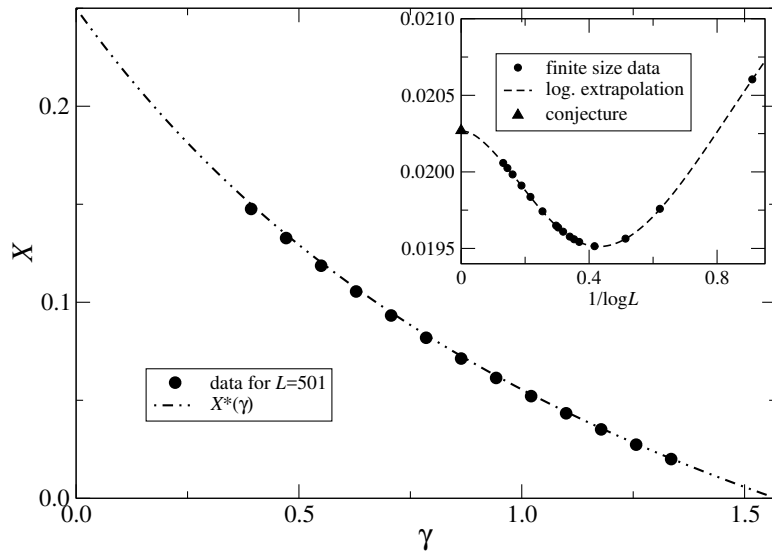


Figure 17: Scaling dimension of the discrete level in the Ramond sector, $\varphi = \pi$, as a function of the anisotropy parameter γ : bullets are the numerical data for system size $L = 501$, the dash-dotted line is the conjectured value (II.67) in the thermodynamic limit. The inset shows the L dependence of the finite size data (\bullet) for $\gamma = 17\pi/40$ together with the extrapolation based on an assumed rational dependence of the data on $1/\log L$ (dashed line).

Increasing the twist beyond $\varphi = \pi$, we find that $X_{(0,0)}^*(\varphi) = X_{(0,0)}^*(2\pi - \varphi)$. For $\varphi > 2\pi - \varphi_{c,2}$ this level coincides with

$$X_{(0,-2)}^* = X_{(0,-2)}^{\text{eff}}(\varphi) - \frac{2k-1}{(k-1)^2} \left(\frac{1}{2} - \frac{k}{2} \left| \frac{\varphi}{\pi} - 2 \right| \right)^2, \quad (\text{II.69})$$

and disappears in the continuum above $X_{(0,-2)}^{\text{eff}}(\varphi)$ at $\varphi = 2\pi - \varphi_c$.

Concluding our analysis of the scaling dimensions under the spectral flow, we note that starting from the lowest state in the continuum above $X_{(1,-1)}^{\text{eff}}(\varphi = \pi)$ (for even L) we have observed another discrete level in the spectrum of the superspin chain

$$X_{(1,-1)}^*(\varphi) = X_{(1,-1)}^{\text{eff}}(\varphi) - \frac{2k-1}{(k-1)^2} \left(1 - \frac{k}{2} \left| \frac{\varphi}{\pi} - 1 \right| \right)^2, \quad |\varphi - \pi| > \frac{2\pi}{k}. \quad (\text{II.70})$$

Let us now analyze the quasimomentum of the state with dimension X^* (II.66) identified above. As discussed in sec. 1.3, the quasimomentum allows to label the continua of scaling dimensions: For the lowest state at antiperiodic boundary conditions

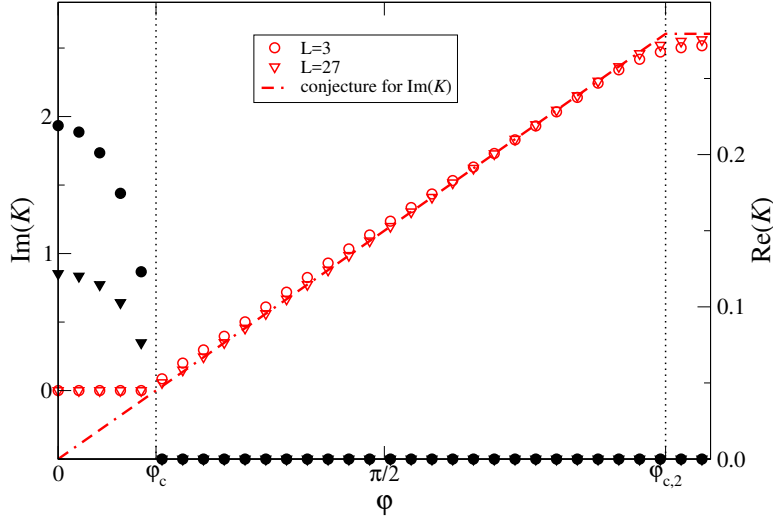


Figure 18: quasimomentum of the discrete level for $\gamma = 17\pi/40$ vs. twist angle φ : filled (open) symbols are the numerical data for the real (imaginary) part of K for system sizes $L = 3$ and 27. Dash-dotted line (in red) is the conjecture for $\text{Im}(K)$, eq. (II.71), saturating at $\varphi = \varphi_{c,2}$.

but outside of the XXZ subspace (i.e. the $\Delta N = 1$ state which was also part of the numerical study in 1.3), the corresponding eigenvalue K is found to take real values not only at $\varphi = 0$ but in the region $|\varphi| < \varphi_c$, see figure 18.

The amplitude vanishes as $1/\log L$ in the thermodynamic limit. This observation agrees with the density of states observed in the continua [20, 21].

For $|\varphi| > \varphi_c$, however, i.e. as the discrete level (II.66) emerges from the continuum of scaling dimensions, the quasimomentum becomes purely imaginary with a linear dependence on the twist angle φ ,

$$K^*(\varphi) = \frac{i}{2(\pi - 2\gamma)} (|\varphi| - \varphi_c) = i \left(\frac{k|\varphi|}{2\pi} - \frac{1}{2} \right) \quad \text{for } \varphi_c \leq \varphi \leq \varphi_{c,2}, \quad (\text{II.71})$$

where we have chosen the branch of the logarithm in (II.59) such that $\text{Im}(K) \in [0, (k-1)/2]$. Corrections to scaling in this expression are small which allows to observe this behaviour already for $L = 3$, see figure 18.

As for the scaling dimension (II.66), the φ -dependence of the quasimomentum changes when the twist is increased beyond $|\varphi| = \varphi_{c,2}$: while K remains purely imaginary its value saturates at

$$\text{Im}(K^*(\varphi)) = \frac{4\gamma^2}{\pi^2 - 4\gamma^2} = \frac{(k-1)^2}{2k-1} \quad \text{for } \varphi \geq \varphi_{c,2}. \quad (\text{II.72})$$

Note that $\text{Im}(K^*(\pi))$ is smaller than the maximum $\gamma/(\pi - 2\gamma) = (k-1)/2$ which is possible according to the definition and the choice of the branch of the logarithm, see (II.59).

The emergence of a discrete level out of the continuum at a finite twist φ_c is strongly reminiscent to the situation in the $a_2^{(2)}$ spin chain [27]: in the black hole CFT describing the low-energy behaviour of this lattice model it is understood as a consequence of the inclusion of principal discrete representations of $SL(2, \mathbb{R})$ as Kac-Moody primaries in the field theory. For operators corresponding to normalizable states in the parent WZNW theory of the model (i.e. states with a finite norm in the Hilbert space defined by the CFT), the spin of these representations (related to the momentum along the non-compact direction of the target space, an infinite cigar for the $SL(2, \mathbb{R})/U(1)$ sigma model) is restricted to values $j \leq -1/2$ (see e.g. [109] for the normalizability of states in WZNW models). To satisfy this bound a finite, non-zero twist has to be applied [92, 93].

For the bosonic $SL(2, \mathbb{R})/U(1)$ coset at level k the spectrum of discrete representations also needs to be truncated by the 'unitarity bound' $j \geq -(k-1)/2$ to guarantee non-negative conformal weights [89, 92, 106].

The appearance of the discrete level X^* (II.66) in the spectrum of the superspin chain at the critical twist φ_c accompanied with the change of quasimomentum from real to imaginary can be interpreted in a similar way: states in the continuum of scaling dimensions have real K , the discrete levels are characterized by an imaginary quasimomentum. The observed bound $\text{Im}(K) \geq 0$ for states in the lattice model can be attributed to the normalizability of the corresponding primaries. Continuing (II.71) to $|\varphi| < \varphi_c$ would yield imaginary quasimomenta $-1/2 \leq \text{Im}(K) < 0$ which is not realized in the spectrum of the superspin chain. Hence, these results allow for a direct interpretation of the quasimomentum of a state to be related to the spin of the primary in the CFT for the thermodynamic limit by means of $j = -1/2 + iK$, in strong reminiscence of the staggered six vertex model [25].

As for a restriction of $\text{Im}(K)$ from above (similar to the unitarity bound in the string theory), our data for the lattice model do not provide a conclusive answer. We would need to see a level being 'absorbed' by the continuum at such a bound under the spectral flow (as is the case for the $a_2^{(2)}$ spin chain [27]). It would be tempting to associate this bound with $\text{Im}(K) \leq (k-1)/2$ as implied by our choice of the branch for the logarithm in (II.59). Since the quasimomentum for the discrete level studied above saturates at the value (II.72) below $(k-1)/2$, however, our data cannot support this conjecture.

1.5 Summary

In this section, we have reviewed the construction of the staggered $U_q[sl(2|1)]$ superspin chain and its consecutive solution by means of the nested Algebraic Bethe Ansatz. We have also briefly mentioned how a subset of the spectrum of scaling dimensions can be obtained by mapping certain subsectors of the superspin chain to the XXZ spin-1

Heisenberg model.

A particular feature of several superspin chains is the emergence of continuous components in the spectrum of scaling dimensions. For the staggered $U_q[sl(2|1)]$ superspin chain, this feature was first discovered in [21]. The existence of continua in the spectrum of scaling dimensions translates to a non-compact target space for the Conformal Field Theory describing the thermodynamic limit. We have extended the picture presented in [21] as we have found continua of scaling dimensions also for other quantum numbers parametrizing the different sectors.

Motivated by the approach of Ikhlef *et al.* [23–25] we have sought a characterization of the observed continuous components of the spectrum by means of a conserved charge. To this purpose, we have defined a quasimomentum operator (II.59). In contrast to the Hamiltonian and momentum operator which are both generated by an expansion of $\log \tau_3(\lambda)\tau_{\bar{3}}(\lambda)$, the quasimomentum originates in an odd combination of single-row transfer matrices, i.e. $\log \tau_3(\lambda)(\tau_{\bar{3}}(\lambda))^{-1}$.

By numerically solving the Bethe Ansatz equations for states belonging to the different continua of scaling dimensions, we have shown that the quasimomentum operator parametrizes the continuous components of the spectrum and thereby determines the logarithmic corrections to scaling. Since the eigenvalues of the quasimomentum operator allow for an extraction of the density of states for the continuous components of the spectrum, we have compared the outcome to the known results for the $SL(2, \mathbb{R})/U(1)$ CFT. Unfortunately, the results do not coincide. Since the identification of the CFT for the thermodynamic limit by calculating the density of states for the continuous component of the spectrum is reliant on the knowledge of the latter for ‘candidate CFTs’, the study of other symmetries on the target space of $SL(2, \mathbb{R})/U(1)$, a semi-infinite cigar which allows for both a continuous and discrete part of the spectrum, seems to be promising. This might help to identify the Conformal Field Theory for the thermodynamic limit.

Subsequently, we turned to a different characteristic of non-unitary CFTs, namely the emergence of discrete levels. To this purpose we have studied the spectral flow in the spectrum of the superspin chain under a twist in the boundary conditions. Based on solutions of the Bethe Ansatz equations for twisted boundary conditions we have identified a state from the continuous part of the spectrum in the Neveu-Schwarz sector (i.e. with antiperiodic boundary conditions for the fermionic degrees of freedom) which under variation of the twist becomes a discrete level in the Ramond sector. We have found the following behaviour of the scaling dimension for this state with the twist angle in the boundary conditions,

$$X_{(0,0)}^*(\varphi) = \begin{cases} X_{(0,0)}^{\text{eff}}(\varphi) & \text{for } |\varphi| < \varphi_c \\ X_{(0,0)}^{\text{eff}}(\varphi) - \frac{2k-1}{(k-1)^2} \left(\frac{1}{2} - \frac{k}{2} \left| \frac{\varphi}{\pi} \right| \right)^2 & \text{for } \varphi_c \leq |\varphi| \leq \varphi_{c,2} \\ \frac{k}{2} \left(1 - \frac{\varphi}{\pi} \right)^2 + \frac{1}{4} \frac{1}{2k-1} & \text{for } \varphi_{c,2} \leq \varphi \leq \pi. \end{cases} \quad (\text{II.73})$$

In the CFT, levels can be attributed to the continuous or discrete part of the spectrum based on their quasimomentum: We have found that states belonging to a continuum of scaling dimensions have *real* quasimomenta while for discrete levels the quasimomentum is purely *imaginary*. The need of a non-zero twist in the boundary conditions for the discrete levels to appear in the spectrum of the lattice model has been argued to be related to the normalizability of primary fields in the non-rational Conformal Field Theory describing the thermodynamic limit.

Again, our results allow for a comparison with expectations from ‘candidate CFTs’ for the thermodynamic limit of the staggered superspin chain. The $SL(2, \mathbb{R})/U(1)$ -symmetric bosonic black hole theory would yield [110]

$$X_{(0,0)}^*(\varphi)^{\text{bos. } SL(2, \mathbb{R})/U(1)} = X_{(0,0)}^{\text{eff}}(\varphi) - \frac{2}{k-2} \left(\frac{1}{2} - \frac{k}{2} \left| \frac{\varphi}{\pi} \right| \right)^2 \quad (\text{II.74})$$

for $-\frac{k-1}{2} \leq j \leq -\frac{1}{2}$,

the corresponding supersymmetric Kazama-Suzuki theory [111]

$$X_{(0,0)}^*(\varphi)^{\text{SUSY } SL(2, \mathbb{R})/U(1)} = X_{(0,0)}^{\text{eff}}(\varphi) - \frac{2}{k} \left(\frac{1}{2} - \frac{k}{2} \left| \frac{\varphi}{\pi} \right| \right)^2 \quad (\text{II.75})$$

for $-\frac{k+1}{2} \leq j \leq -\frac{1}{2}$,

rather than our results, eq. (II.73), which is in accordance with our findings from the study of the density of states in the continuous component of the spectrum.

In summary, we have uncovered and characterized two interesting features of the thermodynamic limit of the staggered $3 \otimes \bar{3}$ superspin chain, namely the emergence of continua of scaling dimensions in the thermodynamic limit as well as the existence of non-normalizable states which gives rise to discrete states appearing when a twist in the boundary conditions is applied. To completely understand the thermodynamic limit and its description in terms of a Conformal Field Theory, additional investigations have to be performed.

2 The operator content of the $U_q[osp(3|2)]$ superspin chain

A few years ago, the isotropic spin chains invariant under the action of the $osp(n|2m)$ superalgebra have been shown to exhibit a number of states in the eigenspectrum leading to the same scaling dimension in the thermodynamic limit [19, 22]. This degeneracy in the critical dimensions grows with the lattice size and has been seen as the signature of the presence of non-compact degrees of freedom in the Conformal Field Theory describing the thermodynamic limit [112]. Hence, this scenario is strongly reminiscent of the $U_q[sl(2|1)]$ superspin chain studied above.

One of the models contained in the aforementioned series, the $osp(3|2)$ superspin chain, may be used to describe the diffusion of particles moving on a square lattice equipped with barriers which are placed randomly [19]. The barriers are tilted left and right w.r.t. the lattice. An incoming particle will change its direction when hitting a scatterer but will pass through a node if it is empty, see fig. 19. Thus, the particles' paths form intersecting loops on the lattice which is eponymous for the model. The local configurations of an intersecting loop at each node and the associated Boltzmann weights are depicted in fig. 20.

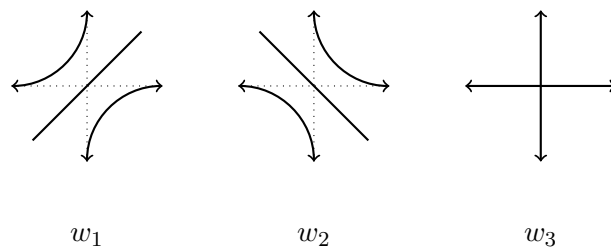


Figure 19: The scattering of incoming particles depends on the existence of barriers at each node. The probabilities for the different vertices to appear are given by w_1 , w_2 and w_3 , respectively.

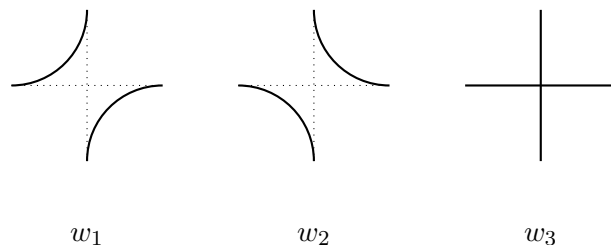


Figure 20: Possible local configurations of an intersecting loop at each node with the corresponding Boltzmann weight w_1 , w_2 and w_3 , respectively.

To calculate the partition function we may sum the contributions for each particle's path [18],

$$Z = \sum_{\text{loop configurations}} w_1^{m_1} w_2^{m_2} w_3^{m_3} z^N \quad (\text{II.76})$$

where m_i are the amount of the weights w_i and N denotes the number of loops in the corresponding configuration. The number z is called fugacity. In the case $z = 1$, the intersecting loop model can be formulated as a supersymmetric vertex model corresponding to the superspin chain which is built from the five-dimensional fundamental representation of the $osp(3|2)$ superalgebra.

In this section we turn towards the study of quantum deformations of the above-quoted $osp(3|2)$ superspin chain. Particularly, we are interested in uncovering the structure of the scaling dimensions X with the deformation parameter q for the compact part of the eigenspectrum. We will argue that the dependence of such critical exponents with q can be expressed in terms of the conformal content of two Coulomb gases with distinct compactification radii. In the rational limit $q \rightarrow 1$, one of the Coulomb gases does not contribute to the critical behaviour since the respective vortex exponent diverges. This allows for a reasoning for the abundance of states with divergent scaling dimensions found in previous work on the isotropic $osp(3|2)$ superspin chain [19]. As for the $U_q[sl(2|1)]$ staggered superspin chain, we find that the feature of having a family of distinct states with the same leading finite-size correction appears to persist for generic values of $q \neq 1$.

This section is organized as follows. In the first subsection 2.1, we will define the Lie superalgebra $osp(3|2)$ and briefly discuss the representation that will be used as the carrier space for the local degrees of freedom in the $osp(3|2)$ superspin chain. Subsequently in 2.2 we will shortly review the Bethe Ansatz solution for the $U_q[osp(3|2)]$ superspin chain using two suitable distinct grading bases with generic toroidal boundary conditions. Before we will investigate the operator content, we will compute certain thermodynamic properties such as the low momenta dispersion relation for low lying excitations in 2.3 and analytically study the leading finite-size corrections in certain spectral sectors of the superspin chain using the root density method. This will provide some insights to conjecture a generic Ansatz for the behaviour of the scaling dimensions with the deformation parameter. In addition, we will point out a correspondence between the Bethe Ansatz description and the energies of certain eigenstates of the superspin chain with those of the integrable spin $S = 1$ Heisenberg XXZ model for a particular value of the deformation parameter. This relationship will turn out to be useful to verify our working proposal for the scaling dimensions. In subsection 2.4, we will solve the Bethe Ansatz equations numerically to compute the eigenenergies and scaling dimensions of the superspin chain for many states in nine sectors corresponding

2. The operator content of the $U_q[osp(3|2)]$ superspin chain

to different eigenvalues of the generators of the Cartan subalgebra of $osp(3|2)$.

Altogether we have investigated the finite-size corrections of around seventy distinct states. The analysis of the subleading finite-size corrections suggests that some states exhibit a combination of a power law and a logarithmic behaviour. The results presented in this section are published in [113], the corresponding research data can be accessed online [114].

2.1 The $osp(3|2)$ Lie superalgebra

Within this subsection we briefly define the $osp(3|2)$ Lie superalgebra and discuss its irreducible representations following [115].

The even part of the $osp(3|2)$ Lie superalgebra is given by the direct sum

$$osp(3|2)_0 = so(3) \oplus sp(2) \cong su(2) \oplus su(2). \quad (\text{II.77})$$

Hence, the associated generators are composed of two sets of $su(2)$ generators s_{\pm}, s_3 and t_{\pm}, t_3 fulfilling

$$\begin{aligned} [s_3, s_{\pm}] &= \pm s_{\pm}, & [s_+, s_-] &= 2s_3 \\ [t_3, t_{\pm}] &= \pm t_{\pm}, & [t_+, t_-] &= 2t_3 \\ [s_{\mu}, t_{\nu}] &= 0 \quad (\mu, \nu = \pm, 3). \end{aligned} \quad (\text{II.78})$$

The odd part however is built from the elements of the tensor product of a three-dimensional $so(3)$ tensor with a two-dimensional $sp(2)$ tensor [115]. We will call the corresponding generators $Z_{\alpha,\beta}$ with $\alpha = -1, 0, +1$ and $\beta = -1/2, +1/2$. Their super Lie products with the elements of the even part read

$$\begin{aligned} [s_3, Z_{\alpha,\beta}] &= \alpha Z_{\alpha,\beta} \\ [s_{\pm}, Z_{\alpha,\beta}] &= ((1 \mp \alpha)(2 \pm \alpha))^{1/2} Z_{\alpha \pm 1, \beta} \\ [s_3, Z_{\alpha,\beta}] &= \beta Z_{\alpha,\beta} \\ [t_{\pm}, Z_{\alpha,\beta}] &= \left(\left(\frac{1}{2} \mp \beta \right) \left(\frac{3}{2} \pm \alpha \right) \right)^{1/2} Z_{\alpha, \beta \pm 1} \end{aligned} \quad (\text{II.79})$$

whereas the non-vanishing supercommutators of the elements of Z are given by

$$\begin{aligned} [Z_{1,1/2}, Z_{0,-1/2}] &= \frac{1}{\sqrt{2}} s_+, & [Z_{0,1/2}, Z_{0,1/2}] &= 2t_+, \\ [Z_{1,1/2}, Z_{-1,1/2}] &= -2t_+, & [Z_{0,1/2}, Z_{0,-1/2}] &= -2t_3, \\ [Z_{1,1/2}, Z_{-1,-1/2}] &= -s_3 + 2t_3, & [Z_{0,1/2}, Z_{-1,-1/2}] &= -\frac{1}{\sqrt{2}} s_-, \end{aligned} \quad (\text{II.80})$$

$$\begin{aligned}
[Z_{1,-1/2}, Z_{0,1/2}] &= -\frac{1}{\sqrt{2}}s_+, & [Z_{0,-1/2}, Z_{0,-1/2}] &= -2t_-, \\
[Z_{1,-1/2}, Z_{-1,1/2}] &= s_3 + 2t_3, & [Z_{0,-1/2}, Z_{-1,-1/2}] &= \frac{1}{\sqrt{2}}s_-, \\
[Z_{1,-1/2}, Z_{-1,-1/2}] &= 2t_-.
\end{aligned}$$

Due to the algebra inclusion

$$su(2) \oplus su(2) \cong osp(3|2)_0 \subset osp(3|2), \quad (\text{II.81})$$

every irreducible representation of $osp(3|2)$ is also an irrep of $su(2) \oplus su(2)$ and therefore can be decomposed into the direct sum of two $su(2)$ irreps. For example, the five-dimensional fundamental representation of $osp(3|2)$ contains $(1, 0)$ and $(0, 1/2)$ $su(2)$ representations, e.g. it can be seen as a direct sum of each one spin 1 and one spin 1/2 representation. Within this irrep, the elements of $osp(3|2)$ are of the following form [116],

$$\begin{pmatrix} a & 0 & b & x & u \\ 0 & -a & c & y & v \\ -c & -b & 0 & z & w \\ v & u & w & d & e \\ -y & -x & -z & f & -d \end{pmatrix} \quad (\text{II.82})$$

where all non-zero entries are complex numbers. The even elements fulfill $x = y = z = u = v = w = 0$, while for the odd elements $a = b = c = d = e = f = 0$.

A quantum deformation²¹ of this $osp(3|2)$ irrep will be used in the remaining section as local Hilbert space for a corresponding superspin chain. A detailed analysis of all (finite- and infinite-dimensional) irreducible representations of $osp(3|2)$ can be found in [115].

2.2 Definition and solution of the $U_q[osp(3|2)]$ superspin chain

In the following, we will investigate a spin chain which can be derived from a vertex model based on the quantum deformation of the five-dimensional fundamental representation of the Lie superalgebra $osp(3|2)$. Its R -matrix in the Weyl-basis reads [117]

$$\begin{aligned}
\mathcal{R}_{a,b}(\lambda) &= P_{a,b} \check{\mathcal{R}}_{a,b}(\lambda) \text{ with} \\
\check{\mathcal{R}}_{a,b}(\lambda) &= \sum_{\substack{j=1 \\ j \neq j'}}^5 a_j(\lambda) e_{jj}^{(a)} \otimes e_{jj}^{(b)} + b(\lambda) \sum_{\substack{j,k=1 \\ j \neq k, j \neq k'}}^5 e_{kj}^{(a)} \otimes e_{jk}^{(b)}
\end{aligned}$$

²¹See 2.5 in part I for a general scheme for the construction of quantum deformations. More details about the explicit construction of $U_q[osp(3|2)]$ can be found in [68].

2. The operator content of the $U_q[\mathfrak{osp}(3|2)]$ superspin chain

$$\begin{aligned}
& + \bar{c}(\lambda) \sum_{\substack{j,k=1 \\ j < k, j \neq k'}}^5 e_{jj}^{(a)} \otimes e_{kk}^{(b)} + c(\lambda) \sum_{\substack{j,k=1 \\ j > k, j \neq k'}}^5 e_{jj}^{(a)} \otimes e_{kk}^{(b)} \\
& + \sum_{j,k=1}^5 d_{jk}(\lambda) e_{j'k}^{(a)} \otimes e_{j'k'}^{(b)}.
\end{aligned} \tag{II.83}$$

where $P_{a,b}$ denotes graded permutation operator within the grading $(p_1, p_2, p_3, p_4, p_5)$ and $p_j = 0$ (1) for even (odd) indices,

$$P_{a,b} = \sum_{j,k=1}^5 (-1)^{p_j p_k} e_{jk}^{(a)} \otimes e_{kj}^{(b)}. \tag{II.84}$$

To each index j we have defined a conjugated index $j' = 6 - j$. The functions occurring in the \mathcal{R} -matrix are given by

$$a_j(\lambda) = (e^{2\lambda} - q^{-1}) (e^{2\lambda(1-p_j)} - q^2 e^{2\lambda p_j}), \tag{II.85}$$

$$b(\lambda) = q (e^{2\lambda} - 1) (e^{2\lambda} - q^{-1}), \tag{II.86}$$

$$c(\lambda) = (1 - q^2) (e^{2\lambda} - q^{-1}), \tag{II.87}$$

$$\bar{c}(\lambda) = e^{2\lambda} c(\lambda) \tag{II.88}$$

$$d_{jk}(\lambda) = \begin{cases} q (e^{2\lambda} - 1) (e^{2\lambda} - q^{-1}) + e^{2\lambda} (q^2 - 1) (q^{-1} - 1), & j = k = 3 \\ (e^{2\lambda} - 1) \left[(e^{2\lambda} - q^{-1}) (-1)^{p_j} q^{2p_j} + e^{2\lambda} (q^2 - 1) \right], & j = k \neq 3 \\ (q^2 - 1) \left[(e^{2\lambda} - 1) \frac{\epsilon_j}{\epsilon_k} q^{t_j - t_k - 1} - \delta_{j,k'} (e^{2\lambda} - q^{-1}) \right], & j < k \\ (q^2 - 1) e^{2\lambda} \left[(e^{2\lambda} - 1) \frac{\epsilon_j}{\epsilon_k} q^{t_j - t_k} - \delta_{j,k'} (e^{2\lambda} - q^{-1}) \right], & j > k \end{cases} \tag{II.89}$$

where $q = \exp(i\gamma)$ and $0 < \gamma < \pi$ parametrizes the anisotropy. The numbers ϵ_j and t_j depend on the grading in the following way,

$$\epsilon_j = \begin{cases} (-1)^{-p_j/2}, & j = 1, 2, \\ 1, & j = 3, \\ (-1)^{p_j/2}, & j = 4, 5; \end{cases} \tag{II.90}$$

$$t_j = \begin{cases} j + \left(\frac{1}{2} - p_j + 2 \sum_{k=j}^2 p_k \right), & j = 1, 2, \\ 3, & j = 3, \\ j - \left(\frac{1}{2} - p_j + 2 \sum_{k=4}^j p_k \right), & j = 4, 5. \end{cases} \tag{II.91}$$

For the construction of the Hamiltonian by means of the Quantum Inverse Scattering Method, we construct the monodromy and transfer matrix,

$$T(\lambda) = \mathcal{G} \mathcal{R}_{\mathcal{A},L}(\lambda) \mathcal{R}_{\mathcal{A},L-1}(\lambda) \dots \mathcal{R}_{\mathcal{A},1}(\lambda), \quad (\text{II.92})$$

$$\tau(\lambda) = \text{str}_{\mathcal{A}} T(\lambda) \quad (\text{II.93})$$

where \mathcal{G} is a diagonal matrix represented here as

$$\mathcal{G} = \begin{pmatrix} e^{i\phi_1} & 0 & 0 & 0 & 0 \\ 0 & 1 & 0 & 0 & 0 \\ 0 & 0 & e^{i\phi_2} & 0 & 0 \\ 0 & 0 & 0 & e^{2i\phi_2} & 0 \\ 0 & 0 & 0 & 0 & e^{i(2\phi_2-\phi_1)} \end{pmatrix}, \quad 0 \leq \phi_1, \phi_2 \leq \pi. \quad (\text{II.94})$$

Using the matrix \mathcal{G} allows for a study of general toroidal boundary conditions for the superspin chain. Although the focus of this section lies in the case of genuine periodic chains, i.e. $(\phi_1, \phi_2) = (0, 0)$ or $\mathcal{G} = \mathbf{1}$, it will turn out to be convenient to formulate the problem for the generic case. Since \mathcal{R} -matrix commutes with two distinct $U(1)$ symmetries, it also commutes with \mathcal{G} ,

$$[R_{12}(\lambda), \mathcal{G} \otimes \mathcal{G}] = 0, \quad (\text{II.95})$$

hence, the boundary conditions imposed by the matrix \mathcal{G} preserve the integrability of the model.

Specifically, we shall investigate the spectrum of the antiferromagnetic superspin chain with L sites subject to these boundary conditions. The Hamiltonian with nearest neighbour interactions expressed in terms of the R -matrix and the twist matrix \mathcal{G} reads

$$\mathcal{H} = i \sum_{j=1}^{L-1} \frac{\partial}{\partial \lambda} R_{jj+1}(\lambda)|_{\lambda=0} + i \mathcal{G}_L^{-1} \frac{\partial}{\partial \lambda} R_{L1}(\lambda)|_{\lambda=0} \mathcal{G}_L. \quad (\text{II.96})$$

The diagonalization of this Hamiltonian (when expressed as logarithmic derivative of the transfer matrix, eq. (II.93)) can be performed within the Algebraic Bethe Ansatz leading to a set of algebraic equations for the Bethe roots parametrizing the eigenspectrum. The calculation in full detail is presented in [117]. Although the auxiliary space is five-dimensional, the nested Bethe Ansatz solution involves only one step of nesting²². This becomes manifest after the first Bethe Ansatz where we arrive at a model isomorphic to the $su(2)$ -symmetric $S = 1$ Heisenberg XXZ chain. Hence, only one step of nesting is necessary. Note, in the first Bethe Ansatz used, there occur some subtleties in the

²²Mathematically, this stems from the fact that $\text{rank}(U_q[\text{osp}(3|2)]) = 2$.

2. The operator content of the $U_q[osp(3|2)]$ superspin chain

construction of eigenstates by acting with creation operators on the reference state since the right combination of creation operators have to be used, see [118]. Besides, the explicit calculation comprises basically the same steps as the solution of the staggered $U_q[sl(2|1)]$ superspin chain, therefore we will present only the main results.

The presence of two $U(1)$ symmetries allows for a decomposition of the Hilbert space of the model into sectors according to the eigenvalues of the corresponding charges. Labeling these sectors by a pair of integers (n_1, n_2) , there exist two convenient reference states which can be used for the Bethe Ansatz, namely the fully polarized states in the sectors $(0, L)$ and $(L, 0)$. Selecting one of these also fixes the ordering of bosonic and fermionic basis states and therefore the parities p_j to $bfbfb \equiv (0, 1, 0, 1, 0)$ and $fbbbf \equiv (1, 0, 0, 0, 1)$, respectively. Likewise the $U_q[sl(2|1)]$ superspin chain, the Bethe Ansatz equations depend on the chosen grading. Below, we will use whichever turns out to be more convenient for the particular state, hence, the Bethe Ansatz equations in both formulations are presented. As we will emphasize below, the model defined in this way is critical for $0 \leq \gamma \leq \pi$. Thus, we again expect the thermodynamic limit of its low-energy spectrum to be described by a Conformal Field Theory.

2.2.1 Bethe Ansatz in the $bfbfb$ grading

The eigenstates of the Hamiltonian in the grading $bfbfb$ are parametrized by two sets of complex numbers $\lambda_j^{(1)}$, $j = 1, \dots, L - n_2$ and $\lambda_j^{(2)}$, $j = 1, \dots, L - n_1 - n_2$, satisfying the Bethe equations

$$\left[\frac{\sinh(\lambda_j^{(1)} + i\gamma/2)}{\sinh(\lambda_j^{(1)} - i\gamma/2)} \right]^L = e^{i\phi_1} \prod_{k=1}^{L-n_1-n_2} \frac{\sinh(\lambda_j^{(1)} - \lambda_k^{(2)} + i\gamma/2)}{\sinh(\lambda_j^{(1)} - \lambda_k^{(2)} - i\gamma/2)}, \quad (\text{II.97a})$$

$$j = 1, \dots, L - n_2,$$

$$\prod_{k=1}^{L-n_2} \frac{\sinh(\lambda_j^{(2)} - \lambda_k^{(1)} + i\gamma/2)}{\sinh(\lambda_j^{(2)} - \lambda_k^{(1)} - i\gamma/2)} = e^{i(\phi_1 - \phi_2)} \prod_{\substack{k=1 \\ k \neq j}}^{L-n_1-n_2} \frac{\sinh(\lambda_j^{(2)} - \lambda_k^{(2)} + i\gamma)}{\sinh(\lambda_j^{(2)} - \lambda_k^{(2)} - i\gamma)}$$

$$\times \frac{\sinh(\lambda_j^{(2)} - \lambda_k^{(2)} - i\gamma/2)}{\sinh(\lambda_j^{(2)} - \lambda_k^{(2)} + i\gamma/2)}, \quad (\text{II.97b})$$

$$j = 1, \dots, L - n_1 - n_2.$$

Note, in this grading the algebra inclusion $osp(3|2) \supset osp(1|2)$ becomes explicit: the second set of equations coincides with those for an inhomogeneous $osp(1|2)$ vertex model [19, 22, 117].

In terms of these parameters the corresponding energy is given by

$$E(\{\lambda_j^{(a)}\}, L) = - \sum_{j=1}^{L-n_2} \frac{2 \sin \gamma}{\cos \gamma - \cosh(2\lambda_j^{(1)})} - 2L \cot \gamma. \quad (\text{II.98})$$

This choice of grading is particularly convenient to study the thermodynamic limit of the superspin chain in the subsector with charges $(n_1 = 0, n_2)$. In these subsectors, the numbers of Bethe roots for both levels coincides which helps to simplify the analysis. Comparing the spectrum obtained by exact diagonalization of the Hamiltonian with our numerical solution of the Bethe equations (II.97) for small lattice sizes, we find that the Bethe root configurations for levels in these sectors are dominated by pairs of complex conjugate rapidities with $\text{Im}(\lambda_j^{(1)}) \simeq \pm 3\gamma/4$ and $\text{Im}(\lambda_j^{(2)}) \simeq \pm \gamma/4$ ('2-strings'). To compute bulk properties of the superspin chain we concentrate our analysis of the Bethe equations to the case of genuine periodic boundary conditions, $\phi_1 = \phi_2 = 0$. In this case we find that the differences between the real centers of two-strings on both levels become exponentially small for large L . This motivates the following string hypothesis involving two *bfbfb*-Bethe roots from each level for the analysis of the thermodynamic limit, $L \rightarrow \infty$:

$$\lambda_{j,\pm}^{(1)} \simeq \xi_j \pm i \frac{3\gamma}{4}, \quad \lambda_{j,\pm}^{(2)} \simeq \xi_j \pm i \frac{\gamma}{4}, \quad \xi_j \in \mathbb{R}. \quad (\text{II.99})$$

Rewriting the Bethe equations (II.97) in terms of the real ξ_j , we find that the second set of Bethe equations is automatically satisfied. Therefore, we can restrict our study to the analysis of the remaining first level equations which, after taking the logarithm, read

$$\begin{aligned} L \left[\Phi \left(\xi_j, \frac{5\gamma}{4} \right) - \Phi \left(\xi_j, \frac{\gamma}{4} \right) \right] &= -2\pi Q_j + \\ + \sum_{k=1}^{(L-n_2)/2} \left[\Phi \left(\xi_j - \xi_k, \frac{3\gamma}{2} \right) + \Phi(\xi_j - \xi_k, \gamma) - \Phi \left(\xi_j - \xi_k, \frac{\gamma}{2} \right) \right], & \quad (\text{II.100}) \\ j = 1, \dots, \frac{L-n_2}{2}, & \end{aligned}$$

where $\Phi(x, \gamma) = 2 \arctan [\tanh x \cot \gamma]$. The numbers Q_j define the possible branches of the logarithm. They are integers or half-integers, depending on the parity of the number of strings $(L - n_2)/2$ (which is an integer for the states considered here).

In this formulation, the thermodynamic limit can be studied within the root density approach [119] in which the roots ξ_j are expected to fill the entire real axis. Their density $\sigma(\xi)$ can be defined by the condition

$$L\sigma(x)dx = \text{Number of } \xi'_j \text{ s in } [x, x + dx]. \quad (\text{II.101})$$

2. The operator content of the $U_q[\mathfrak{osp}(3|2)]$ superspin chain

The thermodynamic limit $L \rightarrow \infty$ may be studied using the *counting function* $Z(x)$,

$$Z(x) = \frac{-1}{2\pi} \left\{ L\Phi\left(x, \frac{5\gamma}{4}\right) - L\Phi\left(x, \frac{\gamma}{4}\right) - \sum_{k=1}^{(L-n2)/2} \left[\Phi\left(x - \xi_k, \frac{3\gamma}{2}\right) + \Phi(x - \xi_k, \gamma) - \Phi\left(x - \xi_k, \frac{\gamma}{2}\right) \right] \right\}. \quad (\text{II.102})$$

By means of its definition, the counting function maps the centers of Bethe roots to the (half-) integers Q_j , $Z(x)|_{x=\xi_j} = Q_j/L$. Hence, the counting function changes every time its argument passes the center of a Bethe root which allows us to write

$$\begin{aligned} LdZ(x)dx &= L\frac{dZ}{dx}dx = \text{Number of } \xi_j \text{ in } [x, x + dx] \\ \Rightarrow \sigma(x) &= \frac{dZ(x)}{dx}. \end{aligned} \quad (\text{II.103})$$

Thus, deriving the counting function enables us to recast the Bethe equations (II.100) into an integral equation for the density $\sigma(x)$ in the limit $L \rightarrow \infty$,

$$\begin{aligned} 2\pi\sigma(x) &= \Phi'\left(x, \frac{\gamma}{4}\right) - \Phi'\left(x, \frac{5\gamma}{4}\right) + \\ &+ \int_{-\infty}^{\infty} dy \left[\Phi'\left(x - y, \frac{3\gamma}{2}\right) + \Phi'(x - y, \gamma) - \Phi'\left(x - y, \frac{\gamma}{2}\right) \right] \sigma(y) \end{aligned} \quad (\text{II.104})$$

where

$$\Phi'(x, \gamma) = \frac{2 \sin(2\gamma)}{\cosh(2x) - \cos(2\gamma)}. \quad (\text{II.105})$$

The integral equation (II.104) can be solved by the standard Fourier transform method leading to

$$\sigma(x) = \frac{1}{\gamma \cosh(2\pi x/\gamma)}. \quad (\text{II.106})$$

Using this expression, we can calculate the energy per site ε_∞ in the infinite volume limit,

$$\varepsilon_\infty = - \int_{-\infty}^{\infty} dx \frac{\sinh\left(\frac{\gamma x}{2}\right) \cosh\left(\frac{(\pi-3\gamma/2)x}{2}\right)}{\sinh\left(\frac{\pi x}{2}\right) \cosh\left(\frac{\gamma x}{4}\right)} - 2 \cot(\gamma) = -2 \cot \frac{\gamma}{2}. \quad (\text{II.107})$$

Note, the density of roots and the energy density coincide with the corresponding expressions of the spin $S = 1$ XXZ model [120]. Furthermore, since the energy and momentum of elementary excitations above the ground state are given in terms of the root density as

$$\varepsilon(x) = 2\pi\sigma(x), \quad p(x) = \int_x^\infty dy \varepsilon(y), \quad (\text{II.108})$$

we find that the superspin chain, too, has gapless excitations with linear dispersion

$$\varepsilon(p) \sim v_F |p| \quad (\text{II.109})$$

with Fermi velocity $v_F = 2\pi/\gamma$.

2.2.2 Bethe Ansatz in the *fbbbf* grading

Alternatively, the Algebraic Bethe Ansatz can be carried out in the grading *fbbbf*. In this case, the eigenstates are parametrized by roots to a different set of Bethe equations,

$$\left[\frac{\sinh(\lambda_j^{(1)} + i\gamma/2)}{\sinh(\lambda_j^{(1)} - i\gamma/2)} \right]^L = e^{i\phi_1} \prod_{k=1}^{L-n_1-n_2} \frac{\sinh(\lambda_j^{(1)} - \lambda_k^{(2)} + i\gamma/2)}{\sinh(\lambda_j^{(1)} - \lambda_k^{(2)} - i\gamma/2)}, \quad (\text{II.110a})$$

$$j = 1, \dots, L - n_1,$$

$$\prod_{k=1}^{L-n_1} \frac{\sinh(\lambda_j^{(2)} - \lambda_k^{(1)} + i\gamma/2)}{\sinh(\lambda_j^{(2)} - \lambda_k^{(1)} - i\gamma/2)} = e^{i\phi_2} \prod_{\substack{k=1 \\ k \neq j}}^{L-n_1-n_2} \frac{\sinh(\lambda_j^{(2)} - \lambda_k^{(2)} + i\gamma/2)}{\sinh(\lambda_j^{(2)} - \lambda_k^{(2)} - i\gamma/2)}, \quad (\text{II.110b})$$

$$j = 1, \dots, L - n_1 - n_2.$$

These equations are related to (II.97) by a particle-hole transformation in the rapidity space [121]. This transformation implies that the second level roots $\lambda^{(2)}$ coincide in the two formulations while the first level ones, $\lambda^{(1)}$, depend on the choice of grading, *bfbfb* and *fbbbf*. In the following, we shall use the same notation but specify the underlying grading, whenever specific root configurations are discussed.

Using the *fbbbf* grading, the energy of the corresponding eigenstates is given in terms of the Bethe roots by

$$E(\{\lambda_j^{(a)}\}, L) = \sum_{j=1}^{L-n_1} \frac{2 \sin \gamma}{\cos \gamma - \cosh(2\lambda_j^{(1)})}. \quad (\text{II.111})$$

Again, the analysis of the thermodynamic limit is simplified when we consider charge sectors where the numbers of rapidities $\lambda_j^{(a)}$ on both levels $a = 1, 2$ are equal, i.e. $(n_1, n_2 = 0)$ for *fbbbf* grading. Here, we find that the Bethe root configurations for low-energy states of (II.96) are dominated by pairs of complex conjugate rapidities with imaginary parts $\text{Im}(\lambda_j^{(a)}) \simeq \pm\gamma/4$ on both levels, $a = 1, 2$. As the system size L grows, the root configurations on the two levels become exponentially close. Therefore, we can proceed as above. To study these levels in the thermodynamic limit, $L \rightarrow \infty$, we rewrite the Bethe equations in terms of the real centers ξ_j of the roots containing four

2. The operator content of the $U_q[osp(3|2)]$ superspin chain

fbbbf Bethe roots

$$\lambda_{j,\pm}^{(1)} \simeq \xi_j \pm i\frac{\gamma}{4}, \quad \lambda_{j,\pm}^{(2)} \simeq \xi_j \pm i\frac{\gamma}{4}, \quad \xi_j \in \mathbb{R}. \quad (\text{II.112})$$

As a result, the second level of the Bethe equations are automatically satisfied²³ and the spectrum in these sectors is parametrized in terms of the string equations

$$\begin{aligned} L \left[\Phi \left(\xi_j, \frac{3\gamma}{4} \right) + \Phi \left(\xi_j, \frac{\gamma}{4} \right) \right] &= 2\pi Q_j \\ &+ \sum_{k=1}^{(L-n_1)/2} \left[2\Phi \left(\xi_j - \xi_k, \frac{\gamma}{2} \right) + \Phi(\xi_j - \xi_k, \gamma) \right], \\ j &= 1, \dots, \frac{L-n_1}{2}. \end{aligned} \quad (\text{II.113})$$

Again, the numbers Q_j defining the possible branches of the logarithm are integers or half-integers, depending on the parity of the integer $(L-n_1)/2$.

Note, the same set of equations is obtained for the integrable spin $S=1$ XXZ model are rewritten using a suitable string hypothesis [108]. This identification extends to the expressions for the corresponding eigenenergies. Therefore, we can rely on existing results for the spin $S=1$ Heisenberg model to obtain certain properties of the superspin chain in the thermodynamic limit $L \rightarrow \infty$. In complete agreement with our results for the $(0, n_2)$ charge sectors based on the Bethe Ansatz in the *bfbfb* grading, the energy density and dispersion of gapless excitations are given by (II.107) and (II.109), respectively.

2.3 Finite-size spectrum

To initiate the investigation of the operator content of the q -deformed $osp(3|2)$ superspin chain we have studied its spectrum for small system sizes by the exact diagonalization of (II.96) with toroidal boundary conditions $(\phi_1 = 0, \phi_2)$. Based on our results we observe that the lowest energy in the charge sector $(n_1, n_2) = (0, 0)$ is given by

$$E_{(0,0)}(L) \equiv -2L \cot \frac{\gamma}{2}, \quad (\text{II.114})$$

without any finite-size corrections and independent of ϕ_2 . Note, this is exactly the energy $L\varepsilon_\infty$ obtained within the root density approach for $L \rightarrow \infty$, see eq. (II.107). As we will see below, however, this is not the ground state of the superspin chain for finite γ . In spite of this we shall take this level as a point of reference and compute the

²³Strictly speaking, this occurs for the twist $\phi_2 = \pi$ due to the emergence of a minus sign on the left hand side of the second level Bethe equations (II.110) when $\lambda_j^{(1)} = \lambda_j^{(2)}$. Here, however, we are interested in properties of the thermodynamic limit which is assumed to be independent of specific toroidal boundary conditions.

effective scaling dimensions, X_{eff} , for the states considered below by means of

$$X_{\text{eff}}(L) = \frac{L}{2\pi v_F} (E(L) - L\varepsilon_\infty). \quad (\text{II.115})$$

2.3.1 Root density approach

Before we present our numerical results for the spectrum of scaling dimensions based on solutions of the Bethe equations (II.97) and (II.110), we extend our analytic treatment of the thermodynamic limit in the previous subsections to get first insights into the finite-size scaling of the lowest states in the charge sectors $(n_1 = 0, n_2)$ and $(n_1, n_2 = 0)$. Following de Vega and Woynarovich [122] we compute the corresponding finite-size energy gaps at large but finite L within the root density approach based on the respective string hypotheses.

Starting from the *bfbfb* string equations (II.100) for the lowest state in the sector $(0, n_2)$, we find

$$E_{(0, n_2)}(L) - L\varepsilon_\infty \simeq \frac{2\pi v_F}{L} \left(n_2^2 \frac{\gamma}{4\pi} \right) + \mathcal{O}\left(\frac{1}{L}\right), \quad n_2 = 1, 2, 3, \dots \quad (\text{II.116})$$

The root density approach neglects possible contributions to the scaling dimensions due to deviations of the Bethe roots from the string hypothesis (II.99). Here, however, it appears that we are in a fortunate situation as far as the correct $1/L$ behaviour is concerned. Our prediction (II.116) reproduces the exact energy (II.114) for $n_2 = 0$ and is confirmed by our numerical analysis based on the full Bethe equations in the sectors $(0, n_2 > 0)$, see subsection 2.4 below.

Similarly, we can study the finite-size scaling of the lowest states in the sectors $(n_1, 0)$ based on the *fbbbf* string hypothesis (II.112). In fact, the large L corrections resulting from (II.113) have already been studied for the XXZ chain [100]. Adapting this approach to the present model we find that, for n_1 odd, the finite-size scaling is given by

$$E_{(n_1, 0)}(L) - L\varepsilon_\infty \simeq \frac{2\pi v_f}{L} \left(n_1^2 \frac{(\pi - \gamma)}{4\pi} - \frac{1}{4} \right) + \mathcal{O}\left(\frac{1}{L}\right), \quad n_1 = 1, 3, 5, \dots \quad (\text{II.117})$$

Once again, there arise subtleties due to the approximations entering the string hypothesis. Deviations from (II.112), either in the imaginary parts of the roots forming the strings or between the string centers on level one and two, can modify the scaling dimensions substantially. In spite of that we shall see that the numerical analysis performed in subsection 2.4 will in fact confirm the proposal II.117 for the lowest state when n_1 is odd.

2.3.2 Relation to the spin $S = 1$ XXZ model

Here we provide additional support for the proposed finite-size spectrum by uncovering relations between the q -deformed $osp(3|2)$ superspin chain and the $S = 1$ XXZ model. At the particular choice of $\gamma = \pi/2$ for the deformation parameter, the charge sectors $(0, n_2)$ and $(n_1, 2)$ of the superspin chain can be shown to contain the eigenenergies of the spin $S = 1$ XXZ model at the same anisotropy.

We begin by considering the $bfbfb$ Bethe equations in the subsector $(0, n_2)$. It is straightforward to see that for $\gamma = \pi/2$ the root configuration

$$\lambda_j^{(1)} = \lambda_j^{(2)} + i\frac{\pi}{2} = \mu_j + i\frac{\pi}{2}, \quad j = 1, \dots, L - n_2 \quad (\text{II.118})$$

automatically satisfies the second set of Bethe equations (II.97). The remaining first level Bethe equations constrain the rapidities μ_j by the relations

$$\left[\frac{\sinh(\mu_j + i\pi/4)}{\sinh(\mu_j - i\pi/4)} \right]^L = (-1)^{n_2+1} \prod_{\substack{k=1 \\ k \neq j}}^{L-n_2} \frac{\sinh(\mu_j - \mu_k + i\pi/4)}{\sinh(\mu_j - \mu_k - i\pi/4)}, \quad j = 1, \dots, L - n_2. \quad (\text{II.119})$$

These are exactly the Bethe equations of the spin $S = 1$ XXZ model with twisted boundary conditions $\varphi = 0$ ($\varphi = \pi$) in the sector with odd (even) magnetization n_2 . Furthermore, the corresponding energy (II.98) of the superspin chain coincides with the expression for the XXZ model. Therefore, there exists a direct correspondence between some energy levels of the superspin chain in the subsectors $(0, n_2)$ and the spectrum of the $S = 1$ XXZ model with suitably twisted boundary conditions for $\gamma = \pi/2$. This observation supports our proposal (II.116) based on the root density method. In fact, from the conformal content of the periodic, i.e. $\varphi = 0$, Heisenberg XXZ $S = 1$ model with anisotropy $\gamma = \pi/2$ in the sector with odd $n = n_2$ and vorticity $m = 0$ we find

$$E_{n_2,0}^{\text{XXZ}}(L) - L\varepsilon_0 \stackrel{\gamma=\pi/2}{=} \frac{2\pi v_f}{L^2} \left(\frac{n_2^2}{8} + \frac{1}{8} - \frac{c}{12} \right) = \frac{2\pi v_f}{L^2} \left(\frac{n_2^2}{8} \right), \quad (\text{II.120})$$

in perfect agreement with our proposal. The same holds for n_2 even using the operator content of the XXZ $S = 1$ model but now with *antiperiodic* boundary conditions, $\varphi = \pi$. For more details about the main results for the XXZ $S = 1$ Heisenberg model we refer to the appendix A.1.

Similarly, we now consider the $fbbfb$ Bethe equations in the sector $(n_1, 2)$. Substituting a root configuration where the second level roots $\lambda_j^{(2)}$ coincide with $L - n_1 - 2$ of the first level ones, i.e.

$$\lambda_j^{(1)} = \lambda_j^{(2)} \equiv \mu_j \quad \text{for } j = 1, \dots, L - n_1 - 2, \quad (\text{II.121})$$

into the second set of Bethe equations (II.110) we see that they are fulfilled for arbitrary values of the μ_j provided that the two remaining first level roots are given by $\lambda_{L-n_1-1}^{(1)} = \Lambda$ and $\lambda_{L-n_1}^{(1)} = \Lambda + i\pi/2$. For even $L - n_1$, the first level Bethe equations for such a configuration can be satisfied provided that Λ is chosen to be one of the roots of²⁴

$$\left[\frac{\sinh(\Lambda + i\pi/4)}{\sinh(\Lambda - i\pi/4)} \right]^L = \prod_{k=1}^{L-n_1-2} \frac{\sinh(\Lambda - \mu_k + i\pi/4)}{\sinh(\Lambda - \mu_k - i\pi/4)}. \quad (\text{II.122})$$

Further, the set of rapidities $\{\mu_j\}_{j=1}^{L-n_1-2}$ has to fulfill the Bethe equations of the integrable $S = 1$ XXZ model with *antiperiodic* boundary conditions, $\varphi = \pi$, in the sector with magnetization $n = n_1 + 2$

$$\left[\frac{\sinh(\mu_j + i\pi/4)}{\sinh(\mu_j - i\pi/4)} \right]^L = - \prod_{\substack{k=1 \\ k \neq j}}^{L-n_1-2} \frac{\sinh(\mu_j - \mu_k + i\pi/4)}{\sinh(\mu_j - \mu_k - i\pi/4)}, \quad j = 1, \dots, L - n_1 - 2 \quad (\text{II.123})$$

We further note that the contributions of the roots $\lambda^{(1)} = \Lambda, \Lambda + i\pi/2$ to the corresponding energy (II.111) of the superspin chain cancel each other for $\gamma = \pi/2$. Thus, we have established another one-to-one correspondence between certain eigenenergies of the superspin chain, now in the charge sectors $(n_1, 2)$, and the spectrum of the *antiperiodic* spin $S = 1$ Heisenberg model with even magnetization n_1 at $\gamma = \pi/2$. We have checked numerically that the complete spectrum of the latter appears in that of the superspin chain for lengths up to $L = 8$.

The spectral inclusions appearing for the deformation parameter $\gamma = \pi/2$ are summarized as

$$\begin{aligned} \text{Spec}[\text{XXZ}(\varphi = 0)]_n &\subset \text{Spec}[\text{osp}(3|2)]_{(0,n)} \quad \text{for } n \text{ odd,} \\ \text{Spec}[\text{XXZ}(\varphi = \pi)]_n &\subset \text{Spec}[\text{osp}(3|2)]_{(0,n)} \quad \text{for } n \text{ even,} \\ \text{Spec}[\text{XXZ}(\varphi = \pi)]_{n+2} &\subset \text{Spec}[\text{osp}(3|2)]_{(n,2)}, \quad \text{for } n \text{ even.} \end{aligned} \quad (\text{II.124})$$

where $\text{XXZ}(\varphi)$ refers to the Heisenberg XXZ $S = 1$ model with toroidal boundary conditions φ . In Table 1 we exhibit these inclusions explicitly for $L = 7$.

Again, we emphasize that these inclusions are particular for the model with the specially chosen deformation parameter $\gamma = \pi/2$ where we observe additional degeneracies in the finite-size spectrum of the superspin chain. Apart from this special point, we have no evidence for such a relation with the XXZ model. Further, the eigenspectrum

²⁴Note that $\Lambda = 0$ is a solution of this equation for any set $\{\mu_j\}_{j=1}^{L-n_1-2}$ which is invariant under $\mu \leftrightarrow -\mu$.

2. The operator content of the $U_q[osp(3|2)]$ superspin chain

$osp(3 2)_{(n_1, n_2)}$	XXZ(φ) $_n$
(0, 0)	$n = 0, \varphi = \pi$
(0, 1)	$n = 1, \varphi = 0$
(0, 2)	$n = 2, \varphi = \pi$
(0, 3)	$n = 3, \varphi = 0$
(0, 4), (2, 2)	$n = 4, \varphi = \pi$
(0, 5)	$n = 5, \varphi = 0$
(0, 6), (4, 2)	$n = 6, \varphi = \pi$
(0, 7)	$n = 7, \varphi = 0$

Table 1: Spectral inclusion for $L = 7$ between sectors of the $osp(3|2)$ and the Heisenberg XXZ spin- $S = 1$ chains for $\gamma = \pi/2$.

does not appear to be invariant under $\gamma \leftrightarrow \pi - \gamma$.

2.4 Numerical study of the operator content

In this subsection we analyze the finite-size scaling of the low-lying excitations of the superspin chain with an even number of lattice sites in a given charge sector (n_1, n_2) . Specifically we shall consider the nine distinct sectors with n_1 and n_2 taking values from the set $\{0, 1, 2\}$.

As mentioned earlier, the root configurations of the low lying levels are dominated by the string complexes (II.99) and (II.112) depending on the grading used. Apart from these, most of the solutions to the Bethe equations contain a finite number of roots which do not belong to one of these complexes. A complete classification of the patterns formed by these additional roots for the $U_q[osp(3|2)]$ superspin chain is not known. In our numerical work we have observed the following configurations:

1_a^v : 1-strings with parity $v = \pm 1$ on level $a = 1, 2$,

$$\lambda^{(a)} = \xi + i\frac{\pi}{4}(1 - v), \quad (\text{II.125a})$$

2_a^+ : 2-strings with parity $v = 1$ on level $a = 1, 2$,

$$\lambda_{\pm}^{(a)} \simeq \xi \pm i\frac{\gamma}{4}, \quad (\text{II.125b})$$

$\bar{2}_a^v$: wide 2-strings with parity $v = \pm 1$ on level $a = 1, 2$:

$$\lambda_{\pm}^{(a)} \simeq \xi + i\frac{\pi}{4}(1 - v) \pm i\frac{3\gamma}{4}, \quad (\text{II.125c})$$

3_{12}^v : mixed 3-strings with parity $v = \pm 1$, combining two level-1 and one level-2 roots as

$$\lambda_{\pm}^{(1)} \simeq \xi + i\frac{\pi}{4}(1-v) \pm i\frac{\gamma}{2}, \quad \lambda^{(2)} = \xi + i\frac{\pi}{4}(1-v) \quad (\text{II.125d})$$

3_{21}^v : mixed 3-strings with parity $v = \pm 1$, combining one level-1 and two level-2 roots,

$$\lambda^{(1)} = \xi + i\frac{\pi}{4}(1-v), \quad \lambda_{\pm}^{(2)} \simeq \xi + i\frac{\pi}{4}(1-v) \pm i\frac{\gamma}{2}, \quad (\text{II.125e})$$

where $\xi \in \mathbb{R}$.

We note that both the root complexes (II.99) and (II.112) and the string configurations (II.125b)–(II.125e) of length greater than 1 may appear strongly deformed in Bethe root configurations for finite L or large real centers ξ . In such cases it may not be possible to discriminate between 2-strings, wide 2-strings, and the components of mixed three strings with $\text{Im}(\lambda) \notin \{0, \pi/2\}$. In these cases the corresponding roots appear as

z_a : pairs of complex conjugate Bethe roots on level $a = 1, 2$:

$$\lambda_{\pm}^{(a)} = \xi \pm i\eta, \quad \xi \in \mathbb{R}, \quad 0 < |\eta| < \frac{\pi}{2}, \quad (\text{II.125f})$$

where we have used that solutions to the Bethe equations are defined modulo $i\pi$ only.

To describe the root configurations parameterizing a particular eigenstate, we introduce the following notation. Using the patterns (II.125) we will indicate only the roots which are *not* part of the dominant string complexes, i.e. eqs. (II.99) and (II.112) depending on the grading. As an example, consider an excitation which is described by a certain number of $fbbbf$ complexes and, in addition, k real roots and one 1^- -string on the first level as well as a wide 2^- -string on the second level. Such a configuration will be indicated by the short notation

$$f : [(1_1^+)^k, 1_1^-, \bar{2}_2^-].$$

Note, the number of additional $fbbbf$ string complexes in this root configuration is fixed by the charges (n_1, n_2) which determine the total number of Bethe roots for a given grading and system size L . In addition to patterns with finite centers the Bethe roots only, we have also observed solutions containing strings which are located at $\pm\infty$. For these, we do not have to distinguish different parities and extend our notation as, e.g., $[1_1]_{+\infty}$ for a root $\lambda^{(1)} = +\infty$.

Considering our observations in subsection 2.3 we expect the critical regime of the superspin chain to be contained in the interval $\gamma \in [0, \pi]$. Let us emphasize, however, that for much of the numerical analysis in this work we have concentrated on the region

2. The operator content of the $U_q[osp(3|2)]$ superspin chain

$\gamma \leq \pi/2$ where we find that most of the states considered here keep their basic root structure, independent of the deformation parameter.

As a working hypothesis for the respective lowest scaling dimensions, we conjecture that they can be expressed in terms of the sum of several distinct parts. The underlying $U(1)$ symmetries of the superspin chain give rise to two Gaussian fields with distinct compactification radii depending on the deformation parameter γ . Motivated by our preliminary finite-size analysis within the root density approach, we propose that these Coulomb gas contributions to the anomalous dimensions are given by

$$\Xi_{n_1, m_1}^{n_2, m_2} = n_1^2 \frac{\pi - \gamma}{4\pi} + m_1^2 \frac{\pi}{\pi - \gamma} + n_2^2 \frac{\gamma}{4\pi} + m_2^2 \frac{\pi}{4\gamma} \quad (\text{II.126})$$

where m_1 and m_2 take into account the vortex companions of the spin excitations n_1 and n_2 . By the same means we propose that the contribution of the Gaussian fields to the conformal spin of a state is determined by

$$\sigma_{n_1, m_1}^{n_2, m_2} = n_1 m_1 + \frac{1}{2} n_2 m_2. \quad (\text{II.127})$$

Additionally, we anticipate that there are contributions to the anomalous dimensions and to the conformal spin coming from fields associated with discrete symmetries. Support for this expectation comes from the inclusion of levels of the $S = 1$ integrable XXZ chain in the spectrum of the superspin chain discussed in subsection 2.3.2. Recall here that the critical properties of the XXZ chain are known to be described in terms of composites of Gaussian and $Z(2)$ fields, see appendix A.1. Putting these thoughts together we are led to propose for the conformal data of the $U_q[osp(3|2)]$ superspin chain,

$$\begin{aligned} X_{n_1, m_1}^{n_2, m_2} &= \Xi_{n_1, m_1}^{n_2, m_2} + x_0, \\ s_{n_1, m_1}^{n_2, m_2} &= \sigma_{n_1, m_1}^{n_2, m_2} \pm s_0. \end{aligned} \quad (\text{II.128})$$

where x_0 and s_0 take into account the contributions of the potential discrete degrees of freedom which are assumed to be independent of γ .

We remark that the respective value of x_0 will be determined by the quantum numbers in (II.128). This can be seen for instance by comparing our proposal (II.128) with the expected conformal dimensions of the isotropic $osp(3|2)$ superspin chain. We easily see that in the rational limit $\gamma \rightarrow 0$ the conformal dimensions do not depend on the quantum number n_2 while the modes $m_2 \neq 0$ decouple from the low-energy spectrum. This comparison on the subspace of states $n_2 = m_2 = 0$ reveals that for L even the quantum numbers n_1 and m_1 satisfy the following rule,

- for n_1 even $\rightarrow m_1 = \pm\frac{1}{2}, \pm\frac{3}{2}, \dots$,
 - for n_1 odd $\rightarrow m_1 = 0, \pm 1, \pm 2, \dots$,
- (II.129)

where in both cases the isotropic limit yields $x_0 = -1/4$.

In the next subsections we shall see that other values for x_0 are possible when the space of states is enlarged to include states with n_2 and $m_2 \neq 0$. This indicates the presence of additional degrees of freedom besides the Gaussian fields in the operator content of the $U_q[osp(3|2)]$ superspin chain. In addition we find that the vortex quantum number m_1 appears to take values on $\mathbb{Z}/2$ while the quantum number satisfies $m_2 \in \mathbb{Z}$.

We now discuss the results of the numerical solution of the Bethe equations (II.97) and (II.110) in the nine sectors characterized by the charges $n_i \in \{0, 1, 2\}$, $i = 1, 2$, for system sizes up to $L = 8192$.

2.4.1 Sector $(0, 0)$

As we have already mentioned above, the lowest state in the sector with quantum numbers $(n_1, n_2) = (0, 0)$ has the energy $L\epsilon_\infty$ without any finite-size correction, eq. (II.114). In terms of our proposal (II.128), this corresponds to a primary operator with scaling dimension $X_{0,0}^{0,0} = \Xi_{0,0}^{0,0} = 0$. This state has zero momentum, consistent with a conformal spin $s = s_0 = 0$ of the corresponding operator.

For the first excitation in this charge sector, we find that its *fbbbf* root configuration contains a single root on the first and a two-string on the second level at infinity, $\lambda^{(1)} = -\infty$ and $\lambda_{\pm}^{(2)} = -\infty$. As a consequence, the remaining finite roots have to satisfy the Bethe equations (II.110) for $(n_1, n_2) = (1, 1)$ in the presence of twists $(\phi_1, \phi_2) = (2\gamma, \gamma)$ in the boundary conditions. They are arranged in $(L-2)/2$ *fbbbf* two-string complexes (II.112) and an additional first level root $\lambda^{(1)} \in \mathbb{R}$, i.e. $f : [1_1^+] \oplus [1_1, 2_2]_{-\infty}$ in the notation introduced in eqs. (II.125) above. In fact, this is the first of a family of excitations with zero momentum in this sector in which k of the string complexes are replaced by $2k$ real roots $\lambda^{(1)}$ and $2k$ second level roots with $\text{Im}(\lambda^{(2)}) = \pi/2$, i.e.

$$\begin{aligned}
\{\lambda^{(1)}\} &= \left\{ \xi_j^{(1)} \pm i\frac{\gamma}{4}, \xi_j^{(1)} \in \mathbb{R} \right\}_{j=1}^{(L-2)/2-k} \cup \left\{ \lambda_j \in \mathbb{R} \right\}_{j=1}^{2k+1} \cup \{-\infty\} \\
\{\lambda^{(2)}\} &= \left\{ \xi_j^{(2)} \pm i\frac{\gamma}{4}, \xi_j^{(2)} \in \mathbb{R} \right\}_{j=1}^{(L-2)/2-k} \cup \left\{ \lambda_j \in \mathbb{R} + i\frac{\pi}{2} \right\}_{j=1}^{2k} \cup \{-\infty, -\infty\},
\end{aligned}
\tag{II.130}$$

or $f : [(1_1^+)^{(2k+1)}, (1_2^-)^{2k}] \oplus [1_1, 2_2]_{-\infty}$. The root configurations for $k = 0, 1, 2$ are depicted in Figure 21.

We have solved the Bethe equations (II.110) for these configurations with $k = 0, 1, 2$

2. The operator content of the $U_q[osp(3|2)]$ superspin chain

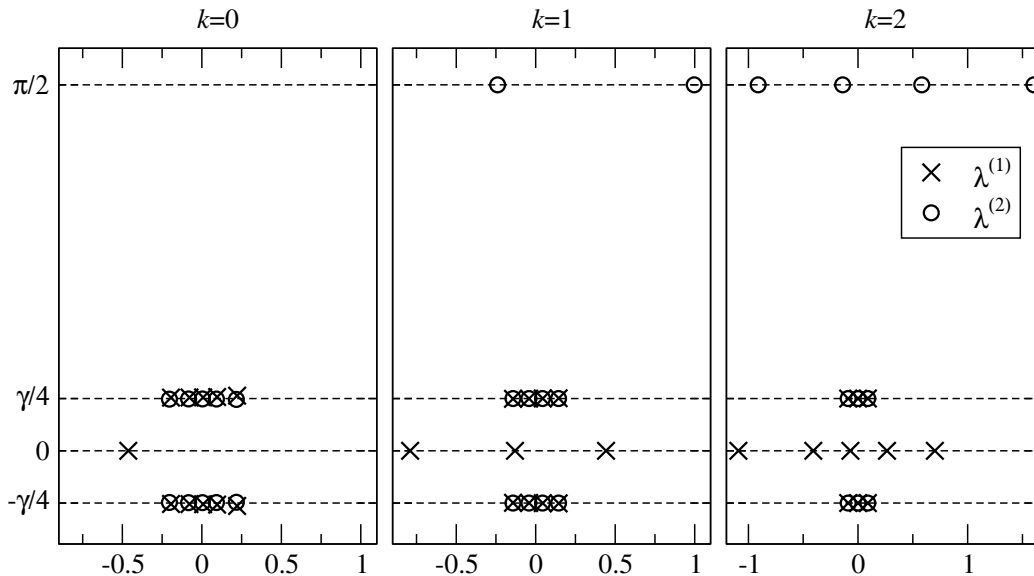


Figure 21: Finite part of the $fbbf$ root configurations (II.130) with $k = 0, 1, 2$ for $L = 12$ and $\gamma = 2\pi/7$.

for chains of up to $L = 2048$ sites. The effective scaling dimensions (II.115) computed from the resulting finite-size energies show strong subleading corrections to scaling, see figure 22.

Assuming a rational dependence on $1/\log L$ we have extrapolated the finite-size data and find that these levels form a 'tower' starting at

$$X_{0,\frac{1}{2}}^{0,0} = \Xi_{0,\frac{1}{2}}^{0,0} - \frac{1}{4} = \frac{\pi}{4(\pi - \gamma)} - \frac{1}{4}, \quad (\text{II.131})$$

with the dominant subleading corrections vanishing as a power of $1/\log L$ in the thermodynamic limit $L \rightarrow \infty$, similar as in the isotropic model [19].

The next excitation for small system sizes corresponds again to an operator with zero conformal spin, $s = 0$. The corresponding Bethe state is described by root configurations $b : [1_1^+] \oplus [1_1, 2_2]_{-\infty}$ or $f : [1_1]_{\infty} \oplus [1_1, 2_2]_{-\infty}$, depending on the grading used. It is studied most conveniently in the $bfbf$ formulation where the finite roots satisfy (II.97) with $(n_1, n_2) = (1, 1)$ and twist angles $(\phi_1, \phi_2) = (2\gamma, \gamma)$. The effective scaling dimensions of this state as calculated from the finite-size energies for chains with up to $L = 2048$ sites extrapolate to

$$X_{0,0}^{0,1} = \Xi_{0,0}^{0,1} - \frac{1}{8} = \frac{\pi}{4\gamma} - \frac{1}{8}, \quad (\text{II.132})$$

see figure 23.

This observation can be underpinned by a relation to the $S = 1$ XXZ chain similar to the ones discussed in subsection 2.3.2. The finite roots in the $fbbf$ configuration satisfy the Bethe equations (II.110) in the sector $(n_1, n_2) = (2, 0)$ with twist angles

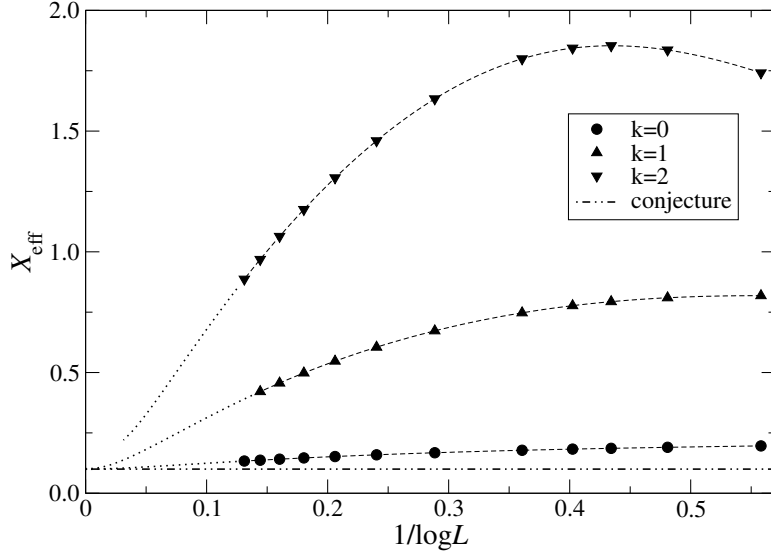


Figure 22: Effective scaling dimensions extracted from the finite-size behaviour of the eigenenergies of the superspin chain in sector $(0, 0)$ described by $fbbbf$ root configurations (II.130) with $k = 0, 1, 2$ for $\gamma = 2\pi/7$. Dotted lines show the extrapolation of the finite-size data assuming a rational dependence on $1/\log L$, the dashed-dotted line is our conjecture (II.131) for this anisotropy.

$(\phi_1, \phi_2) = (2\gamma, 2\gamma)$. Furthermore, at $\gamma = \pi/2$, we find that $\lambda_j^{(1)} = \lambda_j^{(2)} \equiv \mu_j$ for these roots, which satisfy the Bethe equations (A.1) of the XXZ model with periodic boundary conditions for this value of γ . Hence, the proposal (II.132) agrees with the finite size scaling of the lowest zero-momentum excitation in the sector with magnetization $n = 2$ of the XXZ model with periodic boundary conditions, eq. (A.7),

$$E_{2,0}^{\text{XXZ}}(L) - L\varepsilon_0 \stackrel{\gamma=\pi/2}{=} \frac{2\pi v_F}{L} \left(\frac{2^2}{8} - \frac{c}{12} \right) = \frac{2\pi v_F}{L} \left(\frac{3}{8} \right). \quad (\text{II.133})$$

Continuing our finite-size analysis of the low-energy states in the charge sector $(0, 0)$ we have identified an excitation with conformal spin $s = 1$ described by a root configuration $f : [1_1]_\infty \oplus [1_1, 2_2]_{-\infty}$. In this case the finite roots satisfy the Bethe equations (II.110) for $(n_1, n_2) = (2, 0)$ in the presence of twists $(\phi_1, \phi_2) = (2\gamma, 2\gamma)$. From our numerical data, we conclude that this level is a descendant of the lowest state in this sector with scaling dimension

$$X = \Xi_{0,0}^{0,0} + 1 = 1, \quad (\text{II.134})$$

independent of γ , see figure 24.

Again we can relate this proposal to the finite-size scaling of an excitation appearing in the periodic $S = 1$ XXZ model for $\gamma = \pi/2$. More precisely, this state corresponds to $E_{2,1}^{\text{XXZ}}$, see Eq. (A.7).

2. The operator content of the $U_q[osp(3|2)]$ superspin chain

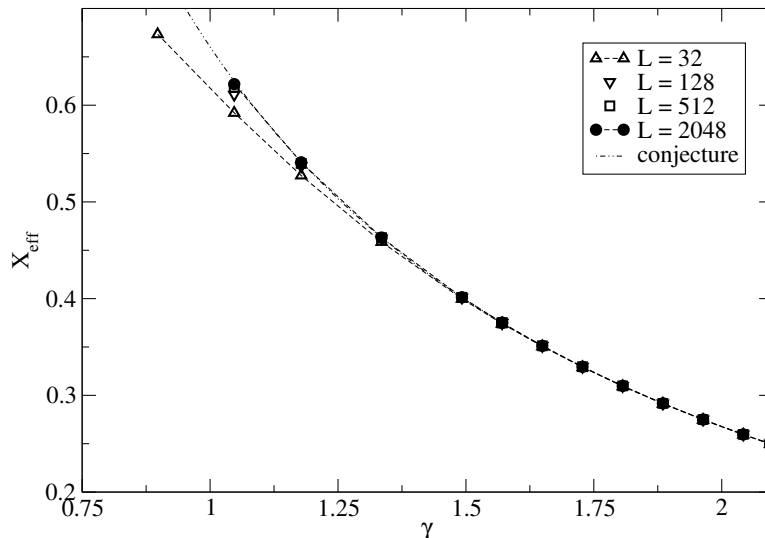


Figure 23: Effective scaling dimensions of the second excitation in the sector $(0,0)$ as a function of γ for various system sizes. The dashed-dotted line indicates our conjecture (II.132).

Among the remaining low-energy states, there are two levels with conformal spin $s = 1$ and scaling dimension extrapolating to

$$X = \Xi_{0, \frac{1}{2}}^{0,0} - \frac{1}{4} + 1 = \frac{\pi}{4(\pi - \gamma)} - \frac{1}{4} + 1, \quad (\text{II.135})$$

see figure 25.

The root structure of one of these states is given by $f : [(1_1^+)^3, z_2] \oplus [1_1, 2_2]_{-\infty}$. We note that this configuration is obtained by breaking one of $fbbb$ string complexes in the first excitation, described by (II.130) with $k = 0$, into two real roots on level 1 and a complex pair on level 2.

The roots for the other level which extrapolates to (II.135) are arranged as $f : [(1_1^+)^2] \oplus [1_1, 2_2]_{-\infty} \oplus [1_1, 2_2]_{\infty}$. In this case, the finite roots satisfy the Bethe equations (II.110) for the charges $(n_1, n_2) = (2, 2)$ with periodic boundary conditions $(\phi_1, \phi_2) = (0, 0)$. This is one example of a more general situation, observed in the exact diagonalization of systems with sizes up to $L = 8$. Many of the low lying eigenenergies in the sector $(2, 2)$ are also present in the sector $(0, 0)$. We defer the discussion of these common levels to subsection 2.4.9 where the low lying states of the sector $(2, 2)$ are studied.

Another spin $s = 1$ level appearing in the charge sector $(0, 0)$ is parametrized by a $bfbfb$ root configuration with the string content $b : [1_1^+] \oplus [1_1, 2_2]_{-\infty}$. Extrapolating its effective scaling dimension we find that it is a descendant of the second excitation, hence

$$X = \Xi_{0,0}^{0,1} - \frac{1}{8} + 1 = \frac{\pi}{4\gamma} - \frac{1}{8} + 1 \quad (\text{II.136})$$

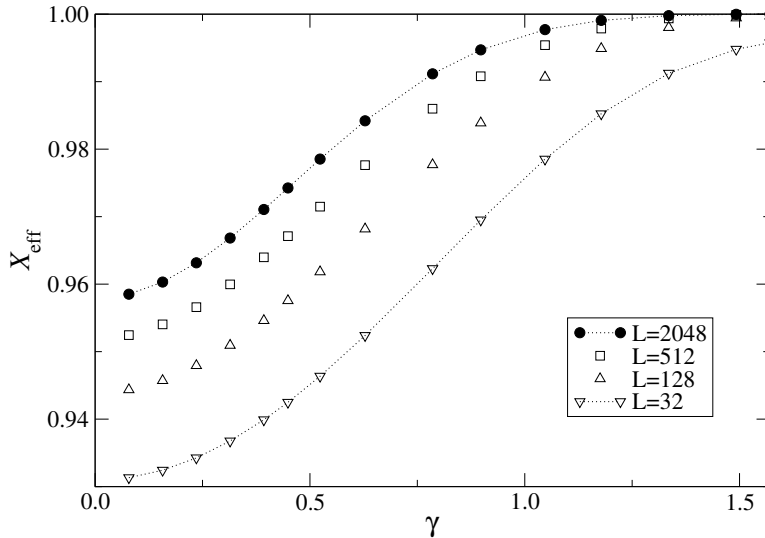


Figure 24: Effective scaling dimensions of the descendant of the ground state of the charge sector $(0, 0)$ as a function of γ for various system sizes. Our conjecture for this state is given by (II.134), $X_{\text{eff}} \equiv 1$, independent of γ .

which, for $\gamma = \pi/2$, can again be related to an eigenenergy in the magnetization $n = 2$ sector of the spin $S = 1$ XXZ model. The finite-size scaling of this state is shown in fig. 25, too.

Among the low-energy states is another spin $s = 1$ level which, depending on the grading chosen, is described by root configurations $f : [(1_1^+)^3, z_2] \oplus [1_1, 2_2]_{-\infty}$ or $b : [1_1^+, 1_1^-, z_2] \oplus [1_1, 2_2]_{-\infty} \oplus [1_1]_{+\infty}$ for small L . In both gradings, one of the real first-level roots, $[1_1^+]$, and the real center of the pair of complex conjugate roots, $[z_2]$, increases considerably as the system size grows. We describe this behaviour in more detail in Appendix A.2. Our observation indicates for a change of the root configuration to a new pattern at some finite-size L_* which we have not been able to identify, unfortunately. The value of L_* where this degeneration takes place depends on the anisotropy, e.g. $L_* \approx 26$ for $\gamma = 2\pi/7$. As a consequence of this scenario we do not have sufficient data for a reliable finite-size analysis of this level.

Our findings for the charge sector $(0, 0)$ are summarized in Table 2.

2.4.2 Sector $(0, 1)$

In this sector, we have analyzed the eight lowest levels present in the spectrum of the superspin chain with $L = 6$ sites and, in addition, some higher excitations which extrapolate to small effective scaling dimensions as well. Based on our numerical finite-size analysis, we find that the effective scaling dimensions of the investigated states extrapolate to four different values fitting into our proposal (II.128).

The lowest state belongs to a family of levels with zero momentum, similar as in the

2. The operator content of the $U_q[osp(3|2)]$ superspin chain

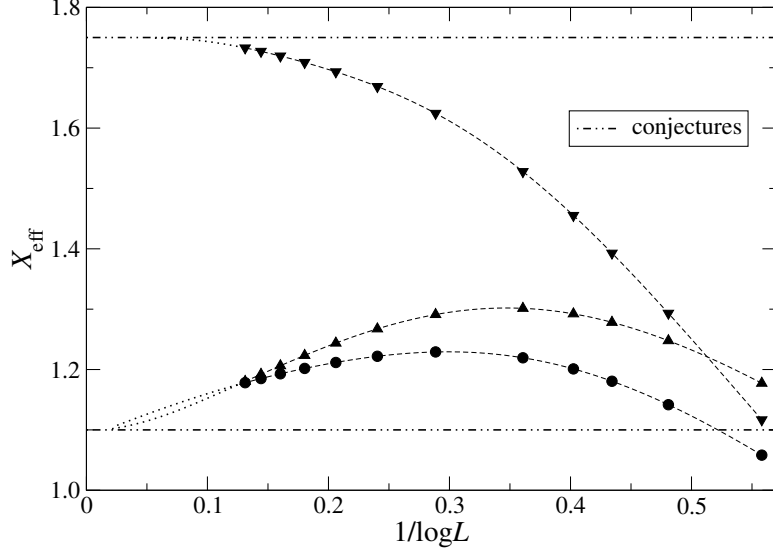


Figure 25: Extrapolation of the effective scaling dimensions of several spin $s = 1$ states in charge sector $(0, 0)$ for $\gamma = 2\pi/7$. The conjectures are given in Eqs. (II.135) and (II.136).

Eq.	X			s			remark
	m_1	m_2	x_0	total spin	$\sigma_{n_1, m_1}^{n_2, m_2}$	s_0	
(II.114)	0	0	0	0	0	0	
(II.131)	$\frac{1}{2}$	0	$-\frac{1}{4}$	0	0	0	tower
(II.132)	0	1	$-\frac{1}{8}$	0	0	0	

Table 2: Summary of the conformal data of primary fields identified in sector $(n_1, n_2) = (0, 0)$. The parametrization is according to our proposal (II.128). In addition we have observed descendants of these primaries, namely (II.134) of (II.114), (II.135) of (II.131), and (II.136) of (II.132).

$(0, 0)$ sector, described by *fbbbf* root configurations

$$\begin{aligned}
 \{\lambda^{(1)}\} &= \left\{ \xi_j^{(1)} \pm i\frac{\gamma}{4}, \xi_j^{(1)} \in \mathbb{R} \right\}_{j=1}^{(L-2)/2-k} \cup \{\lambda_j \in \mathbb{R}\}_{j=1}^{2k} \cup \left\{ \pm i\frac{\gamma}{2} \right\}, \\
 \{\lambda^{(2)}\} &= \left\{ \xi_j^{(2)} \pm i\frac{\gamma}{4}, \xi_j^{(2)} \in \mathbb{R} \right\}_{j=1}^{(L-2)/2-k} \cup \left\{ \lambda_j \in \mathbb{R} + i\frac{\pi}{2} \right\}_{j=1}^{2k} \cup \{0\},
 \end{aligned} \tag{II.137}$$

or $f : [(1_1^+)^{2k}, (1_2^-)^{2k}, 3_{12}^+]$ with integer $k \geq 0$. In this sector, we find another set of levels parametrized by *fbbbf* Bethe roots arranged as

$$\begin{aligned}
 \{\lambda^{(1)}\} &= \left\{ \xi_j^{(1)} \pm i\frac{\gamma}{4}, \xi_j^{(1)} \in \mathbb{R} \right\}_{j=1}^{(L-2)/2-k'} \cup \{\lambda_j \in \mathbb{R}\}_{j=1}^{2k'+1} \cup \left\{ i\frac{\pi}{2} \right\} \\
 \{\lambda^{(2)}\} &= \left\{ \xi_j^{(2)} \pm i\frac{\gamma}{4}, \xi_j^{(2)} \in \mathbb{R} \right\}_{j=1}^{(L-2)/2-k'} \cup \left\{ \lambda_j \in \mathbb{R} + i\frac{\pi}{2} \right\}_{j=1}^{2k'-2} \cup \left\{ i\frac{\pi}{2}, i\frac{\pi}{2} \pm i\frac{\gamma}{2} \right\},
 \end{aligned} \tag{II.138}$$

or $f : [(1_1^+)^{(2k'+1)}, (1_2^-)^{(2k'-1)}, 3_{21}^-]$ for positive integers k' .²⁵

We found that the levels (II.137) and (II.138) with $k = k'$ are almost degenerate. Already for $L = 6$, the relative difference of the energies at $\gamma = 2\pi/7$ is smaller than 10^{-3} .

By solving the Bethe equations (II.110) for these configurations with $k = 0, 1, 2$, $k' = 1, 2$ and system sizes up to $L = 8192$ we found that the scaling dimension for the lowest level ($k = 0$) level extrapolates to

$$X_{0,0}^{1,0} = \Xi_{0,0}^{1,0} = \frac{\gamma}{4\pi}. \quad (\text{II.139})$$

The remaining four levels ($k = 1, 2$ and $k' = 1, 2$) give rise to the same anomalous dimension,

$$X_{0,\frac{1}{2}}^{1,0} = \Xi_{0,\frac{1}{2}}^{1,0} - \frac{1}{4} = \frac{\pi}{4(\pi - \gamma)} + \frac{\gamma}{4\pi} - \frac{1}{4}. \quad (\text{II.140})$$

Again, the associated degeneracy in the thermodynamic limit is lifted for finite L by a fine-structure due to strong subleading corrections to scaling which is shown in fig. 26 for the deformation parameter $\gamma = 2\pi/7$.

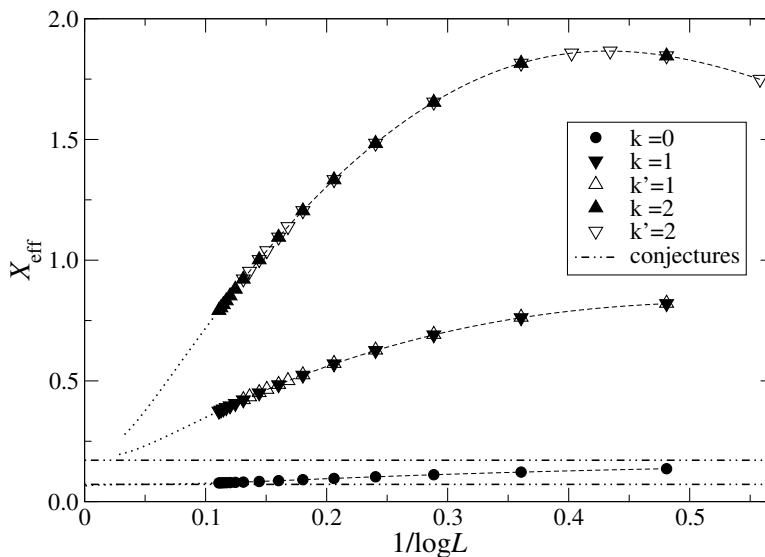


Figure 26: Similar as Fig. 22 but for the eigenenergies of the superspin chain in sector $(0, 1)$ parametrized by the $fbbbf$ root configurations (II.137) with $k = 0, 1, 2$ and (II.138) with $k' = 1, 2$ for $\gamma = 2\pi/7$. The dashed-dotted lines are our conjectures (II.139) and (II.140) for this anisotropy.

We have analyzed the scaling corrections for the $k = 0$ state extrapolating to (II.139) in more detail. For $\gamma = \pi/2$, this state belongs to the class of levels discussed in subsection 2.3.2. Its energy coincides with the lowest eigenvalue of the $S = 1$ XXZ

²⁵We note that the mixed 3-strings in these configurations are exact, i.e. the constituent rapidities are separated by $i\gamma/2$ without deviations.

2. The operator content of the $U_q[osp(3|2)]$ superspin chain

model for magnetization $n = 1$. This motivates to assume a power law dependence of the subleading terms on $1/L$. Extrapolating our numerical data using the VBS method [123, 124] we find

$$X_{\text{eff}}(L) - X_{0,0}^{1,0} \propto L^{-\alpha}, \quad \alpha = \frac{\gamma}{\pi - \gamma}, \quad (\text{II.141})$$

see fig. 27.

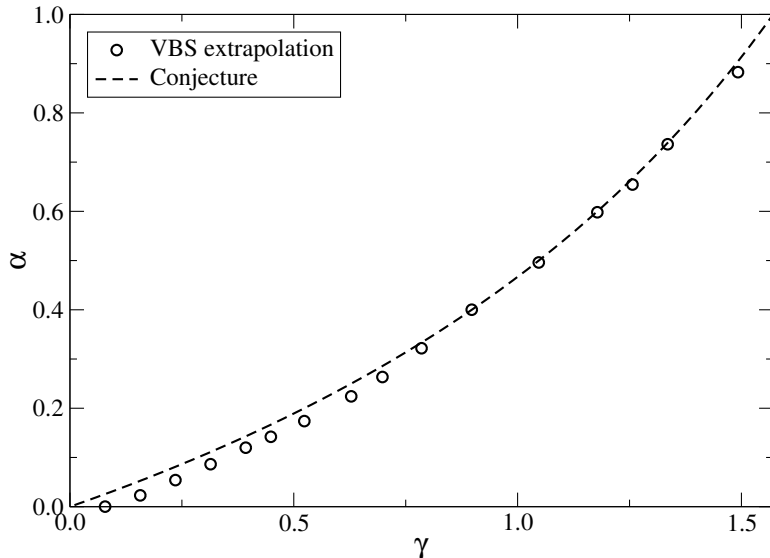


Figure 27: Exponent of the subleading corrections to scaling (II.141) for the ground state of the $(0, 1)$ -sector.

Note, this behaviour coincides with that of the lowest state of the $S = 1$ XXZ model for magnetization $n = 1$ [100] only for the anisotropy where we have established the correspondence to the superspin chain, i.e. at $\gamma = \pi/2$. As $\gamma \rightarrow 0$, the exponent α vanishes indicating the appearance of logarithmic corrections to scaling due to an operator in the theory becoming marginal. This is in accordance with previous studies of the finite-size spectrum of the isotropic $osp(3|2)$ chain [19].

For the other members of this tower, i.e. $k, k' > 0$, we expect the dominant subleading corrections to be logarithmic. A detailed analysis of the corrections to scaling in the combined presence of logarithms and power laws, however, would require data for significantly larger systems which are not accessible by the methods used here.

Continuing our study of low-energy states in the $(0, 1)$ sector we found two states which are described by the root configurations $f : [(1_1^-)^2, (1_2^-)]$ and $b : [1_1^-, 1_2^+, \bar{2}_1^+, 2_2^+]$, respectively. Both carry the conformal spin $s = 1$. In the thermodynamic limit, these states become degenerate since their effective scaling dimensions extrapolate to

$$X = \Xi_{0,0}^{1,0} + 1 = \frac{\gamma}{4\pi} + 1, \quad (\text{II.142})$$

see figure 28, indicating that these levels are descendants of (II.139).

In addition we have identified three low lying levels described by root configurations $b : [1_1^+, 1_2^-]$, $f : [(1_1^+)^2, 1_2^+, 2_1^+, 2_2^+]$, and $f : [(1_1^+)^2, (1_1^-)^2, 1_2^+, \bar{2}_2^-]$, respectively. Extrapolating their effective scaling dimensions yields

$$X_{0,0}^{1,1} = \Xi_{0,0}^{1,1} - \frac{1}{8} + \frac{1}{2} = \frac{\gamma}{4\pi} + \frac{\pi}{4\gamma} + \frac{3}{8}. \quad (\text{II.143})$$

The first and third of these states have conformal spin $s = 0$, the second comes as a doublet of states with the conformal spin $s = 1$. Again this is consistent with primaries being composites of fields with dimensions (II.126) and, according to (II.127), conformal spin $n_2 m_2 / 2 = 1/2$, and an Ising energy operator with conformal weight $1/2$. These factors can be combined to give a scaling dimension (II.143) and conformal spin $s = 0$ and $s = 1$, respectively.

The finite-size scaling for one of the singlets and the doublet is shown in figure 28 for the anisotropy $\gamma = 2\pi/7$. For the lower energy singlet, the Bethe equations have been solved only around $\gamma = \pi/2$, see figure 29.

In table 3 the results presented in this subsection are summed up.

Eq.	X			s			remark
	m_1	m_2	x_0	total spin	$\sigma_{n_1, m_1}^{n_2, m_2}$	s_0	
II.139	0	0	0	0	0	0	
II.140	$\frac{1}{2}$	0	$-\frac{1}{4}$	0	0	0	tower
II.143	0	1	$-\frac{1}{8} + \frac{1}{2}$	1, 0	$\frac{1}{2}$	$\pm \frac{1}{2}$	Ising $(\frac{1}{2}, 0)$, $(0, \frac{1}{2})$

Table 3: Conformal data for the primaries identified in charge sector $(n_1, n_2) = (0, 1)$, see also table 2. We have also observed descendants of (II.139), see (II.142).

2.4.3 Sector $(0, 2)$

Extending our analysis to the $(0, 2)$ sector we found the lowest state to be most conveniently described in the $bfbfb$ grading where all Bethe roots are arranged in $(L - 2)/2$ string complexes (II.99). The root configurations of the first and second excitation are obtained by breaking one of the string complexes into the configurations $b : [(1_1^-)^2, 1_2^+, 1_2^-]$ for the first or $b : [(1_1^-)^2, \bar{2}_2^-]$ for the second excitation, i.e.

$$\lambda_{\pm}^{(1)} = \pm\xi + i\frac{\pi}{2}, \quad \lambda_{\pm}^{(2)} = 0, i\frac{\pi}{2}, \quad (\text{II.144a})$$

$$\lambda_{\pm}^{(1)} = \pm\xi + i\frac{\pi}{2}, \quad \lambda_{\pm}^{(2)} \simeq i\frac{\pi}{2} \pm i\frac{3\gamma}{4}, \quad (\text{II.144b})$$

2. The operator content of the $U_q[osp(3|2)]$ superspin chain

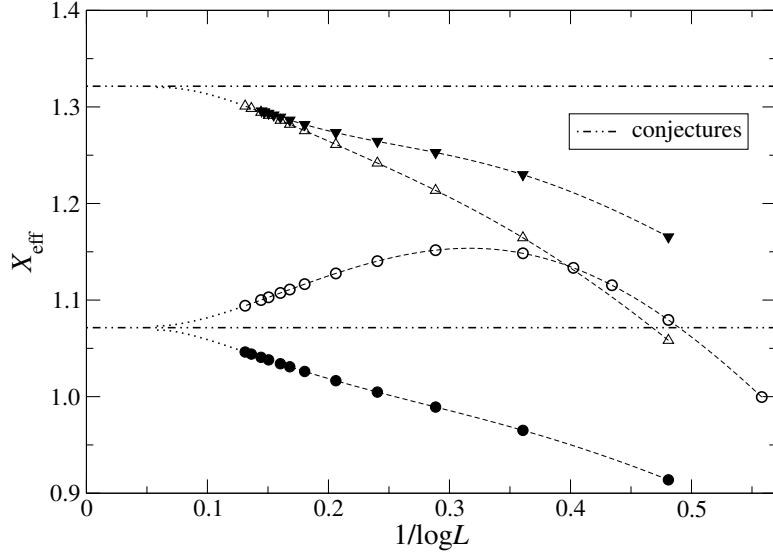


Figure 28: Similar as Fig. 22 but for the levels in sector $(0, 1)$ extrapolating to (II.142) (circles) and (II.143) (triangles) in sector $(0, 1)$ for $\gamma = 2\pi/7$.

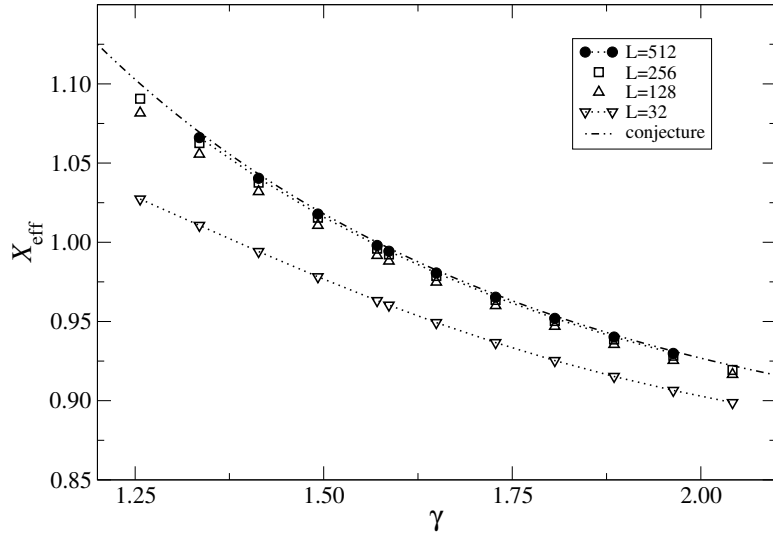


Figure 29: Effective scaling dimensions of the lowest energy singlet in sector $(0, 1)$ with conjectured effective scaling dimension (II.143) as a function of γ for various system sizes.

with real ξ . These three states have zero conformal spin. For large L the effective scaling dimension for the lowest level approaches

$$X_{0,0}^{2,0} = \Xi_{0,0}^{2,0} = \frac{\gamma}{\pi}, \quad (\text{II.145})$$

see figure 30(a).

The subleading corrections are described by a power law in $1/L$. At least for $\gamma \gtrsim \pi/3$ we find that they are described by same exponent as in (II.141) for the ground state in sector $(0, 1)$.

The excitations described in (II.144) belong to a family of excitations obtained by breaking more of the *bfbfb* string complexes forming the ground state leading to root configurations $b : [(1_1^-)^{2k}, 1_2^+, (1_2^-)^{2k-1}]$ or $b : [(1_1^-)^{2k'}, (1_2^-)^{2k'-2}, \bar{2}_2^-]$ with $k, k' > 0$. We have analyzed the finite-size scaling of these levels for $k, k' = 1, 2$, indicating that the members of this family of excitations form another tower of scaling dimensions starting at

$$X_{0, \frac{1}{2}}^{2,0} = \Xi_{0, \frac{1}{2}}^{2,0} - \frac{1}{4} = \frac{\pi}{4(\pi - \gamma)} + \frac{\gamma}{\pi} - \frac{1}{4}. \quad (\text{II.146})$$

For finite L , the degeneracy of these levels is lifted. Likewise the situation in the charge sector $(0, 1)$, for $\gamma > 0$, the excitations are separated from the lowest state by a gap of order $1/L$ with strong subleading corrections. Also, the relative difference of the energies of the levels with $k = k'$ is again very small. e.g. of order 10^{-2} at $L = 6$, see figure 31.

There are two more levels in this sector whose root configurations are described in terms of $(L - 2)/2$ *bfbfb* string complexes. One of them leads to the scaling dimension

$$X_{0,0}^{2,1} = \Xi_{0,0}^{2,1} - \frac{1}{8} = \frac{\gamma}{\pi} + \frac{\pi}{4\gamma} - \frac{1}{8}, \quad (\text{II.147})$$

with conformal spin $s = 1$ in agreement with (II.127). The finite-size data for this state are shown in figure 30(d).

The effective scaling dimension of the other state described by $(L - 2)/2$ *bfbfb* string complexes extrapolates to

$$X = \Xi_{0,0}^{2,0} + 1 = \frac{\gamma}{\pi} + 1, \quad (\text{II.148})$$

see figure 30(b). The conformal spin of this level is given by $s = 1$, indicating that this is a descendant of (II.145). Breaking one of the *bfbfb* string complexes we find another level, also with conformal spin $s = 1$, described by a root configuration $b : [1_1^+, 1_1^-, 1_2^+, 1_2^-]$. The numerical solution of the Bethe equations for this state for sufficiently large systems is limited to anisotropies near $\gamma = \pi/2$ where the extrapolation of the finite-size gives again (II.148), as shown in fig. 30(c).

Additionally, we report on two other low-energy levels in this sector, a spin $s = 0$

2. The operator content of the $U_q[osp(3|2)]$ superspin chain

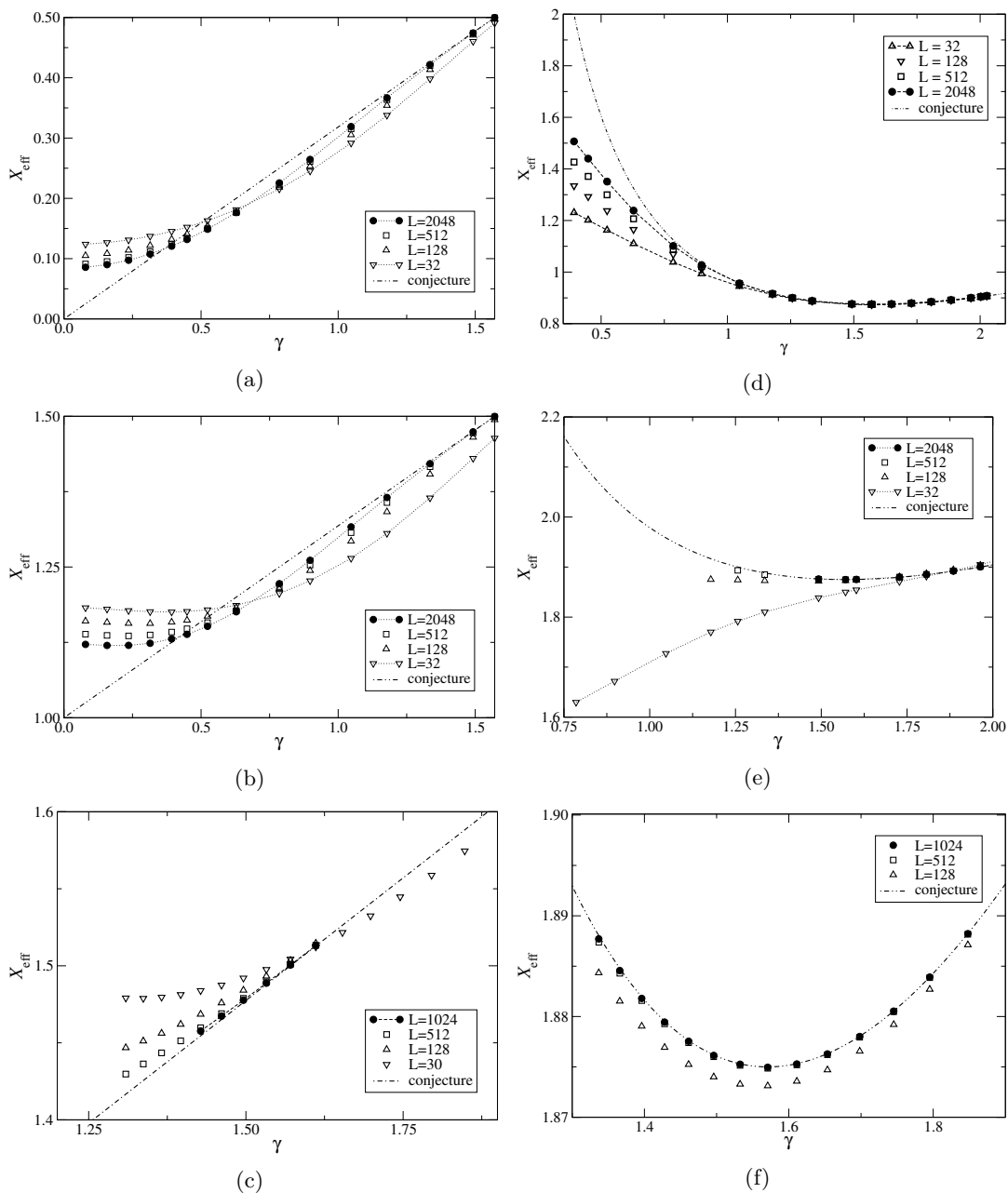


Figure 30: Effective scaling dimensions of several low-energy states in sector $(0, 2)$ as a function of γ for various system sizes: displayed in the left panel are (a) the spin $s = 0$ ground state with effective scaling dimension extrapolating to $X_{0,0}^{2,0}$, eq. (II.145), and in (b) and (c) two spin $s = 1$ levels extrapolating to $X_{0,0}^{2,0} + 1$, eq. (II.148). In the right panel the effective scaling dimension of (d) the spin $s = 1$ level extrapolating to $X_{0,0}^{2,1}$, eq. (II.147), and the spin $s = 0$ and $s = 1$ excitations (e) and (f) extrapolating to $X_{0,0}^{2,1} + 1$, eq. (II.149), are shown. Dotted lines connecting symbols are guides to the eye, dashed-dotted lines show the conjectured γ -dependence.

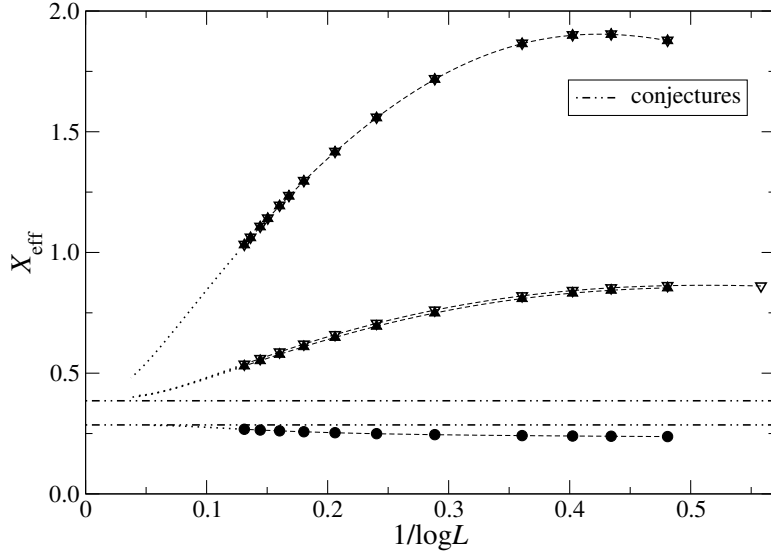


Figure 31: Similar as fig. 22 but for the lowest eigenenergy and the first four excitations forming a tower of scaling dimensions starting at (II.146) in sector $(0, 2)$ for $\gamma = 2\pi/7$. The dashed-dotted lines indicate our conjectures (II.145) and (II.146) for this anisotropy.

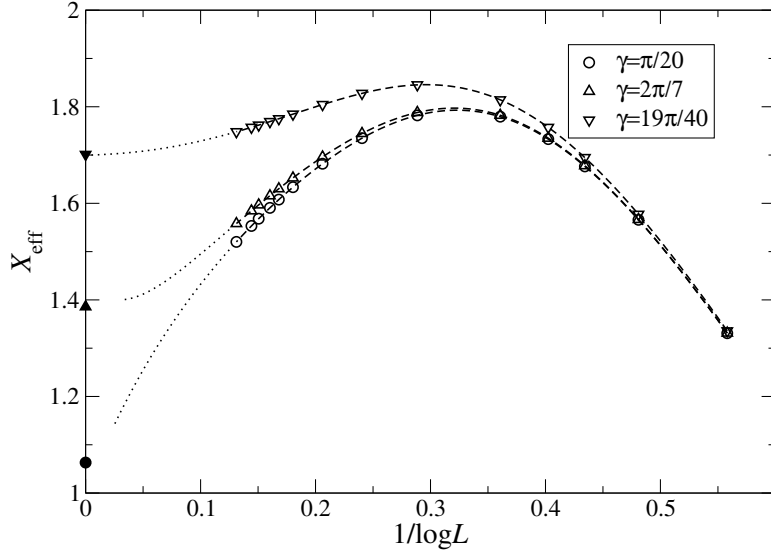


Figure 32: Effective scaling dimensions of the level extrapolating to (II.150) in sector $(0, 2)$ as a function of $1/\log(L)$ for various values of the anisotropy γ . Open (filled) symbols are the numerical data (the conjectured value in the thermodynamic limit $L \rightarrow \infty$). The dotted lines are extrapolations assuming a rational dependence on $1/\log(L)$.

2. The operator content of the $U_q[osp(3|2)]$ superspin chain

state with root configuration $b : [3_{12}^+, 1_2^-]$ and a spin $s = 1$ state with root configuration $b : [1_1^+, 1_1^-, 1_2^+, 1_2^-]$. Both of them are found to extrapolate to the scaling dimension

$$X = \Xi_{0,0}^{2,1} - \frac{1}{8} + 1 = \frac{\gamma}{\pi} + \frac{\pi}{4\gamma} - \frac{1}{8} + 1, \quad (\text{II.149})$$

see figures 30(e) and (f). From these data we conclude that the zero spin level is a descendant of (II.147). The $s = 1$ level appears to be a primary, again the scaling dimension indicates the presence of an Ising field in the effective low-energy description of the superspin chain.

Finally, we have identified a level with spin $s = 1$ and effective scaling dimension extrapolating to

$$X = \Xi_{0,\frac{1}{2}}^{2,0} - \frac{1}{4} + 1 = \frac{\pi}{4(\pi - \gamma)} + \frac{\gamma}{\pi} - \frac{1}{4} + 1. \quad (\text{II.150})$$

In the $bfbfb$ grading, its root configuration is characterized by $b : [(1_1^-)^2, 1_2^+, 1_2^-]$. Based on this configuration we propose that this is a descendant of the state with roots (II.144a) described above. The scaling of this level is displayed in figure 32.

To conclude the investigation of the sector $(n_1, n_2) = (0, 2)$ we present our findings for this sector in table 4.

Eq.	X			s			remark
	m_1	m_2	x_0	total spin	$\sigma_{n_1, m_1}^{n_2, m_2}$	s_0	
(II.145)	0	0	0	0	0	0	
(II.146)	$\frac{1}{2}$	0	$-\frac{1}{4}$	0	0	0	tower
(II.147)	0	1	$-\frac{1}{8}$	1	1	0	
(II.149)	0	1	$-\frac{1}{8} + 1$	1	1	0	Ising $(\frac{1}{2}, \frac{1}{2})$

Table 4: Conformal data for the levels studied in charge sector $(n_1, n_2) = (0, 2)$ (see also table 2). We have also observed descendants of (II.145), see (II.148), one descendant of (II.146), see (II.150) and one descendant of (II.147), see (II.149).

2.4.4 Sector $(1, 0)$

The lowest energy state in the sector with charges $(n_1, n_2) = (1, 0)$ is the overall ground state of the q -deformed $osp(3|2)$ superspin chain for $\gamma > 0$. It is described by a symmetric root configuration $f : [1_1^+, 1_2^-]$ and, thus, has zero conformal spin, $s = 0$. We have solved the Bethe equations (II.110) for this state in systems with up to $L = 8192$ sites. The numerical finite-size data extrapolate to an effective scaling dimension

$$X_{1,0}^{0,0} = \Xi_{1,0}^{0,0} - \frac{1}{4} = -\frac{\gamma}{4\pi}. \quad (\text{II.151})$$

Again, this root configuration can be used as a starting point to construct states forming a tower of scaling dimensions on top of (II.151). Breaking one of the $fbbb$ string complexes into

$$\lambda_{\pm}^{(1)} = \pm\xi, \quad \lambda_{-}^{(2)} = \pm\eta + i\frac{\pi}{2}, \quad \xi, \eta \in \mathbb{R}, \quad (\text{II.152})$$

we obtain the first excitation in this sector. Repeating this procedure leads to excitations described by root configurations $f : [(1_1^+)^{2k+1}, (1_2^-)^{2k+1}]$. For $k = 1, 2$ these excitations have again zero conformal spin, $s = 0$, and their effective scaling dimensions extrapolate to (II.151) as $L \rightarrow \infty$ as well. Strong subleading corrections lift the degeneracy for finite L , see figure 33.

Continuing our analysis within the $(1, 0)$ sector we found two spin $s = 1$ levels described by $f : [1_1^-, 1_2^+]$ and $f : [(1_1^+)^2, 1_1^-, 1_2^-, \bar{2}_2^+]$ root configurations, respectively. Extrapolating their effective scaling dimensions leads to

$$X = \Xi_{1,0}^{0,0} - \frac{1}{4} + 1 = -\frac{\gamma}{4\pi} + 1. \quad (\text{II.153})$$

Hence these levels are descendants of the lowest two states in the tower starting at (II.151). A potential second descendant of the lowest tower state is parametrized in terms of Bethe roots by a $f : [1_1^-, 1_2^+]$ configuration and has conformal spin $s = 2$. Its scaling dimension extrapolates to

$$X = \Xi_{1,0}^{0,0} - \frac{1}{4} + 2 = -\frac{\gamma}{4\pi} + 2. \quad (\text{II.154})$$

The effective scaling dimensions for these three states display strong subleading corrections, see fig. 34.

Moving on, we found two further low-energy levels with root configurations $f : [(1_1^+)^2, 1_1^-, 1_2^-, z_2]$ and $f : [(1_1^+)^2, 1_2^-, 3_{21}^-]$. These have conformal spin $s = 1$ and $s = 0$, respectively. Their effective scaling dimensions are observed to tend to

$$X_{1,\frac{1}{2}}^{0,1} = \Xi_{1,\frac{1}{2}}^{0,1} - \frac{1}{8} + \frac{1}{2} = -\frac{\gamma}{4\pi} + \frac{\pi}{4(\pi - \gamma)} + \frac{\pi}{4\gamma} + \frac{5}{8} \quad (\text{II.155})$$

in the thermodynamic limit. Our finite-size data for these two states can be found in fig 35.

Another scaling dimension in this sector has been identified from the finite-size scaling of a spin $s = 1$ level with root configuration $f : [(1_1^+)^3, 1_2^-, 2_2^+]$. This state approaches

$$X_{1,1}^{0,0} = \Xi_{1,1}^{0,0} - \frac{1}{4} = -\frac{\gamma}{4\pi} + \frac{\pi}{(\pi - \gamma)} \quad (\text{II.156})$$

as $L \rightarrow \infty$. Our numerical results for this state is shown in fig. 36 for several anisotropies.

2. The operator content of the $U_q[osp(3|2)]$ superspin chain

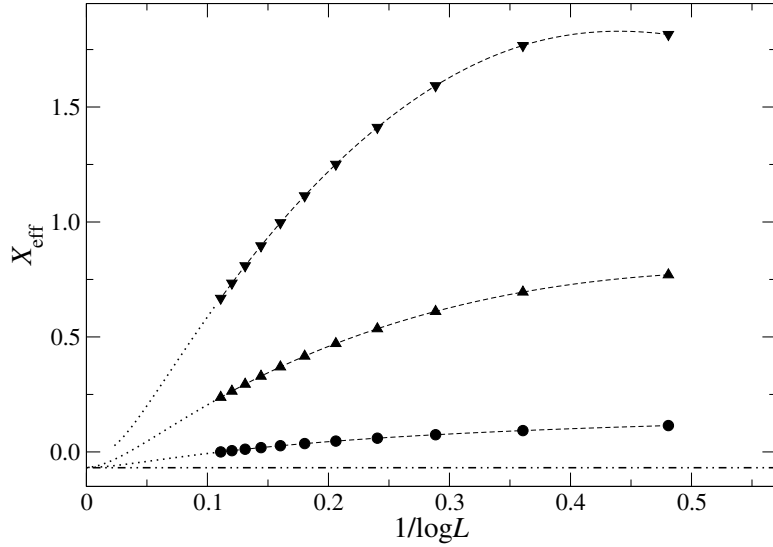


Figure 33: Similar as fig. 22 but for the lowest eigenstate and the related tower of levels in the spectrum of the superspin chain in sector $(1,0)$ for $\gamma = 11\pi/40$. The dashed-dotted line denotes our conjecture (II.151).

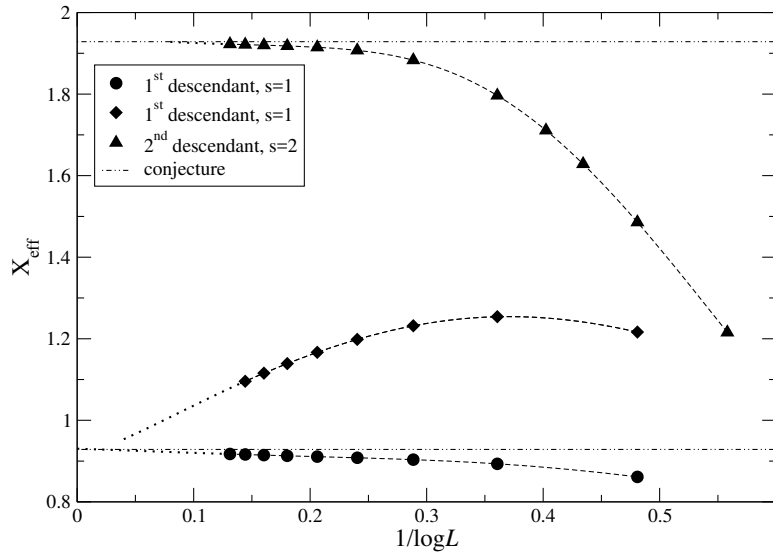


Figure 34: Similar as Fig. 22 but for the three lowest states with nonzero conformal spin in the spectrum of the superspin chain in sector $(1,0)$ for $\gamma = 2\pi/7$. These states are descendants of the lowest two tower states. The dashed-dotted lines are our conjectures (II.153) and (II.154), respectively, for this anisotropy.

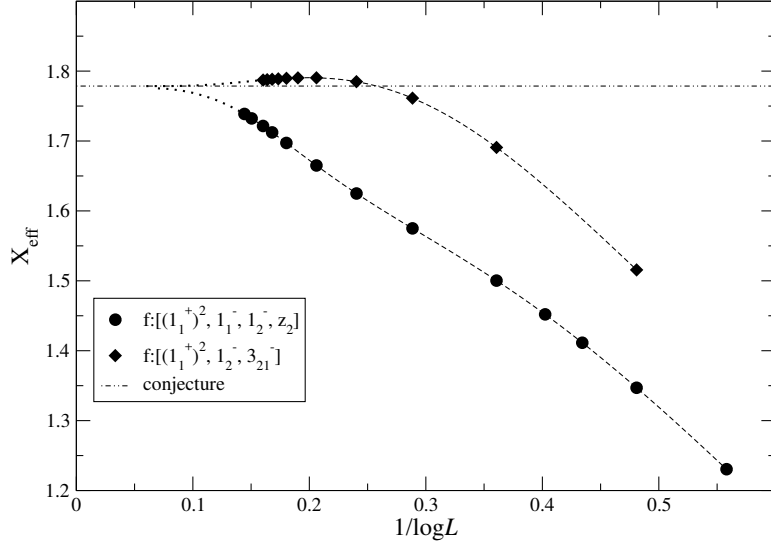


Figure 35: Similar as fig. 22 but for the states in the spectrum of the superspin chain in sector $(1, 0)$ extrapolating to (II.155) for $\gamma = 2\pi/7$. The dashed-dotted line is our conjecture (II.155) for this anisotropy.

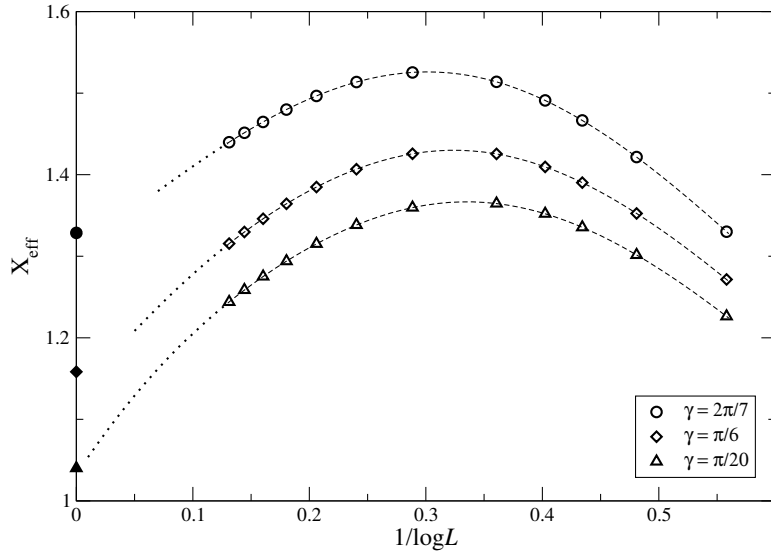


Figure 36: Similar as fig. 32 but for the state in sector $(1, 0)$ extrapolating to (II.156).

2. The operator content of the $U_q[\mathfrak{osp}(3|2)]$ superspin chain

In addition to the levels discussed above, there is another state contained in the low-energy spectrum where we have observed a change of the root pattern as the system size changes. For small L , it is described by root configurations $b : [1_1^-, 1_2^+, 3_{21}^+, z_1]$ and $f : [3_{12}^+, 3_{21}^+]$, depending on the grading. As the system size is increased the $bfbfb$ root structure changes when the pair of complex conjugate first level roots degenerates and is replaced by two one-strings with negative parity, i.e. $[z_1] \rightarrow [(1_1^-)^2]$. For $\gamma = 2\pi/7$, this happens as L grows from 10 to 12. Increasing the system size further, beyond $L = 36$ for $\gamma = 2\pi/7$, another degeneration is observed, this time affecting the roots on the second level. Again, we present more details in appendix A.2. It has not been possible to follow the evolution of the root configuration beyond the second degeneration. Due to the presence of strong corrections to scaling in this state, see fig. 37, our data do not allow for a finite-size analysis.

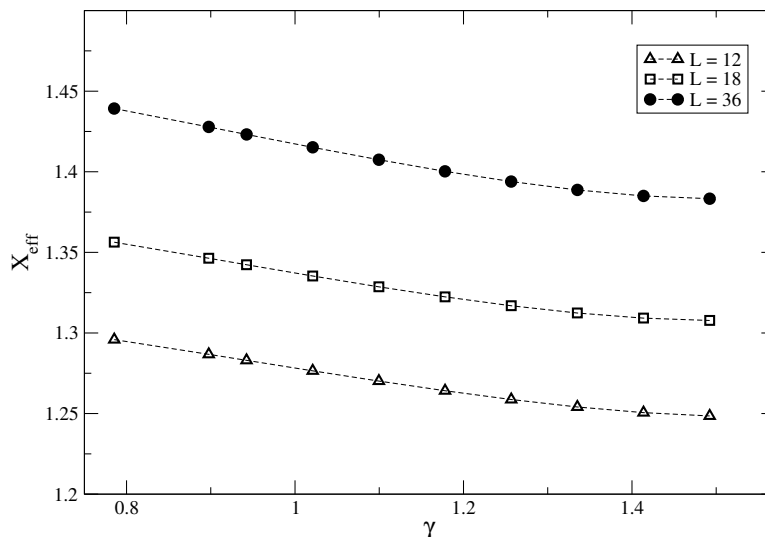


Figure 37: Effective scaling dimension of the state $b : [1_1^-, 1_2^+, 3_{21}^+, z_1]$ or equivalently $f : [3_{12}^+, 3_{21}^+]$ in sector $(1, 0)$ for small system sizes as a function of γ .

We finally remark that for one spin $s = 1$ state in the low-energy spectrum of the superspin chain we have been able to identify the root configuration only for $L = 8$ and $\gamma \leq 2\pi/7$, see appendix A.3.

As before we present our results for the sector $(n_1, n_2) = (1, 0)$ in table 5.

2.4.5 Sector $(1, 1)$

The lowest state for the charges $(n_1, n_2) = (1, 1)$ when using the $fbbbf$ grading is described by a root configuration $f : [1_1^+]$, i.e. $(L - 2)/2$ string complexes (II.112) and one additional root, $\lambda^{(1)} = 0$, on the first level. From our numerical finite-size data for chains with up to $L = 2048$ sites we find that the effective scaling dimension of this

Eq.	X			s			remark
	m_1	m_2	x_0	total spin	$\sigma_{n_1, m_1}^{n_2, m_2}$	s_0	
(II.151)	0	0	$-\frac{1}{4}$	0	0	0	tower
(II.155)	$\frac{1}{2}$	1	$-\frac{1}{8} + \frac{1}{2}$	1, 0	$\frac{1}{2}$	$\pm\frac{1}{2}$	Ising $(\frac{1}{2}, 0), (0, \frac{1}{2})$
(II.156)	1	0	$-\frac{1}{4}$	1	1	0	

Table 5: Conformal data for the levels studied in charge sector $(n_1, n_2) = (1, 0)$ (see also table 2). We have also observed descendants of (II.151), see (II.153) and (II.154).

level tends to

$$X_{1,0}^{1,0} = \Xi_{1,0}^{1,0} - \frac{1}{4} = 0 \quad (\text{II.157})$$

in the thermodynamic limit. As in the charge sector $(1, 0)$, this state is the lowest in a tower of levels with zero conformal spin, $s = 0$, and extrapolating to the same scaling dimension. The root configurations of these excitations are again obtained by breaking string complexes as in (II.152), giving $f : [(1_1^+)^{2k+1}, (1_2^-)^{2k}]$ with integer $k \geq 1$. The finite-size effective scaling dimensions for $k = 0, 1, 2$ and $\gamma = 2\pi/7$ can be found in fig. 38.

We have identified descendants of the two lowest levels in this tower. They are parametrized by root configurations $f : [1_1^-]$ and $f : [(1_1^+)^2] \oplus [1_1, 2_2^+]_{-\infty}$, respectively, and have conformal spin $s = 1$. Our numerical finite-size data extrapolate to

$$X = \Xi_{1,0}^{1,0} - \frac{1}{4} + 1 = 1. \quad (\text{II.158})$$

We also found a potential second descendant with scaling dimension

$$X = \Xi_{1,0}^{1,0} - \frac{1}{4} + 2 = 2 \quad (\text{II.159})$$

and spin $s = 2$. This state is described by a $b : [1_1^+]$ root configuration. The scaling behaviour of these descendants is displayed in fig. 39.

Among the other low-energy states, we have identified two spin $s = 1$ primaries. Both of them are described by Bethe roots arranged as $f : [(1_1^+)^2] \oplus [1_1, 2_2]_{-\infty}$ and scale to

$$X_{1, \frac{1}{2}}^{1,1} = \Xi_{1, \frac{1}{2}}^{1,1} - \frac{1}{8} = \frac{\pi}{4(\pi - \gamma)} + \frac{\pi}{4\gamma} + \frac{1}{8} \quad (\text{II.160})$$

and

$$X_{1,1}^{1,0} = \Xi_{1,1}^{1,0} - \frac{1}{4} = \frac{\pi}{(\pi - \gamma)}, \quad (\text{II.161})$$

respectively. The results of our numerical analysis concerning these two states can be found in fig. 40.

As in sector $(1, 0)$, we have observed degenerations of the root configurations for one

2. The operator content of the $U_q[\mathfrak{osp}(3|2)]$ superspin chain

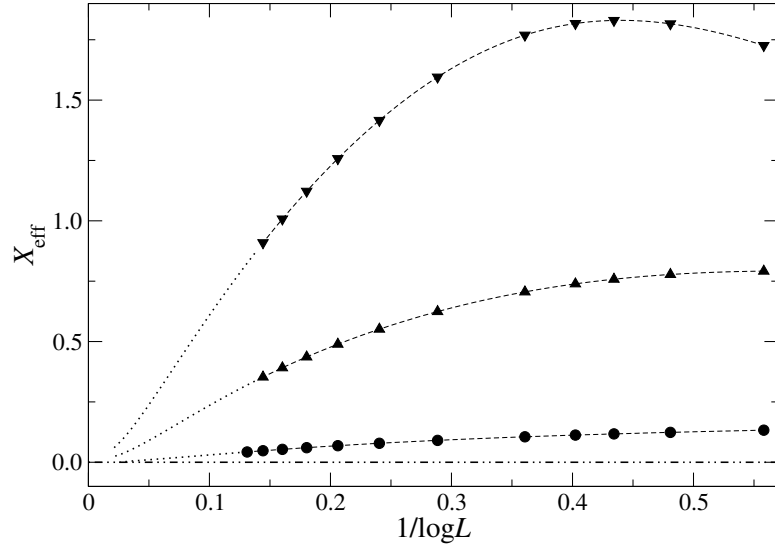


Figure 38: Similar as Fig. 22 but for the lowest eigenenergy and the related tower of levels in the spectrum of the superspin chain in sector $(1, 1)$ for $\gamma = 2\pi/7$. The dashed-dotted line indicates our conjecture (II.157).

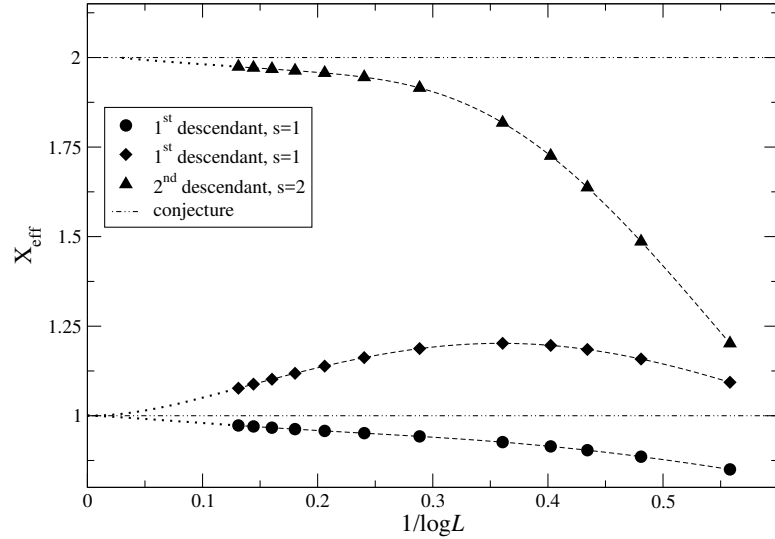


Figure 39: Similar as fig. 22 but for three descendants of the two lowest levels in the spectrum of the superspin chain in sector $(1, 1)$ for $\gamma = 2\pi/7$. The dashed-dotted lines are our conjectures (II.158) and (II.159).

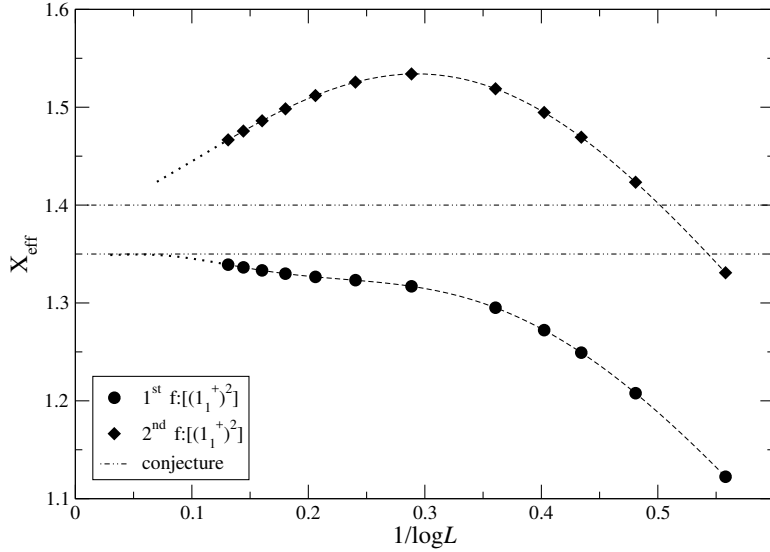


Figure 40: Similar as fig. 22 but for the two $s = 1$ states in the spectrum of the superspin chain in sector $(1, 1)$ for which the finite part of the root configuration is parametrized by $f : [(1_1^+)^2]$ for $\gamma = 2\pi/7$. The dashed-dotted lines denote our conjectures (II.160) and (II.161).

spin $s = 0$ level. For the smallest system sizes considered here, its root configurations is given by $b : [1_1^+]$ or $f : [1_1^-]$, depending on the grading used. As discussed in appendix A.2, these patterns change with growing L . We have succeeded in following these changes up to, e.g. $L = 36$ for $\gamma = 2\pi/7$. The effective scaling dimensions for this state as obtained from the available finite-size data are shown in figure 41. Unfortunately, they do not allow for a reliable extrapolation.

There are two low-energy states remaining which are present in the spectrum of the superspin chain with lengths accessible to exact diagonalization of the Hamiltonian (II.96). Both of these levels have non-zero conformal spin. For one of them we have identified the corresponding Bethe roots for $L = 4, 6$ and anisotropies $\gamma \lesssim \pi/4$, see appendix A.3, but we were not able to go to larger L . For the other one, the parametrization in terms of Bethe roots is still unknown.

To end the discussion of the operator content found in the charge sector $(n_1, n_2) = (1, 1)$ we present our findings in table 6.

Eq.	X			s			remark
	m_1	m_2	x_0	total spin	$\sigma_{n_1, m_1}^{n_2, m_2}$	s_0	
(II.157)	0	0	$-\frac{1}{4}$	0	0	0	tower
(II.160)	$\frac{1}{2}$	1	$-\frac{1}{8}$	1	1	0	
(II.161)	1	0	$-\frac{1}{4}$	1	1	0	

Table 6: Conformal data for the levels studied in charge sector $(n_1, n_2) = (1, 1)$ (see also Table 2). We have also observed descendants of (II.157), see II.158 and (II.159).

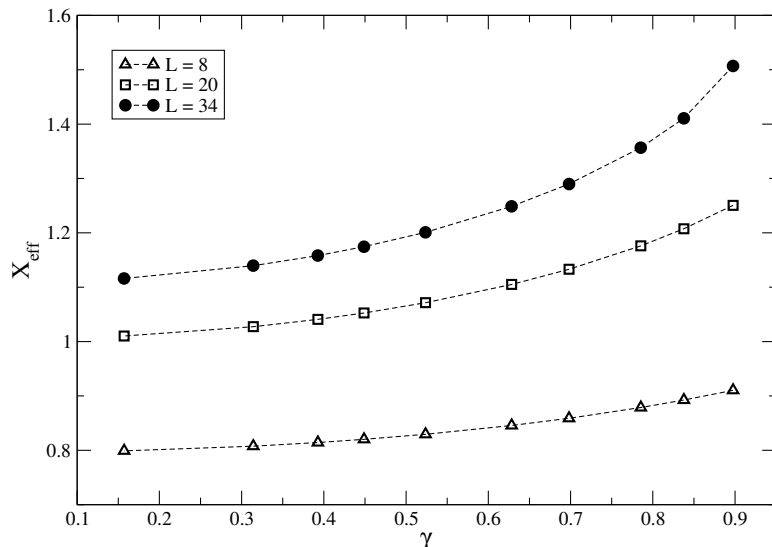


Figure 41: Effective scaling dimension of the state $b : [1_1^+]$ or equivalently $f : [1_1^-]$ in sector $(1, 1)$ for small system sizes as a function of γ .

2.4.6 Sector $(1, 2)$

The Bethe roots for the lowest state in this sector are arranged in a $b : [(1_1^-)^2, 1_2^-]$ configuration, i.e. $(L-4)/2$ $bfbfb$ string complexes (II.99) and two (one) additional roots $\lambda^{(1)}$ ($\lambda^{(2)}$) on the line $\text{Im}(\lambda) = \pi/2$. This states appears as the lowest in a tower of levels with scaling dimensions extrapolating to, see figure 42,

$$X_{1,0}^{2,0} = \Xi_{1,0}^{2,0} - \frac{1}{4} = \frac{3\gamma}{4\pi}. \quad (\text{II.162})$$

The other members of this tower are described by Bethe root configurations with one or more of the $bfbfb$ string complexes replaced by two (1_a^-) -strings on each level $a = 1, 2$, i.e. $b : [(1_1^-)^{2k+2}, (1_2^-)^{2k+1}]$ for $k \geq 0$. All tower states have zero conformal spin, $s = 0$. For $k = 1, 2$, the scaling behaviour of the corresponding excitations is also shown in figure 42.

The next level which we have analyzed in the charge sector $(1, 2)$ is again described by a root configuration $b : [(1_1^-)^2, 1_2^-]$, just as the lowest state in this sector. The extrapolation of the finite-size effective scaling dimensions yields

$$X_{1,\frac{1}{2}}^{2,1} = \Xi_{1,\frac{1}{2}}^{2,1} - \frac{1}{8} + \frac{1}{2} = \frac{3\gamma}{4\pi} + \frac{\pi}{4(\pi - \gamma)} + \frac{\pi}{4\gamma} + \frac{5}{8}. \quad (\text{II.163})$$

This state has conformal spin $s = 2$ in agreement with (II.127) in the presence of a chiral Ising contribution. As $\gamma \rightarrow \pi/2$, the subleading corrections to scaling become small, for $\gamma \rightarrow 0$ the level disappears from the low-energy spectrum, see figure 43.

Three additional excitations in this sector have been identified as descendants of

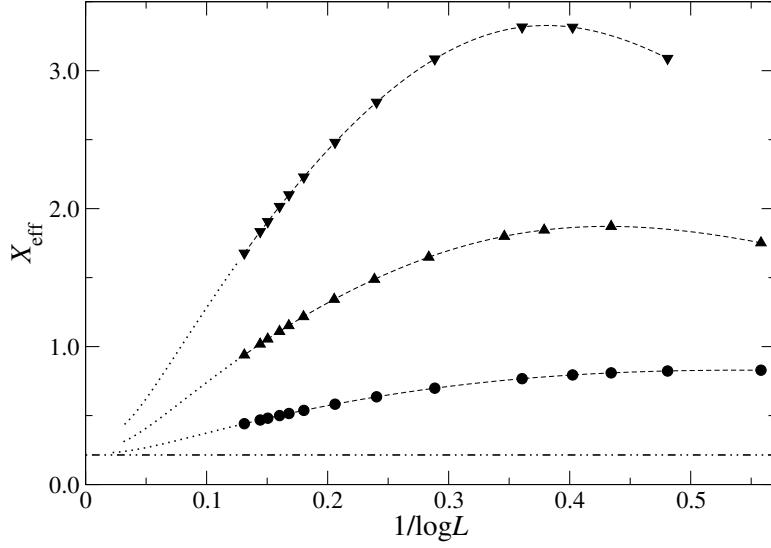


Figure 42: Similar as fig. 22 but for the lowest eigenenergy and the related tower of levels in the spectrum of the superspin chain in the sector $(1, 2)$ for $\gamma = 2\pi/7$. The dashed-dotted line denotes our conjecture (II.162) for this anisotropy.

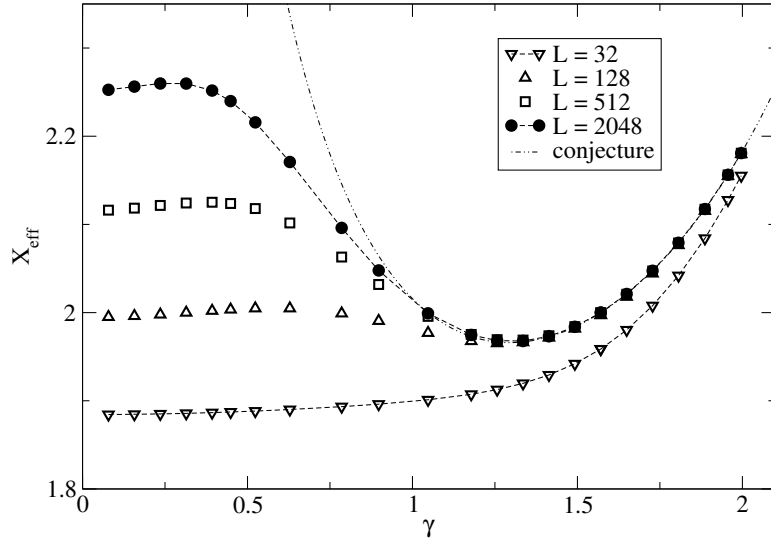


Figure 43: Effective scaling dimension for the charge $(1, 2)$ state with conformal spin $s = 2$ extrapolating to (II.163) as a function of γ for various system sizes.

2. The operator content of the $U_q[osp(3|2)]$ superspin chain

the tower states (II.162). They are described by root configurations $b : [(1_1^-)^2, 1_2^-]$, $b : [(1_1^+)^2, 1_2^-]$, and $b : [(1_1^+)^2, 1_2^+]$, respectively. The first of these levels has conformal spin $s = 1$, the others $s = 0$. Their effective scaling dimensions extrapolate to

$$X = \Xi_{1,0}^{2,0} - \frac{1}{4} + n = \frac{3\gamma}{4\pi} + n, \quad n = 1, 2, \quad (\text{II.164})$$

with $n = 1$ (2) for the spin $s = 1$ (0) states. The L -dependence of the corrections to scaling for $\gamma = 2\pi/7$ is displayed in figure 44.

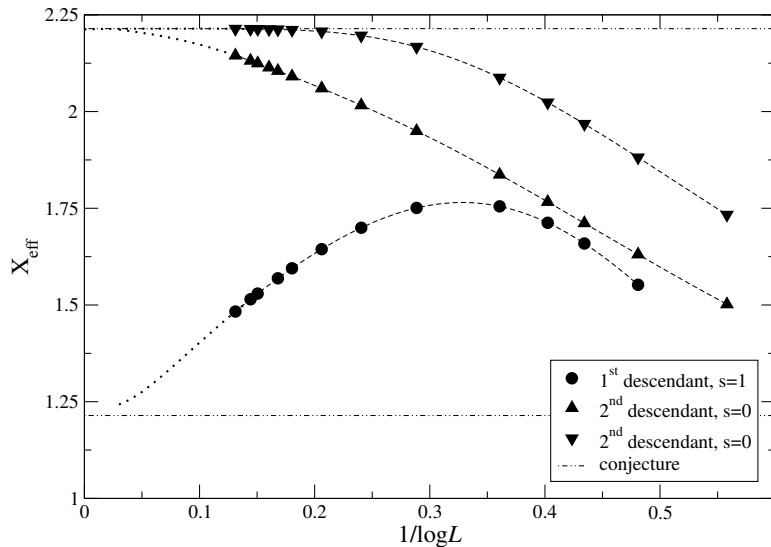


Figure 44: Similar as fig. 22 but for the descendants of the tower states in sector (1,2) extrapolating to (II.164) for $\gamma = 2\pi/7$. The dashed-dotted line are our conjectured values for $L \rightarrow \infty$ for this anisotropy.

Another state belonging to the low-energy spectrum which we have analyzed is described by a Bethe root pattern $f : [(1_1^+)^2, 1_1^-, 1_2^+]$. This excitation has conformal spin $s = 2$. Finite-size data for the effective scaling dimension are available for systems with up to $L = 1024$ lattice sites and anisotropies $0 \leq \gamma \leq 2\pi/3$, see fig. 45(a). Although the corrections to scaling appear to be small, in particular for $\gamma \gtrsim \pi/2$, we did not manage to describe the effective scaling dimensions in terms of our scheme (II.128). A possible explanation for this problem might be a crossing between two levels with similar root configurations for some $\gamma < \pi/2$ which we have not resolved properly. In this situation, the data displayed in fig. 45(a) would correspond to two different operators. For $\gamma \rightarrow 0$ a possible candidate would have, e.g., scaling dimension $X = \Xi_{1,0}^{2,0} - 1/4 + 2 = (3\gamma/4\pi) + 2$. Around $\pi/2$ the data might correspond to an operator with $m_2 = 1$. If this is the case, however, the crossing would come along with huge corrections to scaling which cannot be handled with the available data.

Again, there is one low-energy state present in this charge sector where changes in

the root configuration with the system size aggravate the solution of the corresponding Bethe equations. This level has zero conformal spin, $s = 0$, and is parametrized by Bethe roots arranged as $f : [(1_1^+)^2, 1_1^-, 1_2^+]$ or $b : [3_{12}^+]$ for small system sizes. Similarly as in the $(n_1, n_2) = (0, 0)$ example discussed in appendix A.2, the 1_1^+ -roots diverge at some finite value of the system size so that we cannot extrapolate the scaling dimension from the available finite-size data. Our numerical results for small system sizes, however, are presented in figure 45(b).

We summarize the findings of our study of the sector $(n_1, n_2) = (1, 2)$ in table 7.

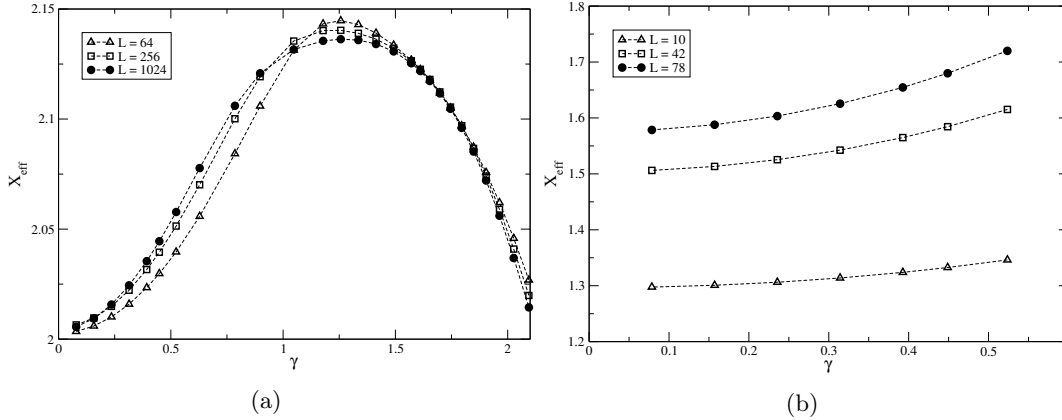


Figure 45: Effective scaling dimension for the charge $(1, 2)$ state with root configuration (a) $f : [(1_1^+)^2, 1_1^-, 1_2^+]$ and (b) $f : [(1_1^+)^2, 1_1^-, 1_2^+]$ or equivalently $b : [3_{12}^+]$ as a function of γ for various system sizes.

Eq.	X			s			remark
	m_1	m_2	x_0	total spin	$\sigma_{n_1, m_1}^{n_2, m_2}$	s_0	
(II.162)	0	0	$-\frac{1}{4}$	0	0	0	tower
(II.163)	$\frac{1}{2}$	1	$-\frac{1}{8} + \frac{1}{2}$	2	$\frac{3}{2}$	$\frac{1}{2}$	Ising $(\frac{1}{2}, 0)$

Table 7: Conformal data for the levels studied in charge sector $(n_1, n_2) = (1, 2)$ (see also table 2). We have also observed descendants of (II.162), see (II.164).

2.4.7 Sector $(2, 0)$

For $L = 6$, the ground state in the charge sector $(2, 0)$ is parametrized by two $fbbbf$ string complexes (II.112). As the system size is increased this configuration degenerates. For example, at $\gamma = 2\pi/7$ the degeneration occurs at $L_* = 10$. Beyond L_* the root configuration consists of $(L-4)/2$ $fbbbf$ string complexes and, in addition, $\lambda_{\pm}^{(1)} = \pm\xi \in \mathbb{R}$ and $\lambda_{\pm}^{(2)} \simeq \pm i\eta$, i.e. $f : [(1_1^+)^2, z_2]$. At least for deformation parameters γ close to $\pi/2$, no further degenerations occur such that we have been able to study the effective scaling dimensions of this level near $\gamma \simeq \pi/2$. From our numerical data we conclude

2. The operator content of the $U_q[\mathfrak{osp}(3|2)]$ superspin chain

that this level has zero conformal spin, $s = 0$. The finite-size effective scaling dimensions extrapolate to

$$X_{2,0}^{0,1} = X_{2,0}^{0,1} - \frac{1}{8} = 1 - \frac{\gamma}{\pi} + \frac{\pi}{4\gamma} - \frac{1}{8}, \quad (\text{II.165})$$

see figure 46(a).

We found a second $s = 0$ state with the same scaling dimension in the thermodynamic limit. It is described by a root configuration $f : [(1_1^+)^2, 1_2^+, 1_2^-]$. Here we had to study deformation parameters from $3\pi/8 \leq \gamma \leq 5\pi/8$ to get finite-size data with sufficiently large L for the extrapolation. The results of our numerical analysis for this state is shown in figure 46(b). Note, the corrections to scaling for both states extrapolating to (II.165) are small for anisotropies $\gamma \geq 3\pi/8$.

Among the set of low-energy levels, we have identified two states in this sector with root configurations consisting only of $(L-2)/2$ $fbbbf$ string complexes (II.112). Their effective scaling dimensions extrapolate to

$$X = \Xi_{2,\frac{1}{2}}^{0,0} - \frac{1}{4} + n = 1 - \frac{\gamma}{\pi} + \frac{\pi}{4(\pi - \gamma)} - \frac{1}{4} + n, \quad n = 0, 1, \quad (\text{II.166})$$

and have conformal spin $s = 1$ (2) for $n = 0$ (1). Their scaling behaviour is shown in figure 47.

In addition we have observed a pair of excitations combining $(L-4)/2$ $fbbbf$ string complexes with different structures for the additional roots. One of these excitations has a root configuration $f : [(1_1^+)^2, (1_2^-)^2]$, the other one is described by a pattern $f : [1_1^+, 1_1^-, z_2]$ where the roots in the pair $[z_2]$ appear to approach $\lambda_{1,2}^{(2)} \simeq \pm i\pi/4$ for large L . Their scaling dimensions also extrapolate to (II.166) while their conformal spins are $s = 1$ ($s = 0$) for $n = 0$ ($n = 1$). From eq. (II.127), we expect the conformal spin $s = 1$ for the $(n_1, m_1) = (2, 1/2)$ primary field, hence, the $s = 0$ and 2 levels are first level descendants. Their finite-size scaling is also displayed in figure 47.

Further, we have studied two excitations with conformal spin $s = 1$ and $s = 0$ described both by root configurations $b : [1_1^+, (1_1^-)^3, (1_2^-)^2]$ or $f : [(1_1^+)^2, (1_2^-)^2]$ for not too large L . Unfortunately, the presence of divergent Bethe roots with growing system size prevented us from getting finite-size data for $L \gtrsim 200$ and therefore a satisfying extrapolation. The results of our numerical study up to $L = 208$ (160) is shown in fig. 48.

Finally, we have studied the scaling of a spin $s = 0$ level with $(L-4)/2$ $fbbbf$ string complexes (II.112) and extra roots $\lambda_{\pm}^{(1)} = \pm i\gamma/2$ as well as two degenerate second level roots at $\lambda^{(2)} = 0$, i.e. $f : [1_2^+, 3_{12}^+]$. The effective scaling dimension extrapolate to

$$X = \Xi_{2,0}^{0,0} + 1 = -\frac{\gamma}{\pi} + 2, \quad (\text{II.167})$$

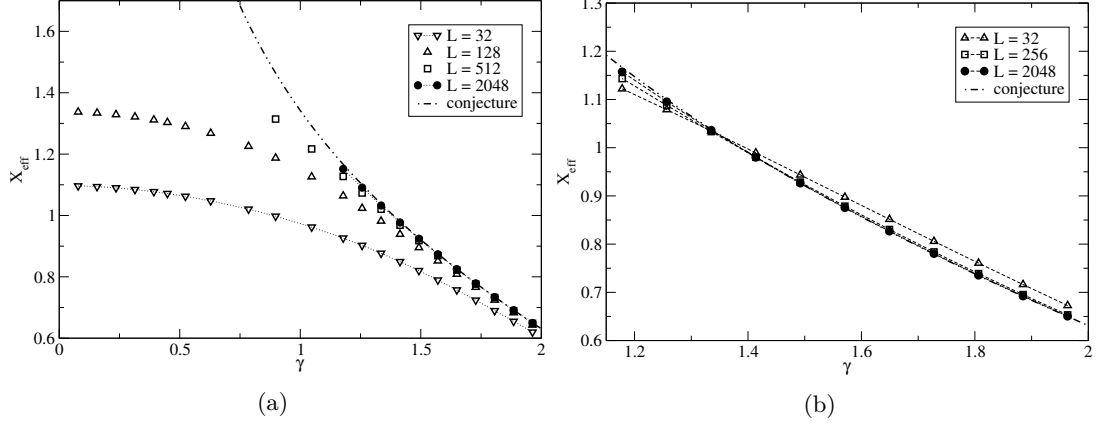


Figure 46: Effective scaling dimension for the state in sector $(2, 0)$ with root configuration (a) $f : [(1_1^+)^2, z_2]$ (Note, this is the lowest state in this charge sector) and (b) $f : [(1_1^+)^2, 1_2^+, 1_2^-]$ as a function of γ for various system sizes. The dashed-dotted lines indicate our conjecture (II.165) for these levels.

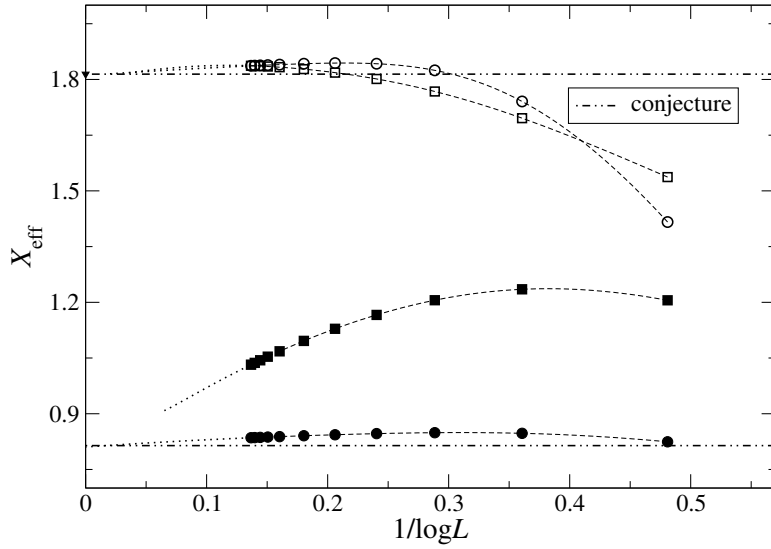


Figure 47: Similar as fig. 22 but for the states in sector $(2, 0)$ extrapolating to (II.166) for $\gamma = 2\pi/7$. The filled symbols denote states with conformal spin $s = 1$, the open ones are levels with $s = 2$ and $s = 0$, respectively. The dashed-dotted lines are our conjectured values for $L \rightarrow \infty$ for this anisotropy.

2. The operator content of the $U_q[osp(3|2)]$ superspin chain

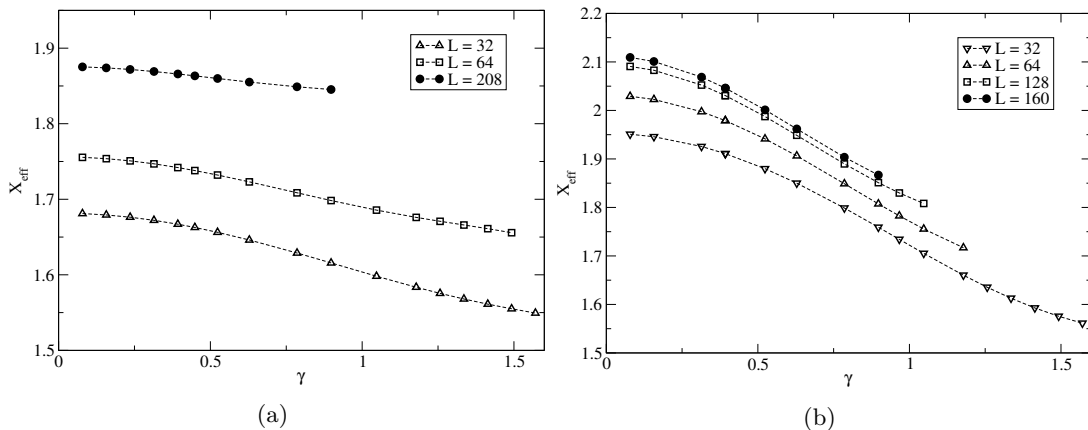


Figure 48: Effective scaling dimension for the states in sector $(2,0)$ with root configuration $b : [1_1^+, (1_1^-)^3, (1_2^-)^2]$ or equivalently $f : [(1_1^+)^2, (1_2^-)^2]$ and conformal spin (a) $s = 1$ and (b) $s = 0$ as a function of γ for various system sizes.

see fig. 49.

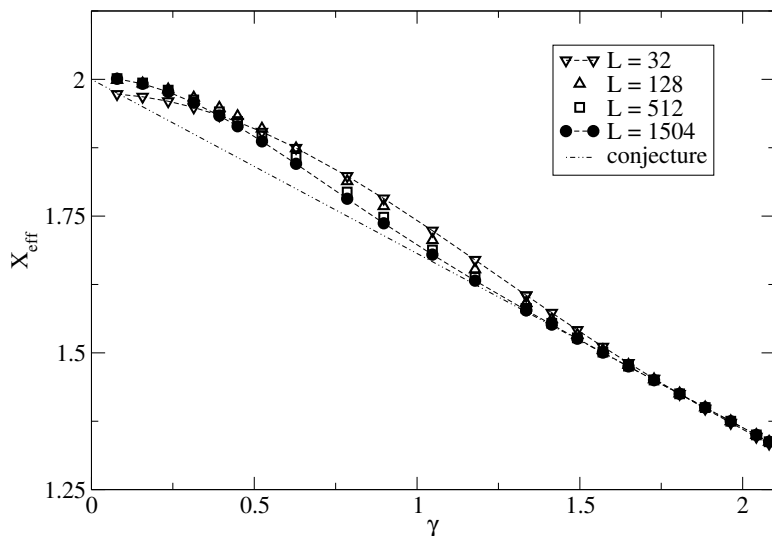


Figure 49: Effective scaling dimension for the state in sector $(2,0)$ conjectured to extrapolate to (II.167) as a function of γ for various system sizes.

Again, there is one low-energy excitation present in the spectrum of small systems for which no Bethe Ansatz solution has been found.

A summary of the numerical study of the sector $(n_1, n_2) = (2, 0)$ is given in table 8.

2.4.8 Sector $(2, 1)$

In this charge sector, the lowest level is described by root configurations $b : [1_1^-, 3_{1_2}^+]$ or $f : [(1_1^+)^2, 1_2^+]$ for small system sizes. Since this configuration degenerates at intermediate

Eq.	X			s			remark
	m_1	m_2	x_0	total spin	$\sigma_{n_1, m_1}^{n_2, m_2}$	s_0	
(II.165)	0	1	$-\frac{1}{8}$	0	0	0	
(II.166)	$\frac{1}{2}$	0	$-\frac{1}{4}$	1	1	0	
(II.167)	0	0	1	0	0	0	Ising $(\frac{1}{2}, \frac{1}{2})$

Table 8: Conformal data for the levels studied in charge sector $(n_1, n_2) = (2, 0)$ (see also table 2). We have also observed descendants of (II.166), see fig. 47.

L we were able to solve the Bethe Ansatz equations only for $L \leq 128$, depending on the anisotropy. However, based on a VBS analysis of our data for $3\pi/8 \leq \gamma \leq 2\pi/3$ we conjecture that its scaling dimension extrapolates to

$$X_{2,0}^{1,1} = \Xi_{2,0}^{1,1} - \frac{1}{8} + \frac{1}{2} = 1 - \frac{3\gamma}{4\pi} + \frac{\pi}{4\gamma} + \frac{3}{8}. \quad (\text{II.168})$$

This level has zero conformal spin, $s = 0$. Our finite-size results for small system sizes are depicted in fig. 50.

The first excitation is described by an $f : [(1_1^+)^2, 1_2^-]$ configuration, i.e. it has $(L-4)/2$ $fbbb$ string complexes (II.112), two additional real roots on the first level, and a single root with $\text{Im}(\lambda^{(2)}) = \pi/2$ on the second. The conformal spin of this excitation is $s = 1$. For $L \rightarrow \infty$ its effective scaling dimension tends to

$$X_{2,\frac{1}{2}}^{1,0} = \Xi_{2,\frac{1}{2}}^{1,0} - \frac{1}{4} = 1 - \frac{3\gamma}{4\pi} + \frac{\pi}{4(\pi - \gamma)} - \frac{1}{4} \quad (\text{II.169})$$

with strong subleading corrections, see figure 51.

Also shown in fig. 51 are two higher excitations with dimension $X = X_{2,\frac{1}{2}}^{1,0} + 1$ and spin $s = 2$ indicating that these levels are descendants of the $s = 1$ level extrapolating to eq. (II.169). Their root configurations are best described in the $bfbfb$ grading where both contain $(L-4)/2$ string complexes (II.99). The full configurations are $b : [1_1^-, 3_{12}^+]$ and $b : [1_1^+, (1_1^-)^2, 1_2^-]$, respectively.

For two other excitations with root configurations $b : [1_1^+, (1_1^-)^2, 1_2^-]$, we had to solve the Bethe equations for $3\pi/8 \leq \gamma \leq 5\pi/8$ to get the energies for sufficient large systems. Based on these data, see fig. 52, we propose that their scaling dimensions extrapolate to (II.168). Their conformal spin is $s = 1$ and $s = 0$, respectively. Given that there is a contribution $n_2 m_2 / 2 = 1/2$ from the γ dependent part of the conformal weights we argue that their degeneracy is a consequence of the combination with an Ising energy operator, similar as in (II.143)). Since $m_2 \neq 0$ these levels disappear from the low-energy spectrum for $\gamma \rightarrow 0$.

The last state we have studied in this sector has a $b : [(1_1^+)^2, 1_1^-, 1_2^-]$ root configuration

2. The operator content of the $U_q[osp(3|2)]$ superspin chain

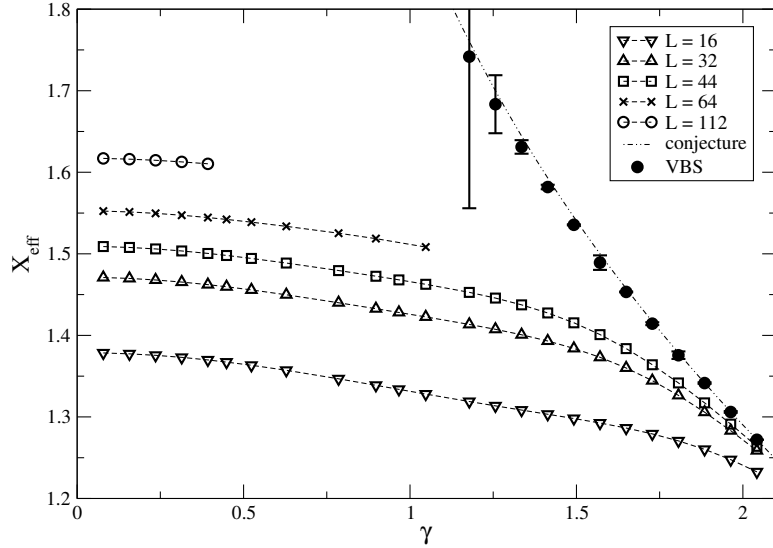


Figure 50: Effective scaling dimension for the lowest state in sector $(2, 1)$ as a function of γ for various system sizes.

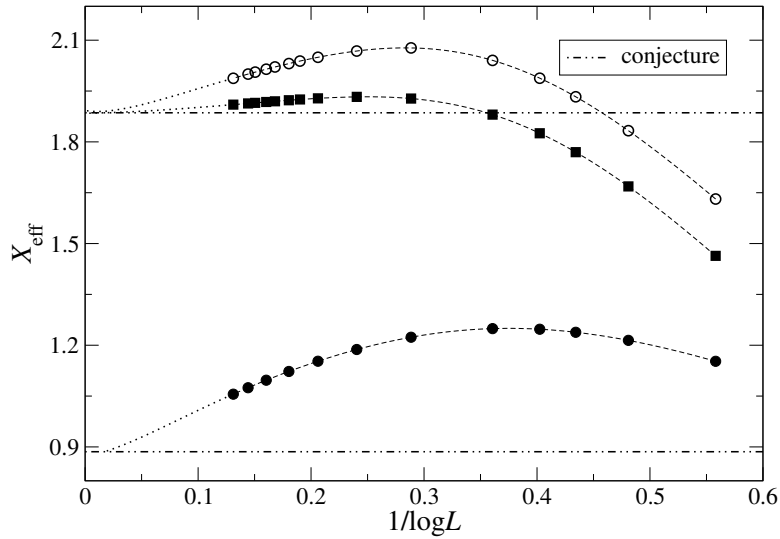


Figure 51: Similar as fig. 22 but for the first excitation with spin $s = 1$ in sector $(2, 1)$ extrapolating to X given by (II.169) and two higher $s = 2$ levels extrapolating to $X + 1$. The data are for $\gamma = 2\pi/7$.

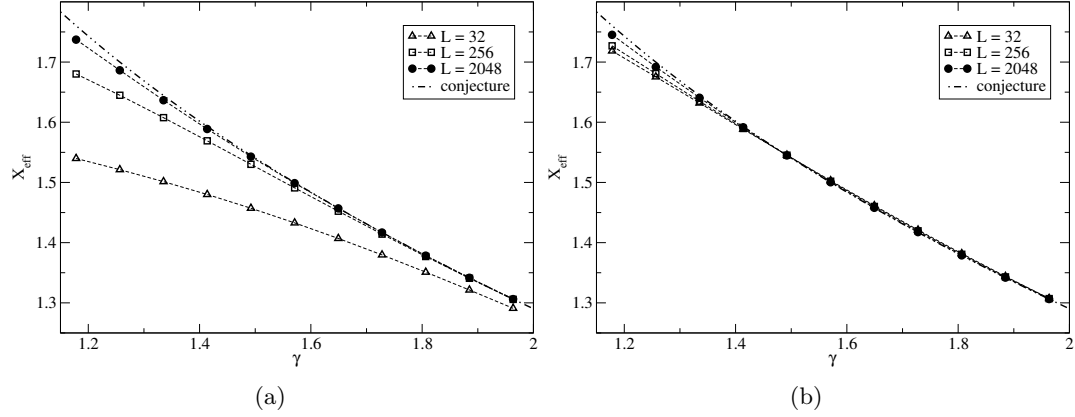


Figure 52: Effective scaling dimension for the states in sector $(2, 1)$ conjectured to extrapolate to (II.168) with conformal spin (a) $s = 1$ and (b) $s = 0$ as a function of γ for various system sizes.

and zero conformal spin, $s = 0$. Its scaling dimension tends to

$$X = \Xi_{2,0}^{1,0} + 1 = -\frac{3\gamma}{4\pi} + 2, \quad (\text{II.170})$$

in the thermodynamic limit, see figure 53.

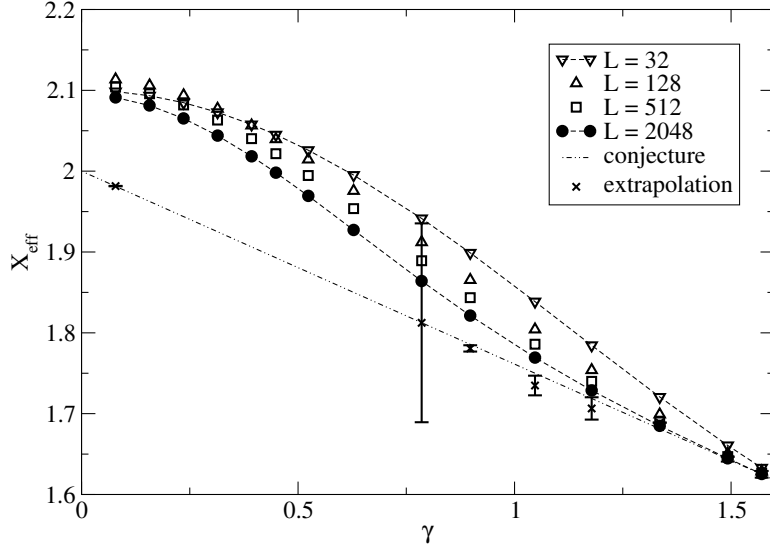


Figure 53: Effective scaling dimension for the state in sector $(2, 1)$ conjectured to extrapolate to (II.170) as a function of γ for various system sizes.

There is one remaining low-energy excitation present in the spectrum of this charge sector for which the corresponding solution to the Bethe equations has been found only for $L \leq 16$, see appendix A.3.

In table 9 we present a summary of our findings in the sector $(n_1, n_2) = (2, 1)$.

2. The operator content of the $U_q[osp(3|2)]$ superspin chain

Eq.	X			s			remark
	m_1	m_2	x_0	total spin	$\sigma_{n_1, m_1}^{n_2, m_2}$	s_0	
(II.168)	0	1	$-\frac{1}{8} + \frac{1}{2}$	1, 0	$\frac{1}{2}$	$\pm\frac{1}{2}$	Ising $(\frac{1}{2}, 0), (0, \frac{1}{2})$
(II.169)	$\frac{1}{2}$	0	$-\frac{1}{4}$	1	1	0	
(II.170)	0	0	1	0	0	0	Ising $(\frac{1}{2}, \frac{1}{2})$

Table 9: Conformal data for the levels studied in charge sector $(n_1, n_2) = (2, 1)$ (see also table 2). We have also observed descendants of (II.169), see fig. 51.

2.4.9 Sector $(2, 2)$

Before we consider the low lying states in this sector, let us recall our discussion at the end of subsection 2.4.1. Although there exist exceptions in the spectra obtained from exact diagonalization of small systems with $L \geq 6$ sites we observe that many of the eigenenergies in the sector $(2, 2)$ appear also in the zero charges sector. In fact, this includes all of the levels discussed below. We expect that the formation of such multiplets can be understood in the context of the $U_q[osp(3|2)]$ symmetry in the presence of periodic boundary conditions. This, however, is beyond the scope of this work.

We note that, in addition to the numerical evidence, this spectral inclusion is compatible with our hypothesis (II.128) for the effective scaling dimensions. The latter implies

$$X_{2, m_1}^{2, m_2} = X_{0, m_1}^{0, m_2} + 1. \quad (\text{II.171})$$

Similarly, the conformal spins according to (II.127) are related as $s_{2, m_1}^{2, m_2} = s_{0, m_1}^{0, m_2} + 2m_1 + m_2$. Therefore, levels with $2m_1 + m_2 = 1$ considered in this subsection may be considered either as primaries in the charge sector $(2, 2)$ or, alternatively, as descendants of a lower energy state with spin $s = 0$ in the sector $(0, 0)$.

As mentioned in subsection 2.4.1, the lowest level in the charge sector $(2, 2)$ is part of a multiplet which also appears as an excitation in the sector $(0, 0)$. Here, its root configuration is given by $f : [(1_1^+)^2]$. It has conformal spin $s = 1$ in agreement with (II.127) and its effective scaling dimension extrapolates to

$$X_{2, \frac{1}{2}}^{2, 0} = \Xi_{2, \frac{1}{2}}^{2, 0} - \frac{1}{4} = 1 + \frac{\pi}{4(\pi - \gamma)} - \frac{1}{4}, \quad (\text{II.172})$$

see figures 54 and 55 (a).

Possible descendants of this level are described by root configurations $b : [1_1^+, 1_1^-]$, $f : [(1_1^+)^3, 1_1^-, z_2]$, and $f : [(1_1^+)^5, (1_2^-)^2, 3_{21}^-]$. They have conformal spin 2, 0, and 0, respectively, and their scaling dimensions extrapolate to

$$X = \Xi_{2, \frac{1}{2}}^{2, 0} - \frac{1}{4} + 1 = 1 + \frac{\pi}{4(\pi - \gamma)} - \frac{1}{4} + 1. \quad (\text{II.173})$$

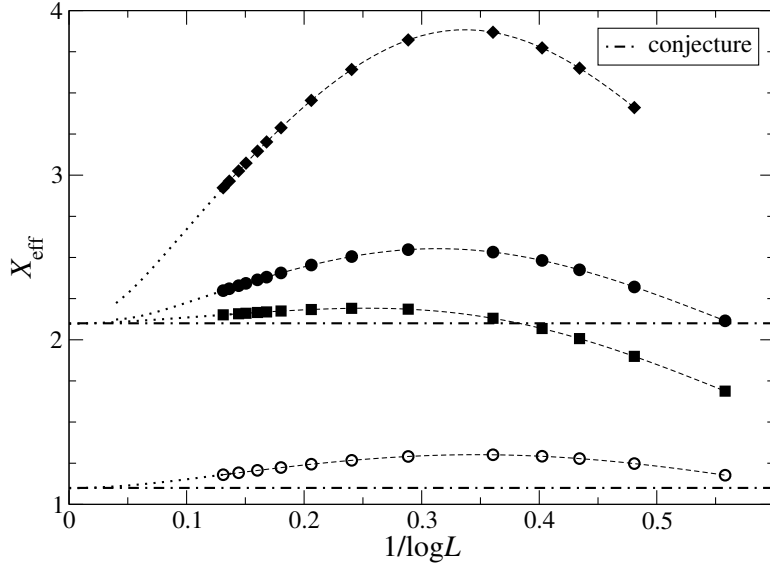


Figure 54: Similar as Fig. 22 for the lowest state in sector $(2, 2)$ extrapolating to $X_{2, \frac{1}{2}}^{2,0}$, eq. (II.172), and three higher levels extrapolating to $X = X_{2, \frac{1}{2}}^{2,0} + 1$, eq. (II.173). The data shown are for $\gamma = 2\pi/7$.

Their scaling behaviour is also shown in figure 54.

Continuing our study in the charge sector $(2, 2)$, we have observed a $s = 1$ level described by a root configuration $f : [(1_1^+)^2]$. This level yields an effective scaling dimension

$$X_{2,0}^{2,1} = \Xi_{2,0}^{2,1} - \frac{1}{8} = 1 + \frac{\pi}{4\gamma} - \frac{1}{8}, \quad (\text{II.174})$$

in the thermodynamic limit, see figure 55(b). Again, we have identified three possible descendants of this level. Their root configurations are given by $b : [1_1^+, 1_1^-]$, $b : [(1_1^+)^2]$, and $f : [(1_1^+)^4, 1_2^+, 1_2^-]$. The conformal spin of these descendants are $s = 2, 2,$ and 0 , respectively, and their scaling dimension extrapolates to

$$X = \Xi_{2,0}^{2,1} - \frac{1}{8} + 1 = 1 + \frac{\pi}{4\gamma} - \frac{1}{8} + 1, \quad (\text{II.175})$$

see also figure 55 (d), (e), and (f).

Further, we have found a level in this sector corresponding to an operator with zero spin $s = 0$ and scaling dimension

$$X = \Xi_{2,0}^{2,0} + 1 = 2, \quad (\text{II.176})$$

see figure 55(c). Its root configuration is described in terms of a $f : [1_1^+, 1_1^-]$ pattern.

Apart from these states, we have identified the Bethe roots for two additional levels: a zero spin $s = 0$ excitation with root configuration $b : [1_1^+, 1_1^-]$ or $f : [(1_1^+)^2]$ and a $s = 1$

2. The operator content of the $U_q[osp(3|2)]$ superspin chain

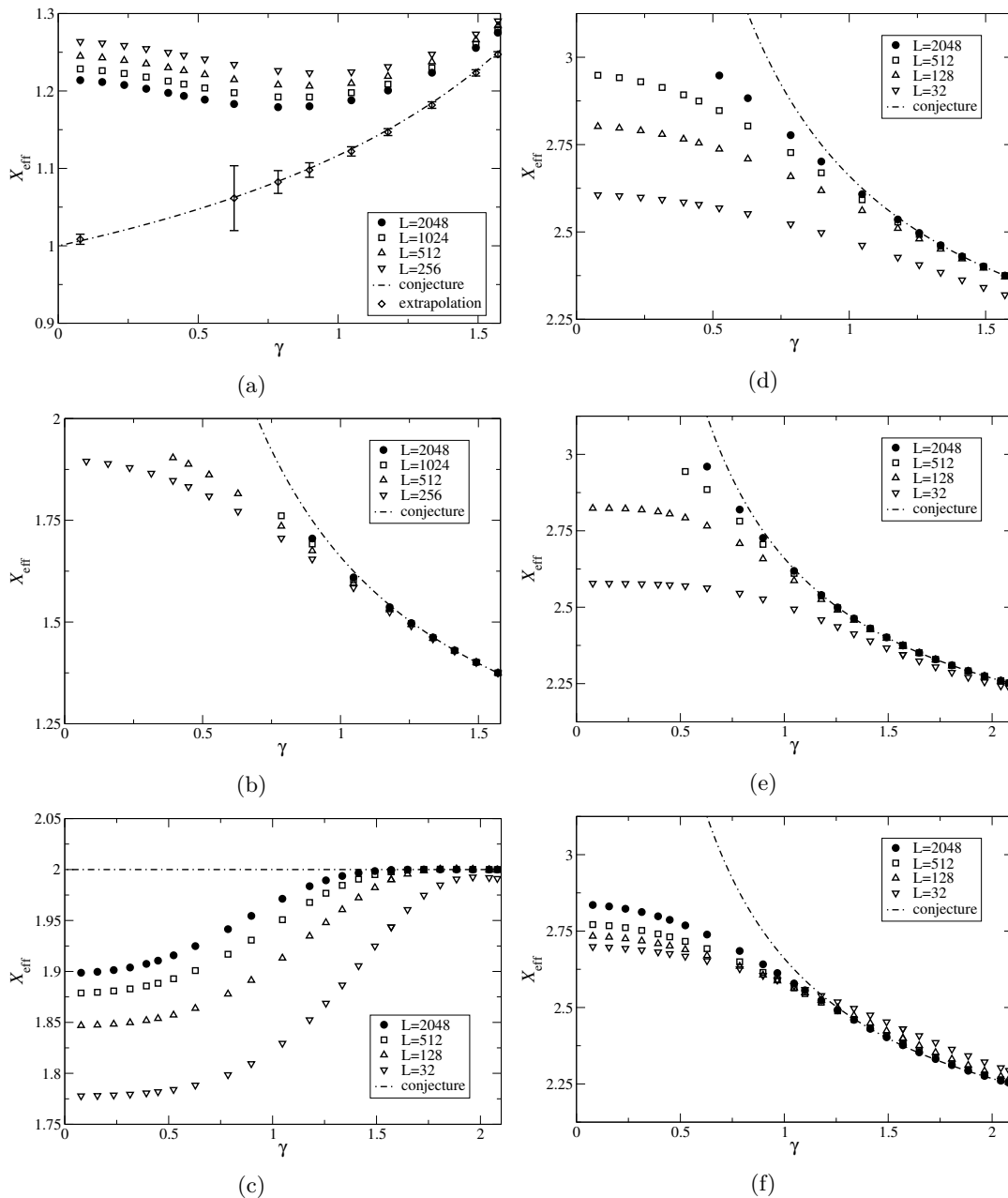


Figure 55: Effective scaling dimensions of several low-energy states in sector $(2, 2)$ as a function of γ for various system sizes: displayed in the left panel are (a) the spin $s = 1$ ground state with effective scaling dimension extrapolating to $X_{2,1/2}^{2,0}$, eq. (II.172), in (b) the spin $s = 1$ level extrapolating to $X_{2,0}^{2,1} + 1$, eq. (II.174) and in (c) the $s = 0$ level extrapolating to $X = 2$, eq. (II.176). In the right panel the effective scaling dimension of three descendants of (b), eq. (II.175) with spin (d) and (e) $s = 2$ and (f) $s = 0$, are shown. Dashed-dotted lines show the conjectured γ -dependence. In (a), the extrapolated data were calculated assuming a rational dependence of the finite-size data on $x = 1/\log L$. Since the finite-size corrections become larger the extrapolation starts to fail for small γ .

excitation described by roots $f : [1_1^+, 1_1^-]$ or $b : [(1_1^+)^2]$. As the system size increases roots in these configurations degenerate, therefore we were not able to perform a satisfying finite-size study.

To conclude our investigation of the sector $(n_1, n_2) = (2, 2)$ we present our results in table 10.

Eq.	X			s			remark
	m_1	m_2	x_0	total spin	$\sigma_{n_1, m_1}^{n_2, m_2}$	s_0	
(II.172)	$\frac{1}{2}$	0	$-\frac{1}{4}$	1	1	0	
(II.174)	0	1	$-\frac{1}{8}$	1	1	0	
(II.176)	0	0	1	0	0	0	Ising $(\frac{1}{2}, \frac{1}{2})$

Table 10: Conformal data for the levels studied in charge sector $(n_1, n_2) = (2, 2)$ (see also table 2). We have also observed descendants of (II.172), see II.173, and descendants of (II.174), see (II.175).

2.5 Summary

In this section, we have reported the results obtained in a comprehensive finite-size study of the q -deformed $osp(3|2)$ superspin chain. We have identified the configurations of roots to the Bethe equations (II.97) and (II.110) for most of the lowest energy states. Taking these configurations as an input, we have computed the corresponding eigenenergies as a function of the system size. With data available for lattices up to several thousand sites, combined with insights from the root density approach and at $\gamma = \pi/2$ as discussed in subsection 2.3, this has allowed for a computation of the effective scaling dimensions even in the presence of very strong corrections to scaling, see e.g. figure 56. There exist a few states where our solution of the Bethe equations has been limited to several tens or a few hundreds of sites usually due to changes or degenerations of the corresponding root configurations when the system size was varied, see appendix A.2. In these cases, a reliable extrapolation has not been possible.

For the majority of states, however, we have been able to extrapolate the numerical data and found that the scaling dimensions of primaries can be described by our proposal, see (II.128),

$$X_{n_1, m_1}^{n_2, m_2} = n_1^2 \frac{\pi - \gamma}{4\pi} + m_1^2 \frac{\pi}{\pi - \gamma} + n_2^2 \frac{\gamma}{4\pi} + m_2^2 \frac{\pi}{4\gamma} + x_0. \quad (\text{II.177})$$

We note that modes with $m_2 \neq 0$ disappear from the low-energy spectrum in the isotropic limit $\gamma \rightarrow 0$. Such a behaviour was also observed in other superspin chains based on deformations of orthosymplectic superalgebras [125].

Based on the finite size scaling of the states we have studied, we find that x_0 takes values from a discrete set depending on the quantum numbers n_1 , m_1 , n_2 , and m_2 of

2. The operator content of the $U_q[osp(3|2)]$ superspin chain

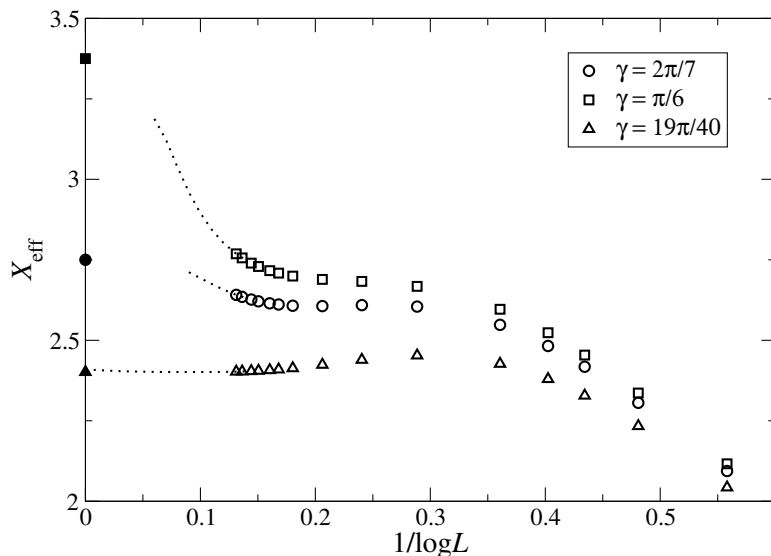


Figure 56: The difficulties with numerical extrapolation based on finite-size data in the presence of the strong corrections to scaling observed in some eigenenergies of the $U_q[osp(3|2)]$ are evident in the scaling behaviour of one of the three descendants (II.175), see fig. 55 (f): open symbols are data from the numerical solution of the Bethe equations for various values of γ and system sizes up to $L = 2048$. The dotted lines are extrapolations assuming a rational dependence of X_{eff} on $1/\log L$. While the radius of convergence of the latter may not be sufficient to read off the effective scaling dimensions for $L \rightarrow \infty$ the extrapolation is consistent with the conjectured values (filled symbols). Thus, this picture indicates the difficulties in using standard numerical extrapolation techniques for the calculation of effective scaling dimensions for this model.

the corresponding level. The formulation of the general pattern of such constraints has eluded us so far, but we note that they should at least include the following rules (for even L),

$$\begin{aligned}
 \text{for } n_1 + 2m_1 \text{ odd and } m_2 = 0 : \quad & x_0 = -\frac{1}{4}, \\
 \text{for } n_1 = 0 \text{ and } m_1 = m_2 = 0 : \quad & x_0 = 0, \\
 \text{for } n_1 + n_2 \text{ even and } m_2 = 1 : \quad & x_0 = -\frac{1}{8}, \\
 \text{for } n_1 + n_2 \text{ odd and } m_2 = 1 : \quad & x_0 = \frac{3}{8}.
 \end{aligned} \tag{II.178}$$

We recall that the rules for $m_2 = 0$ are consistent to what is expected for the conformal spectrum of the isotropic $osp(3|2)$ superspin chain [19]. The two possible values of x_0 observed for $m_2 = 1$ provide a hint that the fields in the low-energy effective continuum description of the model are composites of Gaussian fields and an Ising operator. The connection to the integrable spin $S = 1$ XXZ chain provides additional support for this interpretation. At present we don't have a complete comprehension of this feature and it may require further studies in order to understand the origin of the several allowed values for x_0 .

Another characteristic feature of the conformal spectrum of the isotropic model are macroscopic degeneracies in the thermodynamic limit $L \rightarrow \infty$. Their presence appears to be a general feature of spin chains invariant under the superalgebras $osp(n|2m)$ [22] and is consistent with the expected low temperature behaviour of the related intersecting loop models [18, 112].

Here, i.e. for the anisotropic deformation of the $osp(3|2)$ superspin chain with general values of γ , we have observed a similar feature. In each of the charge sectors (n_1, n_2) we have identified groups of levels extrapolating to the same effective scaling dimension. They are subject to strong corrections to scaling which vanish as a function of $1/\log L$. In this model, such towers of levels have been found to appear on top of the following dimensions,

$$X_{\text{tower}} = X_{n_1, m_1}^{n_2, 0} = n_1^2 \frac{\pi - \gamma}{4\pi} + m_1^2 \frac{\pi}{\pi - \gamma} + n_2^2 \frac{\gamma}{4\pi} - \frac{1}{4} \quad (\text{II.179})$$

for $(n_1, m_1) = (0, 1/2)$, see figures 22, 26, 31, and $(n_1, m_1) = (1, 0)$ as shown in figures 33, 38 and 42.

With these results, we provide a first phenomenological picture of the finite size spectrum of the deformed $osp(3|2)$ superspin chain. We emphasize that although most of our numerical data have been calculated for anisotropies in the interval $0 \leq \gamma \leq \pi/2$ we expect that the proposal (II.128) also captures the behaviour of the conformal dimensions in the complementary region $\pi/2 < \gamma < \pi$. The confirmation of this expectation, however, requires a large amount of additional numerical work which is beyond the scope of this work.

Additionally, there are issues remaining which are not captured by our conjecture: for a complete understanding of the effective low-energy theory, the combined presence of discrete levels (II.128) and a possible continuous component in the conformal spectrum leading to the existence of towers of levels starting at scaling dimensions (II.179) in the lattice model needs to be explained. Furthermore, the appearance of the states with the lowest energy of the lattice model, eq. (II.151), in a sector with non-zero charge quantum numbers, i.e. $(n_1, n_2) = (1, 0)$, is still an unanswered question.

In other models showing such peculiar features, studies of the spectral flow under the change of toroidal boundary conditions have provided further insights [27], see also section 1 and reference [85]. For the $U_q[osp(3|2)]$ superspin chain, this amounts to an extension of the finite-size analysis presented in this section to its integrable modifications obtained by including the generic toroidal twists (II.94). Following the evolution of the low-energy levels under varying twist angles (ϕ_1, ϕ_2) it is possible to connect the superspin chain to several, closely related models and thereby obtain additional evidence supporting the conjecture for the conformal spectrum, see figure 57.

For an exhaustive discussion of these relations, a lot of additional work is required. Here, we restrict ourselves to list a few observations, mostly concerning the lowest state

2. The operator content of the $U_q[osp(3|2)]$ superspin chain

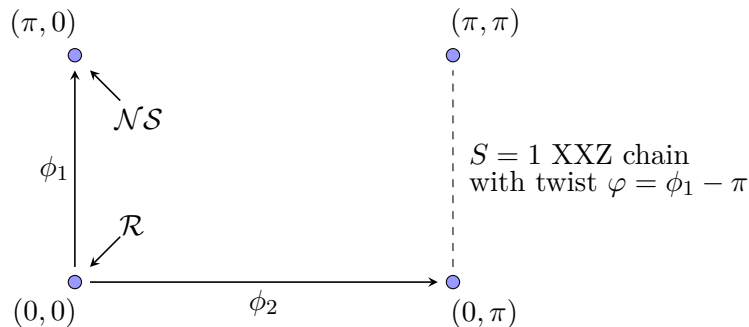


Figure 57: Models connected by variation of the twists (II.94): the symbol \mathcal{R} (\mathcal{NS}) denote periodic (antiperiodic) boundary conditions for the fermionic degrees of freedom of the $U_q[osp(3|2)]$ superspin chain in analogy to the Ramond (Neveu-Schwarz) sector of Conformal Field Theories. On the dashed line for $\phi_2 = \pi$ the spectrum of the superspin chain contains the eigenenergies of the integrable spin $S = 1$ Heisenberg chain.

in the zero charge sector.

We have pointed out already in our discussion of the Bethe Ansatz solution in the *fbbbf* grading, eqs. (II.110), that the spectrum of the $U_q[osp(3|2)]$ chain contains the eigenenergies of the integrable $S = 1$ XXZ Heisenberg model on the line $(\phi_1, \phi_2) = (\pi + \varphi, \pi)$. The Virasoro central charge of the latter model varies between $c = 3/2$ for periodic ($\varphi = \pi - \phi_1 = 0$) and $c = 0$ for antiperiodic ($\varphi = \pi - \phi_1 = \pi$) boundary conditions of the spin $S = 1$ XXZ chain, see appendix A.1.

The energy of the latter state has no corrections to scaling and does not change under the spectral flow $(\phi_1, \phi_2) = (0, \pi) \rightarrow (0, 0)$. It therefore connects to that of the lowest state in the zero charge sector of the periodic superspin chain, eq. (II.114), that we have used as reference state for our finite-size analysis.

The variation of the twist along the line $(\phi_1, \phi_2) = (0, 0) \rightarrow (\pi, 0)$ corresponds to an adiabatic change of the boundary conditions for the fermionic degrees of freedom from periodic to antiperiodic. In the field theory describing the thermodynamic limit of the superspin chain, this corresponds to the Ramond (\mathcal{R}) and Neveu-Schwarz (\mathcal{NS}) sector, respectively. The spectral flow connects the reference state with energy (II.114) and the zero charge ground state of the lattice model for twists $(\phi_1, \phi_2) = (\pi, 0)$. In the *fbbbf* grading, the latter is parametrized by roots arranged in $L/2$ complexes (II.112). As shown in figure 58 for $\gamma = 2\pi/7$, its effective scaling dimension extrapolates to $X_{0,\text{eff}}^{\mathcal{NS}} = -1/4$ which coincides with the observation of a central charge $c_{\mathcal{NS}} = 3$ in the isotropic model [18, 19, 112].

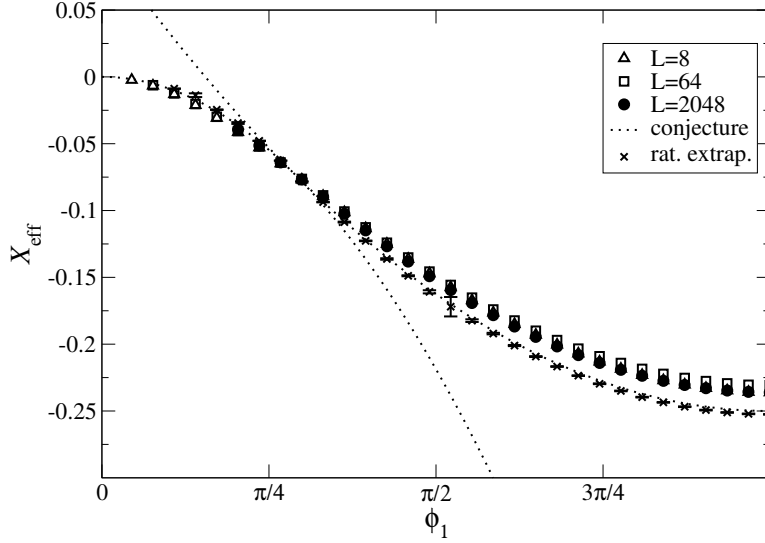


Figure 58: Spectral flow of the lowest level in the charge sector $(0, 0)$ as function of the twist angle ϕ_1 for $\gamma = 2\pi/7$. The effective scaling dimension for $\phi_1 = 0$ (π) appears in the Ramond (Neveu-Schwarz) of the low-energy effective theory, respectively. Symbols are finite-size data from the solution of the Bethe equations (II.110), lines show the conjectured analytical behaviour (II.180).

Curiously, following the scaling dimension as a function of the twist ϕ_1 we find different analytical expressions near $\phi_1 = 0$ and π ,

$$X(\phi_1) = \begin{cases} X_{\text{eff}}^{\mathcal{R}}(\phi_1) = -\frac{\pi}{4\gamma} \left(\frac{\phi_1}{\pi}\right)^2, & 0 \leq \phi_1 \leq \gamma, \\ X_{\text{eff}}^{\mathcal{NS}}(\phi_1) = -\frac{1}{4} + \frac{\pi}{4(\pi-\gamma)} \left(\frac{\pi-\phi_1}{\pi}\right)^2, & \gamma \leq \phi_1 \leq \pi. \end{cases} \quad (\text{II.180})$$

Note, the dependence on the twist near $\phi_1 = \pi$ can be related to the vortex contribution m_1 in our proposal for the scaling dimensions (II.177). Near $\phi_1 = 0$, however, the flow under the twist resembles the γ -dependence of the m_2 vortices albeit with the 'wrong' sign. Now suppose that it is possible to extend the amplitude $X_{\text{eff}}^{\mathcal{R}}(\phi_1)$ to the twist angle domain of the Neveu-Schwarz sector by means of a well defined analytical continuation procedure. Using this hypothesis, we observe that $X_{\text{eff}}^{\mathcal{R}}(\pi) = -\pi/4\gamma$ is in fact smaller than the lowest observed scaling dimension in the Neveu-Schwarz sector, i.e. $X_{\text{eff}}^{\mathcal{NS}}(\pi) = -1/4$. Following the arguments of refs. [20, 27, 85] (see also section 1), we may speculate that this can be taken as an indication for the presence of operators in the non-unitary effective field theory for the Neveu-Schwarz sector that correspond to non-normalizable states and therefore are absent in the spectrum of the lattice model. To put this on firm ground, however, further studies are required.

Conclusions

Non-unitary Conformal Field Theories show several extremely interesting features. While the spectrum of unitary CFTs can be characterized by a discrete set of conformal weights only, the spectrum of non-unitary CFTs may include continua of scaling dimensions, meaning their target space is non-compact. A second striking feature of non-unitary CFTs is the existence of non-normalizable states. In lattice realizations these correspond to discrete states which emerge for certain boundary conditions only. Interestingly, several lattice models including superspin chains have been argued to correspond to non-unitary CFTs in the thermodynamic limit [19, 21, 22, 26] although the local degrees of freedom are finite. Even though some of their features as listed above are known, the thermodynamic limit of such models is not completely understood. In contrast, spin chains based on simply laced Lie algebras are believed to correspond to Wess-Zumino-Novikov-Witten models in the thermodynamic limit [7]. Hence, within this work we have studied two superspin chains in order to contribute to a characterization of their thermodynamic limit.

The first model we have investigated within this work is the staggered $U_q[sl(2|1)]$ superspin chain which is one of the toy models for order-disorder transitions in Quantum Hall systems. The construction of this model is based on the three-dimensional fundamental representation of $U_q[sl(2|1)]$ and its dual. As mentioned above, a special feature of this model is the emergence of continuous components in the spectrum of scaling dimensions [21]. We have extended this picture by discovering continua of scaling dimensions in other sectors as well. Motivated by the approach of Ikhlef *et al.* for the staggered six-vertex model [23–25] we have sought for a characterization of the different continua by means of a conserved charge. To this purpose we have defined a quasimomentum operator. In contrast to the Hamiltonian and the momentum operator which are generated by an expansion of the logarithm of the double row transfer matrix, the quasimomentum originates from an expansion of an odd combination of single-row transfer matrices. By numerical solutions of the Bethe Ansatz equations for states from the continua of scaling dimensions we have shown that the quasimomentum operator parametrizes the continuous components of the spectrum and thereby determines the logarithmic corrections which lift the macroscopic degeneracies of these states on the lattice. Since the quasimomentum eigenvalues also allow for an extraction of the density of states for the continuous components of the spectrum, we have compared the outcome to the known results for the $SL(2, \mathbb{R})/U(1)$ sigma model. Unfortunately, the results do not coincide. Certainly, the identification of the CFT for the thermodynamic limit by calculating the density of states for the continuous component of the spectrum is reliant on its knowledge for ‘candidate CFTs’. Therefore, the study of other symmetries on

the target space of the $SL(2, \mathbb{R})/U(1)$ sigma model, a semi-infinite cigar which allows for both a continuous and discrete part of the spectrum, seems to be promising. The corresponding results might help to identify the CFT for the thermodynamic limit.

Subsequently, we have turned to a different characteristic of non-unitary CFTs, namely the emergence of non-normalizable levels. In the spectrum of the staggered $U_q[sl(2|1)]$ superspin chain, the corresponding states appear as discrete states for twisted boundary conditions only, that is, when the corresponding primary field in the CFT becomes normalizable. Hence, we have studied the spectral flow in the spectrum of the superspin chain under a twist in the boundary conditions. Based on numerical solutions of the Bethe Ansatz equations, we have identified a state from the continuous part of the spectrum in the Neveu-Schwarz sector which under variation of the twist becomes a discrete level in the Ramond sector. Note, for the discrete state to appear a non-zero twist has to be applied. Thus, our observations coincide with the expectations in the context of non-unitary CFTs as described above. Additionally, we have found that in the CFT, levels can be attributed to the continuous or discrete part of the spectrum based on their quasimomentum: States belonging to a continuum of scaling dimensions have real quasimomenta while for discrete levels the quasimomentum is purely imaginary. To entirely understand the thermodynamic limit of the q -deformed staggered $sl(2|1)$ superspin chain and its description in terms of CFTs, however, additional investigations have to be performed.

Consecutively, we have studied a superspin chain based on the five-dimensional fundamental representation of the q -deformed $osp(3|2)$ superalgebra. In the isotropic limit, this model corresponds to a reformulation of the intersecting loop model. As a first step for the characterization of the thermodynamic limit for the q -deformed model, we have investigated its operator content. To this purpose, we have performed a comprehensive finite-size study thereby identifying the configurations of roots to the Bethe equations in two different gradings for most of the lowest energy states. Taking these configurations as an input we have computed the corresponding eigenenergies as a function of the system size. With data available for lattices up to several thousand sites, combined with insights from the root density approach and at $\gamma = \pi/2$, this has allowed for a computation of the effective scaling dimensions even in the presence of very strong corrections to scaling. For the majority of states we have found that the scaling dimensions of primaries can be described by our proposal. We note that modes with quantum number $m_2 \neq 0$ disappear from the low-energy spectrum in the isotropic limit $\gamma \rightarrow 0$. Such a behaviour was also found in other superspin chains based on deformations of orthosymplectic superalgebras [125]. Among the investigated states from the low-energy spectrum we have observed groups of levels extrapolating to the same effective scaling dimension. They are subject to strong corrections to scaling which

vanish as a function of $1/\log L$. We have found such towers of levels on top of the states with quantum numbers $(n_1, m_1) = (0, 1/2)$, $(n_1, m_1) = (1, 0)$, $n_2 = 0, 1, 2$ and $m_2 = 0$. With these results we provide a first phenomenological picture of the finite size spectrum of the deformed $osp(3|2)$ superspin chain. Note, the rational $osp(3|2)$ superspin chain was shown to exhibit continua of scaling dimensions previously. The amplitudes of the corresponding logarithmic corrections were shown to be related to the quadratic Casimir of $osp(3|2)$ [19, 22].

There are still some issues remaining which are not captured by our conjecture. For a complete understanding of the effective low-energy theory, the combined presence of discrete levels entering our conjecture and a possible continuous component in the conformal spectrum leading to the existence of towers of levels needs to be further elaborated. As discussed above, towers of excitations have been found also in the staggered $U_q[sl(2|1)]$ superspin chain, in which the corresponding continua have been shown to be parametrized by a quasimomentum operator. Since the latter originates from an expansion of an odd combination of single-row transfer matrices, its existence is a direct consequence of the staggering in the model. Therefore, the construction of a quasimomentum in the absence of staggering should be a major goal of future research. Intuitively, the framework of quasilocal charges [126] might provide a good starting point for such a construction.

In our conjecture for the operator content of the q -deformed $osp(3|2)$ superspin chain, we have taken into account the contributions of potential discrete degrees of freedom by introducing the γ -independent summand x_0 . Some of its possible values which depend on the quantum numbers n_i and m_i ($i = 1, 2$) can be fixed by the isotropic limit. However, it is not clear whether, in terms of the corresponding Bethe roots, x_0 originates from finite size string deviations or from isolated roots. A detailed study thereof would be of great interest and seems to be auspicious.

Additionally, the reason for the appearance of the states with the lowest energy of the q -deformed $osp(3|2)$ superspin chain in a sector with non-zero charge quantum numbers, i.e. $(n_1, n_2) = (1, 0)$, remains unclear. In the context of non-unitary CFTs, this might be an indication for the existence of non-normalizable states: For the ‘true ground state’ to appear in the spectrum of the lattice model, a non-zero twist in the boundary conditions may be needed. However, these thoughts are highly speculative such that further studies are required.

For both models under consideration our study was reliant on a numerical solution of the Bethe Ansatz equations. When using this method, the system size determines the numerical effort needed for a solution with satisfying precision. Assuming the possibility to deduce nonlinear integral equations not for the thermodynamic limit but for *finite* system sizes as in refs. [25, 26] for the (staggered) six-vertex model, the

system size would appear only as a parameter allowing for a numerical study up to, in principle, arbitrary large system sizes. Both studied models would greatly benefit from an investigation based on nonlinear integral equations, if such exist: For the q -deformed $sl(2|1)$ superspin chain, larger system sizes may allow for a more precise extraction of the density of states in the continua of scaling dimensions similar to [26]. The higher precision might be needed when comparing the calculated density of states in the continuous components of the spectrum with predictions from ‘candidate CFTs’ if known. In the q -deformed $osp(3|2)$ model, an approach based on integral equations would allow for a more precise verification of our conjecture as well as a better understanding of the subleading finite-size corrections. Admittedly, there may be technical difficulties to overcome when deducing the needed nonlinear integral equations since some of the states either involve isolated roots or have huge finite-size corrections in the imaginary parts of the string complexes. In addition, as mentioned above, such an approach is well-established for the (staggered) six vertex model only. For higher rank models like the two superspin chains studied within this work, there is no general scheme how to deduce the correct set of equations.

Recently, it became clear furthermore that the contribution of only the primary levels to the density of states in the continuous components of the spectrum is not sufficient for the identification of the thermodynamic limit of superspin chains [90]. Hence, when seeking for an identification of the thermodynamic limit of the $U_q[sl(2|1)]$ superspin chain by calculating the density of states using the quasimomentum operator also descendant states have to be considered.

Moreover, as briefly mentioned in the preliminaries, the Hamiltonians for both the staggered $U_q[sl(2|1)]$ and the q -deformed $osp(3|2)$ superspin chain are not hermitian operators. Hence, some energies might have a non-zero imaginary part. In fact, when studying the full spectrum for small lattice sizes, we found complex eigenenergies in the spectra of both models. However, previous studies of both models focused on the real part of the low-energy spectrum and the corresponding low-energy effective field theory in the thermodynamic limit [20–22, 84], hence we acted in a similar way. Since a rigorous proof for the permission of the negligence of complex eigenenergies is lacking, this procedure has to be seen as the desire for a simplification to end up with a theory with well-known properties. On the other hand, for superspin chains with a non-unitary CFT as effective field theory, the Hamiltonian fulfills a different role, that is, it serves as the generating functional for correlation functions. In this context, the usage of a non-hermitian operator is admissible. For the isotropic staggered $sl(2|1)$ superspin chain, this connection has been elaborated explicitly [127, 128]. Due to its different role, however, it is unclear whether the formalism to extract the scaling dimensions out of the finite size spectrum as discussed in I.3.3 needs slight adjustments when being applied to

superspin chains. Therefore, in this context, the role of non-hermitian Hamiltonians should be investigated in future research. The mentioned complex eigenenergies might turn out to be an essential part of the CFT describing the thermodynamic limit of superspin chains even though this may lead to rather unusual (in a physical context) field theories.

Allover, this work showed two striking features of the thermodynamic limits of superspin chains, in fact, the emergence of continua of scaling dimensions and the appearance of discrete states when imposing general toroidal boundary conditions. By establishing notable results for both studied models, the q -deformed $sl(2|1)$ and $osp(3|2)$ superspin chain, a solid basis was set for future research ultimately aiming to unveil their thermodynamic limit in the context of Conformal Field Theories.

A Supplements for the $U_q[osp(3|2)]$ superspin chain

A.1 The integrable XXZ spin-1 chain

We start by recalling the Bethe Ansatz solution of the integrable $S = 1$ Heisenberg XXZ spin chain with generic toroidal boundary conditions [48]. The Hilbert space of this model can be separated into disjoint sectors labeled by the total magnetization $S^z \equiv n$. The spectrum of the lattice model with L sites in a given sector n is parametrized by $L - n$ roots μ_j of the Bethe equations

$$\left[\frac{\sinh(\mu_j + i\gamma/2)}{\sinh(\mu_j - i\gamma/2)} \right]^L = e^{i\varphi} \prod_{\substack{k=1 \\ k \neq j}}^{L-n} \frac{\sinh(\mu_j - \mu_k + i\gamma/2)}{\sinh(\mu_j - \mu_k - i\gamma/2)}, \quad j = 1, \dots, L - n \quad (\text{A.1})$$

where $0 \leq \varphi \leq \pi$ corresponds to the twist angle around the z -axis. Given a solution $\{\mu_j\}$ to eqs. (A.1) the corresponding eigenenergy can be calculated by means of

$$E_n^{\text{XXZ}}(L, \varphi) = \sum_{j=1}^{L-n} \frac{2 \sin \gamma}{\cos \gamma - \cosh(2\mu_j)}. \quad (\text{A.2})$$

For the analysis of the system in the thermodynamic limit, $L \rightarrow \infty$, we utilize the string hypothesis [108, 129], that is, for $0 \leq \gamma \leq \pi$ we observe for the root configurations of the ground state and low lying excitations to be dominated by pairs of complex conjugate rapidities

$$\mu_{j\pm} = \xi_j \pm i\frac{\gamma}{4}, \quad (\text{A.3})$$

which are continuously distributed along the real ξ -axis. Based on this observation the root density formalism [119] allows for a computation of the density of these two-strings [120],

$$\sigma(\xi) = \frac{1}{\gamma} \frac{1}{\cosh(2\pi\xi/\gamma)} \quad (\text{A.4})$$

leading to the ground state energy per lattice site,

$$\varepsilon_\infty = \lim_{L \rightarrow \infty} E_0(L)/L = -2 \cot \frac{\gamma}{2}. \quad (\text{A.5})$$

In this approach, the elementary low-lying excitations above the ground state are found to be described by their dressed energy and momentum,

$$\varepsilon(\xi) = 2\pi\sigma(\xi) \quad \text{and} \quad p(\xi) = \int_\xi^\infty dx \varepsilon(x), \quad (\text{A.6})$$

yielding a linear dispersion relation $\varepsilon(p) \sim v_F |\sin p|$ with Fermi velocity $v_F = 2\pi/\gamma$. The complete finite-size spectrum of this model has been studied using a combination of analytical and numerical methods leading to [100–102]

$$E_{n,m}^{\text{XXZ}}(L, \varphi) - L\varepsilon_\infty = \frac{2\pi v_F}{L} \left[n^2 \frac{\pi - \gamma}{4\pi} + \left(m + \frac{\varphi}{\pi} \right)^2 \frac{\pi}{4(\pi - \gamma)} + X_I(r, j) - \frac{c}{12} \right]. \quad (\text{A.7})$$

The central charge of the Conformal Field Theory describing the low-energy behaviour of the integrable $S = 1$ Heisenberg XXZ spin chain reads $c = 3/2$ [130]. Within this theory, the operators are given in terms of composites of a $U(1)$ Kac-Moody field with charge n and vorticity m and an Ising (or $Z(2)$) operator with scaling dimension $X_I(r, j)$. The latter takes values

$$X_I(0, 0) \in \{0, 1\}, \quad X_I(1, 0) = X_I(0, 1) = \frac{1}{8}, \quad X_I(1, 1) = \frac{1}{2}, \quad (\text{A.8})$$

depending on n , m and the parity of the system size by means of the selection rules $r = n + L \bmod 2$ and $j = m + L \bmod 2$. In particular, $X_I = 1/8$ for $n + m$ odd.

Note, within the root density approach based on the string hypothesis (A.3) only the contributions from the Kac-Moody field to the finite-size energies (A.7) are obtained [122, 131]. The differences between the true root configurations solving the Bethe equations (A.1) and the string hypothesis add up to give the Ising part X_I [100].

A.2 Degeneration of root configurations

Usually, the finite-size analysis of a particular level in a Bethe Ansatz solvable lattice system relies on the fact that the roots to the Bethe equations form characteristic patterns which allow to characterize this level uniquely for any finite system and in the thermodynamic limit $L \rightarrow \infty$. For most of the studied low-energy states in the q -deformed $osp(3|2)$ superspin chain, we have found this statement to be true. However, we have also encountered a number of situations in which at a finite lattice size L_* some of the Bethe roots either diverge or degenerate leading to a qualitative change in the corresponding root configuration.

Unfortunately, it is not always possible to identify the new pattern of roots in order to follow the state for larger systems sizes. Moreover, such degenerations can occur even for intermediate system sizes which cannot be reached by an exact diagonalization of the Hamiltonian preventing us to identify the new pattern of the Bethe roots.

In this appendix we present such degenerations which have been observed in our finite-size study in more detail.

At the end of section 2.4.1, we have discussed a level in the charge sector $(0, 0)$ where we have found that the corresponding Bethe root configuration changes as the

system size is increased. For small L , the $fbbf$ roots for this state are arranged as $f : [(1_1^+)^3, z_2] \oplus [1_1, 2_2]_{-\infty}$, the finite ones are shown in Figure 59 for $L = 10$ and $L = 16$ and anisotropy $\gamma = 2\pi/7$.

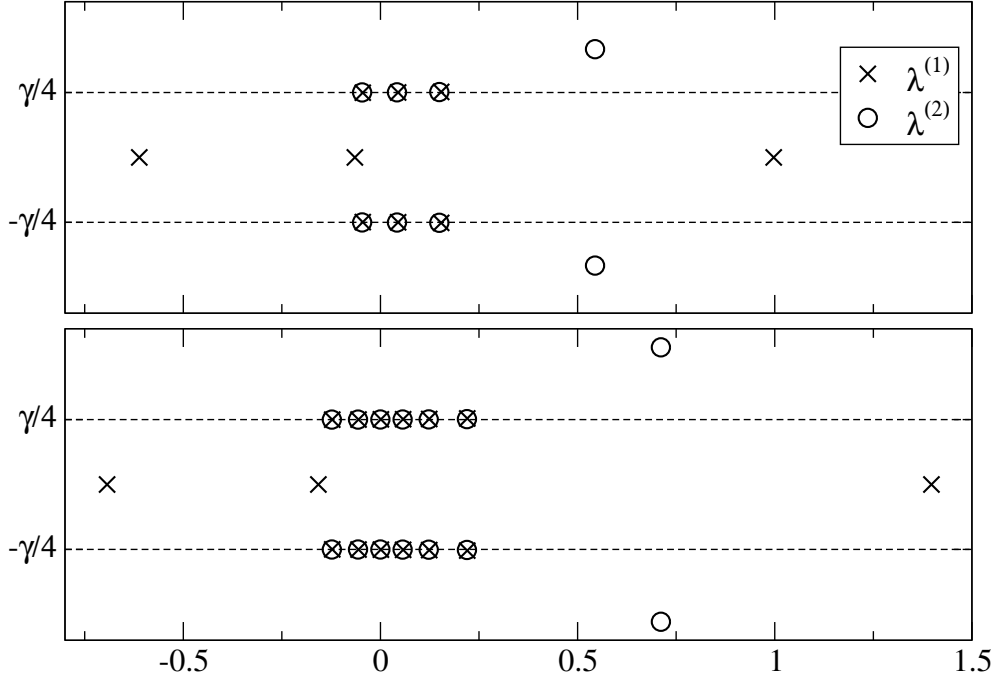


Figure 59: Finite part of the $fbbf$ root configurations for the spin $s = 1$ state in sector $(0, 0)$ for $L = 10$ (top) and $L = 16$ (bottom) and $\gamma = 2\pi/7$. As L is increased we notice a growth in the real part of one of the roots at the first level and of the real part of a complex pair at the second level.

As can be seen from this figure, three of the roots which are not part of the complexes (II.112), namely one of the real first level roots $[1_1^+]$ and the pair of complex conjugate level-2 roots, $[z_2]$, increase considerably as the system size grows. We can follow this behaviour based on our numerical solution of the Bethe equations (II.110) up to some finite system size L_* which depends on the anisotropy, e.g. $L_* = 26$ for the parameters used in figure 59. Beyond L_* , the root configuration degenerates and it is likely to change forming a different pattern. In principle, it might be possible to identify such a new pattern by solving the Bethe equations for $L \gtrsim L_*$. However, whether this describes an eigenstate of the superspin chain cannot be checked since an exact diagonalization of the Hamiltonian for systems of that size is not feasible.

In some cases it may be possible to avoid the degenerations described above by working in the other grading. Here, however, the $bfbf$ root configuration degenerates at the same system size L_* . As a consequence of this scenario we do not have sufficient data for a reliable finite-size analysis.

A second example for a state where the patterns formed by the Bethe roots changes

with the system size has been observed in the charge sector $(1, 0)$.

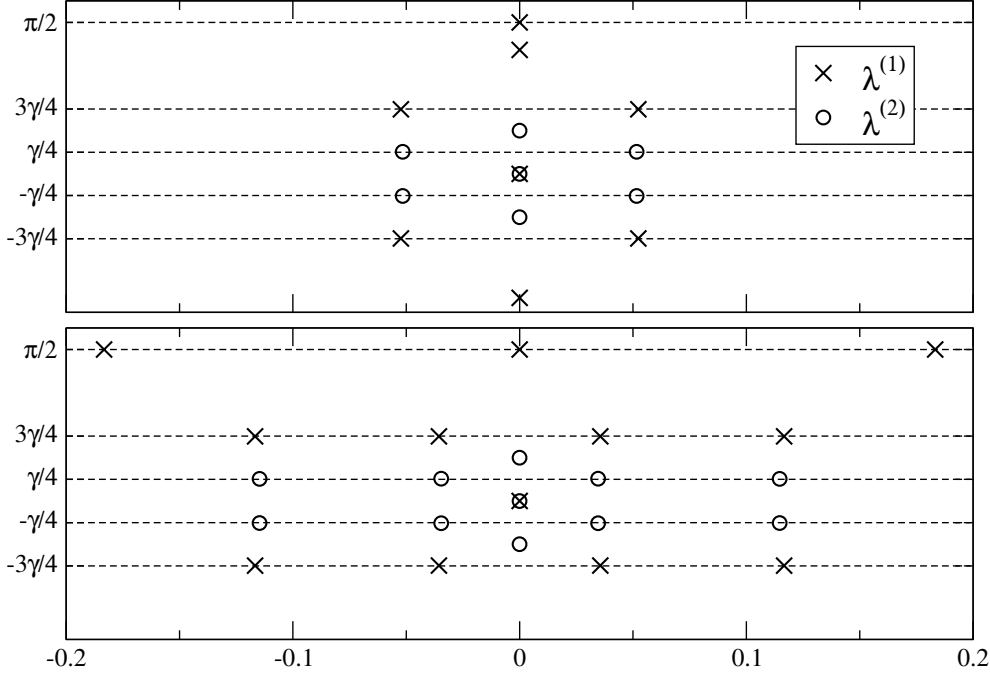


Figure 60: Degeneration of Bethe roots for a state in charge sector $(1, 0)$: for anisotropy $\gamma = 2\pi/7$ the root configuration changes from $b : [1_1^-, 1_2^+, 3_{21}^+, z_1]$ for system size $L = 10$ (top) to $b : [(1_1^-)^3, 1_2^+, 3_{21}^+]$ for $L = 12$ (bottom).

In fig. 60 we show how the *bfbfb* root configuration of this state changes when the system size is increased. We first note that the complex pair $[z_1]$ at the first level degenerates at $L_* = 12$ into the root pattern $[(1_1^-)^2]$ with a rather large real part. This configuration remains unchanged until we reach another finite system size \bar{L}_* which again depends on the anisotropy, e.g. for $\gamma = 2\pi/7$ we found $\bar{L}_* = 42$. Now for $L \gtrsim \bar{L}_*$ we find that the second level roots in two of the *bfbfb* complexes degenerate giving rise to yet another pattern of root configurations making it difficult to follow this state for large L . We remark that this kind of degeneracies is also present when we use the *fbbbf* grading. Therefore, the situation is similar to the one described previously.

Another example of a state whose root configuration changes twice, at distinct lattice sizes, has been observed in the $(1, 1)$ sector. The degenerations are exhibited in fig. 61 for $\gamma = 2\pi/7$.

In (a) we show the root pattern for $L = 8$ which is built from a configuration $f : [1_1^-]$. By increasing the system size to $L = 10$ we see that one of the 2-strings at level one splits into two real roots giving rise to new configuration $f : [(1_1^+)^2, 1_1^-, 2_2^+]$, see fig. 61(b). In addition, for $L > 12$ we note that one of the two-strings at level two starts to be deformed into a $[z_2]$ root configuration which is displayed in fig. 61(c) and (d). This latter root pattern remains stable for system sizes up to $L = 36$. Beyond this size the

solution of the Bethe equations failed due to numerical instabilities.

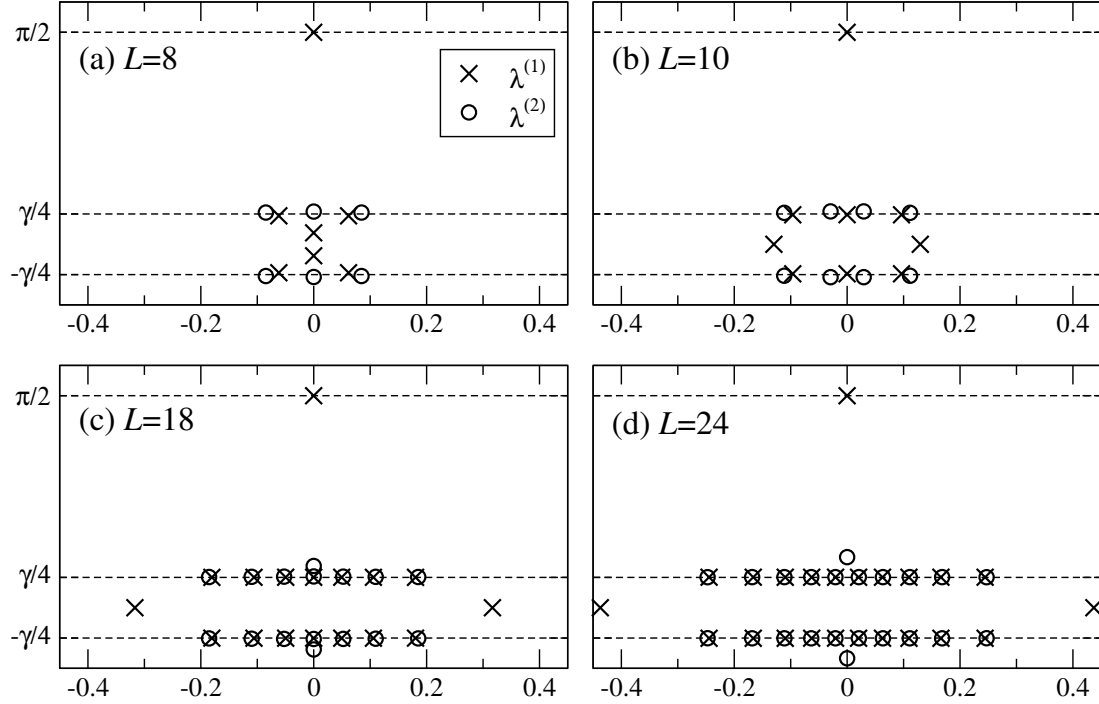


Figure 61: Sequence of degenerations of the Bethe root patterns for a state in charge sector $(1, 1)$ at anisotropy $\gamma = 2\pi/7$: the root configuration changes from $f : [1_1^-]$ for $L = 8$ (a) to $f : [(1_1^+)^2, 1_1^-, 2_2^+]$ for $L = 10$ (b), and further to $f : [(1_1^+)^2, 1_1^-, z_2]$ for $L = 18$ (c) and $L = 24$ (d).

A.3 Missing and unclassified states

In addition to states changing their root configuration which have been discussed in appendix A.2, we have also found states for which we could find the root configuration only for specific values of the anisotropy γ and system size L . In this appendix, we list these states and their root configurations if known.

The first of these states belongs to the charge sector $(1, 0)$ and is described in terms of a $f : [1_1^-, 1_2^+, z_1, z_2]$ or equivalently $b : [3_{12}^+, z_1, z_2]$ root configuration. The Bethe roots for both gradings and anisotropy $\gamma = 2\pi/7$ can be found in table 11.

In the $(1, 1)$ charge sector there is again one state for which the root configuration is known only for certain parameters. For $L = 6$ and $\gamma < \pi/4$, this state has a $b : [1_1^-, z_1, z_2]$ root configuration, see tab. 12. When $\gamma \rightarrow \pi/4$ the imaginary part of the $[z_1]$ configuration shrinks such that at $\gamma = \pi/4$ it passes into $[(1_1^+)^2]$ to avoid degenerations. For $\gamma > \pi/4$ we haven't been able to find a root configuration.

For the charges $(n_1, n_2) = (2, 1)$ we found one additional state with a very peculiar root configuration which does not fit to our notation introduced in section 2.4. Using

$\lambda^{(1)}/\gamma$ (<i>bfbfb</i>)	$\lambda^{(1)}/\gamma$ (<i>fbbbf</i>)	$\lambda^{(2)}/\gamma$
$-0.0614037 + 0.7497763i$	$-0.0497337 + 0.2308725i$	$-0.0594249 + 0.2575524i$
$-0.0614037 - 0.7497763i$	$-0.0497337 - 0.2308725i$	$-0.0594249 - 0.2575524i$
$0.2775207 + 0.7511673i$	$-0.1104048 + 0.1852444i$	$0.2586970 + 0.2364768i$
$0.2775207 - 0.7511673i$	$-0.1104048 - 0.1852444i$	$0.2586970 - 0.2364768i$
$-0.1083635 + 0.4999904i$	$0.2434987 + 0.2732079i$	$-0.1052276 + 0.3794159i$
$-0.1083635 - 0.4999904i$	$0.2434987 - 0.2732079i$	$-0.1052276 - 0.3794159i$
$-0.1077535 + 1.0052139i$	$-0.0869949 + \pi/(2\gamma)i$	-0.1083634
$-0.1077535 - 1.0052139i$		

Table 11: Root configuration of the $b : [3_{12}^+, z_1, z_2]$ or equivalently $f : [1_1^-, 1_2^+, z_1, z_2]$ state in the $(1, 0)$ sector for $L = 8$ and $\gamma = 2\pi/7$ [114].

$\lambda^{(1)}/\gamma$	$\lambda^{(2)}/\gamma$
$0.0802213 + 0.7496060i$	$0.0802934 + 0.2503739i$
$0.0802213 - 0.7496060i$	$0.0802934 - 0.2503739i$
$0.7922719 + 0.6098025i$	$0.9907590 + 0.3621826i$
$0.7922719 - 0.6098025i$	$0.9907590 - 0.3621826i$
$-0.6739339 + \pi/(2\gamma)i$	

Table 12: Root configuration of the $b : [1_1^+, z_1, z_2]$ state in the $(1, 1)$ sector for $L = 6$ and $\gamma = 2\pi/9$ [114].

the *fbbbf* grading it consist of two (one) purely imaginary roots on the first (second) level. In contrast to the string complexes occurring at all of the other states, here the remaining roots on both levels are *not* complex conjugates. Instead their imaginary parts are slightly shifted which can be seen explicitly in tab. 13 where we list the corresponding Bethe roots for $L = 8$ and $\gamma = 2\pi/7$. We have been able to calculate the Bethe roots for this state up to $L \leq 16$ and $0 < \gamma \leq \pi/3$.

$\lambda^{(1)}/\gamma$	$\lambda^{(2)}/\gamma$
$-0.0574347 + 0.2561136i$	$-0.0576961 + 0.2563855i$
$0.0574347 + 0.2561136i$	$0.0576961 + 0.2563855i$
$-0.0635931 - 0.2340169i$	$-0.0573882 - 0.2442878i$
$0.0635931 - 0.2340169i$	$0.0573882 - 0.2442878i$
$-0.1620614i$	$0.5803344i$
$1.3092483i$	

Table 13: Root configuration of the discussed state in the $(2, 1)$ sector using the *fbbbf* grading for $L = 8$ and $\gamma = 2\pi/7$ [114].

References

- [1] W. Heisenberg. „Zur Theorie des Ferromagnetismus.“ In: *Original Scientific Papers Wissenschaftliche Originalarbeiten*. Springer, 1985, pp. 580–597.
- [2] P. A. M. Dirac. „On the theory of quantum mechanics.“ In: *Proceedings of the Royal Society of London. Series A, Containing Papers of a Mathematical and Physical Character* 112.762 (1926), pp. 661–677.
- [3] H. Bethe. „Zur Theorie der Metalle.“ In: *Zeitschrift für Physik* 71.3-4 (1931), pp. 205–226.
- [4] R. Baxter. *Exactly solved models in statistical mechanics*. Academic Press, 1982.
- [5] V. Bazhanov. „Trigonometric solutions of triangle equations and classical Lie algebras.“ In: *Physics Letters B* 159.4-6 (1985), pp. 321–324.
- [6] M. Jimbo. „Quantum R -matrix for the generalized Toda system.“ In: *Communications in Mathematical Physics* 102.4 (1986), pp. 537–547.
- [7] I. Affleck and F. Haldane. „Critical theory of quantum spin chains.“ In: *Physical Review B* 36.10 (1987), p. 5291.
- [8] J. Wess and B. Zumino. „Supergauge transformations in four dimensions.“ In: *Nuclear Physics B* 70.1 (1974), pp. 39–50.
- [9] L. Corwin, Y. Ne’eman, and S. Sternberg. „Graded Lie algebras in mathematics and physics (Bose-Fermi symmetry).“ In: *Reviews of Modern Physics* 47.3 (1975), p. 573.
- [10] K. v. Klitzing, G. Dorda, and M. Pepper. „New method for high-accuracy determination of the fine-structure constant based on quantized Hall resistance.“ In: *Physical Review Letters* 45.6 (1980), p. 494.
- [11] J. Chalker and P. Coddington. „Percolation, quantum tunnelling and the integer Hall effect.“ In: *Journal of Physics C: Solid State Physics* 21.14 (1988), p. 2665.
- [12] M. Morgenstern et al. „Real-space observation of drift states in a two-dimensional electron system at high magnetic fields.“ In: *Physical Review Letters* 90.5 (2003), p. 056804.
- [13] H. Levine, S. B. Libby, and A. M. Pruisken. „Electron delocalization by a magnetic field in two dimensions.“ In: *Physical Review Letters* 51.20 (1983), p. 1915.
- [14] A. M. Pruisken. „On localization in the theory of the quantized hall effect: A two-dimensional realization of the θ -vacuum.“ In: *Nuclear Physics B* 235.2 (1984), pp. 277–298.

- [15] M. R. Zirnbauer. „Towards a theory of the integer quantum Hall transition: From the nonlinear sigma model to superspin chains.“ In: *Annalen der Physik* 506.7-8 (1994), pp. 513–577.
- [16] H. A. Weidenmüller. „Single electron in a random potential and a strong magnetic field.“ In: *Nuclear Physics B* 290 (1987), pp. 87–110.
- [17] K. Efetov. „Supersymmetry and theory of disordered metals.“ In: *Advances in Physics* 32.1 (1983), pp. 53–127.
- [18] M. Martins, B. Nienhuis, and R. Rietman. „An intersecting loop model as a solvable super spin chain.“ In: *Physical Review Letters* 81.3 (1998), p. 504.
- [19] H. Frahm and M. J. Martins. „Finite-size effects in the spectrum of the $OSp(3|2)$ superspin chain.“ In: *Nuclear Physics B* 894 (2015), pp. 665–684.
- [20] F. H. Essler, H. Frahm, and H. Saleur. „Continuum limit of the integrable $sl(2|1)_{3-\bar{3}}$ superspin chain.“ In: *Nuclear Physics B* 712.3 (2005), pp. 513–572.
- [21] H. Frahm and M. J. Martins. „Finite size properties of staggered $U_q[sl(2|1)]$ superspin chains.“ In: *Nuclear Physics B* 847.1 (2011), pp. 220–246.
- [22] H. Frahm and M. J. Martins. „The fine structure of the finite-size effects for the spectrum of the $OSp(n|2m)$ spin chain.“ In: *Nuclear Physics B* 930 (2018), pp. 545–562.
- [23] Y. Ikhlef, J. Jacobsen, and H. Saleur. „A staggered six-vertex model with non-compact continuum limit.“ In: *Nuclear Physics B* 789.3 (2008), pp. 483–524.
- [24] Y. Ikhlef, J. L. Jacobsen, and H. Saleur. „Integrable spin chain for the $SL(2, \mathbb{R})/U(1)$ black hole sigma model.“ In: *Physical Review Letters* 108.8 (2012), p. 081601.
- [25] C. Candu and Y. Ikhlef. „Nonlinear integral equations for the black hole sigma model.“ In: *Journal of Physics A: Mathematical and Theoretical* 46.41 (2013), p. 415401.
- [26] H. Frahm and A. Seel. „The staggered six-vertex model: Conformal invariance and corrections to scaling.“ In: *Nuclear Physics B* 879 (2014), pp. 382–406.
- [27] É. Vernier, J. L. Jacobsen, and H. Saleur. „Non compact conformal field theory and the (Izergin–Korepin) model in regime III.“ In: *Journal of Physics A: Mathematical and Theoretical* 47.28 (2014), p. 285202.
- [28] E. Vernier, J. L. Jacobsen, and H. Saleur. „The continuum limit of $a_{N-1}^{(2)}$ spin chains.“ In: *Nuclear Physics B* 911 (2016), pp. 52–93.

- [29] J.-S. Caux and J. Mossel. „Remarks on the notion of quantum integrability.“ In: *Journal of Statistical Mechanics: Theory and Experiment* 2011.02 (2011), P02023.
- [30] L. Faddeev. *Integrable models in 1+1 dimensional quantum field theory*. Tech. rep. CEA Centre d'Etudes Nucleaires de Saclay, 1982.
- [31] A. Izergin and V. Korepin. „The most general \mathcal{L} -operator for the \mathcal{R} -matrix of the XXX model.“ In: *Letters in Mathematical Physics* 8.4 (1984), pp. 259–265.
- [32] L. Faddeev. „How Algebraic Bethe Ansatz works for integrable model.“ In: *arXiv preprint hep-th/9605187* (1996).
- [33] F. Franchini. *An introduction to integrable techniques for one-dimensional quantum systems*. Vol. 940. Springer, 2017.
- [34] C.-N. Yang. „Some exact results for the many-body problem in one dimension with repulsive δ -function interaction.“ In: *Physical Review Letters* 19.23 (1967), p. 1312.
- [35] C. N. Yang. „ S matrix for the one-dimensional N -body problem with repulsive or attractive δ -function interaction.“ In: *Physical Review* 168.5 (1968), p. 1920.
- [36] L. Šamaj and Z. Bajnok. *Introduction to the statistical physics of integrable many-body systems*. Cambridge University Press, 2013.
- [37] V. E. Korepin, N. M. Bogoliubov, and A. G. Izergin. *Quantum inverse scattering method and correlation functions*. Vol. 3. Cambridge university press, 1997.
- [38] A. N. Kirillov and N. Y. Reshetikhin. „Exact solution of the Heisenberg XXZ model of spin s .“ In: *Journal of Soviet Mathematics* 35.4 (1986), pp. 2627–2643.
- [39] A. M. Grabinski. *Functional Bethe Ansatz Methods for the Exact Solution of Integrable Super Spin Chains with Non-Diagonal Boundary Fields*. Dr. Hut, 2013.
- [40] E. H. Lieb and F. Wu. „The one-dimensional Hubbard model: A reminiscence.“ In: *Physica A: Statistical Mechanics and its Applications* 321.1-2 (2003), pp. 1–27.
- [41] Y. Wang et al. *Off-diagonal Bethe ansatz for exactly solvable models*. Springer, 2015.
- [42] T. Deguchi. „Regular XXZ Bethe states at roots of unity as highest weight vectors of the \mathfrak{sl}_2 loop algebra.“ In: *Journal of Physics A: Mathematical and Theoretical* 40.27 (2007), p. 7473.
- [43] P. P. Kulish and N. Y. Reshetikhin. „Diagonalisation of $GL(N)$ invariant transfer matrices and quantum N-wave system (Lee model).“ In: *Journal of Physics A: Mathematical and General* 16.16 (1983), p. L591.

- [44] O. Babelon, H. De Vega, and C. Viallet. „Exact solution of the $Z_{n+1} \times Z_{n+1}$ symmetric generalization of the XXZ model.“ In: *Nuclear Physics B* 200.2 (1982), pp. 266–280.
- [45] A. Nijenhuis. „Jacobi-type identities for bilinear differential concomitants of certain tensor fields, I.“ In: *Proceedings of Koninklijke Nederlandse Akademie van Wetenschappen A* 58 (1955), p. 390.
- [46] A. Frölicher and A. Nijenhuis. „A theorem on stability of complex structures.“ In: *Proceedings of the National Academy of Sciences of the United States of America* 43.2 (1957), p. 239.
- [47] P. P. Kulish. „Integrable graded magnets.“ In: *Journal of Soviet Mathematics* 35.4 (1986), pp. 2648–2662.
- [48] F. Zhang and T. Rice. „Effective Hamiltonian for the superconducting Cu oxides.“ In: *Physical Review B* 37.7 (1988), p. 3759.
- [49] F. H. Essler and V. E. Korepin. „Higher conservation laws and algebraic Bethe Ansatz for the supersymmetric $t - J$ model.“ In: *Physical Review B* 46.14 (1992), p. 9147.
- [50] M. Scheunert. *The theory of Lie superalgebras: An introduction*. Vol. 716. Springer, 2006.
- [51] V. G. Kac. „Lie superalgebras.“ In: *Advances in Mathematics* 26.1 (1977), pp. 8–96.
- [52] J. Cornwell. „Group Theory in Physics. Volume III: Supersymmetries and Infinite-Dimensional Algebras.“ In: *Techniques in Physics* 10 (1989), pp. 1–628.
- [53] M. Scheunert, W. Nahm, and V. Rittenberg. „Irreducible representations of the $osp(2, 1)$ and $spl(2, 1)$ graded Lie algebras.“ In: *Journal of Mathematical Physics* 18.1 (1977), pp. 155–162.
- [54] M. Marcu. „The representations of $spl(2, 1)$ — an example of representations of basic superalgebras.“ In: *Journal of Mathematical Physics* 21.6 (1980), pp. 1277–1283.
- [55] M. Marcu. „The tensor product of two irreducible representations of the $spl(2, 1)$ superalgebra.“ In: *Journal of Mathematical Physics* 21.6 (1980), pp. 1284–1292.
- [56] L. Frappat, A. Sciarrino, and P. Sorba. „Dictionary on Lie superalgebras.“ In: *arXiv preprint hep-th/9607161* (1996).
- [57] V. Kac. „A sketch of Lie superalgebra theory.“ In: *Communications in Mathematical Physics* 53.1 (1977), pp. 31–64.

- [58] P. Francesco, P. Mathieu, and D. Sénéchal. *Conformal field theory*. Springer Science & Business Media, 2012.
- [59] M. Chaichian and P. Kulish. „Quantum Lie superalgebras and q -oscillators.“ In: *Physics Letters B* 234.1-2 (1990), pp. 72–80.
- [60] T. Ostrowski. „A note on semidirect sum of Lie algebras.“ In: *Discussiones Mathematicae-General Algebra and Applications* 33.2 (2013), pp. 233–247.
- [61] D. J. Benson. *Representations and Cohomology: Cohomology of groups and modules*. Cambridge University Press, 1998.
- [62] G. Götz, T. Quella, and V. Schomerus. „Representation theory of $sl(2|1)$.“ In: *Journal of Algebra* 312.2 (2007), pp. 829–848.
- [63] P. Kulish and E. Sklyanin. „Lecture notes in physics.“ In: *Springer, Berlin* 151 (1982), p. 61.
- [64] E. K. Sklyanin. „Some algebraic structures connected with the Yang—Baxter equation.“ In: *Functional Analysis and its Applications* 16.4 (1982), pp. 263–270.
- [65] V. Pasquier and M. Saleur. „Symmetries of the XXZ chain and quantum groups.“ In: *Saclay. SPhT/88-187* (1988).
- [66] V. G. Drinfeld. „Quantum groups.“ In: *Proceedings of the International Congress of Mathematicians, Berkeley*. 1986, pp. 798–820.
- [67] L. D. Faddeev, N. Y. Reshetikhin, and L. A. Takhtajan. „Quantization of Lie groups and Lie algebras.“ In: *Algebraic Analysis*. Elsevier, 1988, pp. 129–139.
- [68] R. Floreanini, V. P. Spiridonov, and L. Vinet. „ q -Oscillator realizations of the quantum superalgebras $sl_q(m, n)$ and $osp_q(m, 2n)$.“ In: *Communications in Mathematical Physics* 137.1 (1991), pp. 149–160.
- [69] H. Weyl. *Raum, Zeit, Materie*. Vol. 7. Springer, 1918.
- [70] A. M. Polyakov. „Conformal symmetry of critical fluctuations (originally published in russian volume 12, number 11).“ In: *Soviet Journal of Experimental and Theoretical Physics Letters* 12 (1970), p. 381.
- [71] A. A. Belavin, A. M. Polyakov, and A. B. Zamolodchikov. „Infinite conformal symmetry of critical fluctuations in two dimensions.“ In: *Journal of Statistical Physics* 34 (1984), pp. 763–774.
- [72] A. A. Belavin, A. M. Polyakov, and A. B. Zamolodchikov. „Infinite conformal symmetry in two-dimensional quantum field theory.“ In: *Nuclear Physics B* 241 (1984), pp. 333–380.
- [73] J. L. Cardy. „Conformal Invariance.“ In: *Phase Transitions and Critical Phenomena* 11 (1987), pp. 55–126.

- [74] M. Henkel. *Conformal invariance and critical phenomena*. Springer Science & Business Media, 2013.
- [75] Y. Nakayama. „Scale invariance vs conformal invariance.“ In: *Physics Reports* 569 (2015), pp. 1–93.
- [76] S. Ribault. „Conformal field theory on the plane.“ In: *arXiv preprint arXiv:1406.4290* (2014).
- [77] D. Friedan, Z. Qiu, and S. Shenker. „Superconformal invariance in two dimensions and the tricritical Ising model.“ In: *Physics Letters B* 151.1 (1985), pp. 37–43.
- [78] P. Ramond. „Dual theory for free fermions.“ In: *Physical Review D* 3.10 (1971), p. 2415.
- [79] A. Neveu and J. H. Schwarz. „Tachyon-free dual model with a positive-intercept trajectory.“ In: *Physics Letters B* 34.6 (1971), pp. 517–518.
- [80] D. Tong. „Lectures on the quantum Hall effect.“ In: *arXiv preprint arXiv:1606.06687* (2016).
- [81] P. W. Bridgman. *Biographical Memoir of Edwin Herbert Hall, 1855-1938*. National Academy of Sciences, 1939.
- [82] E. Hall. „On a New Action of the Magnet on Electric Currents.“ In: *American Journal of Mathematics* 2.3 (1879), pp. 287–292.
- [83] K. Von Klitzing. „The quantized Hall effect.“ In: *Reviews of Modern Physics* 58.3 (1986), p. 519.
- [84] H. Frahm and M. J. Martins. „Phase diagram of an integrable alternating $U_q[sl(2|1)]$ superspin chain.“ In: *Nuclear Physics B* 862.2 (2012), pp. 504–552.
- [85] H. Frahm and K. Hobeuß. „Spectral flow for an integrable staggered superspin chain.“ In: *Journal of Physics A: Mathematical and Theoretical* 50.29 (2017), p. 294002.
- [86] I. A. Gruzberg, A. W. Ludwig, and N. Read. „Exact exponents for the spin quantum Hall transition.“ In: *Physical Review Letters* 82.22 (1999), p. 4524.
- [87] H. Saleur and V. Schomerus. „On the $SU(2|1)$ WZNW model and its statistical mechanics applications.“ In: *Nuclear Physics B* 775.3 (2007), pp. 312–340.
- [88] E. Witten. „String theory and black holes.“ In: *Physical Review D* 44.2 (1991), p. 314.
- [89] R. Dijkgraaf, H. Verlinde, and E. Verlinde. „String propagation in a black hole geometry.“ In: *Nucl. Phys. B* 371 (1992), pp. 269–314.
- [90] V. V. Bazhanov et al. „On the scaling behaviour of the alternating spin chain.“ In: *arXiv preprint arXiv:1903.05033* (2019).

- [91] A. Izergin and V. Korepin. „The inverse scattering method approach to the quantum Shabat-Mikhailov model.“ In: *Communications in Mathematical Physics* 79.3 (1981), pp. 303–316.
- [92] A. Hanany, N. Prezas, and J. Troost. „The partition function of the two-dimensional black hole conformal field theory.“ In: *Journal of High Energy Physics* 2002.04 (2002), p. 014.
- [93] S. Ribault and V. Schomerus. „Branes in the 2D black hole.“ In: *Journal of High Energy Physics* 2004.02 (2004), p. 019.
- [94] R. Gade. „An integrable $sl(2|1)$ vertex model for the spin quantum Hall critical point.“ In: *Journal of Physics A: Mathematical and General* 32.41 (1999), pp. 7071–7082.
- [95] A. Foerster and M. Karowski. „Algebraic properties of the Bethe ansatz for an $spl(2,1)$ -supersymmetric $t - J$ model.“ In: *Nuclear Physics B* 396.2-3 (1993), pp. 611–638.
- [96] M. P. Pfannmüller and H. Frahm. „Algebraic Bethe ansatz for $gl(2,1)$ invariant 36-vertex models.“ In: *Nuclear Physics B* 479.3 (1996), pp. 575–593.
- [97] M. Pfannmüller and H. Frahm. „A new algebraic Bethe ansatz for $gl(2,1)$ invariant vertex models.“ In: *Journal of Physics A: Mathematical and General* 30.15 (1997), p. L543.
- [98] G. Ribeiro and M. Martins. „Algebraic Bethe ansatz for an integrable $U_q[Sl(n|m)]$ vertex model with mixed representations.“ In: *Nuclear Physics B* 738.3 (2006), pp. 391–408.
- [99] J. Abad and M. Rios. „Method for solving integrable A_2 spin chains combining different representations.“ In: *Physical Review B* 53.21 (1996), p. 14000.
- [100] F. C. Alcaraz and M. J. Martins. „Conformal invariance and the operator content of the XXZ model with arbitrary spin.“ In: *Journal of Physics A: Mathematical and General* 22.11 (1989), p. 1829.
- [101] F. C. Alcaraz and M. J. Martins. „The spin- S XXZ quantum chain with general toroidal boundary conditions.“ In: *Journal of Physics A: Mathematical and General* 23.8 (1990), p. 1439.
- [102] H. Frahm, N.-C. Yu, and M. Fowler. „The integrable XXZ Heisenberg model with arbitrary spin: construction of the Hamiltonian, the ground-state configuration and conformal properties.“ In: *Nuclear Physics B* 336.3 (1990), pp. 396–434.
- [103] D. Gepner and Z. Qiu. „Modular invariant partition functions for parafermionic field theories.“ In: *Nuclear Physics B* 285 (1987), pp. 423–453.

- [104] C. Hagendorf. „The nineteen-vertex model and alternating sign matrices.“ In: *Journal of Statistical Mechanics: Theory and Experiment* 2015.1 (2015), P01017.
- [105] W. H. Press et al. *Numerical Recipes in C: The Art of Scientific Computing*. Cambridge University Press, 1992, pp. 111–113.
- [106] J. Maldacena and H. Ooguri. „Strings in AdS_3 and the $SL(2, \mathbb{R})$ WZW model. I: The spectrum.“ In: *Journal of Mathematical Physics* 42.7 (2001), pp. 2929–2960.
- [107] P. Bowcock, M. Hayes, and A. Taormina. „Characters of Admissible Representations of the Affine Superalgebra $\hat{sl}(2|1; \mathbb{C})_k$.“ In: *Nuclear Physics B* 510.3 (1998), pp. 739–763.
- [108] M. Takahashi and M. Suzuki. „One-dimensional anisotropic Heisenberg model at finite temperatures.“ In: *Progress of Theoretical Physics* 48.6 (1972), pp. 2187–2209.
- [109] L. Eberhardt. *Wess-Zumino-Witten Models*. Feb. 2019.
- [110] E. Vernier. „Non compact conformal field theories in statistical mechanics.“ PhD thesis. Ecole Normale Supérieure & IPhT, Saclay, 2015.
- [111] K. Hori and A. Kapustin. „Duality of the fermionic 2d black hole and $N=2$ Liouville theory as mirror symmetry.“ In: *Journal of High Energy Physics* 2001.08 (2001), p. 045.
- [112] J.-L. Jacobsen, N. Read, and H. Saleur. „Dense loops, supersymmetry, and Goldstone phases in two dimensions.“ In: *Physical Review Letters* 90.9 (2003), p. 090601.
- [113] H. Frahm, K. Hobuß, and M. Martins. „On the critical behaviour of the integrable q -deformed $OSp(3|2)$ superspin chain.“ In: *Nuclear Physics B* 946 (2019), p. 114697.
- [114] H. Frahm, K. Hobuß, and M. J. Martins. *Dataset: Finite size data for the q -deformed $OSp(3|2)$ superspin chain*. <https://doi.org/10.25835/0064330>. 2019.
- [115] J. Van der Jeugt. „Finite-and infinite-dimensional representations of the orthosymplectic superalgebra $OSP(3, 2)$.“ In: *Journal of Mathematical Physics* 25.11 (1984), pp. 3334–3349.
- [116] T. Palev and N. Stoilova. „Wigner quantum oscillators. $osp(3/2)$ oscillators.“ In: *Journal of Physics A: Mathematical and General* 27.22 (1994), p. 7387.
- [117] W. Galleas and M. J. Martins. „ \mathcal{R} -matrices and spectrum of vertex models based on superalgebras.“ In: *Nuclear Physics B* 699.3 (2004), pp. 455–486.
- [118] M. Martins and P. Ramos. „The algebraic Bethe ansatz for rational braid-monoid lattice models.“ In: *Nuclear Physics B* 500.1-3 (1997), pp. 579–620.

- [119] C.-N. Yang and C. P. Yang. „Thermodynamics of a One-Dimensional System of Bosons with Repulsive Delta-Function Interaction.“ In: *Journal of Mathematical Physics* 10.7 (1969), pp. 1115–1122.
- [120] K. Sogo. „Ground state and low-lying excitations in the Heisenberg XXZ chain of arbitrary spin S .“ In: *Physics Letters A* 104.1 (1984), pp. 51–54.
- [121] P.-A. Bares et al. „Charge-spin recombination in the one-dimensional supersymmetric $t - J$ model.“ In: *Physical Review B* 46.22 (1992), p. 14624.
- [122] H. De Vega and F. Woynarovich. „Method for calculating finite size corrections in Bethe ansatz systems: Heisenberg chain and six-vertex model.“ In: *Nuclear Physics B* 251 (1985), pp. 439–456.
- [123] J.-M. V. Broeck and L. W. Schwartz. „A one-parameter family of sequence transformations.“ In: *SIAM Journal on Mathematical Analysis* 10.3 (1979), pp. 658–666.
- [124] C. Hamer and M. N. Barber. „Finite-lattice methods in quantum Hamiltonian field theory. I. The Ising model.“ In: *Journal of Physics A: Mathematical and General* 14.1 (1981), p. 241.
- [125] W. Galleas and M. Martins. „Exact solution and finite size properties of the $U_q[osp(2|2m)]$ vertex models.“ In: *Nuclear Physics B* 768.3 (2007), pp. 219–246.
- [126] E. Ilievski et al. „Quasilocal charges in integrable lattice systems.“ In: *Journal of Statistical Mechanics: Theory and Experiment* 2016.6 (2016), p. 064008.
- [127] T. Senthil, J. Marston, and M. P. Fisher. „Spin quantum Hall effect in unconventional superconductors.“ In: *Physical Review B* 60.6 (1999), p. 4245.
- [128] T. Senthil and M. P. Fisher. „Quasiparticle density of states in dirty high- T_c superconductors.“ In: *Physical Review B* 60.9 (1999), p. 6893.
- [129] A. N. Kirillov and N. Y. Reshetikhin. „Exact solution of the integrable XXZ Heisenberg model with arbitrary spin. I. The ground state and the excitation spectrum.“ In: *Journal of Physics A: Mathematical and General* 20.6 (1987), p. 1565.
- [130] H. M. Babujian and A. Tsvetick. „Heisenberg magnet with an arbitrary spin and anisotropic chiral field.“ In: *Nuclear Physics B* 265.1 (1986), pp. 24–44.
- [131] C. Hamer. „Finite-size corrections for ground states of the XXZ Heisenberg chain.“ In: *Journal of Physics A: Mathematical and General* 19.16 (1986), p. 3335.

Acknowledgements

At first I deeply thank my supervisor Prof. Dr. Holger Frahm for all his support during my time as a PhD candidate. Without our countless discussions this work would not have been possible in the present way. In the same manner I would like to thank also all the present and former members of our working group at the ITP, in particular I want to mention Daniel Borcharding and Daniel Westerfeld.

I also want to thank Prof. Dr. Andreas Klümper and PD Dr. Michael Flohr for acting as second reviewers of this thesis as well as Prof. Dr. Rolf Haug for chairing the PhD organization committee.

It was a great pleasure to work together with Prof. Marcio J. Martins during his two stays at the ITP in early 2018 and 2019. His profound knowledge and our detailed discussions influenced our joint work in a very positive way.

I am very grateful to the Deutsche Forschungsgemeinschaft for providing the funding for this work as part of the research unit *Correlations in Integrable Quantum Many-Body Systems* (FOR2316) under grant No. Fr 737/9-1. I really enjoyed being part of this research unit. In this context I especially want to express my thanks for the great scientific exchange during the corresponding workshops.

Finally I want to express my deepest thanks to my family and friends for the huge support during the past years. The friendship and love I received from all of you cannot be overstated for the existence of this thesis.

Konstantin Hobuß

Selbstständigkeitserklärung

Hiermit erkläre ich, diese Arbeit selbständig und nur mit den angegebenen Hilfsmitteln angefertigt zu haben. Alle Stellen der Arbeit, die wörtlich oder sinngemäß aus anderen Werken übernommen wurden, sind als solche kenntlich gemacht. Diese Arbeit lag weder in dieser, noch in ähnlicher Form bereits einer Prüfungsbehörde vor.

Hannover, 11. Dezember 2019

Curriculum Vitae

Personal

Name Konstantin Hobuß

Date of birth 08.08.1991

Place of birth Hannover

Education

01/2016 - 12/2019 Research associate, Leibniz University Hannover,
Dissertation: Spin chains and vertex models based on
superalgebras

10/2013 - 09/2015 M.Sc. Physics, Philipps University Marburg,
Master's thesis: Calculation of the single particle Green's
function using the Gutzwiller wave function

10/2010 - 09/2013 B.Sc. Physics, Philipps University Marburg,
Bachelor's thesis: Fabrication and characterization of THz-
metamaterials on thin piezoelectric films

06/2009 Allgemeine Hochschulreife, Ratsgymnasium Osnabrück